EXPERIMENTAL INVESTIGATION OF CI ENGINE PERFORMANCE, EMISSIONS AND COMBUSTION USING ADVANCED BIOFUELS

By

Md Abul Kalam Azad

A Thesis

Submitted in Fulfilment of the Requirements for the Degree of

Doctor of Philosophy

School of Engineering and Technology

Central Queensland University, Australia

December, 2016

This thesis is dedicated to my parents, wife

and

our lovely daughter Samara Azad

Abstract

There is an ongoing interest in developing new alternative fuels (such as biofuel) for both aviation and road transport sectors to meet increasing energy demand and assist in reducing greenhouse gas (GHG) emissions. The major contribution of this work is to develop an aviation biofuel from a new feedstock and create the best possible biodiesel-diesel blends for the transport sector. This study focuses on improving engine performance and reducing emissions by enhancing combustion efficiency using these newly developed fuels without any modification of the modern engine. The combustion and emissions were closely monitored to evaluate the pollutants formation in a compression ignition (CI) engine. Better performing fuels were identified and their tribological behaviour was also studied to assess their impact on engine life.

A wide range of biofuel feedstocks (over 150 species) was initially investigated to identify the most prospective feedstocks for producing biodiesels. The study eventually identified six prospective feedstocks namely Mandarin peel waste, Crambe, Tamanu, Borage, Waste Avocado flesh and Bush nut for biofuel production. The biofuels were produced in the laboratory from these selected feedstocks. The fatty acid methyl esters (FAMEs) composition and physio–chemical properties of these newly produced biofuels were evaluated using ASTM and EN standards.

The fuel properties of these biodiesels revealed that the properties of the Mandarin biofuel closely fit with the properties of commercial jet fuel with a calorific value of 44.66 MJ/kg (4.3% higher than commercial jet fuel) and a higher flash point of 52 °C. This biofuel has a lower viscosity (about 2.13 mm^2/s at minus 20 degree C.) which is desirable and is self–oxygenated and sulphur free. Therefore, it is seen as a prospective new source of aviation biofuel production which is a new finding. This has not been studied earlier.

As an aviation engine was not available, Mandarin aviation biofuel was tested in a lean diesel engine and showed excellent performance and a large reduction in engine emissions. It can achieve reductions of up to 30.0% CO, about 33.5% HC and around 19.2% PM (particulate matter) at full load with variable speed and 33.0% CO, 32.8% HC, 28.5% PM emission

reduction at variable load as compared to ultra – low – sulphur diesel (ULSD) by blending 20% with fossil fuel.

Other biodiesel (Crambe, Tamanu, Borage, Avocado, Bush nut) blends (B5 to B20) were also tested in a four stroke diesel engine to evaluate the performance and emission parameters at different operating and load conditions. The results revealed that Avocado biodiesel shows overall better performance (about 0.50% less BP, 0.83% more BSFC, and 0.18% less BTE as compared to ULSD at full load and rated speed) compared to other fuels. However, Crambe, Borage, and Bush nut also show close performance with Avocado biodiesel. Blending up to 20% of this biodiesel can reduce emissions by up to about 50% CO, 27% HC and 36% PM, however it increases NO_x emission by about 26% compared to ULSD at full load and rated speed. On the other hand, Tamanu biodiesel blends show poor engine performance though emission reduction is comparable with other biodiesels at the same operating conditions.

For further improvement in engine performance and emission reduction this study developed four mixture blends by combining two biodiesels (totalling 5% at different proportions) and paraffin as an additive at 4% with the remaining 91% being ULSD. The mixture blends are described as ManCr_Pa (Mandarin-Crambe_Paraffin), TaMan_Pa (Tamanu-Mandarin_Paraffin), BoMan_Pa (Borage-Mandarin_Paraffin) and AvBn_Pa (Avocado-Bush nut_Paraffin). The mixture blends show improved performance compared to each B5 blend and significantly reduce emissions like B20 blends due to their improved fuel properties. Among these mixture blends, the Avocado-Bush nut and paraffin (AvBn_Pa) ternary mixture demonstrates comparable performance with ULSD. It reduces about 48.0% CO, 30.0% HC, 40.0% PM emissions compared to ULSD. This equates to about 16.0% CO, 8.7% HC and 28.0% PM more reduction of emissions compared to an Avocado B5 blend. This mixture blend produces about 9% less NO_x compared to the B5 blend of Avocado biodiesel. On the other hand, the ManCr_Pa mixture blend reduces about 62% HC emission compared to ULSD with about 12% lower NO_x emission.

The advanced combustion analysis was done on the better performing blends (i.e. for ManCr_Pa and AvBn_Pa mixture blends) to evaluate pollutant formation mechanisms during combustion. The results revealed shorter ignition delay and longer combustion duration for AvBn_Pa. This blend also exhibits higher cylinder pressure and higher heat release rate with a longer duration of the diffusion combustion phase. Additionally, a knocking characteristic was

identified for ManCr_Pa mixture blend. The tribological characteristics such as friction, wear, lubrication stability and metal surface morphology were also evaluated using high-resolution SEM/EDX microscopy to assess energy savings, engine reliability, and impacts on engine life. This study revealed an excellent tribological performance of AvBn_Pa blend compared to ULSD with about 21% less friction coefficient at steady state condition, around 19% less wear scar diameter, higher lubrication film stability, as well as less wear debris and metal corrosion. The study concluded that AvBn_Pa blend is the best mixture blend in all aspects of performance considered, namely emission reduction, improved combustion and tribological behaviour for a sustainable environment as well as sustainable engine health for the transport sector.

The study will provide useful information and guidelines to biofuel stakeholders, the transport sector, engine designers, the aviation industry and policy makers involved with newly developed aviation biofuels and other biodiesel usage in a full-scale diesel engine. It will provide new opportunities to future researchers to develop Mandarin aviation biofuel as a commercial aviation fuel. This research will help engine designers to develop more efficient and sustainable engines and to customise newly developed biodiesels for application in the transport sector.

Declaration of Originality

I hereby declare that the thesis entitled "Experimental investigation of CI engine performance, emissions and combustion using advanced biofuels" is entirely my own effort, idea and knowledge except where otherwise acknowledged. The material contained in this thesis is original and has not been submitted for a degree or certificate elsewhere.

Signature Redacted

Md Abul Kalam Azad

Date: 21/12/2016

Rockhampton, QLD, Australia.

Acknowledgment

I would like to express my deepest gratitude to Almighty ALLAH who has provided the opportunity with good health, patience, and ability to complete such a wonderful research work. I express my utmost gratitude to my principal supervisor Associate Professor Mohammad Rasul for his inspiring guidance, constant support, and encouragement in every step of this study. I also express gratitude to Professor Masud Khan and Dr Subhash Sharma (Associate Supervisors) for their constructive suggestions, skilled guidance, constant encouragement and useful discussions throughout the course of this study.

I am thankful to all of my research colleagues for their inspiration and support from the beginning of this study. My gratitude and special thanks go to Associate Professor Nanjappa Ashwath for his kind assistance and guidance in preparing biofuels in the laboratory. Special thanks to Heather Smyth, Senior Laboratory Supervisor, for her assistance in use of the chemical laboratory. I am also thankful to all technical stuff in the School of Engineering and Technology for their technical assistance. Special thanks go to Patrick O'Grady, Technical Officer of Mechanical Engineering for his kind, friendly and continuous assistance during the experiment on the dyno engine setup located in the thermodynamics laboratory. Special thanks to Mohammad Anwar, Laboratory Supervisor of Mechanical Engineering, for his technical assistance during the experiment on rheometer. I am thankful to Mr. Tim McSweeney, Adjunct Research Fellow, Centre for Railway Engineering, CQUniversity for his kind assistance in English proofreading of this thesis and publications produced from this work.

I am most thankful to Central Queensland University, Australia, for awarding me the Strategic Research Scholarship (SRS) to support this study. I would like to acknowledge the Office of Research Services team for their assistance during this study. Special thanks go to Associate Professor Susan Kinnear, Dean of Graduate Studies, for her kind support of this study. I am also thankful to Leslie Walker, Denise Lentell and Natasha Toon for their assistance and friendly cooperation during the period of this study. Special thanks to Professor Steven Moore, Deputy Dean for Research, School of Engineering and Technology, for his encouragement to publish the findings of this work. Finally, I would like to express gratitude from my heart to my wife Sharmin Sultana for her unbelievable sacrifices, endurance and continuous mental support to complete this study.

List of Publications and Award

The list of publications and award from this study is given below. The publications have been sorted as patent, book chapter, refereed journal and refereed conference from recent years to follows. The author contributions are given together at the end of each type because similar contributions were made by the supervisory panel. Other co-author contributions are specified separately in the particular article as discussed below.

Patent

"***Aviation biofuel from Mandarin peel oil***" by **A. K. Azad**, M. G. Rasul, M.M.K. Khan, Subhash Sharma (In preparation and under internal review)

Statement of Author Contribution:

The patent application for IP protection is under preparation. This patent is mainly based on the incredible findings of this research work. The author (A. K. Azad) has prepared this patent under the supervision of M. G. Rasul, M.M.K. Khan, and Subhash Sharma. The supervisory panel gave feedback on it to improve its quality. They also provided guidance through several meetings and discussion on different aspects of scientific issues.

Book Chapter (Refereed)

1. **A. K. Azad**, M. G. Rasul, M.M.K. Khan, Subhash C. Sharma (2016) "Biodiesel from Queensland bush nut (*Macadamia integrifolia*)", Chapter 13, Page 419-439, the book entitled "*Clean Energy for Sustainable Development*, ELSEVIER, editors: M.G. Rasul, A.K. Azad and Subhash Sharma (DOI: 10.1016/B978-0-12-805423-9.00013-2)

Statement of Author Contribution:

This book has been edited by M.G. Rasul as editor–in–chief, ***A.K. Azad*** *and Subhash Sharma as co–editors with Academic Press (AP), ELSEVIER. Chapter 13 of this book was written on fuel preparation. The author (A.K. Azad) initially prepared the draft of this chapter. M.G. Rasul and M.M.K. Khan contributed to the design of the experimental procedure and gave feedback on the draft in several iterations to improve the quality. Subhash Sharma has contributed to assess the experimental data, and gave feedback and help to address the reviewer comments.*

Refereed Journal Articles

1. **A. K. Azad**, M. G. Rasul, M.M.K. Khan, Subhash C. Sharma, M. Mofigur and M.M.K. Bhuiya, "Prospects, feedstocks and challenges of biodiesel production from beauty leaf oil and castor oil: A nonedible oil sources in Australia", *Renewable and Sustainable Energy Reviews, (2016) 61: 302-318*. (DOI: 10.1016/j.rser.2016.04.013) (**ISI Impact Factor 6.798**)

2. **A. K. Azad**, M. G. Rasul, M.M.K. Khan, Subhash C. Sharma and M.M.K. Bhuiya, "Recent development of biodiesel combustion strategies and modelling for compression ignition engines", *Renewable and Sustainable Energy Reviews, (2016) 56: 1068-1086*. (DOI: 10.1016/j.rser.2015.12.024) (**ISI Impact Factor 6.798**)

3. **A. K. Azad**, M.G. Rasul, M.M.K. Khan, Subhash C. Sharma, M.M.K. Bhuiya, and M. Mofijur, (2016) "A review on socio-economic aspects of sustainable biofuels", International Journal of Global Warming, *(2016) 10(1-3): 32-54* (**ISI Impact Factor 1.043**)

4. **A. K. Azad**, M. G. Rasul, M.M.K. Khan, Subhash C. Sharma and M.A. Hazrat, "Prospect of Biofuels as an Alternative Transport Fuel in Australia", *Renewable and Sustainable Energy Reviews, (2015) 43: 331-351*. (DOI: 10.1016/j.rser.2014.11.047) (**ISI Impact Factor 6.798**)

5. **A. K. Azad**, M. G. Rasul, M.M.K. Khan, Subhash C. Sharma and M.M.K. Bhuiya, "Study on Australian energy policy, socio-economic, and environment issues", *Journal of Renewable and Sustainable Energy, (2015) 7: 063131-(1-20).* (DOI: http://dx.doi.org/10.1063/1.4938227) (**ISI Impact Factor 0.961**)

6. **A. K. Azad**, M. G. Rasul, Brady Giannangelo "Comparative study of diesel engine performance and emission with soybean and waste oil biodiesel fuels", *International Journal of Automotive and Mechanical Engineering, (2015) 12: 2866-2881*. (DOI: 10.15282/ijame.12.2015.6.0241)

7. **A. K. Azad,** M. G. Rasul, M.M.K. Khan, T. Ahasan, S.F. Ahmed, "Energy scenario: Production, consumption and prospect of renewable energy in Australia", *Journal of Power and Energy Engineering, (2014) 2(4): 19-25*. (DOI: 10.4236/jpee.2014.24004)

Articles in Preparation

8. **A. K. Azad**, M. G. Rasul, M.M.K. Khan and Subhash C. Sharma, "Experimental investigation of diesel engine performance and emissions analysis using Tamanu and Borage biodiesel", *Applied Energy* (**ISI Impact Factor 5.746**)
9. **A. K. Azad**, M. G. Rasul, M.M.K. Khan and Subhash C. Sharma, "Combustion analysis of advanced biofuel in CI engine at full load condition", *Applied Energy* (**ISI Impact Factor 5.746**)
10. **A. K. Azad**, M. G. Rasul, M.M.K. Khan and Subhash C. Sharma, "Investigation of tribological behaviour of ternary mixture blends to assess diesel engine health", *Energy Conversion and Management* (**ISI Impact Factor 4.801**)
11. **A. K. Azad**, M. G. Rasul, M.M.K. Khan and Subhash C. Sharma, "Assessment of Avocado and Bush nut biodiesel performance and emissions at variable load condition", *Applied Thermal Engineering* (**ISI Impact Factor 3.043**)

Statement of Author Contribution:

The author (A.K. Azad) discussed with his supervisory team (M.G. Rasul, M.M.K. Khan, Subhash Sharma) regarding different issues of the extensive literature review of this thesis which was published in various referred journals (as mentioned above). They guided him in the right direction to identify research gaps from this review. Azad initially prepared the draft of these manuscripts. M.G. Rasul provided feedback on overall content, organisation and presentation of these manuscripts. M.M.K. Khan and Subhash Sharma provided their feedback on revised manuscripts and instructed on how to improve the quality of those papers. The supervisory team reviewed the revised manuscripts and helped to address reviewers' comments before publication.

Other co-authors such as M.M.K. Bhuiya (article 1, 2, 3 and 5), M. Mofijur (article 1, and 3), M.A. Hazrat (article 4), S.F. Ahmed (article 7) and T. Ahasan (article 7), contributed to collect data from the literature, analyse these data, and assess to prepare the initial draft of those manuscript. They also helped in formatting and revision of these articles. Co–author Brady Giannangelo (article 6) contributed in experimental work and data analysis. All the co-authors' contributions facilitated these articles being published in the above mentioned refereed journals.

Refereed Conference Papers

1. **A. K. Azad,** Mohammad Rasul, Masud Khan, Subhash Sharma, "Macadamia biodiesel as a sustainable and alternative transport fuel in Australia", Energy Procedia, (2017) (**In press**)
2. **A.K. Azad,** M.G. Rasul, M.M.K. Bhuiya and Rubayat Islam, "Effect of first and second generation biodiesel blends on engine performance and emission", AIP Conference Procedia, (2016), 1754:050031 (1-6). (DOI: 10.1063/1.4958422)
3. **A.K. Azad**, M.G. Rasul, M.M.K. Khan, Subhash C. Sharma and Rubayat Islam, "Prospect of Moringa seed oil as a sustainable biodiesel fuel in Australia: A review" Procedia Engineering, (2015); 105: 601-606 (DOI: 10.1016/j.proeng.2015.05.037).
4. **A. K. Azad**, M. G. Rasul, B. Glannangelo and S.F. Ahmed, "Diesel engine performance and emission study using soybean biodiesel blends with fossil diesel" 7th International Exergy, Energy and Environment Symposium, April 27-30, (2015), Valenciennes, France.
5. **A. K. Azad**, M. G. Rasul, M.M.K. Khan, Anis Omri, M.M.K. Bhuiya, M. A. Hazrat, "Modelling of renewable energy economy in Australia", *Energy Procedia*, (2014), 61: 1902-1906. (DOI: 10.1016/j.egypro.2014.12.238)
6. **A. K. Azad**, M. G. Rasul, M.M.K. Khan and Subhash C. Sharma, "Review of non-edible biofuel resources in Australia for second generation (2G) biofuel conversion", International Green Energy Conference, Tainjin, China, (2014), Pages: 867-878.
7. **A. K. Azad**, M. G. Rasul, M.M.K. Khan and Subhash C. Sharma, "Review of biodiesel production from microalgae: A novel source of green energy", International Green Energy Conference, Tainjin, China, (2014). Page 879-888.
8. **A. K. Azad**, M. G. Rasul, M.M.K. Khan and Subhash C. Sharma, "Socio-economic prospect of second generation bio-fuel in Australia: A Review", *International Conference on Clean Energy*, Turkey, (2014), pp. 210-221.

Statement of Author Contribution:

The author (A.K. Azad) discussed the methodology, experimental plan, and data measurements in fortnightly meetings with his supervisory team (M.G. Rasul, M.M.K. Khan, Subhash Sharma). They guided him in the right direction to perform the experiments using standard procedures. Azad initially prepared drafts for the above mentioned conferences on the

experiments (paper 1, 2 and 4), economic analysis (paper 5) and relevant literature reviews (paper 3, 6, 7 and 8) related to this thesis. M.G. Rasul provided feedback on overall content, organisation and presentation of these papers in several iterations. M.M.K. Khan and Subhash Sharma provided their feedback on revised papers. The supervisory team also contributed in addressing reviewers' comments.

Co–author Anis Omri assessed simulation data on energy economy for modelling (paper 5). Co-authors M.M.K. Bhuiya (paper 5), M.A. Hazrat (paper 5), Rubayat Islam (paper 2 and 3), B. Glannangelo (paper 4) and S.F. Ahmed (paper 4) contributed in data analysis and helped in preparing the initial draft of those papers. They also assisted in formatting and revision of these articles. Co–authors Rubayat Islam (paper 2 and 3) and S.F. Ahmed (paper 4) also contributed through oral presentation of these papers in the conferences. All the co-authors' contribution improved the quality of these papers for publication in the above mentioned refereed conferences.

Awards:

A. K. Azad was awarded the **First Prize** of **$2000.00** for his research excellence and presentation on the topic of "*Biodiesel: A sustainable and alternative transport fuel in Australia*" in the School of Engineering and Technology RHD Symposium, 2nd to 3rd November' 2016, Rockhampton, Australia.

Table of Contents

List of Figures

List of Tables

List of Abbreviations and Acronyms

ABG	Aviation Bio-Gasoline
AES	Australian Energy Statistic
ANN	Artificial Neural Network
ASTM	American Society of Testing Materials
AV	Acid Value
Av	Avocado
AvBn_Pa	(3% Avocado + 2% Bush nut + 4% Paraffin) ternary mixture + 91% ULSD
BPC	British Petroleum Corporation
BoM	Bureau of Meteorology
BSC	Biofuel Supply Chain
Bo	Borage
Bn	Bush Nut or Macadamia
BP	Brake Power
BT	Brake Torque
BSFC	Brake Specific Fuel Consumption
BTE	Brake Thermal Efficiency
BMEP	Brake Mean Effective Pressure
B5	5% biodiesel + 95% ULSD by volume
B10	10% biodiesel + 90% ULSD by volume
B15	15% biodiesel + 85% ULSD by volume
B20	20% biodiesel + 80% ULSD by volume
BoMan_Pa	(3% Borage + 2% Mandarin + 4% Paraffin) ternary mixture + 91% ULSD
BDC	Bottom Dead Centre
CSIRO	Commonwealth Science and Industrial Research Organisation
CV	Calorific Value
CN	Cetane Number
CCL	Carbon Chain Length
CFPP	Cold Filter Plugging Point
Cr	Crambe
CI	Compression Ignition
CO	Carbon Monoxide Emission
CO_2	Carbon Dioxide Emission
CP	Cylinder Pressure
CD	Combustion Duration
CA	Crank Angle
DoE	Department of Environment
DU	Degree of Unsaturation
DI	Direct Injection

EN	European Standard
EGT	Exhaust Gas Temperature
EGA	Exhaust Gas Analyser
FAME	Fatty Acid Methyl Esters
FP	Flash Point
FT	Friction Torque
FTP	Flash Temperature Parameter
FC	Friction Coefficient
GHG	Greenhouse Gas
GC	Gas Chromatography
HC	Hydrocarbons Emission
HRR	Heat Release Rate
ID	Ignition Delay
ISO	International Organization for Standardization
IEO	International Energy Outlook
Man	Mandarin / Citrus
ManCr_Pa	(3% Mandarin + 2% Crambe + 4% Paraffin) ternary mixture + 91% ULSD
Man_B5	5% Mandarin biodiesel + 95% ULSD by volume
NO_x	Nitrogen Oxides Emission
NDIR	Non-Dispersive Infrared
OH	Hydroxyl
PM	Particulate Matter Emission
REN21	Renewable Energy Policy Network for the 21st Century
R&D	Research and Development
SN	Saponification Number
SI	Spark Ignition
SOI	Start of Injection
SOC	Start of Combustion
SEM/EDX	Scanning Electron Microscope / Energy Dispersive X-Ray
Ta	Tamanu
TaMan_Pa	(3% Ta + 2% Man + 4% Paraffin) ternary mixture + 91% ULSD
TDC	Top Dead Centre
USEPA	United States Environmental Protection Agency
ULSD	Ultra-low Sulphur Diesel
WSD	Wear Scar Diameter

Nomenclature

A	Area of the cylinder in mm^2
A_i	Percentage of each fatty acid component
C	Fatty acid methyl ester content in %
D	Cylinder bore in mm
D_b	Number of double bonds presence in the carbon chain
d	Wear scar diameter in mm
HV_{output}	Heating value of the output products in MJ/kg
HV_{input}	Heating value of the input products in MJ/kg
l	Connecting rod length in mm
$M_{Biodiesel}$	Mass of purified methyl esters in g
M_{Oil}	Mass of crude vegetable oil used in g
MW_i	Molecular mass of each component by FAMEs
P	Cylinder pressure in Pa (N. m)
r	Crank radius in mm
r_c	Distance from the centre of the lower ball contact surface to the axis of rotation in mm
T	Friction torque in kg-mm
V	Cylinder volume in m^3
V_c	Clearance volume in mm^3
W	Applied load in kg
W_{input}	Mass of input feedstock in kg
W_{output}	Mass of output biodiesel in kg
θ	Crank angle in °CA
$\frac{dQ}{d\theta}$	Heat release rate in J/°CA
γ	Specific heat constant = 1.35
μ	Friction coefficient

Chapter 1

INTRODUCTION

This chapter introduces the general background of this study and the importance of potential aviation biofuel and biodiesels in the transport sector. It also presents the significance of the study, aims, and objectives based on the key research questions as well as the scope and limitations of this study. The chapter gives an overview of this research and briefly outlines the structure of the thesis at the end.

1.1. Background

The world's total energy demand has increased at the rate of 1.52% per year (IEO, 2016a) which is faster than the total population growth of 1.14% per year (World Bank, 2016). This increase attributed to the development of modern civilisation, improvements of lifestyle, dependency on more electronic devices, the significant increase in the usage of automobiles, increasing industrialisation and recent commercial development particularly in developing countries. Figure 1.1 illustrates the history and projection of world total population growth and total energy consumption. The world total energy consumption will increase about 56% between 2010 and 2040 as projected by the International Energy Outlook (IEO, 2016a). The total energy consumption includes liquid fuel, coal, natural gas, and nuclear energy. Figure 1.2 shows the world's total energy consumption by various sources. The highest consumption of liquid fuels was recorded at about 33% of total energy consumption in 2015 which is one of the main concerns with regard to energy security, environmental sustainability and higher oil prices in the near future (IEO, 2016a). Liquid fuel consumption is increasing at the rate of about 2.10% per year and is mainly consumed by the transport sector (IEO, 2016a). This sector accounts for about 28% of global energy consumption since 2000 (REN21, 2016). For example, the transport sector (including aviation, road, rail, and marine) consumed about 25% of total world energy in 2012 is expected to increase at the rate of 1.4% per year from 2012 to 2040 as projected by IEO (2016a). This increasing energy demand in the transport sector could be met by low-emitting, renewable, and liquid eco-fuel (such as biofuels) as an alternative transport fuel in this sector. Renewables 2016 Global Status Report revealed that biofuels met about 4% of global transport energy demand in 2015 (REN21, 2016). The transport sector

involves around 67% in road transport, 23% shipping, 4% rail and the remainder in aviation transport worldwide (REN21, 2016). The biofuel usage includes biodiesel for road, rail and marine, and bioethanol for light passenger vehicles.

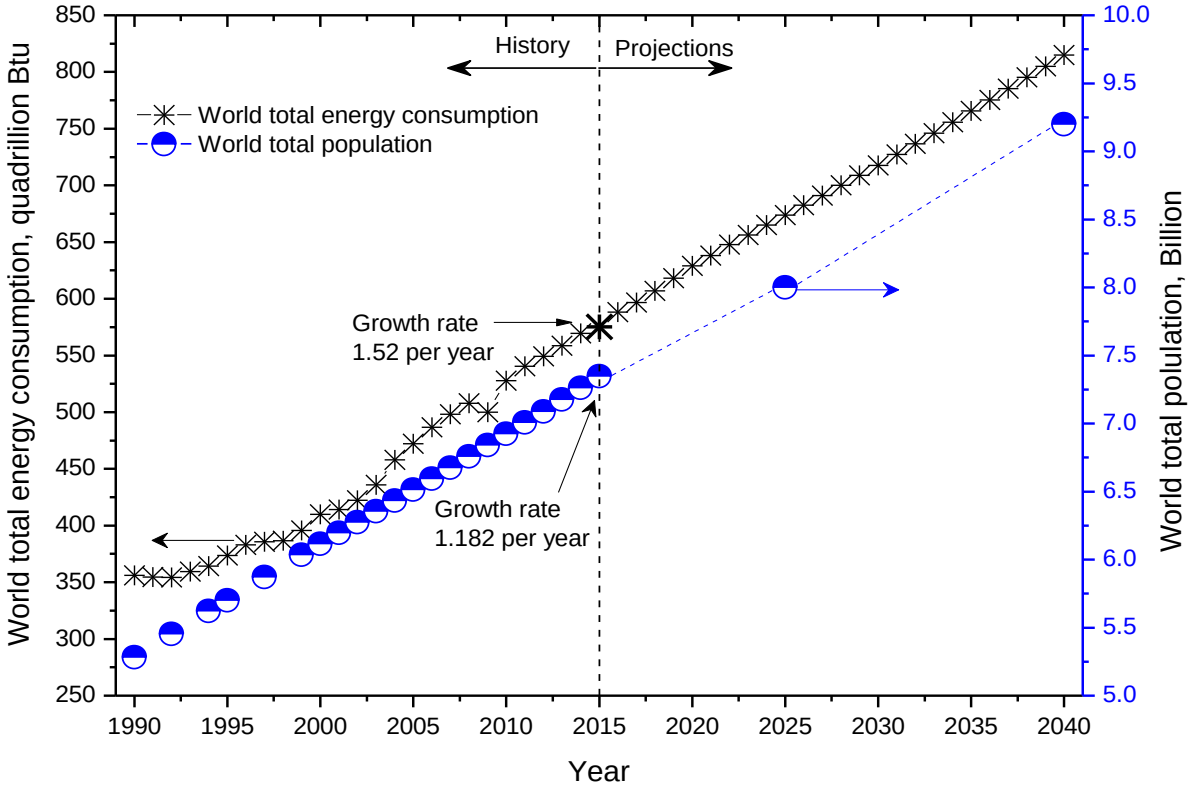

Figure 1.1: World total energy consumption and total population growth

Source: International Energy Outlook (IEO, 2016a) and (World Bank, 2016)

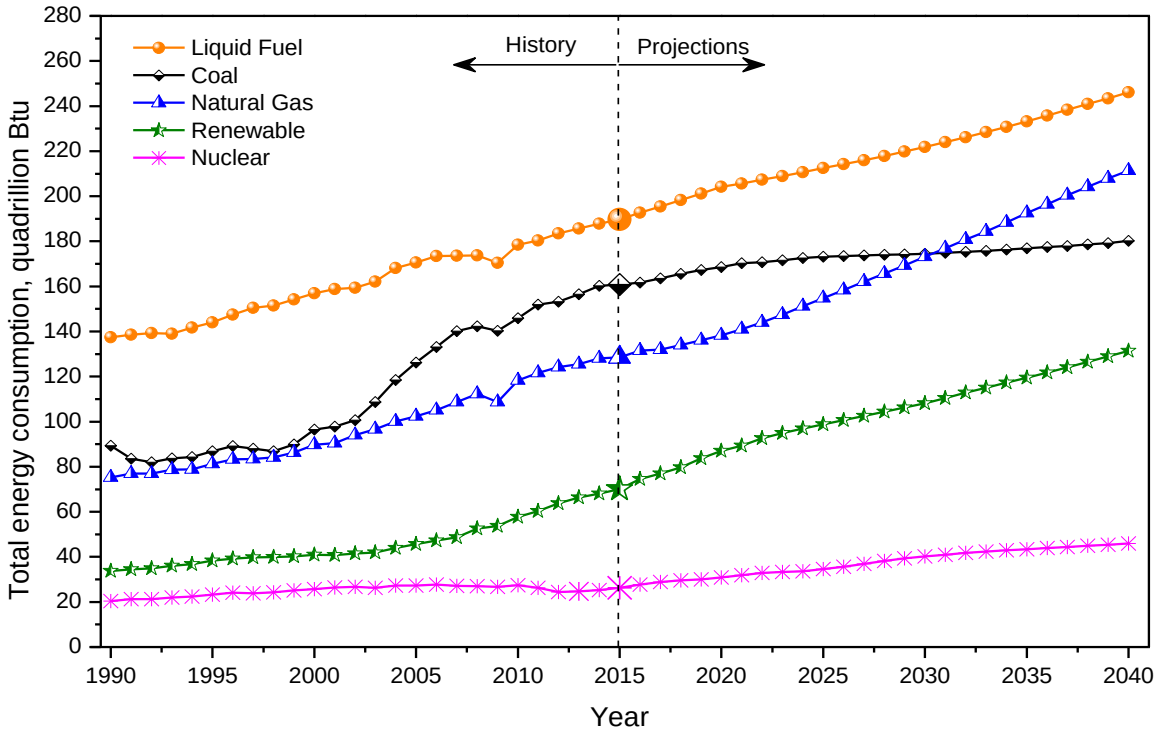

Figure 1.2: World total energy consumption by energy sources (IEO, 2016a)

In recent years, biofuel created new markets including its usage in the aviation sector as aviation biofuel (REN21, 2016). The aviation sector consumes about 10% of total global energy which is responsible for 2% of total CO_2 emissions worldwide as reported by Chiaramonti et al. (2014). The United States Environmental Protection Agency (USEPA) revealed that about 14% of total global greenhouse gas (GHG) emissions were recorded in 2010 due to the usage of petroleum fuels in road, rail, air and marine transport (EPA, 2016). In recent years, aviation biofuel and biodiesel have become more attractive because of their excellent capability to mitigate adverse environmental effects and future energy security concerns by replacing some energy produced from fossil fuels (Demirbas, 2007).

Figure 1.3 illustrates the world's total biofuels production from 2005 to 2015 (bar graph) and total production by region (line graphs) which show an increasing trend. In addition, liquid biofuel production industries created around 1678 direct and indirect jobs worldwide (REN21, 2016). According to British Petroleum Corporation (BPC), the world's total biofuels production increased about 0.9% in 2015 due to an increase in bio-ethanol production (BP, 2016). Figure 1.3 shows that the North America (primarily the United States) region produced the highest volumes of biofuels in the world. They replaced 30% of their total energy consumption with biofuels. The South and Central America produced the second largest biofuel

and Brazil was the major contributor. They met about 23% of their transport energy demand with biofuels from 2009 (Azad et al., 2015c). The Middle East and African countries are only at the beginning of biofuel production at this stage. In the Asia Pacific region, China produces the largest quantity of biofuels whereas Australia started biofuel production in 2004 and has been increasing its production rate in recent years. Therefore, a detailed study on biofuel production and usage is most relevant and important.

Australia is the 19th largest energy consumer on a per capita basis and ranks as the 17th prime non-renewable energy consumer in the world (Azad et al., 2015c). Australia has abundant energy resources including one-third of the world's total uranium resources, one-tenth of black coal resources, and about 2% of total natural gas resources (Pham et al., 2016). Australia makes a significant contribution as the 9th largest energy producer in the world (Azad et al., 2014a). Australian Energy Statistic (AES) revealed that Australia's energy consumption was sourced from about 32.2% coal, 37.8% oil, 24.2% gas and 5.8% renewable energy in 2015 (AES, 2016). The detailed energy scenario is discussed in the literature review in Chapter 2. The highest share of liquid oil is primarily consumed by the road transport, mining and manufacturing sectors in Australia. Among those, the transport sector consumed about 27.20% of total energy consumption in 2015 (AES, 2016). Ball et al. (2016) reported that the consumption of energy by this sector has increased by about 1.70% per year in recent decades. Australia's Department of Environment (DoE) revealed that transport sector GHG emissions increased about 24% between 1999-2000 and 2013-2014 (DoE, 2015). So this sector is energy and emissions intensive in Australia as well as all over the world. The use of biofuels can reduce the emissions and that is why the Australian Government took the initiative and set mandatory targets of about 5% to 10% biofuel in different states in recent years. In 2015, Australia produced about 130 million litres of biofuel (including bioethanol and biodiesel) and imported 159 million litres to make up its 289 million litres of total biofuel consumption.

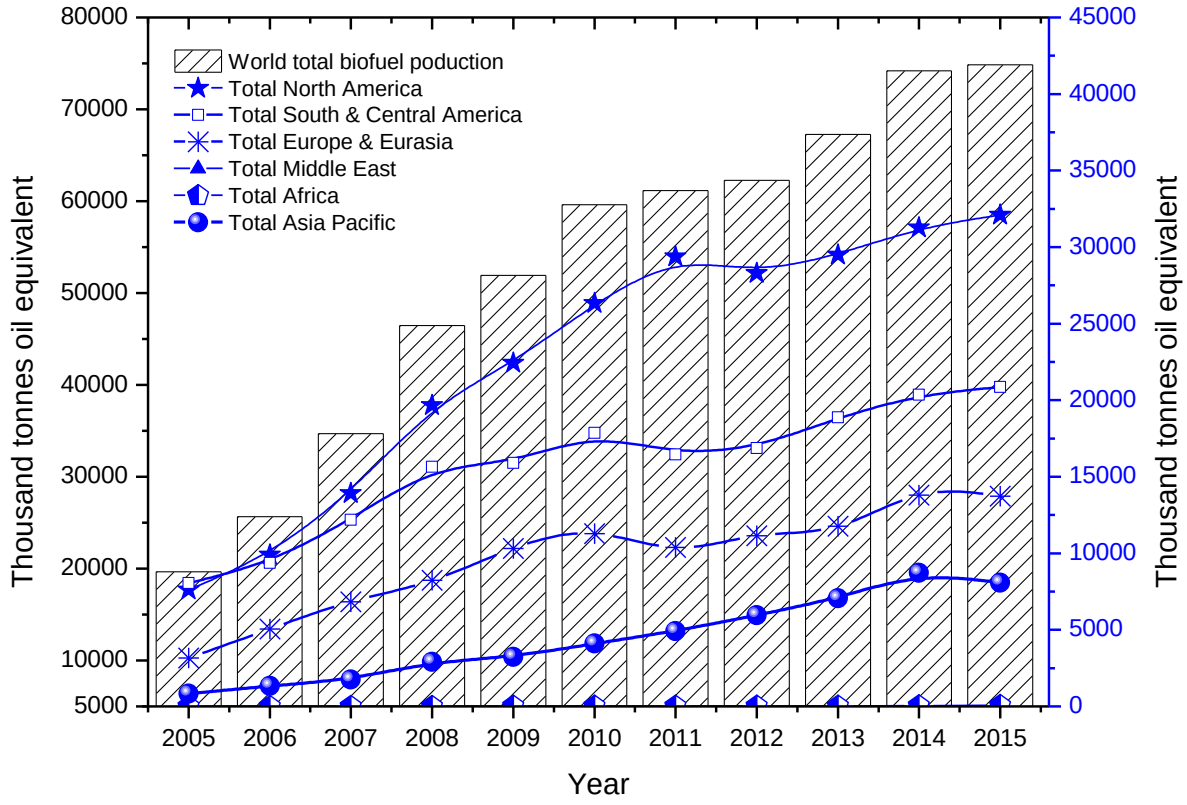

Figure 1.3: The world total biofuels production and the production by regions (BP, 2016)

Advanced biofuels have also created a new market in the aviation sector in recent years. A study made by the Commonwealth Science and Industrial Research Organisation (CSIRO) in 2011 supported by major aviation companies identified that a 20% GHG emission reduction is possible by using aviation biofuels (Farrell, 2016). As a result, Qantas first experimentally operated a flight from Sydney to Adelaide with a 50% biofuel blend with commercial jet fuel. Now Australia and New Zealand are expecting use of about 5% by 2020 to 40% by 2050 of bio-derived aviation fuel from various feedstocks (Farrell, 2016). Hence aviation biofuel and biodiesel produced from different feedstocks have a good prospect in the energy market in Australia as well as throughout the world. This study focuses on the investigation of these biofuels and related issues.

The key points of the background to this study are shown in Figure 1.4. In summary, liquid fuel consumption is increasing day-by-day all over the world which is depleting total oil reserves as well as the future fuel security. The fuel price has also been increasing over the last few decades in a long term comparison. However, the oil price has been quite stable in recent years. The largest share of liquid fuel is mainly consumed by the fast growing transport sector

(including aviation, road transport etc.) around the world. The huge consumption of liquid fuel by the transport sector creates serious environmental pollution. One of the key tools to tackle this situation is alternative fuel for the transport sector which is renewable, biodegradable and low pollutant emitting. It follows that the use of aviation biofuel and biodiesel could be one of the promising solutions for future energy security and environmental sustainability.

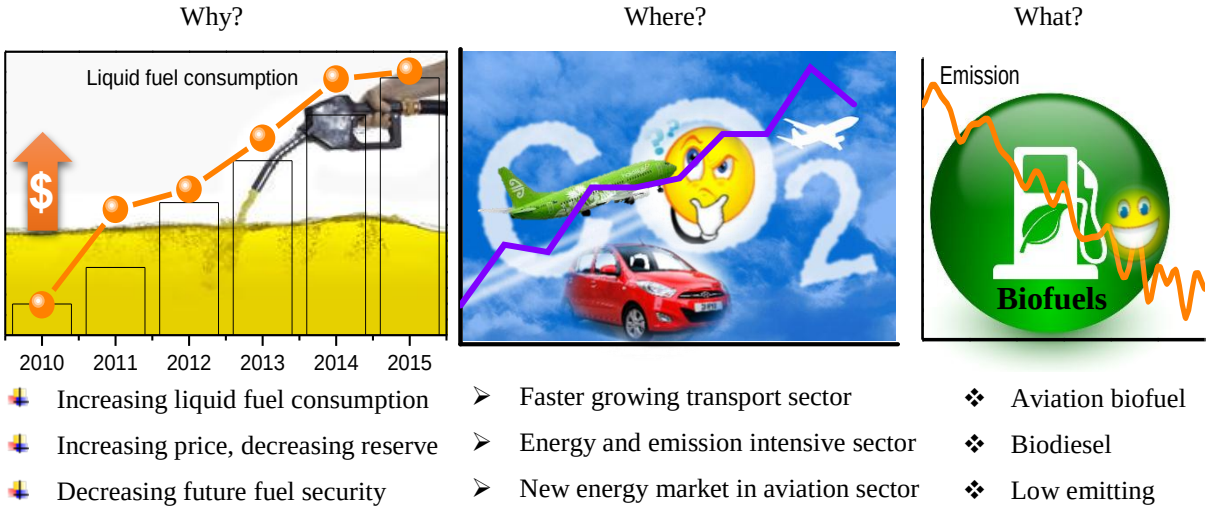

Figure 1.4: Key points of background study

1.2. Is Biofuel a Possible Solution for Future Energy Security and Environmental Sustainability?

Biofuels are renewable eco-fuel produced from biological resources such as vegetable oil, animal fat or green wastes which are mainly composed of fatty acid methyl esters and fulfil the requirements of the ASTM D6751 biodiesel standard (Sarin et al., 2010b, Azad et al., 2015c). In other words, biofuels are liquid fuels which can be extracted from lignocellulosic biomass and waste including animal fats. The biofuels are of different types that include bioethanol (Rosegrant et al., 2008), renewable methanol (Cifre and Badr, 2007), aviation biogasoline (Chiaramonti et al., 2014), biodiesel (Stevens and Verhé, 2004), biogas (Blanca and Juan, 2008), biobutanol (Blanca and Juan, 2008) and biohydrogen (Cherubini et al., 2009). These fuels can replace and serve as alternatives to fossil fuels. There are some excellent benefits in using biofuels because they are non-toxic, biodegradable, low emission, safer and environmentally acceptable fuels (Demirbas, 2011b). In addition, environmental carbon can be recycled through plants from which it can be extracted as fuel to produce energy. It can also be described as carbon recycling renewable energy. Figure 1.5 illustrates the lifecycle of biofuels showing different steps for carbon recycling.

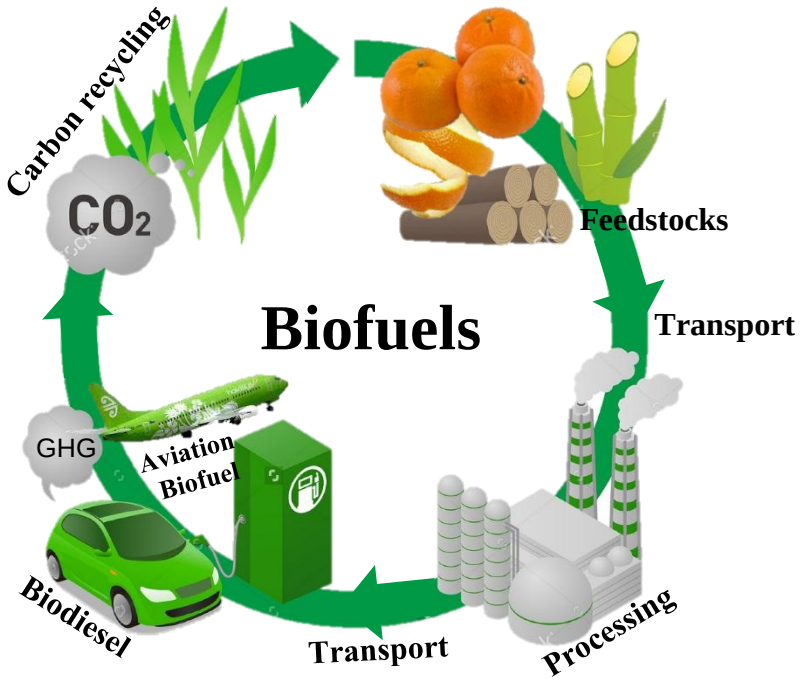

Figure 1.5: Biofuels lifecycle for feedstocks regrown as environmental carbon recyclers

As shown in Figure 1.5 the biofuels lifecycle involves steps such as feedstock preparation, processing, transportation and usage in the transport sector including the aviation sector. Compared to fossil fuels, the use of biofuels produces lower GHG emissions which can also be recycled by re-growing the feedstock plants. The summation of carbon emissions from cultivation machines, processing equipment, transportation, and combustion is almost equivalent to the amount extracted by the feedstock plants from the environment as they re-grow. For this reason, biofuels are also called carbon neutral, renewable eco-fuel. There are some other benefits in using of biofuels, namely that it is a sulphur free fuel and it can reduce GHG emissions by up to 60% compared to fossil fuel as reported by Hoekman and Robbins (2012) and Mofijur et al. (2016a). Another benefit of using biofuels from 2G feedstocks is to remove pressure from food and land usage as discussed by Azad et al. (2016b). Therefore, biofuels have strong sense of balancing between agriculture, environment and economic development as reported by Demirbas (2007) and Meher et al. (2006).

1.3. Search for Biofuel Feedstocks in this Study

Biofuel feedstocks are broadly categorised as edible or first generation (1G) (Naik et al., 2010), non-edible or second generation (2G) (Naik et al., 2010) and microorganism or third generation (3G) (Lee and Lavoie, 2013). Some examples are given here for each category. This study is

mainly focused on the prospect of aviation biofuel and biodiesel feedstocks from available sources considering a broad range of technical issues.

Edible sources or 1G biofuels are produced from edible biomass such as food crops and vegetable oils as reported by Lee and Lavoie (2013). Food crops include wheat, barley, rice, whey, and sugar beets etc. which are marginally used in biofuel production (Karmakar et al., 2010). Vegetable oil feedstocks for biodiesel production include soybean oil (Azad et al., 2015b), sunflower oil (Hoekman et al., 2012), olive oil (Demirbas, 2005), palm oil (Sarin et al., 2009a), coconut oil (Demirbas, 2005), and rapeseed oil (Saka and Kusdiana, 2001). In addition, corn waste and sugarcane are widely used feedstocks for bio-ethanol production.

Non-edible sources or 2G biofuels can be produced from a wide array of feedstocks such as non-food crops, animal fats and lignocellulosic solid waste (Lee and Lavoie, 2013, Demirbas, 2009b). The non-edible oil seed includes jatropha curcas (Sarin et al., 2010b), *pongamia glabra* (Sarin et al., 2009a), castor oil (Meneghetti et al., 2006), beauty-leaf oil (Bhuiya et al., 2015d), and animal fats like beef tallow (Tashtoush et al., 2004). The non-edible feedstocks can overcome the main economic, social and environmental challenges of 1G biofuel feedstocks without creating any pressure on land use and hindering the food supply since it is non-edible and can grow on marginal land.

The microorganism or 3G biofuels are mainly produced from microalgae biomass which has some remarkable advantages such as self-productivity, fast growing, require less water and can grow in undeveloped land (Lee and Lavoie, 2013). However, the key factor to extracting biofuel is the lipid content. For instance, Scott et al. (2010) investigated *Chlorella protothecoides, Chlorella vulgaris, Dunaliella salina, Chamydomonas reinhardtii* etc. species and found about 60% to 70% lipid content in them. Chen et al. (2011) reported higher productivity of lipid in *Chlorella vulgaris* of about 7.4 g/l/day. This feedstock can also be used to produce bioethanol, jet fuel or aviation biogasoline (Demirbas, 2011c). In addition, some authors also studied other 2G feedstocks such as pongamia, sugarcane molasses, waste cooking oil, jatropha, camelina, and tallow, for aviation biofuel production (Chiaramonti et al., 2014, Cox et al., 2014).

This study investigated around 150 prospective species aiming for aviation biofuel and biodiesel production as shown in Figure 1.6 and identified six most prospective feedstocks from the green waste and oil seeds for producing aviation biofuel and biodiesel as presented in Figure 1.7.

Figure 1.6: Total studied biofuel feedstocks for aviation biofuel and biodiesel production

Mandarin rind waste

Crambe

Tamanu

Borage

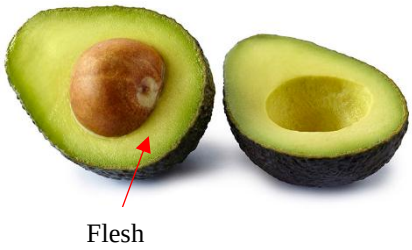

Waste Avocado flesh

Bush nut

Figure 1.7: Selected feedstocks for aviation biofuel and biodiesel production in this study

The selected species for aviation biofuel and biodiesel production are Mandarin peel or rind waste, Crambe oil seed, Tamanu oil seed, Borage oil seed, waste Avocado flesh, and Bush nut oil seeds. These feedstocks were selected based on their higher oil yield, availability, sustainability and FAMEs composition as well as excellent fuel properties. This study mainly focuses on these selected feedstocks for detailed analysis as a prospective biofuel feedstock.

1.4. Significance of the Study

There has been an ongoing interest in both the road and aviation transport sector in developing new and alternative fuels for future energy security and sustainable environment. For instance, the aviation industries are struggling to find new and sustainable feedstocks for alternative aviation fuels because this fuel accounts for about 30% of their operating cost worldwide (Farrell, 2016). The aviation sector accounts for about 10% of global liquid fuel consumption and 2% of the world's total CO_2 emissions (Chiaramonti et al., 2014). The use of alternate aviation fuels can optimise costs and reduce environmental pollution. Biodiesel can be used by blending up to 20% with fossil fuel in the modern engine which can reduce GHG emissions from the transport sector by up to 60% as discussed above (Mofijur et al., 2016b).

The proposed research aims to assess new, sustainable and technically viable advanced aviation biofuels and biodiesels for reducing emissions because Australian renewable energy resources are largely undeveloped. As mentioned earlier, this study investigated six prospective feedstocks for producing aviation biofuel and biodiesel from Australian native species. The commercial applications of these biofuels could create a new economic direction by creating new energy markets (such as aviation biofuel) and trading biodiesels which can create future energy security by reducing dependency on fossil fuels. This study is significant because:

- the biofuel industries will get new feedstock information for increasing their production and fuel quality,
- the transport sector, including the aviation sector, will get more improved biofuels to meet their demands and reduce operating and maintenance costs,
- the engine designers will get novel guidelines to develop more efficient engines with sustainable engine health (including less friction and wear, increased durability with longer engine life) which will help to customise newly developed aviation fuels and more biodiesel applications in transport vehicles.

1.5. Research Strategies and Gaps

Sustainability of biofuel applications depends on some key parameters such as availability of feedstocks, oil yield, conversion process, fuel properties, and capability for emissions reduction. Application of pure biofuel in engine requires modification of the engine combustion system which may cause some technical problems such as higher specific fuel consumption, higher NO_x emission, lower thermal efficiency, heavy gum and wax formation (Murillo et al.,

2007, Bozbas, 2008). However, it can be used for blending with fossil fuel up to 20% without any modification of the combustion system (Tan et al., 2012). As an oxygenated fuel (general formula -CHO-), biofuels have excellent capability for emissions reductions compared to fossil fuel (-CH-). This self-oxygenation in the biofuels enhances combustion quality which promotes complete combustion. The improvement of the main fuel properties (such as density, viscosity, calorific value) can also play an important role in complete combustion by overcoming the major drawbacks. Different combustion strategies such as alteration of fuels, alteration of combustion processes and after-treatment of the exhaust gas can be used to reduce emissions. The alteration of the combustion process (i.e. low-temperature combustion) and after-treatment of the exhaust gas involves a lot of investment and modification of engine systems which is still not economically viable.

This study aims to achieve the goal of maximum possible emissions reduction without any modification of the modern engine using the alteration of fuel strategy. The study selected the following key parameters to achieve this goal:

a) Identification of more oxygenated biofuels (about 10% to 12% more self-oxygen),
b) Development of ternary blends by mixing two biodiesels with a low viscous high heating value additive by considering three fuel properties (density, viscosity, and calorific value) which directly impact combustion,
c) Maintaining the blend density as low as possible,
d) Maintaining the fuel viscosity as low as possible,
e) Maintaining calorific value of the blend fuel as close to fossil fuel as possible.

Considering the above mentioned parameters, an extensive literature review on feedstock searching, fuel processing, combustion and emissions analysis etc. has been conducted to identify research gaps which is presented in Chapter 2. Based on the literature review, the following research gaps have been identified:

a) A limited number of studies are available on aviation biofuel from green waste. This study identified Mandarin juice factory waste (i.e. Mandarin peel or rind waste) as a prospective source of aviation biofuel. To the best knowledge of the author, so far no study has been conducted to produce aviation biofuel from this green waste. This study has filled this gap by investigating performance, emissions, combustion, and tribological (friction, wear, corrosion and lubrication) behaviour of this new aviation fuel.

b) No study has been found on engine performance, emissions, combustion and tribological characteristics of Borage and Avocado biodiesels at variable speed and load condition. This review also revealed that very limited research is available on the above-mentioned behaviour of the Crambe and Bush nut biodiesel and its blends at variable load condition. So far no study has been found that has developed a ternary mixture blend of low performing Tamanu biodiesel with aviation biofuel which can be compatible with other blends in a CI engine.
c) No study has been found on ternary mixture blends prepared from two biodiesels (from these selected feedstocks) and an additive to enhance combustion efficiency by improving the properties of the fuel mixture.
d) No study has been found on tribological characteristics such as friction, wear, and metal surface morphology via SEM/EDX microscopy on these selected biodiesel blends and their mixture blends.

This study aims to address the above-mentioned research gaps.

1.6. Research Questions

The key research questions that will be addressed in this study are as follows:

a) What are the prospective aviation biofuel and biodiesel feedstocks?
b) What are the best bio-quality (i.e. higher calorific value) and oxygenated fuels?
c) What are the key factors involved in engine performance and emissions of the new fuels?
d) How do these fuels perform and how much can emissions be reduced?
e) What are the most appropriate combustion strategies for proper combustion?
f) How do the newly developed fuels behave with regard to engine tribology?

1.7. Aim and Objectives of the Research

The main aim of this study is to investigate the prospect of the application of these newly developed biofuels in a CI engine without any modification of engine design and with a specific focus on improving combustion efficiency to enhance engine performance and reduce emissions. The tribological behaviour of the best performing fuel is also evaluated to assess engine health, durability and engine life expectancy. The specific objectives of the study are to:

- Obtain aviation biofuel and biodiesel from the selected feedstocks by an efficient process.
- Evaluate the FAMEs composition and physio-chemical properties of the extracted fuels and compare them with those of fossil fuels.
- Determine engine performance (BP, BSFC, and BTE) and emissions (CO, CO_2, HC, PM, NO_x) at varying speed and load using different blends.
- Analyse combustion phenomena by evaluating cylinder pressure, HRR, ignition delay and combustion duration for better performing fuel blends.
- Evaluate tribological behaviour of the fuel by analysing friction, wear scar diameter and FTP to assess sustainability of the lubrication behaviour of the fuel.
- Analyse metal surface morphology to evaluate corrosive characteristics by SEM/EDX.

1.8. Scopes and Limitations

The study investigated engine performance, emission, combustion and tribological characteristics of the aviation biofuel and biodiesel produced from selected feedstocks. The study initially evaluated 150 feedstocks and selected the six most prospective feedstocks for aviation biofuel and biodiesel production. Then oil extraction and biodiesel conversion were carried out from the selected feedstocks. The fatty acid compositions were identified by gas chromatography tests for the extracted biofuels, and the physio-chemical fuel properties were measured to compare with commercial jet fuel and Ultra-Low Sulfur Diesel (ULSD). The behaviour of the fuels at different temperatures were evaluated. The blends were prepared by adding 5% to 20% by volume of biodiesel into ULSD. The study developed several ternary mixture blends by mixing two biodiesels totalling 5% with 4% paraffin as an additive to achieve a calorific value close to diesel but with lower density and viscosity than diesel.

The fuels were tested in a 4-cylinder, 4-stroke DI diesel engine at variable engine speed and load conditions for each blend. The engine performance parameters such as BP, BT, BSFC, BTE, and emission parameters including CO, λ, CO_2, HC, PM and NO_x and EGT were examined for each operating condition. The combustion analysis was conducted on the better performing fuel blends by quantifying the combustion parameters such as CP, HRR, ID, and CD at different engine speeds and load conditions. The tribological behaviour of the better performing fuel blends was evaluated by determining the friction coefficient and wear scar diameter using the ASTM D4172 standard. Then the metal surface morphology of tested balls

was obtained by a scanning electron microscope (SEM) with energy dispersive X-ray (EDX) analysis. The images from the SEM/EDX test were analysed to determine the wear on the metal surface showing the corrosive behaviour of the tested fuels.

This study has identified that the aviation biofuel from Mandarin peel waste contains about 92 to 97% gasoline range hydrocarbon. The fuel properties of this aviation biofuel were well matched with the commercial jet fuels. However, the octane rating was not determined for this fuel due to the unavailability of an octane analyser. Further, the newly developed aviation biofuel has not been tested in an aviation engine due to non-availability of aviation engine test facilities. Therefore, the aviation biofuel was tested in a CI engine by blending up to 20% with ULSD to predict fuel performance and emissions. The CI engine was selected over an SI engine for aviation biofuel combustion because CI is a lean combustion engine as reported by Reşitoğlu et al. (2015).

Engine performance and emissions testing was conducted at constant injection pressure and fixed fuel injection timing. The test setup constraints did not allow changing injection pressure and timing to assess the effects on engine performance and emissions. The setup also was not equipped to measure engine vibration and noise level. The combustion analysis was conducted by analysing cylinder pressure and heat release rate data. The combustion phenomena could be analysed more effectively using an optical engine to capture combustion images with a high performance camera. This study was conducted under limited research funding which was insufficient to install the above mentioned equipment for investigation.

1.9. Study Overview

The study overview is presented graphically in Figure 1.8. The main steps are presented as prospective feedstock searching, fuel preparation, engine performance and emissions study, combustion and tribological study on better performing mixture blend. An aviation biofuel and the best blend for the transport sector as final outcomes of this study.

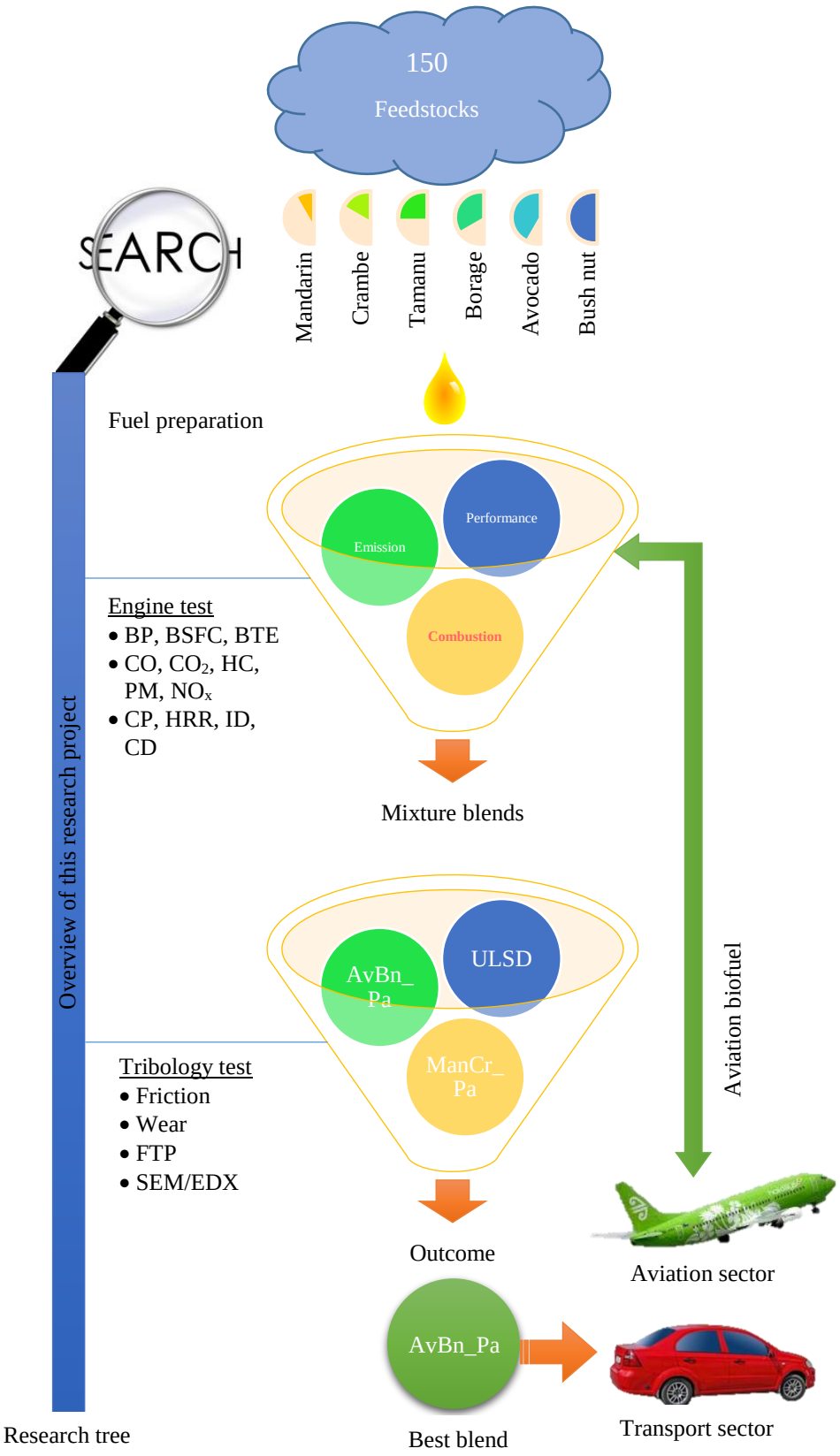

Figure 1.8: Study overview

1.10. Organisation of the Thesis

The structure of the thesis is shown in Figure 1.9. It contains eight chapters. A brief description of each chapter is given below.

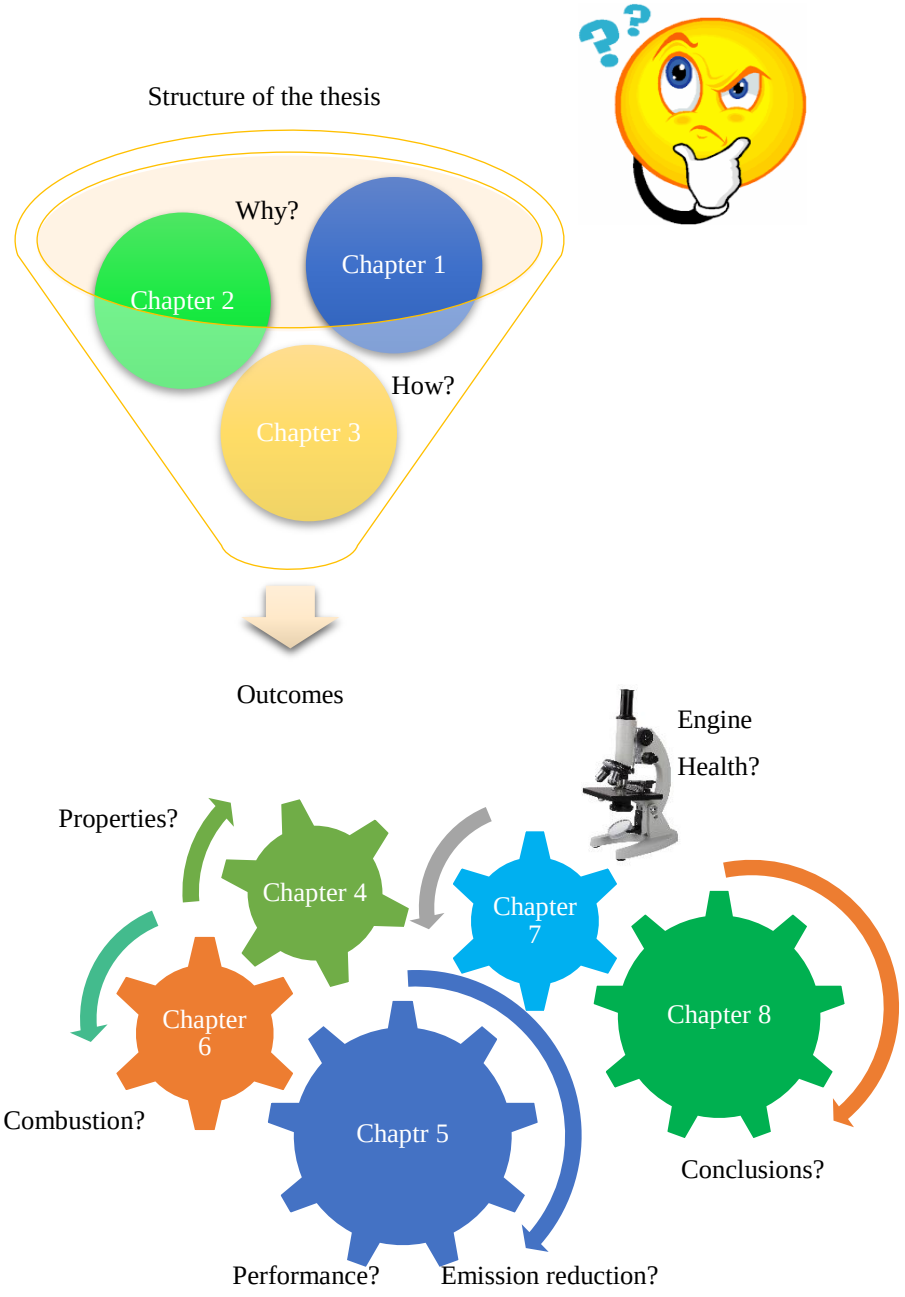

Figure 1.9: Structure of the thesis

Chapter 1 introduces the background information of the study and briefly discusses the significance of the study in the present context. It also provides research strategies and gaps, the general aim and objectives, and the scope and limitations. Finally, the structure of the thesis and a description of each chapter are briefly outlined.

Chapter 2 presents a detailed review of literature on various biofuel feedstocks and relevant works. It also covers the energy scenario, biodiesel production, consumption, biofuel supply chain, and prospective feedstocks for biodiesel production. Oil extraction processes, biodiesel conversion, and fuel properties are briefly outlined. Previous studies on engine performance parameters and emission parameters are also reported. Combustion strategies for biodiesel are briefly discussed. Finally, the research gaps have been identified in detail in this chapter.

Chapter 3 describes the detailed methodology used in this study. Experimental design, research plans and measurement techniques are briefly discussed. The developed neural network for the experimental investigation is briefly discussed. It also provides a summary of the experimental procedures for engine performance, emissions, combustion and the tribological study of the fuels.

Chapter 4 presents the results of fatty acid composition of the tested fuels by the GC test. The physio-chemical fuel properties of the fuels are evaluated and compared to fossil fuels. The behaviour of the fuel at various temperatures is also examined and discussed in this chapter.

Chapter 5 describes engine performance and emissions characteristics of different blends at variable engine speeds and load conditions. The study compares the experimental results of the biofuels with ULSD and other biodiesel blends.

Chapter 6 presents the combustion study of the better performing fuel blends by analysing CP, HRR and ID and CD with crank angle during combustion. It also presents the correlation of CP and HRR with colour maps for better demonstration and variation of crank angle.

Chapter 7 describes the detailed analysis of the tribological behaviour of the fuel using the four-ball testing procedure to determine the friction coefficient, and wear scar diameter and metal surface morphology were examined using SEM/EDX microscopy.

Finally, conclusions and recommendation from this study are drawn in Chapter 8. It also contains recommendations for future study.

Chapter 2

LITERATURE REVIEW

This chapter presents an in-depth literature review related to this work. The energy scenario and present biofuel scenario are briefly discussed. A biofuel supply chain (BSC) relationship model was developed in this study. As secondary resources according to that BSC, over 150 biofuel feedstocks have been studied for identifying prospective biodiesel feedstocks. The study identified six most prospective feedstocks for detailed analysis in this work. The recent development of biodiesel combustion strategies for diesel engines is briefly discussed. Literature related to tribological studies on various biodiesels are also presented in this chapter. The content of this chapter has already been published in various journals.

2.1. Introduction

The world's total energy consumption rose to about 575.37 quadrillion Btu in 2015 which is increasing faster than its population growth rate day-by-day due to sustainable development worldwide (IEO, 2016a). The higher rate of energy consumption causes serious environmental pollution as well as creating uncertainty regarding the future energy supply. To maintain the continuity of the world development and sustainability of the environment, the world is progressively moving towards renewable, alternative and low-emitting energy applications. On the other hand, economic growth is directly related to the energy usage. Therefore, energy consumption, economic growth, and environmental pollution are the multidisciplinary concerns nowadays (Azad et al., 2015c). The world's total energy supply is broadly categorised as non-renewable and renewable energy sources. The renewable energy contributed about 19.2% to total global energy consumption in 2014-2015 (Azad et al., 2014a, REN21, 2016). On the other hand, over 80% of the global energy demand has been meet by non-renewable energy sources which include coal, liquid fuel, and natural gas (Koh and Ghazoul, 2008, IEO, 2016b). The history of the global energy consumption revealed that it grows about 1.5% per year (IEO, 2016a). According to IEO projections, the total energy demand will grow by 56% between 2010 and 2040 (IEO, 2016b). This study also reported that developing countries are the main consumer of this energy to accelerate their development. The total energy consumed by the most energy intensive sectors such as power generation, manufacturing industries and transport sectors worldwide (Fattah et al., 2013). These sectors are emissions intensive sectors which cause serious GHG emissions around the globe (Körbitz, 1999). The transport sector is the second largest energy and emissions intensive

sector in the world which consumes mainly liquid fuel. The world consumed one-third of total energy (about 33%) from liquid fuels, 28% coal, 22% natural gas, 12% renewable and 5% nuclear energy (Figure 2.1). The trend of energy consumption history shows that higher consumption of liquid fuels will be unsustainable in the future due to the gradual depletion of those energy reserves. Therefore, the globe is looking towards alternative energy sources which are renewable, friendly for the environment and cost-effective. For this reason, renewable energy consumption increases every year throughout the world by discovering new sources which can be subdivided as clean energy and bioenergy.

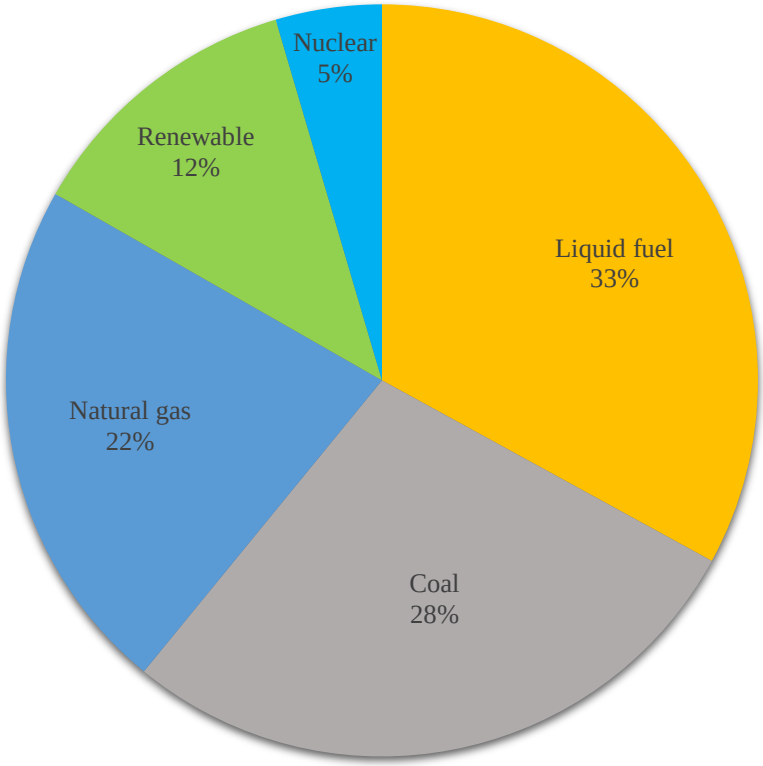

Figure 2.1: World total energy consumption by fuel type in 2015 (IEO, 2016a)

Liquid biofuels are one of the efficient forms of bioenergy which can be used as alternative fuels for the transport sector. Biofuels include biodiesel, bioethanol, biogas, and bio-hydrogen etc. which are self-oxygenated long chain hydrocarbon eco-fuels produced from bio-materials and animal fats (Janaun and Ellis, 2010, Sarin et al., 2010a). The different types of biofuels have different usages such as biodiesel for heavy transport vehicles, and bioethanol for light cars (Cherubini et al., 2009). In recent years, biofuel has found new usage in the aviation sector as aviation biofuel. These fuels are non-toxic, sulphur free, renewable, low pollutant emitting, safer and environment friendly energy sources (Demirbas, 2011b). The feedstock sources of biodiesel can

be classified as first generation (edible oil) (Demirbas, 2009b, Naik et al., 2010), second generation (non-edible oil) (Demirbas, 2009b, Naik et al., 2010), and third generation (algae oil) (Lee and Lavoie, 2013, Lü et al., 2011) biodieisels. It is reported in literature that sustainable energy development strategies typically involve three major technical changes, namely consumer energy savings (Blok, 2005), improvements of efficient energy production systems (Lior, 2002) and wide applications of renewable energy (Afgan and Carvalho, 2004). Renewable energy is the fastest growing sector in the world in which biofuels are the most prominently growing segment. This section aims to review and briefly discuss the prospect of biofuels in the transport sector including the aviation sector as a newly growing sector. Logistically, this section follows the path through total energy, renewable energy, bioenergy, and then biofuel as a prospective source of alternative energy. The energy scenario in Australia is briefly discussed below.

2.2. Energy Scenario in Australia

Australia has abundant, high quality and diverse energy resources both in non-renewable and renewable energy. Australia is the ninth largest energy producer in the world. In 2014-15, Australia exported two-thirds of its domestic energy production. For instance, they exported 90% of the black coal from their total production. In recent years, Australia's total energy production and consumption has risen about 1.0% from the previous year. Figure 2.2 illustrates the total energy consumption by fuel type from 1960 to 2015 in Australia. Table 2.1 summarises the energy consumption, growth and share in 2014-15 by primary fuel type. Australia primarily consumes 94.2% of its total energy from non-renewable resources such as coal (32.2%), liquid oil (37.8%), gas (24.2%) and the remaining 5.8% is from renewables (AES, 2016). Australia imported about 45% of its need for refined products to manage the higher consumption of liquid oil. On the other hand, about 63% of electricity was generated from coal and 14% from renewables in 2015 (AES, 2016). The total energy consumption rose to 5919.6 PJ in 2015 (Ball et al., 2016). Renewable generation increased by 1.6% in 2014-15 with an average growth rise of 2.1% per year over the last ten years (Ball et al., 2016). So, the growth in renewable energy consumption is increasing steadily every year.

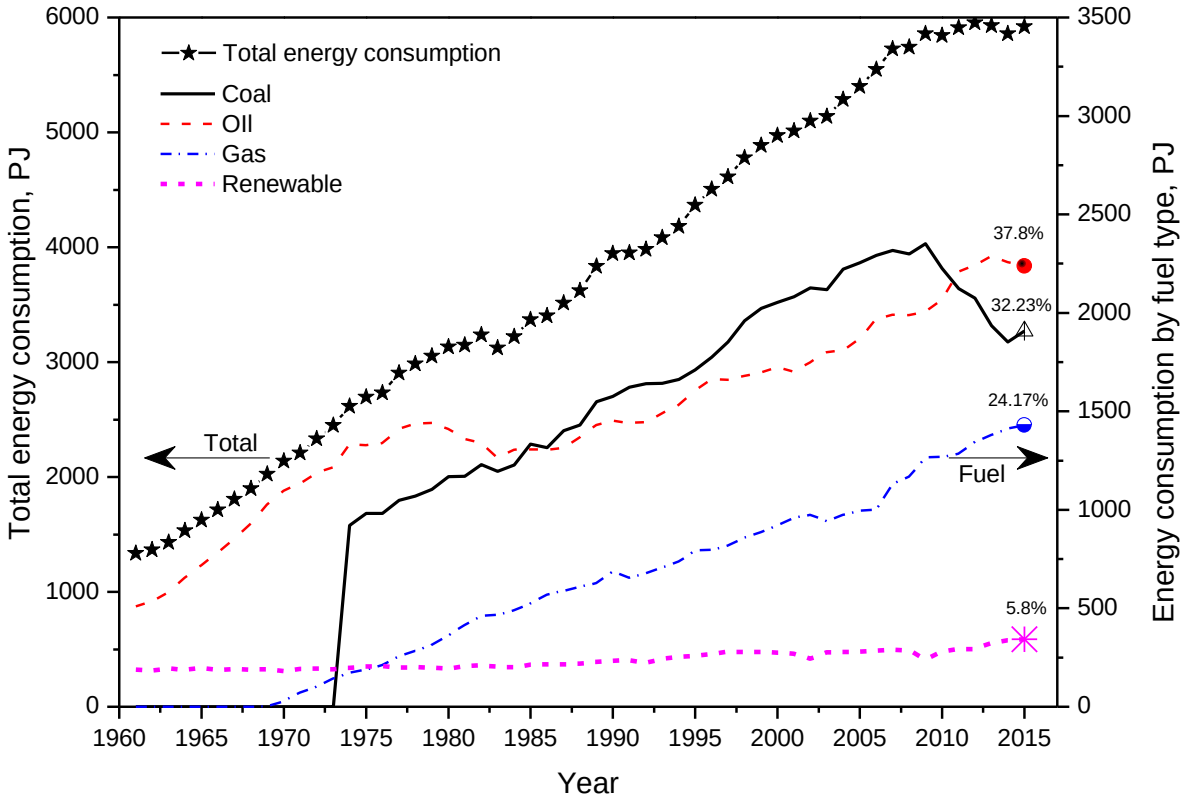

Figure 2.2: The energy consumption in Australia by fuel type [Unit 1 petajoule, PJ= 1015J]

Source: Australian Energy Statistics, Table C (AES, 2016)

Table 2.1: Summary of Australia's primary energy status

Fuel type	Consumption (PJ)	Growth (%)		Share (%)
	2014-15	2014-15	10 years average	
Coal	1907.80	3.00	-2.00	32.20
Oil	2237.40	-0.90	1.40	37.80
Gas	1431.00	1.30	4.10	24.20
Renewable	**343.30**	**1.60**	**2.10**	**5.80**
Total	5919.60	1.00	0.70	100.00

Sources: Australian Energy Statistic Data, Table C (AES, 2016)

Figure 2.3 illustrates the total energy consumption by primary sectors in 2015. As seen from the figure, 28.2% energy has been consumed for electricity generation whereas 27.2% energy was consumed by the transport sector in 2014-15. Energy consumption increased by about 1.7% per year in the transport sector which mainly consumed liquid fuels (Ball et al., 2016). The higher consumption of liquid fuel and the faster growth rate of this sector has become an important issue for future energy security. The higher consumption also leads to serious environmental pollution with GHG emissions from this sector having increased by 24% in the last decade (DoE, 2015). Alternative fuels could be one of the promising solutions to meet the increasing energy demand

while also decreasing environmental pollution. Eco-fuel resources as well as other renewable energy resources are largely undeveloped (Ball et al., 2016). Further study is therefore needed to investigate how biodiesel resources can be used as an alternative fuel in the transport sector.

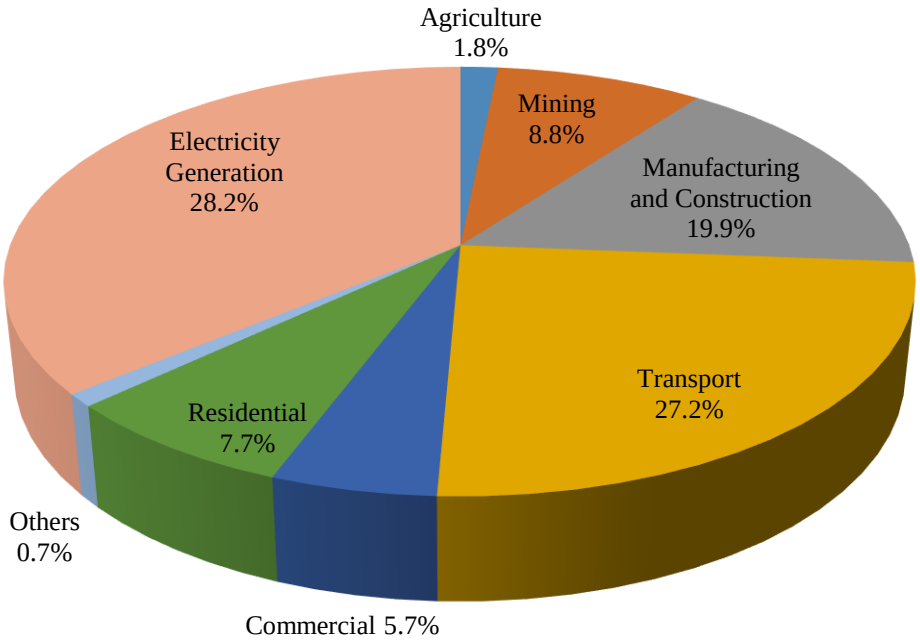

Figure 2.3: The total energy consumption in Australia by sector

Source: Australian Energy Statistics, Table E (AES, 2016)

2.3. Renewable Energy

Renewable energy is eco-friendly, cost effective and low pollutant emitting as reported by Kelly (2007). The main renewable energy resources such as wind, solar, hydro, and wave energy are pollution free and biomass, geothermal, biogas and biofuel are low pollutant emitting (Jacobson and Delucchi, 2011). The increased usages of renewable energy can significantly reduce GHG emissions. Due to its desire to save the environment, the Australian Government set a target of about 20% electricity generation from renewable sources by 2020 (RET, 2013). The target has almost been achieved because about 14% of electricity was already being generated by renewable resources in 2015 as discussed above. Table 2.2 summarises the 2014-15 renewable energy scenario in Australia. A significant growth of solar energy (35.1%) occurred in 2014-15 when its share accounted for 10.6% of total renewable energy consumption. Hydro-energy consumption decreased 27% due to reduced water in-flows in southeast Australia caused by low rainfall with respect to previous years. Bio-ethanol growth also reduced about 22.7% due to the lack of a rebound in the sugarcane harvest in Queensland. Biodiesel consumption growth of about 10% was recorded in 2014-15. The production and uses of biodiesel have grown quickly in recent years due

to increased public consciousness of the potential for biodiesel to assist in maintaining environmental safety. It is expected that biodiesel will grow over the next 30 years worldwide as a prospective sector.

Table 2.2: Australia's renewable energy scenario in 2014-15

Renewable energy type	Energy source type	Consumption (PJ) 2014-15	Growth (%) 2014-15	Share %)
Clean energy	Hydro	48.40	- 27.00	14.10
	Wind	41.30	11.80	12.00
	Solar PV & HW	36.30	35.10	10.60
Bioenergy	Biomass	186.70	6.80	54.40
	Biogas	19.10	17.00	5.60
	Bioethanol	6.70	-22.70	2.00
	Biodiesel	**4.70**	**9.70**	**1.40**
	Total	343.30	1.60	100.00

Source: Australian Energy Statistic Data, Table D, F, O (Ball et al., 2016).

2.4. Biofuel Scenario in Australia

Figure 2.4 illustrates the present biofuel scenario in Australia including production, consumption and trade from 2006 to 2015. Australia started biofuel production in 2004 with only 100 barrels per day which has been increasing every year until 2015. As seen from Figure 2.4, biofuel consumption significantly increased from 2013 and a peak was recorded in 2014 due to the noticeably heavy demand and the resulting huge increase in imports (about 371 million litres) (Table 2.3). The trend of the consumption curve shows higher in every year which implies more demand in Australian energy market. Australia imported biofuels every year to meet this demand. For to this reason, the Australian Government has aimed to support 350 million litres of biofuel production per year from 2010 (Rodriguez et al., 2011). To desire to achieve energy independency in the transport sector is one of the main reasons for Government investment to develop biodiesel industries in Australia as mentioned by Farrell (2016). At present, Australia produces biodiesel from waste cooking oil, and some oil seeds and animal fats such as beef tallow as shown in Table 2.4. The State Governments have taken some initiatives to produce biofuels including aviation biofuels to meet their liquid fuel demand. There are probably two main reasons for this. One could be that Australia wants energy independency for transport fuel because a large part of this fuel (about 45%) has been imported every year as reported by Farrell (2016). Another reason could be that the Australian Government has set a target to reduce GHG emissions by 80% against 2000 levels by the year of 2050 (CEFC, 2014). The exploration of new renewable energy resources and their applications could have significant impacts on environmental sustainability and energy security. It could create a new energy market area which can contribute to the economy. Trade of biofuels (both exports and imports) can

play an important role in the economic growth of Australia. Australia started biofuel exports from 2012 of about 10 to 20 million litres per year until 2015 (Farrell, 2016). In 2014, the policy was changed so that the imported biodiesel would be fully subject to excise whereas only a partial excise applied for locally produced biodiesel (Farrell, 2016). For this reason, imports of biodiesel dropped significantly in 2015 as is clearly shown in Figure 2.4.

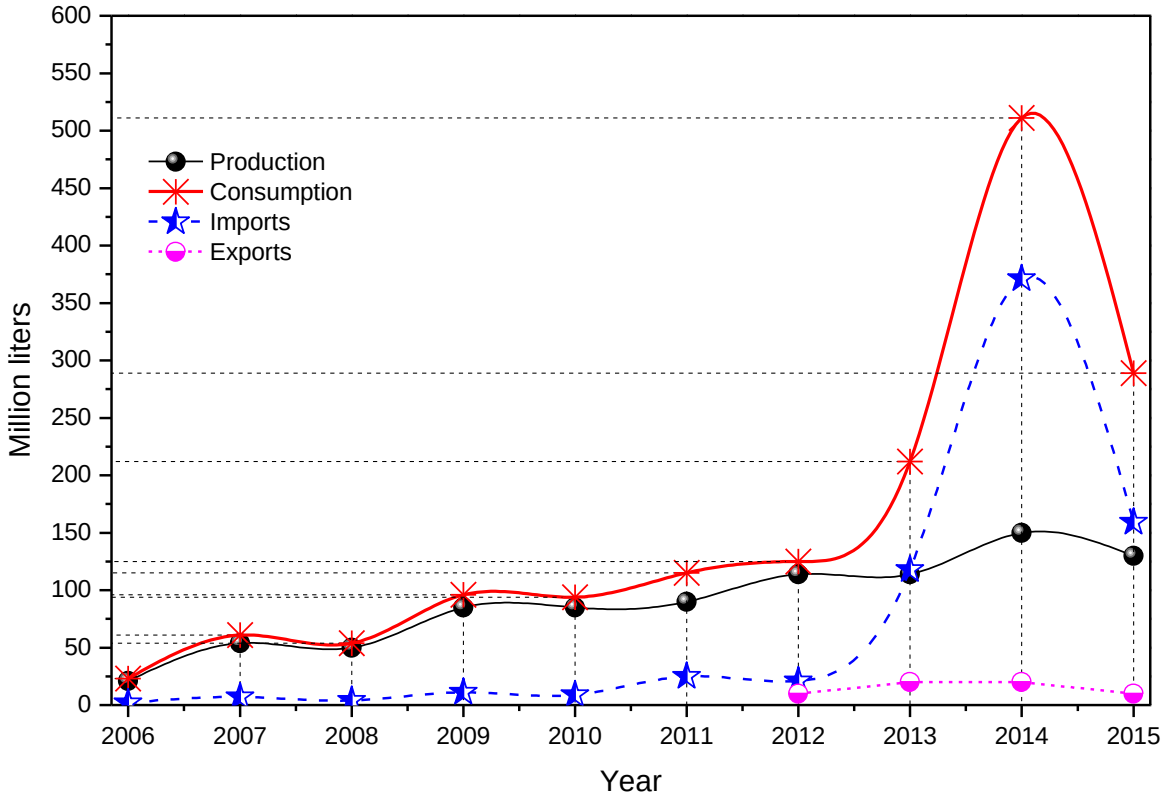

Figure 2.4: Australia's biofuel scenario including production, consumption, imports and exports

Source: Australia Biofuels Annual (Farrell, 2016)

Table 2.3: Australia's biofuel scenario including production, consumption and trade in millions of litres

Year-end July	2006	2007	2008	2009	2010	2011	2012	2013	2014	2015
Production	43.0	54.0	98.0	80.0	80.0	115.0	114.0	114.0	150.0	130.0
Imports	5.0	4.0	11.0	8.5	25.0	20.0	21.0	118.0	371.0	159.0
Exports	0.0	0.0	0.0	0.0	0.0	0.0	10.0	20.0	20.0	10.0
Consumption	47.0	58.0	109.0	88.5	105.0	125.0	125.0	212.0	511.0	289.0
Ending stocks	2.0	2.0	6.0	7.0	9.0	10.0	0.0	0.0	0.0	0.0
Production capacity (Conventional biofuel)										
No. of bio-refineries	7	9	8	6	7	7	7	7	8	8
Capacity	174	136	283	215	215	280	400	400	400	400

Source: Australia Biofuels Annual (Farrell, 2016).

2.4.1. Present biofuel production facilities in Australia

As discussed above, the number of biofuel production facilities in Australia is increasing due to the significant demand in the local energy market. The production capacity of biofuel facilities are being increased by the development of new projects or by extending existing projects. The three largest bioethanol production facilities are Sarina Distillery in north Queensland, the Manildra facility in Nowra (NSW), and the Dalby bio-refineries in Queensland (Puri et al., 2012). Table 2.4 summarises the present biofuel production facilities available in Australia. The State of Queensland produces around 120ML/year of bioethanol from 1G feedstocks such as sugar cane and grain (Puri et al., 2012). The Queensland government recently invested in an advanced biofuel project called the ‘‘Queensland Sustainable Aviation Fuel Initiative’’. Three feedstocks were selected for use under this project, namely bagasse, algae, and karanja oil (Azad et al., 2015c). Australian research is focused on understanding how nationally available feedstocks can be used for biofuel, and on how to resolve the challenges involved in its production.

Table 2.4: Present status of Australia’s biofuels industry, production capacity and feedstocks

Bioenergy producer	Industry owner	Location	Feedstocks	Capacity (ML/year)	Status at (01/06/15)
ARFuels Largs Bay	Australian Renewable Fuels*	Largs Bay, SA	Waste cooking oil, tallow	45.0	In production
ARFuels Barnawartha	Australian Renewable Fuels*	Barnawartha, VIC	Waste cooking oil, tallow	60.0	In production
EcoTech BioDiesel	Gull Group*	Narangba, QLD	Waste cooking oil, tallow	30.0	In production
ARFuels Picton	Australian Renewable Fuels*	Picton, WA	Waste cooking oil, tallow	45.0	In production
Biodiesel Industries	Biodiesel Industries Australia Pty Ltd*	Rutherford, NSW	Waste cooking oil, vegetable oil	20.0	In production
Macquarie Oil	Macquarie Oil Co	Cressy, TAS	Poppy oil & waste oil	15.0	In production
EcoFuels Australia	EcoFuels Australia Pty Ltd	Echuca, VIC	Canola oil	1.50	In production
ASHOIL	Ashburton Aboriginal Corporation*	Tom Price, WA	Waste cooking oil	Unknown	In production
Territory Biofuels	Territory Biofuels Ltd	Darwin, NT	Waste cooking oil, tallow, refined palm oil	140.0	Closed
Smorgon Fuels-BioMax Plant	Smorgon Fuels Pty Ltd	Laverton, VIC	Canola, Juncea and tallow	N/A	Closed
Neutral Fuels	Neutral Fuels (Melbourne) Pty Ltd	Dandenong, VIC	Waste cooking oil	Unknown	Closed
Total production capacity in million litres per year =				**360.0**	

Source: Biofuels Association of Australia (BAA), * indicates BAA members.

Development of the biofuel industry has been facing lot of challenges throughout the world. A few of them are briefly discussed here. The challenges relate to the need for a constant supply of raw materials, the food versus energy debate, the higher pricing of biofuels, and a lack of public awareness regarding the usage of biofuels, shorter oxidation stability, different FAMEs compositions, and some other technological challenges. It is reported in the literature that government support and productivity policy can play an important role for sustainability of the biofuel industry (Lim and Teong, 2010). Research and development is also needed to identify new feedstocks with good prospects in all aspects of biofuel production. The biofuel trade in the international energy market could open a new direction in economic development. This study has developed a biofuel supply chain representation for better understanding of the relationships involved between biofuel productions from raw materials to the end user applications as is briefly discussed below.

2.4.2. Biofuel supply chain

The biofuel supply chain is simply the symbolic representation of the biofuels lifecycle (Azad et al., 2015c). Figure 2.5 illustrates the relationship flows between the energy producing resources to the end users in the biofuel supply chain. It consists of several steps including primary resources, secondary resources, development and production projects, processing, transport and storage, and finally end users and their applications of biofuels. In this supply chain, the sun, atmospheric CO_2 and water are considered as primary resources whereas plants and animals are considered as secondary resources. The secondary resources are directly or indirectly dependent on primary resources and store the energy as biomass and animal fats. Secondary resources recycle the emitted carbon in energy form through biological processes. The third step is the most important step of the conversion of the energy of secondary resources into useable forms of energy. Generally, three types of conversion techniques are used for the energy conversion, namely biomass, biogas and biofuel projects. The available bioenergy is processed, transported or stored as required and finally reaches the end user or customer. Note that biomass can also be used to produce biofuels such as bio-ethanol. Bio-ethanol and biodiesel are the most efficient forms of recycling carbon as alternative fuels in the transport sector. This study reveals that the transport sector is a fast growing and emissions intensive sector which needs to have its adverse impacts managed by the application of the largely undeveloped renewable energy resources of biofuels. The study focuses on the special interest in aviation biofuel and biodiesel as an alternative fuel to meet the increasing energy

demand and to reduce the harmful emissions from this sector. The study investigated biodiesel resources to identify new and prospective feedstocks which are presented in the following section.

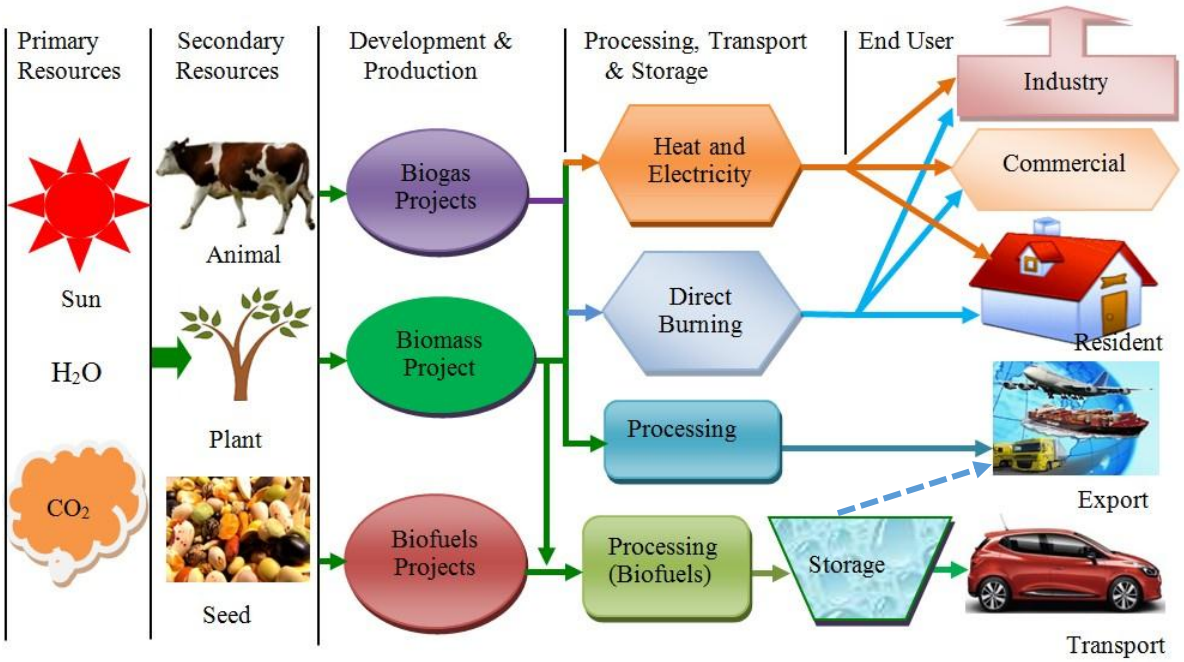

Figure 2.5: The relationship between resources and end user in biofuel supply

2.5. Biodiesel Sources and Potential Feedstocks

Biofuels are liquid eco-fuels which are generally produced from biological materials such as biomass and animal fats (Azad et al., 2015c). A narrower concept says that "*biofuel is a renewable source of carbon*" as reported by Lee and Lavoie (2013) (page 6). It is a renewable fuel composed of long chain fatty acid methyl esters which can meet the requirements of ASTM D6751 standards (Janaun and Ellis, 2010, Sarin et al., 2010b). Biofuels include bio-ethanol, biodiesel, biogas etc. which can be used as alternative fuels. This study is mainly focused on biodiesel and aviation biofuel for the transport sector. Sources of biodiesel continue to be investigated with a view to finding new resources. Biodiesel resources can be classified based on social, economic and environmental factors as briefly discussed below.

2.5.1. Edible sources (first generation biodiesel)

The first generation (1G) biodiesels are generally derived from edible food crops or oil seeds (Lee and Lavoie, 2013, Azad et al., 2012). Food crops including wheat, rice, potato wastes, barley, and sugar beets etc. are marginal 1G feedstocks. However, corn and sugarcane are generally used to

produce bio-ethanol. The edible vegetable oils such as mustard oil, soybean oil, palm oil, sunflower oil, coconut oil, corn oil, rapeseed oil, and olive oil etc. are the main sources of biodiesel production as reported by Balat (2011) and Hoekman et al. (2012). However, vegetable oils are widely used for food processing. A selection of the edible feedstocks, their oil content and productivity yields are presented in Table 2.5. The table shows that some of these feedstocks have high oil yields and high production rate. Conventional oil extraction techniques can be applicable to extract oil from these feedstocks. Furthermore, 1G biofuel faces social, economic and environmental challenges because these are derived from food crop feedstocks. Their use leads to increased food prices and also creates pressure on land use which makes it unlikely to be sustainable. Consequently, technologies are starting to develop for the use of alternative feedstocks to overcome the major shortcomings of the 1G biodiesel (Azad et al., 2016c). Table 2.5 clearly identifies the higher oil yield feedstocks such as Borage, Avocado, and Bush nut etc. which would be the more prospective feedstocks for biodiesel production.

Table 2.5: Biodiesel feedstocks from edible sources in literature

	Edible sources	Oil yield (%)		Production yield	References
	Food Crops	Seed	Kernel	(Litres/hectare)	
1.	Wheat	-	2.50	-	(Sanford et al., 2009)
2.	Corn	48.0	-	172.0	(Karmakar et al., 2010)
3.	Whey	4.5-5.0	-	-	(Guimarães et al., 2010)
4.	Barley	2.5-5.0	-	-	(Hahn-Hägerdal et al., 2006)
5.	Potato waste	20.0	-	-	(Arapoglou et al., 2010)
6.	Sugar beets	40.0	-	-	(Mussatto et al., 2010)
	Vegetable oil				
7.	Rice burn oil	15.0-23.0	-	825.0	(Karmakar et al., 2010)
8.	Coconut oil	63.0-65.0	-	2689.0	(Karmakar et al., 2010)
9.	Rapeseed oil	37.0-50.0	-	1190.0	(Karmakar et al., 2010)
10.	Palm oil	30.0-60.0	-	5950.0	(Ramos et al., 2009)
11.	Soybean oil	15.0-20.0	-	446.0	(Sanford et al., 2009)
12.	Canola oil	43.0	-	-	(Hoekman et al., 2012)
13.	Sunflower oil	25.0-35.0	45.0-55.0	952.0	(Hoekman et al., 2012)
14.	Hemp oil	30.0-35.0	-	-	(Hoekman et al., 2012)
15.	Palm oil	44.0-65.0	-	-	(Ramos et al., 2009)
16.	Borage oil	95.0	-	-	(Soto et al., 2007)
17.	Sesame oil	41.0	-	-	(Banapurmath et al., 2008a)
18.	Moringa oil	35.0-40.0	-	250.0	(Ramos et al., 2009)
19.	Mustard oil	30.0	-	-	(Azad and Uddin, 2013)
20.	Peanut oil	45.0-55.0	-	1059.0	(Sanford et al., 2009)
21.	Olive oil	45.0-70.0		1212.0	(Ramos et al., 2009)
22.	Bush nut oil	-	60.0-72.0	1413.0	(Knothe, 2010)
23.	Cotton seed	18.0-25.0		325.0	(Ramos et al., 2009)
24.	Linseed	40.0-44.0	-	-	(Sanford et al., 2009)
25.	Avocado oil	-	59.0-67.0	270.0	(Ortiz et al., 2004)
26.	Grape seed oil	12.0	-	-	(Fernández et al., 2010)
27.	Apricot oil	-	50.2	-	(Wang and Yu, 2012)
28.	Pumpkin oil	45.0	-	-	(Schinas et al., 2009)

2.5.2. Non-edible sources (second generation biodiesel)

The second generation (2G) biodiesels are produced from a wide array of lignocellulosic feedstocks and animal fats (Lee and Lavoie, 2013, Demirbas, 2009b). In addition, they can be obtained from pyrolytic biomass oil, (Alcantara et al., 2000), non-food crops (Azad et al., 2014c), waste cooking oil (Vasudevan and Briggs, 2008). A wide range of feedstocks are available for 2G biodiesel production including castor oil, jatropha curcas, pongamia oil, lesquerella oil etc. which have already been investigated for biofuel production (Sarin et al., 2010b, Azad and Prince, 2012). The 2G biodiesels can overcome the social, economic and environmental challenges without hampering our food costs and creating pressure on land use because it is non-edible, biodegradable and can grow on marginal land (Azad et al., 2014d). The 2G biodiesels have some other advantages. They have some excellent fuel properties including higher flash point, higher cetane number, excellent lubricity and very favourable energy balance (Xue et al., 2011, Li et al., 2014). Table 2.6 summarises the available 2G feedstocks, their distribution, oil yield and other uses which has been arranged in descending order of their oil content.

Table 2.6 provides brief information about 75 feedstocks including Australian native species considered to have potential for biodiesel conversion. This study identified some more prospective native species, namely Tamanu (beauty leaf), Crambe, Karanja, Queen palm, Castor oil, and Mandarin peel waste due to their high oil yield, ready availability, fast growing rate and their environmentally sustainable as feedstocks. These species can be grown in largely unproductive areas and are mostly located in degraded forest and coastal areas. These oils contain some fatty acids which are not edible. In addition, these biodiesels have some desirable physio-chemical properties compared to fossil fuel. There are some key factors which directly influence the fuel properties, namely fatty acid composition, feedstock quality, relatively simple production and refining techniques of the fuel. The properties of the biodiesel are within the acceptable range of ASTM and EN standards. For the above mentioned reasons, this fuel can overcome the major shortcomings of 1G biofuel such as the food versus fuel controversy, and the economic and environmental issues.

Table 2.6: Non-edible biodiesel feedstocks with scientific name, distribution, oil content and uses

No	Feedstocks name	Distribution	Used part	Oil yield		General usage	Reference
				Seed (Wt.%)	Kernel (Wt.%)		
1.	Kusum oil (*Sleichera triguga*)	Malaysia, Indonesia, Himalayas, China, Java, Sri-Lanka etc.	Seed		55 to 70	Skin oil, hairdressing	(Atabani et al., 2013b, Sharma and Singh, 2010)
2	Stillingia oil (*Sapium sebifeum*)	USA, Japan, China, India etc.	Seed, kernel	13 to 32	53 to 64	Drying and strillengia oil	(Wang et al., 2011, Atabani et al., 2013b)
3.	Sea lemon oil (*Ximenia Americana*)	Australia, New Zealand, Africa, India etc.	kernel	–	49 to 61	Bio-lubricant and vegetable oil	(Saeed and Bashier, 2010)
4.	Niger oil (*Guizotia abyssinica L.*)	India, Ethiopia etc.	Seed	50 to 60	–	Biodiesel, vegetable oil	(Sarin et al., 2009b)
5.	Rubber seed oil (*Hevea brasiliensis*)	Southeast Asia, West Africa, Brazil Nigeria etc.	Seed	40 to 60	40 to 50	Rubber or plastic raw material, printing ink	(Singh and Singh, 2010b)
6.	Jamaal Gota oil (*Croton tiglium*)	Philippines, China, Java, Malabar, Ceylon etc.	Seed, kernel	30 to 45	50 to 60	Resin, vegetable oil biodiesel	(Mohibbe Azam et al., 2005)
7.	Jatropha oil (*Jatropha curcas*)	Malaysia, Indonesia, Pakistan, Philippines, Nepal etc.	Seed, kernel	20 to 60	40 to 60	Biodiesel, bio- lubricant, vegetable oil	(Kumar and Reddy, 2012, Chen et al., 2012a)
8.	Jojoba oil (*Simmondsia chinensis*)	Arizona, California and Mexico etc.	Seed	45 to 55	–	Skin protector, moisturiser, and hairdressing.	(Singh and Singh, 2010b, Basha et al., 2009)
9.	Sea mango oil (*Cerbera odollam*)	Southern Asia	Seed, kernel	54	6.4	Illuminate	(Wang et al., 2012)
10.	Soap nut oil (*Sapindus mukorossi*)	Europe, Asia, America	Kernel	51.8	–	Biodiesel, vegetable oil	(Chhetri and Watts, 2013)
11.	Castor oil *(Ricinus communis)*	Italy, China, Brazil, India, Cuba, French etc.	Seed	45 to 50	–	Bio-lubrication, oil fuel	(da Silva César and Otávio Batalha, 2010)
12.	Mesua ferrea oil *(Cobra's saffron)*	Malaysia, Philippines, Nepal, India	Seed	35 to 50	–	Bio-lubricants, Soaps, illumination	(Gui et al., 2008, Kushwah et al., 2008)
13.	Mahwa oil *(Madhuca indica)*	India	Seed, kernel	35 to 50	50	Biodiesel	(Balat, 2011, Kumari et al., 2007)
14.	Karanja oil *(Pongamia pinnata)*	Asia, Australia, Fiji	Seed, kernel	25 to 50	30 to 50	Timber, firewood, oil-illumination	(Atabani et al., 2013a)
15.	Bengal almond oil *(Terminalia catappa)*	Brazil, Asia, Australia, Africa	Seed	49	–	Biodiesel, timber oil	(Singh and Singh, 2010a)

16.	Desert date oil *(Balanites aegyptiaca)*	Asia and African arid regions	Kernel		36 to 47	Biodiesel, vegetable oil	(Gour and Kant, 2012, Gutti et al., 2012)
17.	Kukui nut *(Aleurites moluccana)*	South Asia, Malaysia, Java, Australia	Kernel	46.73	-	-	(Kibazohi and Sangwan, 2011)
18.	Beauty Leaf oil *(Calophyllum inophyllum)*	Australia, Malaysia, East Africa, India		46.51±4	-	Biodiesel, candle oil	(Ong et al., 2011, Sanjid et al., 2013)
19.	Kokum oil *(Garcinia indica)*	Africa, Asia	Seed	45.5	–	Resin, biodiesel, vegetable oil	(No, 2011, Hosamani et al., 2009)
20.	Radish oil *(Raphanus sativus)*	Australia and almost every country in the world	Seed	40 to 45	-	Biodiesel and vegetable oil	(Moser, 2011)
21.	Vann oil *(Salvadora oleoides)*	Southern Iran, Pakistan, India etc.	Seed	45	–	Candle oil	(Al-Sohaibani and Murugan, 2012)
22.	Yellow jade orchid oil *(Michela chaampaca)*	India, China	Seed	45	–	Biodiesel, vegetable oil	(Atabani et al., 2013b)
23.	Linseed oil *(Linum usitatissimum)*	Canada, Europe, Middle East, Argentina, India	Seed	35 to 45	–	Biodiesel, floor oil, resin, fibre	(Guzatto et al., 2011)
24.	Neem oil *(Azadirachta indica)*	Australia, Malaysia, Cuba, Bangladesh, Pakistan Sri Lanka	Seed, kernel	20 to 30	25-45	Biodiesel, timber, firewood	(Ragit et al., 2011, Karmakar et al., 2012)
25.	White cedar oil *(Melia azedarach)*	Asia, Australia, Indomalaya	Seed, kernel	10 to 45	2.8	Biodiesel	(Stavarache et al., 2008)
26.	Putranjiva oil *(Putranjiva roxburghii)*	India	Seed	41 to 42	–	Oil burning	(Tong et al., 2011)
27.	Ethiopian mustard oil *(Brassica carinata)*	Ethiopia	Seed	42	2.2-10.8	Jet fuel, biodiesel	(No, 2011, Pinzi et al., 2009)
28.	Queen palm *(Syagrus romanzoffiana)*	South America, Brazil, Australia, Argentina, Bolivia.	Seed	41.64	-	Biodiesel	(Ashwath, 2010, Falasca et al., 2012)
29.	Tobacco oil *(Nicotiana tabacum)*	Bangladesh, Pakistan, Turkey, India, England, Brazil, Cuba, Africa	Seed, kernel	36 to 41	17	Ethno medicinal, bio-oil	(Atabani et al., 2013b, Usta et al., 2011)
30.	Kapok oil *(Ceiba pentandra)*	America, Mexico, Indonesia (Java)	Seed	24 to 40	–	Biodiesel, timber oil	(Silitonga et al., 2013b, Ong et al., 2013)
31.	Tung oil *(Vernicia fordii)*	Taiwan, Vietnam, China	Seed	35 to 40	–	Oil, biodiesel	(Zhou et al., 2011)
32.	Pongam Oil tree *(Millettia pinnata)*	Japan, Malaysia, Australia, India, China	Seed	27 to 39	-	Biodiesel, vegetable oil	(Kumar and Sharma, 2011)
33.	Argan oil *(Argania spinosa)*	Morocco	Kernel	30 to 50	–	Bio-oil, cosmetic oil	(Atabani et al., 2013b)
34.	Cuphea oil *(Cuphea hyssopifolia)*	USA, Argentina	Seed	20 to 38	–	Biodiesel	(Moser and Vaughn, 2010)

35.	Tomato seed oil *(Solanum lycopersicum)*	Mexico, Australia, Greece, Turkey	Seed	32 to 37	–	Vegetable oil, soaps	(Atabani et al., 2013b, Moser et al., 2011)
36.	Moringa oil *(Moringa oleifera)*	Asia, Latin America, Africa, Oceania	Seed	35		Biodiesel, vegetable oil	(Rashid et al., 2011)
37.	Pithraj oil *(Aphanamixis piolystachya)*	China, India	Kernel	-	35	Oil illuminant	(Uddin, 2009, Atabani et al., 2013b)
38.	Garden rocket *(Eruca sativa)*	South Asia, Europe, America, South Africa, Australia, New Zealand	Seed	35	–	Biodiesel, vegetable oil	(Chakrabarti et al., 2011, Qin et al., 2010)
39.	Samadera oil *(Samadera indica)*	Tropical region, Indonesia	Seed	~35	–	Vegetable oil	(Atabani et al., 2013b)
40.	Foambark oil *(Jagera pseudorhus)*	New Guinea, Australia	Seed	34.01	-	Biodiesel	(Ashwath, 2010)
41.	Koroch seed oil *(Pongamia glabra)*	Malaysia, Japan, Thailand, Australia	Seed	33.6	-	Biodiesel, firewood	(Razon, 2009, Atabani et al., 2013b)
42.	Mall-leaved oil *(Ochna serrulata)*	South Africa, New Zealand, Australia	Seed	31.16	-	Biodiesel	(Bandi et al., 2012)
43.	Platyloba oil *(Passiflora platyloba)*	Asia, South America	Seed	19 to 28	-	Biodiesel, hair care	(Zahedi and Azarpour, 2011)
44.	Wonder oil *(Idesia polycarpa)*	Asia, Japan, Korea	Fruit, Seed	26.26	–	Oil, biodiesel	(Yang et al., 2009)
45.	Cotton seed oil *(Bombax malabaricum)*	Asia, Europe	Seed	18 to 26	–	Biodiesel, vegetable oil	(Hossain et al., 2012, Atabani et al., 2013b)
46.	Milkweed oil *(Asclepias syriaca)*	USA	Seed	20 to 25	0.019	Bio-oil	(Pinzi et al., 2009)
47.	Sandalwood oil *(Santalum album)*	India, Sri Lanka, Australia	Seed	24.49±3	-	Biodiesel, vegetable oil	(Misra and Dey, 2013)
48.	Chinese rain tree oil *(Koelreuteria formosana)*	Taiwan, Australia	Seed	22.17	-	Biodiesel	(Lin et al., 2014)
49.	Orange jasmine oil *(Murraya exotica)*	Australia	Seed	21.86	-	Biodiesel	(Wu et al., 2013, Zhang et al., 2013)
50.	Quinine bush oil *(Petalostigma pubescens)*	Australia	Seed	21.13	-	Biodiesel	(Grace et al., 2006)
51.	Illawarra Flame Tree oil *(Brachychiton acerifolius)*	Australia	Seed	19.86	-	Essential oil	(Ashwath, 2010)
52.	Coffee seed oil (*Coffea arabica*)	Brazil	Seed	17	-	Essential oil, biodiesel	(Sarıbıyık et al., 2010, Berman et al., 2011)
53.	Long-leaved Bitter Bark *(Petalostigma triloculare)*	Asia, Australia	Seed	19.06	-	Vegetable oil	(Heard et al., 2009)

54.	Blue flax-lily oil *(Dianella caerulea)*	Tasmania in Australia	Seed	18.66	-	Bio-oil	(Ashwath, 2010)
55.	Cardosanto oil *(Argemone Mexicana)*	UAS, Mexico, Australia		18.38	-	Biodiesel	(Sharma et al., 2012)
56.	Sugar-apples oil *(Annona squamosa)*	Indonesia, Caribbean, Central America, Australia	Seed	15 to 20	-	Biodiesel, vegetable oil	(Reyes-Trejo et al., 2014)
57.	Broad Leafed Palm Lily *(C. manners-suttoniae)*	Australia	Seed	15.84	-	Biodiesel	(Ashwath, 2010)
58.	Whitewood oil *(Atalaya hemiglauca)*	Swaziland, Australia, Southern Africa	Seed	15.62	-	Bio-oil	(Ashwath, 2010)
59.	Fabaceae oil *(Crotalaria retusa L.)*	Africa, Native in Asia	Seed	15	–	Biodiesel, vegetable oil	(Umerie et al., 2010)
60.	Red silky oak oil *(Grevillea banksii)*	Australia	Seed	13.85	-	-	(Ashwath, 2010)
61.	Balanco oil *(Aleurites trisperma)*	South America, Asia	Kernel	-	–	Bio-lubricant, paraffin	(Martín et al., 2010)
62.	Mandarin oil *(Citrus reticulate)*	China, India, Australia, Pakistan	Seed	28.5	-	Skin oil, biodiesel	(Rashid et al., 2013)
63.	Racemosa oil *(Barringtonia racemosa)*	Asia and the Pacific islands, East Africa	Seed	19.5	–	Oil illuminate	(Kong et al., 2012)
64.	Dwarf kurrajong oil *(Brachychiton bidwillii)*	Australia	Seed	11.15		Biodiesel	(Ashwath, 2010)
65.	Crambe oil *(Crambe abyssinica)*	Brazil, USA	Seed	69 to 81	-	Biodiesel	(Wazilewski et al., 2013)
65.	Curare oil *(Acacia tetragonophylla)*	Australia	Seed	-	-	Treat warts	(McHenry and Anwar, 2013)
67.	Eucalyptus oil (*Eucalyptus globulus*)	Australia	Peel	-	-	Biodiesel	(Tarabet et al., 2012)
68.	Waste cooking oil	All countries	-	97.02	-	Biodiesel	(Sharma et al., 2008)
70.	Rich Straw	Throughout the world	-		-	Biodiesel	(Amiri et al., 2014)
69.	Bagasse	Throughout the world	Biomass		-	Bio-ethanol	(Ojeda et al., 2011, Chandel et al., 2012)
71.	Wheat straw	Throughout the world	Biomass		-	Biodiesel	(Qureshi et al., 2008)
72.	Barley straw	Throughout the world	Biomass		-	Biodiesel	(Qureshi et al., 2010)
73.	Poultry fats	Throughout the world	Fat	-	-	Biodiesel	(Tang et al., 2008)
74.	Lard	Throughout the world	Fat		-	Biodiesel	(Canakci and Sanli, 2008)
75.	Tallow	Throughout the world	Fat		-	Biodiesel	(Canakci and Sanli, 2008)

2.5.3. Microalgae (third generation biodiesel)

The third generation (3G) biodiesels are produced from microalgal biomass. The microalgae are a single celled photosynthetic aquatic micro-organism having the ability to convert CO_2 into oil through a photosynthetic process. It is capable of self-rejuvenation with a high growth rate (4 new cells per 17 to 20 hours). It has some remarkable advantages such as being very fast growing, containing high energy per unit mass, requiring less water per unit of biomass production, and being renewable and environmentally friendly. In addition, it consumes CO_2 as a nutrient which may contribute to reduce environmental GHG levels as reported by Hossain et al. (2008). It also has a very distinctive growth yield compared to classical lignocellulosic biomass (Lee and Lavoie, 2013, Brennan and Owende, 2010). The fuels that are related to algae biomass are also called oilgae (Demirbas, 2009b, Demirbas, 2011c). It is reported in the literature that microalgae is the 3G biodiesel feedstock (Zhao and Su, 2014, Azad et al., 2014b). The literature also reported that microalgae have higher biomass and lipid content capability per unit area compared to conventional crops (Chisti, 2007, Demirbas, 2010, Amin, 2009). It can grow using undeveloped land and water which is not suitable for food production, therefore reducing the strain on already depleted water sources (Azad et al., 2015c). Hossain et al. (2008) reported that microalgae oil potential production yield is 7 to 31 times higher than that of palm oil. The comparisons between vegetable oil and microalgae oil productivity are presented in Table 2.7. From the table it seems that microalgae can produce 58700 to 136900 litres of oil per hectare per year whereas palm, coconut, jatropha, olive, canola can produce only 5950, 2689, 1992, 1212, 1190 litres of oil per hectare per year, respectively (Demirbas, 2011a, Azad et al., 2015c).

Table 2.7: Oil yield and land usage for vegetable oil resources compared with microalgae

Feedstock	Scientific name	Oil yield (Litres/ha)	Required land for cultivation (M ha)	Percentage of existing US cropping area
Corn	*Zea mays*	172.0	1540.0	84.6
Cotton seed	*Gossypium hirsutum*	325.0	-	-
Soybean	*Glycine max*	446.0	594.0	32.6
Sunflower	*Helianthus annuus*	952.0	-	-
Peanut	*Arachis hypogaea*	1059.0	-	-
Canola	*Brassica napus*	1190.0	223.0	12.2
Castor	*Ricinus communis*	1413.0	-	-
Jatropha	*Jatropha curcas*	1992.0	140.0	77.0
Coconut	*Cocos nucifera*	2689.0	99.0	54.0
Palm	*Elaeis guineensis*	5950.0	45.0	24.0
Microalgae	*Chlorella vulgaris*	58700.0	4.5	2.5
Microalgae	*Chlorella photothecoides*	136900.0	2.0	1.1

The lipid content in algae biomass is the key factor in their use to produce biodiesel. However, their harvesting and oil extraction techniques are highly complicated and costly which is one of the main drawbacks of algae biomass production. The species used for 3G biofuel production are reviewed here. A selection is arranged by descending order of their oil content in Table 2.8. A lot of research work has been conducted to develop algae oil extraction and conversion techniques with which to produce biodiesel. The literature reported that the algae species with the higher lipid contents are the primary potential source for biodiesel production (Demirbas and Fatih Demirbas, 2011, Halim et al., 2011). The physio-chemical fuel properties of the algae biodiesel satisfy the requirements of the biofuel standard ASTM D6751. For example, Chen et al. (2012b) investigated the fuel properties of *Chlorella protothecoides* and found satisfactory fuel properties including 65.20 wt% methyl oleate and 18.50 wt% methyl linoleate as predominant components. Sari et al. (2013) extensively studied enzyme assisted protein extraction from different oil seeds including microalgae and found that microalgae achieved the lowest protein yield. Talebi et al. (2013) investigated the fatty acid profile and lipid content of different groups of microalgae. Their research found the highest volumetric lipid content of about 79.08 $mgL^{-1}day^{-1}$ for *Chlorella vulgaris*. On the other hand, Seo et al. (2015) used pyrite (F_eS_2) for lipid extraction from microalgae for biodiesel production. They observed around a 90% biodiesel conversation rate during esterification from microalgae biodiesel conversation. No waste was produced during oil extraction and biodiesel conversion from microalgae feedstocks. After oil extraction, leftover materials are suitable for soil fertilisation or can be used for ethanol production (Demirbas, 2011c). Moreover, microalgae cultivation for biodiesel production is still under investigation for large-scale production under suitable conditions and technologies (Brunet et al., 2012, Zhu et al., 2013).

Recent studies have mainly focused on microalgae cultivation, harvesting, oil extraction and biodiesel conversion techniques. A few studies have been conducted on engine performance and emissions for selected species (Campbell, 2008, Mata et al., 2010). For instance, Tüccar and Aydın (2013) evaluated the diesel engine performance and emissions using microalgae biodiesel blends up to B50 and found significant improvement of the emissions level, however the product slightly reduced brake torque and power. Furthermore, the recent investigation shows that the use of this biodiesel can reduce air toxicity by about 90% compared with petroleum diesel. Tüccar et al. (2014a) experimented on a binary biodiesel (microalgae biodiesel and butanol) and diesel blends in a four cylinder diesel engine to observe engine performance and emissions. They found

that these blends caused a slight reduction of brake power and torque of the engine but emission levels were improved.

Table 2.8: List of the spaces used for 3G biofuel production in the literature

	Name of microorganisms	Oil content per tonne of biomass (w_t% dry mass)	Lipid content (%, w/w_{dw})	Lipid productivity (mg/L/day)	References
	Microalgae				
1.	*Schizochytrium sp.*	50.0-77.0	35.0-55.0	-	(Meng et al., 2009, Yan et al., 2014)
2.	*Botryococcus braunii*	64.0	25.0-75.0	-	(Balat, 2011)
3.	*Nitzschia laevis*	69.1	-	-	(Chen et al., 2008)
4.	*Neochloris oleoabundans*	35.0-65.0	29.0-65.0	90.0-134.0	(Yan et al., 2014, Goiris et al., 2012)
5.	*Chlorella vulgaris*	63.2	5.0-58.0	11.2-40.0	(Tran and Chang, 2014)
6.	*Parietochloris incise*	62.0	-	-	(Solovchenko et al., 2008)
7.	*Crypthecodium cohnii*	56.0	20.0-51.1	-	(Balat, 2011)
8.	*S. obiquus*	35.0-55.0	11.0-55.0	-	(Lardon et al., 2009)
9.	*Nannochloris sp.*	-	20.0-56.0	60.9-76.50	(Balat, 2011)
10.	*Nannochloropsis oculata*	50.0	22.7-29.7	84.0-142.0	(Crowe et al., 2012)
11.	*Nitzschia sp.*	45.0-47.0	16.0-47.0	-	(Yan et al., 2014, Balat, 2011)
12.	*Scenedesmus dimorphus*	16.0-40.0			(Mata et al., 2010)
13.	*Monodus subterraneus*	39.3	16.0	30.4	(Yan et al., 2014)
14.	*Cylindrotheca* sp.	16.0-37.0			(Meng et al., 2009)
15.	*Phaeodactylum tricornutum*	20.0-30.0	18.0-57.0	44.8	(Balat, 2011)
16.	*Chamydomonas reinhardtii*	25.3			(Siaut et al., 2011)
17.	*Haematococcus pluvialis*	25.0	25.0	-	(Scott et al., 2010, Razon and Tan, 2011)
18.	*Dunaliella primolecta*	23.0	23.1	-	(Balat, 2011)
19.	*Tetraselmis sueica*	15.0-23.0	8.5-23.0	27.0-36.4	(Balat, 2011)
20.	*Chlorella sorokiana*	22.0	19.0-22.0	44.7	(Yan et al., 2014, Wan et al., 2011)
21.	*Monallanthus salina*	> 20.0	20.0-22.0	-	(Balat, 2011)
22.	*Dunaliella salina*	14.0-20.0	6.0-25.0	116.0	(Scott et al., 2010)
23.	*Porphyridium cruentum*	19.3	9.0-18.8	34.8	(Yan et al., 2014)
24.	*Spirulina platensis*	5.0-17.0	4.0-16.6	-	(Yan et al., 2014)
25.	*Isochrysis galbana*	14.5	7.0-40.0	-	(Yan et al., 2014)
	Bacterium				
26..	*Arthrobacter sp.*	> 40.0	24.0-31.0	-	(Meng et al., 2009)
27.	*Acinetobacter calcoaceticus*	27.0-38.0	-	-	(Meng et al., 2009)
28.	*Rhodococcus opacus*	24.0-25.0	-	-	(Meng et al., 2009)
29.	*Bacillus alcalophilus*	18.0-24.0	-	-	(Meng et al., 2009)
	Yeast				
30.	*Rhodotorula glutinis*	72.0	-	-	(Meng et al., 2009)
31.	*Rhodotorula glutinis*	72.0	-	-	(Xue et al., 2010)
32.	*Rhodosporidium toruloides*	48.0-67.5	-	-	(Zhao et al., 2011, Wu et al., 2011)
33.	*Cryptococcus albidus*	65.0	-	-	(Meng et al., 2009)
34.	*Lipomyces starkeyi*	64.0	-	-	(Meng et al., 2009)
35.	*Candida curvata*	58.0	-	-	(Meng et al., 2009)

	Fungi				
36.	*Mortierella isabellina*	86.0	-	-	(Ruan et al., 2012)
37.	*Humicola lanuginosa*	75.0			(Meng et al., 2009)
38.	*Mortierella vinacea*	66.0	-	-	(Meng et al., 2009)
39.	*Aspergillus oryzae*	57.0	-	-	(Meng et al., 2009, Yan et al., 2014)
40.	*M. ramanniana*	54.2	-	-	(Yan et al., 2014)
41.	*Cunninghamella japonica*	50.0	-	-	(Yan et al., 2014, Lunin et al., 2013)
42.	*Cunninghamella echinulata*	46.0	-	-	(Fakas et al., 2008)
43.	*Mortierella alpina*	42.0	-	-	(Wynn et al., 2001)
44.	*C. bainieri*	38.0	-	-	(Yan et al., 2014, Taha et al., 2010)
45.	*Mucor rouxii*	32.0	-	-	(Jeennor et al., 2008)
46.	*Mucor circinelloides*	23.0	-	-	(Zhang et al., 2007)
47.	*Mucor* sp.	3.0-17.0	-	-	(Somashekar et al., 2003)

2.6. Selection of Prospective Biodiesel Feedstocks

Feedstock selection is one of the important and primary steps for biodiesel production. The feedstocks (as listed below) have been selected due to their higher oil yield, availability, sustainability, and excellent fatty acid composition and fuel properties (as discussed in Chapter 4). Considering the factors mentioned above, the study investigated some selected new feedstocks as well as some feedstocks which require more investigation for biodiesel production. The microalgae feedstocks were not selected for this study due to the highly complicated and costly cultivation, harvesting and oil extraction techniques which required some sophisticated equipment. These facilities were not available for this study. So, this study investigated the following prospective feedstocks in detail:

a) Mandarin (*Citrus reticulate*)
b) Crambe (*Crambe abyssinica*)
c) Tamanu (*Calophyllum inophyllum*)
d) Borage (*Borago officinalis*)
e) Avocado (*Persea americana*)
f) Bush nut (*Macadamia integrifolia*)

The study undertook a comprehensive literature survey on the selected feedstocks for appropriate oil extraction techniques followed by biodiesel conversion process and characterisation of the biodiesel as discussed in the following sections.

2.7. Oil Extraction Techniques

Oil extraction involves some preliminary steps such as feedstock preparation, kernel extraction, kernel drying and moisture control. Kernel drying is an important pre-treatment step for oil extraction. The moisture content directly influences the oil yield. Bhuiya et al. (2015c) and Jahirul et al. (2013) studied the effect of moisture content on oil yield for various feedstocks such as jatropha, beauty-leaf, karanja etc., and found maximum oil yield at an optimum moisture content of about 15% for mechanical and chemical extraction. There are many oil extraction methods available in the literature including mechanical extraction, chemical or solvent extraction and enzymatic extraction. These methods are briefly discussed below.

2.7.1. Mechanical extraction

Mechanical extraction is the most conventional oil extraction method in which a manual ram press or engine driven screw press is used. It is a widely used method and also called cold press oil extraction. It is reported in the literature that an engine driven screw press can extract more oil (68-80%) than a ram press (60-65%) (Azad and Prince, 2012, Shahid and Jamal, 2011). For instance, Jahirul et al. (2013) extracted oil from BLT using the screw press. The literature revealed that seed pre-treatment can enhance the oil yield by up to 89% (single pass) and 91% (dual pass) in a screw press (Achten et al., 2008a, Atabani et al., 2012). Singh et al. (2002) extracted oil from Crambe seed by screw press and found 69.0% to 80.9% oil yield from dried seed. Soto et al. (2007) experimented on Borage oil extraction by double cold pressing at 20.0% moisture content and found 77.7% oil yield by achieving 95.0% oil recovery. Various seeds required specially designed machines, however the yield is affected if used for other seeds. Oil extracted by this method sometime requires pretreatment such as screening and degumming.

2.7.2. Chemical extraction

Chemical extraction or solvent extraction is the technique of extracting oil from kernels using a liquid solvent, usually with a higher oil yield (Atabani et al., 2012). There are several factors which affect oil yield by this method, namely the type of solvent chosen, particle size, speed of shaking, time, temperature and agitation of the solvent. Rashid et al. (2013) examined the citrus seed oil yield by solvent extraction and found about 28.5% oil in the dry seed. Jahirul et al. (2013) used the chemical extraction technique for Tamanu using n-hexane to extract oil due to the higher oil yield of this method. Ortiz et al. (2004) applied a new method, namely microwave-squeezing, and compared it with hexane extraction of oil from Avocado pulp. They

found about 67% and 59% oil yield by microwave-squeezing and hexane extraction, respectively. Azad et al. (2016a) extracted oil from Bush nut by the n-hexane method and found about 73.07% oil yield from dry kernels. Three techniques described as soxhlet extraction, hot water extraction and ultrasonication are available in this method. Soxhlet extractors with n-hexane as the solvent have been used to extract oil from Drumstick tree, Sea mango, Niger, and Coriander (Kansedo et al., 2009, Moser and Vaughn, 2010, Rashid and Anwar, 2008, Sarin et al., 2009b). The literature reported that this technique is not cost effective on a small scale. However, this method is economic for large-scale production (more than 50 tons of biodiesel per day) as reported by Achten et al. (2008b). Atabani et al. (2013b) also noted some adverse environmental impacts such as higher specific energy consumption and waste water generation for this method. The process also emits higher amounts of volatile organic compounds and has some bad impacts on human health due to handling of the hazardous and inflammable chemicals associated with n-hexane (Izah and Ohimain, 2013).

2.7.3. Enzymatic extraction

Enzymatic oil extraction is a technique to extract oil from plant materials using suitable enzymes while crushing (Rosenthal et al., 2001, Shah et al., 2005). The process is environmentally friendly. However, the long processing time is the main disadvantage associated with this technique (Mahanta and Shrivastava, 2004). Shah et al. (2005) experimented on jatropha oil extraction using this method combined with ultrasonication. Factors such as pH, reaction temperature, reaction time etc. have a direct impact on oil yield in this method. The use of alkaline protease provides better results in aqueous enzymatic oil extraction. Additionally, ultrasonication pre-treatment is a more useful step in aqueous oil extraction (Atabani et al., 2012, Achten et al., 2008b, Shah et al., 2005).

In summary, mechanical extraction is simpler and cheaper than other techniques, however initial investment cost is higher. On the other hand, high oil yield has been found in chemical extraction, though the ongoing operating cost (i.e. cost of n-hexane) is higher. In addition, enzymatic extraction is cost effective for large scale production but higher time consuming. This study selected cold press for Mandarin peel oil extraction and the n-hexane chemical method for the other oil extractions due to the higher oil yield.

2.8. Biodiesel Conversion

The direct application of vegetable oil in internal combustion (IC) engines is not practical due to their high density, high viscosity, free fatty acid content, low volatility, and polyunsaturated characteristics as reported by Nigam and Singh (2011). To resolve these issues, a lot of effort has been made globally to improve vegetable oil fuel properties as a substitute for fossil fuel (Atabani et al., 2013b, Abbaszaadeh et al., 2012, Salvi and Panwar, 2012a). Four different methods (chemical cracking, thermal cracking, transesterification and dilution) have been developed to convert vegetable oil into biodiesel which are presented in Figure 2.6 (Atabani et al., 2013b, Moser, 2011). Lin et al. (2011) reviewed and compared these different methods and identified that transesterification is the most efficient conversion technique (Azad et al., 2016b).

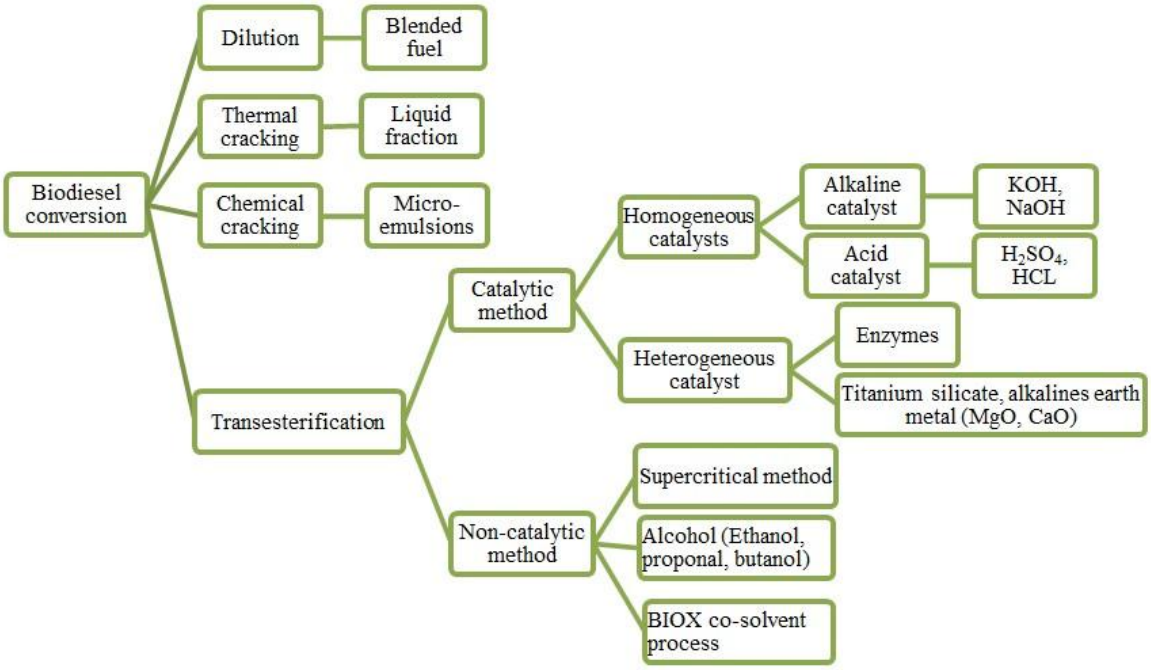

Figure 2.6: Biodiesel conversion techniques available in the literature

Transesterification is a bidirectional reaction which is widely used to convert triglycerides into methyl esters (Ghaly et al., 2010, Azad et al., 2015a). Figure 2.6 shows that there are two methods available namely catalytic and non-catalytic transesterification (Atabani et al., 2013b, Salvi and Panwar, 2012b, Yusuf et al., 2011). In the catalytic reaction, a catalyst is used to commence the reaction. Alkaline catalysts including KOH, NaOH, $KOCH_3$, $NaOCH_3$, and NaMeO (Rashid and Anwar, 2008, Demirbas, 2009a, Cao and Zhao, 2013) and acid catalysts

including hydrochloric acid, phosphoric acid, sulphuric acid, ferric sulphate are commonly used in the reaction (Lotero et al., 2005, Jothiramalingam and Wang, 2009).

High conversion yields of about 85-98% can be achieved by transesterification reactions (Atabani et al., 2013b, Atabani et al., 2012). Considerable efforts have been made to improve conversion rates by applying different techniques. For example, Atabani and César (2014) used a two stage method, i.e. acid catalyst esterification before alkali catalyst transesterification for Tamanu oil. They found 85% and 92% conversion yields, respectively. Rashid et al. (2013) also used two stage transesterification for Mandarin seed oil using 1% sodium methoxide catalyst with 6:1 methanol-oil molar ratio at 60 °C for one hour. They have not mentioned any conversion yield. Some research groups investigated Mandarin (*Citrus unshiu* species) peel waste to produce bioethanol (Choi et al., 2015, Kaur Sandhu et al., 2012). Single stage transesterification was used by Wazilewski et al. (2013), Knothe (2013b) and Azad et al. (2016a) for Crambe, Borage and Bush nut biodiesel conversion using various catalysts under standard reaction conditions. In addition, Knothe (2013a) extracted Avocado methyl ester by a two stage transesterification reaction with 1% sodium methoxide catalyst and 6:1 methanol-oil molar ratio at 65 °C for one hour. The literature also reveals that the above mentioned authors also investigated fatty acid methyl esters (FAMEs) composition and important fuel properties of their biodiesels. Characterisation of any new fuel is very important before application in a CI engine as is briefly discussed below.

2.9. Characterisation

The characteristics of the biodiesels need to be analysed to ensure the quality of the fuel. First of all, fatty acid composition analysis should be carried out in accordance with the European AOCS Ce1a-13 standard. The main physio-chemical properties such as calorific value, density, cetane number, viscosity, flash point, acid value, pour point, cloud point etc. are measured and compared with standard biodiesel. The property measurement should be followed according to the American Society for Testing and Materials standard (ASTM D6751-3) and the European Standard (EN 14214) for pure biodiesel (Atadashi et al., 2010, Sanjid et al., 2013). The density and viscosity are important physical properties which have direct impacts on fuel consumption and poor atomisation, vaporisation and mixing during combustion (Silitonga et al., 2013a, Sarin, 2012). The calorific value (CV) is another important thermodynamic property which indicates the total amount of heat contained in the fuel. The literature reports that biodiesel has a lower CV compared to fossil diesel, however, it also contains 10% to 12% self-oxygen

(Silitonga et al., 2013a). According to EN 14213, the minimum acceptable value for CV is 35 MJ/kg (Silitonga et al., 2013a). The cetane number (CN) indicates the ignition delay of the fuel. Higher CN implies shorter ignition delay and smoother combustion. It has been observed from the literature that the CN increases with increasing fatty acid composition, chain length, and saturation of fatty acids (Atabani et al., 2012, Keera et al., 2011). Biodiesel has higher CN than diesel fuel (Atabani et al., 2013b, Lapuerta et al., 2008b). The flash point is a safety indication for the fuel. The flash point of biodiesel is higher than diesel which denotes safer fuel. The detailed analysis of other important fuel properties is given in Chapter 4.

2.10. Engine Performance and Emissions Study

The use of biodiesel in diesel engines is not a recent innovation. Rudolf Diesel (1858-1913), the inventor of the diesel engine, first used peanut vegetable oil to validate his invention at Paris in 1900. Many modifications have been made to the diesel engine to improve engine efficiency and limit the emissions to produce an efficient modern diesel engine. Due to the lower energy content in the biodiesel, the main challenge is to obtain optimum efficiency for biodiesel fuelled engines (Murugesan et al., 2009). The literature reports that up to 20% biodiesel blends with fossil diesel do not require any modification of the engine combustion chamber (Jain and Sharma, 2010, Dantas et al., 2011). Higher blends and pure biodiesel usages in a CI engine requires engine modification (combustion chamber) to improve the engine efficiency as well as to limit the harmful emissions (Vashist and Ahmad, 2011, Qi et al., 2010). Tüccar et al. (2014b) experimented on four-cylinder diesel engine performance and emissions by varying the speed at full load condition. They extracted biodiesel from another Mandarin species (*Citrus sinensis*) and prepared three blends of B5, B10, and B20 for testing. Their results reveal that the tested fuel slightly reduced BP and BT as well as reduced CO emissions, but also increased NO_x emissions. Karthikeyan et al. (2015) experimented on a spark ignition engine using bio-ethanol produced from citrus peel waste by fermentation. The study found a lack of investigation on other performance and emissions parameters at full load as well as for variable load conditions. No experiment has been done to have been carried out on engine performance, emissions and combustion fuelled with Mandarin peel or rind aviation biofuel.

Rosa et al. (2014) investigated BSFC and engine efficiency as performance parameter and CO, NO, NO_x, and SO_2 emissions parameters for a diesel engine generator fuelled with 100% Crambe biodiesel at variable load conditions. They found engine performance compared

closely with diesel but with emissions reductions of 43.42% CO, 38.56% NO, 9.06% NO_x and 65.73% SO_2, respectively. Their study recommends more detailed investigation on engine performance, emissions and combustion by varying engine speed at particular loads for different blends. No study has been found on the combustion behaviour of this biodiesel.

Sahoo et al. (2007) have done an experiment on a single cylinder diesel engine using Tamanu biodiesel blends of B20, B40, B60, B80 and B100. An emissions and combustion study was carried out by Hassan et al. (2015) and Harch et al. (2014). They found that the optimum engine operating condition based on lower brake specific fuel consumption and higher brake thermal efficiency occurs at 100% load for pure biodiesel (Buyukkaya, 2010, M. Mofijur, 2013). A significant number of studies have been found for variable speeds, but a limited number of studies have been conducted on combustion characteristics of this fuel at partial load conditions.

This current study has found limited works on Borage and Avocado biodiesel conversion, FAMEs and fuel properties testing and virtually no study has been found on engine performance, emissions and combustion characteristics. On the contrary, Rahman et al. (2016b) examined engine performance for B5 and B20 Macadamia biodiesel blends at variable engine speed and undertook an emissions investigation for 800 rpm and 1400 rpm speed. More detailed research is required on emissions and combustion characteristics throughout the entire range of engine speed. This study also identified very limited information on engine performance, emissions and combustion at variable or partial engine load. The study also identified that NO_x emissions for biodiesel combustion is higher than for diesel, but can be reduced by modification of combustion techniques.

2.11. Combustion Analysis

In combustion analysis, the key parameters are cylinder pressure (CP), cylinder temperature (CT), heat release rate (HRR), ignition delay (ID) and combustion duration (CD) which are related to the in-cylinder combustion. Emissions formation is directly involved with combustion phenomena of the fuel. Biodiesel is an alternative fuel having different physio-chemical fuel properties to diesel and is used as a substitute for diesel fuel in CI engines (Azad et al., 2015c). Due to the different biodiesel fuel properties, the combustion phenomena are not same as for diesel fuel. For instance, Vallinayagam et al. (2014) studied pine biodiesel

combustion and identified the variation of CP and HRR with crank angle (°CA). Islam et al. (2015) described emissions parameters associated with the combustion of microalgae at variable load. They analysed CP and HRR at power stroke and found higher CP and lower HRR for algae biodiesel combustion. Gogoi and Baruah (2011) analysed combustion of Koroch biodiesel in a CI engine. They investigated start of injection, start of combustion, CP, HRR, cumulative heat release, ID and CD for the tested biodiesel blends. They found insignificant variation of CD up to 30% biodiesel blend, but shorter ID for biodiesel compared to diesel. Sajjad et al. (2015) analysed combustion phenomena of *Calophyllum inophyllum* biodiesel B20 blend in a four cylinder diesel engine. They investigated CP and HRR at power stroke for -20 °CA to 40 °CA and found higher CP and lower HRR for biodiesel. The combustion of biodiesel in a CI engine reduces some harmful emissions; however, it also increases NO_x emissions compared to fossil fuel which can be controlled by applying different combustion techniques (Kumar and Sharma, 2011, Fazal et al., 2011).

A lot of effort has been made by scientists and engineers to develop different combustion phenomena to understand the characteristics and behaviour of biodiesel combustion in CI engine (Agarwal et al., 2011). For example, Lai et al. (2011a) proposed an advanced chemical kinetic modelling of biodiesel combustion which will aid development of clean and efficient combustors. Over the past few decades, several combustion models have been proposed by different research groups (Veynante and Vervisch, 2002). For instance, Sun et al. (2010) investigated NO_x emissions using biodiesel blends. They reported some advantages of their combustion model which indicated some reduction of CO, CO_2, HC and PM emissions for the same fuel properties in a diesel engine. On the other hand, Banapurmath et al. (2012) experimentally investigated the effects of injection timing, injection pressure and compression ratio on engine performance and emissions parameters on a diesel engine fuelled with Honge biodiesel (Banapurmath et al., 2008a). Steinberg et al. (2012) reported on both the statistics and dynamics of turbulent flame alignment in premixed combustion of biofuel. They concluded that the orientation of turbulence structures was clearly affected by the flame surface. Further, Ranzi et al. (2012) proposed a hierarchical and comparative kinetic modelling of laminar flame speeds of hydrocarbon and oxygenated fuels.

On the other hand, Tran et al. (2012) demonstrated the quantifiable sooting propensity of biodiesel–diesel fuel blend flames using classical smoke point observations with the help of laser induced-incandescence and laser extinction optical techniques. Pandey et al. (2012) and

Varatharajan and Cheralathan (2012) studied biodiesel properties and emissions, analysing the impact of alternative fuel properties on fuel spray behaviour, atomisation and mixing. They also studied the effect of biodiesel fuel properties on NO_x emissions in a diesel engine (Bhuiya et al., 2015a). Benjumea et al. (2010) studied the effect of unsaturated biodiesel fuels on engine performance and emissions as well as combustion characteristics. This research group found that the degree of unsaturation has insignificant effects on the engine performance and the start of injection. They also identified that it had a noticeable impact on combustion characteristics and emissions due to the change of cetane number. They also observed that the higher degree of unsaturation of biodiesel led to longer ignition delay and consequently a more retarded start of combustion (Benajes et al., 2015, Benajes et al., 2014).

Lai et al. (2011b) reviewed the advanced chemical kinetic modelling for biodiesel combustion. They identified some key limitations of kinetic modelling such as (a) need for high-pressure kinetic methodology, and (b) need for continuous improvement of kinetic mechanisms with theoretical modelling validated by experimental results. On the other hand, Mohamed Ismail et al. (2013) developed a reduced chemical kinetics mechanism and validated it under zero-dimension and multi-dimension engine simulations for a range of engine operating conditions with B50 blends of coconut, palm, soy methyl esters biodiesel fuel (Puri et al., 2012, Sanjid et al., 2013). Their proposed mechanism was well matched for predictions of in-cylinder combustion and emission. Giakoumis et al. (2012) carried out a thorough review on exhaust emissions of diesel engines operating with biodiesel blends under transient conditions. They found a decreasing trend in PM, HC and CO emissions and an increasing trend in NO_x emissions (Giakoumis et al., 2012). Komninos and Rakopoulos (2012) reviewed the simulation models for homogeneous charge compression ignition (HCCI) biofuel combustion. Ra and Reitz (2011) developed a combustion model for multi-component fuels using the MultiChem mechanism. Their developed model was experimentally applied to simulate HCCI and direct injection (DI) engine combustion. They found that the model gives reliable performance for combustion predictions. A detailed chemical kinetic mechanism has been developed by Herbinet et al. (2010). They studied the oxidation of methyl decanoate, a surrogate for biodiesel fuel. Their proposed methyl decanoate mechanism can provide a realistic kinetic tool for biodiesel combustion in CI engines.

An et al. (2014) developed and discussed a tri-component skeletal reaction model for biodiesel combustion in diesel engines which consists of methyl decanoate, methyl-9-decenoate, and n-

heptane. They found that the developed model was able to give accurate predictions for ignition delay of n-heptane biodiesel. Sahoo and Das (2009) tested the combustion of non-edible filtered Jatropha, Karanja and Polanga oil based biodiesel blends with diesel as a substitute fuel in a diesel engine. They found that the ignition delay is shorter for pure Jatropha biodiesel than diesel. It varies between 5.9º and 4.2º crank angles, the difference increasing with load. Imtenan et al. (2014b) reviewed the impact of LTC attaining strategies on diesel engine emissions for both diesel and biodiesel blends. They reported that LTC strategies decrease NO_x and PM simultaneously, but slightly increase HC and CO emissions (Romeiro et al., 2012, Soloiu et al., 2013). The LTC models consist of longer liquid-fuel penetration and an extended ignition delay which allows more premixing of fuel. It also includes extended two-stage ignition which can be reduced to alter soot formation regions. Various biodiesel combustion models are newly developed, but every model has some limitations. Not a single model is perfect to describe the combustion phenomena of biodiesel in a CI engine.

Low Temperature Combustion (LTC) is a recently developed combustion strategy for biodiesel combustion. Though the LTC strategy reduces NO_x emissions, it still faces different challenges when implemented in real application vehicles. The study identified some drawbacks of the LTC strategy which are briefly discussed here. The literature shows that one of the main challenges is controlling the LTC combustion reaction which can badly affect engine performance (Carlucci et al., 2014). Under this strategy, BSFC is higher than for the ordinary combustion technique due to the higher EGR rate and later injection timing which lead to significant increases of UHC and CO emissions in the exhaust steam. Lower BT and BP are also recorded under the LTC strategy (Musculus et al., 2013). On the contrary, the installation of an LTC system creates a more complex engine system which leads to increased manufacturing costs of the engine. Biodiesel combustion under this strategy also leads to increased PM emissions by condensation of UHC. The main reasons behind these drawbacks are late injection timing, degree of atomisation and mixing of air-fuel during combustion. This study did not consider the LTC strategy for experimental investigation due to the number of drawbacks as presented above. However, it did consider the alternation of fuel properties technique through developing new blends for reducing emissions without any modification of the modern engine.

2.12. Tribological Study

The IC engine combustion system involves both moving and stationary parts such as the piston reciprocating inside the cylinder. When the engine runs, they produce friction forces which cause wear between the contact surfaces of the sliding components. Engine life and reliability degrades due to this effect which amplifies the maintenance cost of the engine. Lubrication undertakes an important role to minimise this effect. As a result, fuel (such as biodiesel) with self-lubricating characteristics can enhance engine life as well as improve engine durability and reliability. It is important to analyse the friction, wear and corrosive characteristics of any new fuel to maintain engine health before introducing it to the engine. The coefficient of friction and the wear scar diameter analysis quantifies the parametric analysis of friction and wear of the engine. In addition, cylinder metal surface morphology can be analysed by an optical microscope and scanning electron microscope (SEM) with energy dispersive X-ray spectroscopy (EDX) analysis. Recently, Mosarof et al. (2016c) investigated the friction and wear characteristics of *Calophyllum inophyllum* biodiesel B100 and palm biodiesel blend B10 and B20 at different temperatures and load conditions with constant speed. They found higher metal elements in pure biodiesel and lower metal elements in blends (Mosarof et al., 2016b). They also investigated lubrication characteristics of *Millettia pinnata* and rice bran biodiesel (Mosarof et al., 2016a). They found that *Millettia pinnata* resulted in a low coefficient of friction which indicates better lubricating performance and rice bran biodiesel demonstrated lower wear scar diameter. Fazal et al. (2010) were investigated the corrosive behaviour of biodiesel for long term durability of the engine moving parts. They experimented and compared corrosive characteristics of the tested biodiesel on aluminium, copper and stainless steel metal at 80 °C temperature for a period of 1200 h. They found that biodiesel does not attack stainless steel, but copper and aluminium were more susceptible to attack by the fuel in comparison to diesel. It is obvious that a tribological study of any new fuel is really important to ensure sustainable engine health.

2.13. Chapter Conclusion and Research Gaps

The extensive literature survey concluded that biodiesel could be one of the promising solutions for the world's large liquid fuel consumption in the transport sector. Biodiesel could be an alternative fuel in this sector to achieve a sustainable environment. The study reviewed over 150 species of biodiesel feedstocks and selected six most prospective feedstocks for further study. The biodiesel production steps of oil extraction, biodiesel conversion and

characterisation of the biodiesel are briefly described in this chapter. The study reviewed engine performance and emissions parameters. The widespread literature on combustion techniques that can be applied to mitigate emissions are presented. Finally, the study reviewed friction, wear, and corrosion behaviour by four-ball tests of other biodiesels which can be applied to the selected biodiesels to identify combustion surface morphology and self-lubricating characteristics for sustainable engine health. Based on the extensive literature review presented in this chapter, the following research gaps have been identified.

e) A limited number of studies are available on Mandarin oil extraction. Virtually, no study has been found on the production of "Aviation Bio-Gasoline" from Mandarin rind waste. No experimentation has been done using aviation bio-gasoline to investigate performance, emissions, combustion, and tribological (friction, wear, corrosion and lubrication) behaviour.
f) No study has been conducted on engine performance, emissions, combustion and tribological characteristics of Borage and Avocado biodiesels at variable speed and load conditions. This study also revealed that there are very limited studies available on the above-mentioned behaviour of the Crambe and Bush nut biodiesel and its blends at variable load conditions. Moreover, no study of friction, wear and corrosion behaviour of Tamanu biodiesel blends has been found in the literature.
g) No study has been found on the ternary mixture blends prepared from two biodiesels and an additive to improve fuel properties and reduce emission.
h) Very limited information is available on combustion modelling of the selected biodiesels and their blends.
i) No tribological study (such as friction, wear, and corrosion characteristics) has been found on the selected biodiesel blends and their mixture blends.

This study aims to address these gaps.

Chapter 3

EXPERIMENTAL PROCEDURE & MEASUREMENTS

This chapter discusses materials and methods used in this study. Complete methodologies for seed preparation, kernel extraction, drying, oil extraction and biodiesel conversion are presented. The appropriate method for fatty acid composition analysis and ASTM standards and European standards for determining physio-chemical fuel properties are outlined. The blend preparation process and the experimental neural network prediction technique are also presented. Furthermore, a test bed engine setup under ISO 8178-4 C1 testing method was used for engine performance; emissions and combustion studies of these biodiesel blends are also outlined. Tribological test parameters and methods are also briefly discussed.

3.1. Introduction

The study involves the experimental investigation of oil extraction, biodiesel conversion, engine performance, emissions, and combustion study as well as tribological characteristics of the biodiesel. This study has three key parts, namely fuel processing (including oil extraction and biodiesel conversion), characterisation (i.e. FAMEs and fuel properties) and engine performance, emissions and combustion study. The tribological characteristics of coefficient of friction, wear scar diameter and corrosive behaviour quantified by SEM/EDX are examined for the tested biodiesel. The steps of this research are briefly discussed below.

3.2. Materials and Methods

There are six biodiesel feedstocks that were selected for biodiesel production in this study. As discussed in Chapter 2, these feedstocks are Mandarin rind/peel, Crambe, Tamanu, Borage, Avocado (flesh) and Bush nut. The vegetable oils were extracted from different parts of the selected species. For instance, oil was obtained from the rind of Mandarin fruits, from Avocado flesh (no oil found in seed), and from Crambe, Tamanu, Borage, and Bush nut seeds. The Crambe and Borage oils were collected from Australian Wholesale Oils supplier in Australia. The seeds were collected from an Australian native plant supplier in Central Queensland, Australia. The Mandarin and Avocado fruits were collected from local farms in Central Queensland, Australia. The n-hexane and 98% concentrated methanol were supplied by Chem-supply in South Australia for oil extraction and chemical reaction, respectively. The KOH and N_aOH pellets were collected from a local distributor for this work.

3.2.1. Vegetable oil preparation

The vegetable oil preparation involves three main steps, namely kernel extraction, kernel drying, and oil extraction. Tamanu and Bush nut kernels were extracted from seeds, Mandarin peel from fresh fruits and Avocado flesh from waste Avocado fruits were sourced from farms. Then, the moisture was removed from the fresh kernel using a microprocessor temperature controlled incubator (IM550) at 60ºC for 24 hours before oil extraction. The kernels were crushed using a grinder to about 0.5-0.8 mm particle size to facilitate removing the moisture, uniform drying and maximising chemical contact surface area. Kernel drying is an important pre-treatment step for oil extraction because moisture content directly influences the oil yield. After achieving the optimum moisture content (around 15%), the dried kernels were crushed again to less than 0.5 mm particle size to maximise particle contact surface area. The oil was extracted by the n-hexane method. The acid value of the crude oils was determined before biodiesel conversion.

3.2.2. Biodiesel conversion

The biodiesel conversion is the most sensitive step in the fuel processing technique. Transesterification is one of the most efficient techniques to convert triglycerides into methyl esters and remove glycerine from the vegetable-oil (Figure 3.1). The biodiesel conversion requires some specific steps of chemical reaction, glycerine separation, and excess methanol removing, washing, and drying. The schematic diagram for biodiesel conversion is presented in Figure 3.2. The study also critically examined the effect of various reaction parameters such as catalyst concentration, methanol to oil molar ratio, reaction time and reaction temperature on the biodiesel conversion yield. The oil was preheated to 60°C before adding the catalyst. The potassium methoxide ($KOCH_3$) solution was prepared separately by adding 1%wt. KOH pellets into methanol (6:1 molar ratio of methanol to oil). The mixture was stirred on a hot plate until all the crystals were completely dissolved into the methanol. Then the $KOCH_3$ solution was slowly added into the preheated mandarin oil. The reaction temperature was maintained at 60ºC and stirred continuously at 750rpm for 60 minutes reaction time. The glycerine was separated in three different steps from the converted biodiesel. The unreacted methanol was removed by heating at 80°C for 1 hour. The remaining catalyst was also removed by washing with warm demineralised water several times in the separating funnel. Finally, the biodiesel was dried at 110°C for 45-60 minutes to remove moisture and residual water particles. The

total conversion yield of methyl esters was calculated using equation (3.1) (Ullah et al., 2015, García-Moreno et al., 2014).

$$Yield = \frac{M_{Biodiesel} \times C}{M_{Oil}} \times 100 \quad (3.1)$$

where $M_{Biodiesel}$ = mass of purified methyl esters obtained, C = fatty acid methyl ester content, M_{Oil} = mass of crude vegetable oil used.

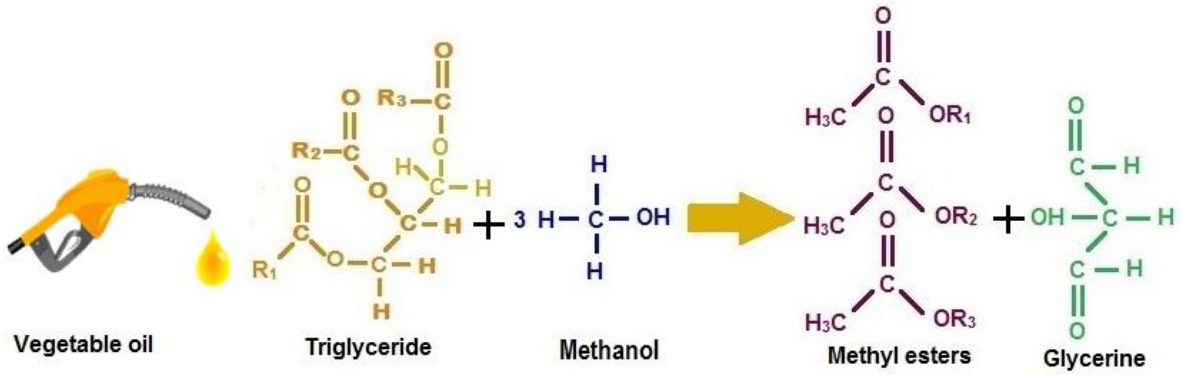

Figure 3.1: Transesterification reaction to convert vegetable oil to biodiesel

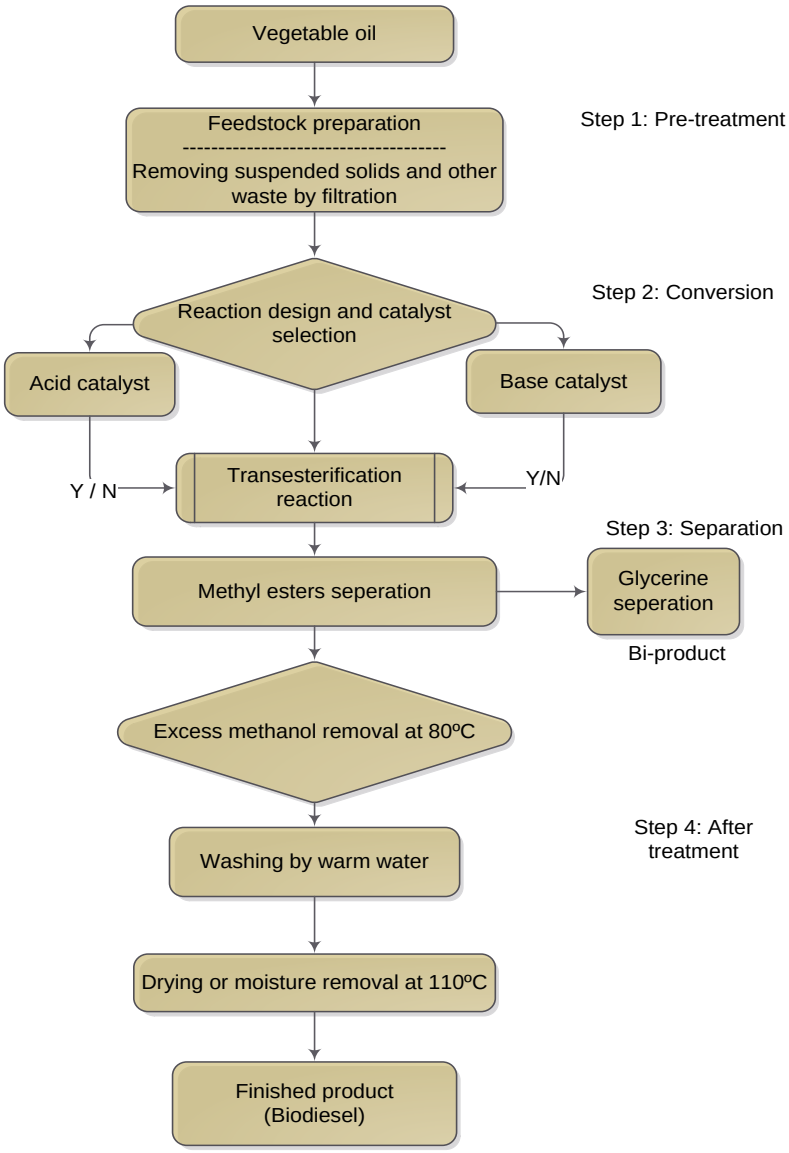

Figure 3.2: Schematic diagram for biodiesel production by transesterification reaction

After biodiesel conversion, the analysis of mass and energy balance for biodiesel conversion was carried out according to the input (feedstock) and output (final products) variables. It is very important to analyse total production loss to optimise the entire process. Mass balance is calculated numerically based on input mass of the feedstock and output mass of the products plus waste. On the other hand, the energy distribution is calculated based on input energy to the system (mass of feedstock x gross heating value) and output energy from the system. Total output energy is the summation of the energy (energy = mass × gross heating value) of the individual products, by-products, and waste. The mass and energy balances are calculated using the following equations (Kongkasawan and Capareda, 2012).

Mass balance:

% of mass recovery, $M_{recovery} = \frac{W_{output}}{W_{input}} \times 100\%$ (3.2)

% of mass loss = $100\% - \sum M_{recovery}$ (3.3)

Energy balance:

% of energy recovery, $E_{recovery} = \frac{W_{outtput} \times HV_{output}}{W_{input} \times HV_{input}} \times 100\%$ (3.4)

% of energy loss = $100\% - \sum E_{recovery}$ (3.5)

where W_{input} is the mass (kg) of input feedstock, W_{output} denotes total mass (kg) of output products (i.e. oil, biodiesel, glycerine etc.), $\sum M_{recovery}$ is the summation of mass recovery from all output products, HV_{output} is the heating value (MJ/kg) of the product and by-product, HV_{input} represents the heating value (MJ/kg) of the vegetable oil and $\sum E_{recovery}$ is the summation of energy recovery from all output products.

3.3. Characterisation of Biodiesels

The fatty acid methyl esters (FAMEs) compositions were identified using AOCS Ce 1a-13 standard methods. The key fuel properties of density, kinematic viscosity, calorific value, flash point, pour point, cloud point, acid value, carbon residue, cold filter plugging point were measured in accordance with the ASTM and EN standards. The behaviour of the fuel i.e. variation of density and viscosity at different temperatures (from 10 to 40°C) were investigated. In this study, some properties such as saponification number (SN), iodine value (IV) and cetane number (CN) were calculated numerically using Equations (3.6) to (3.8) (Fattah et al., 2014). The degree of unsaturation (DU) can be calculated with Equation (3.9) by considering monounsaturated and polyunsaturated fatty acids as reported by (Ramos et al., 2009).

Saponification number, $SN = \sum \left(\frac{560 \times A_i}{MW_i} \right)$ (3.6)

Iodine value, $IV = \sum \left(\frac{254 \times D_b \times A_i}{MW_i} \right)$ (3.7)

Cetane number, $CN = 46.3 + \left(\frac{5458}{SN} \right) - \left(0.225 \times IV \right)$ (3.8)

Degree of unsaturation = (monounsaturated Cn:1 wt.%) + 2 × (polyunsaturated Cn:2,3 wt.%) (3.9)

where, A_i indicates the percentage of each fatty acid component, MW_i is the molecular mass of each component by FAMEs analysis and D_b is the number of double bonds present in the component.

3.4. Blend Preparation

The biodiesel blends were prepared by volumetric mixing of pure biodiesel and ULSD which implies pure fossil diesel fuel. In this study, 5% by volume of biodiesel and 95% by volume ULSD is denoted as B5, 10% by volume of biodiesel and 90% by volume of ULSD is denoted as B10, and 20% by volume of biodiesel and 80% by volume of ULSD is denoted as B20. In addition, ternary mixture blends were prepared by an agreeable combination of two biodiesels (about 5% by volume), paraffin as an additive (about 4% by volume) and rest of the 91% ULSD. The study determined the make-up of these mixture blends by considering calorific values (CV) close to ULSD and keeping density and viscosity as low as possible. On this basis, the following four mixture blends were prepared. ManCr_Pa is the mixture of 3% Mandarin and 2% Crambe with 4% Paraffin and 91% ULSD. Similarly, TaMan_Pa, BoMan_Pa and AvBn_Pa mixture blends were prepared by mixing 3% Tamanu and 2% Mandarin, 3% Borage and 2% Mandarin, and 3% Avocado and 2% Bush Nut with 4% Paraffin and 91% ULSD, respectively. The blends were prepared in 5 litre lots and stirred by a magnetic stirrer at 750rpm at ambient temperature. The properties of the biodiesel blends were measured and compared with the ASTM D6751.

3.5. Test Engine Setup

A Kubota V3300 four stroke, four cylinder, direct injection (DI) diesel engine was used for examining engine performance, emissions and combustion characteristics of the prepared blends. The test engine was directly coupled to the dyno dynamics eddy current dynamometer. The schematic diagram of the experimental setup is presented in Figure 3.3. The detailed engine specification of the experimental setup is presented in Table 3.1. The torque was measured by the load cell located on the dynamometer arm. The fuel and air flow meter and the thermocouples in the exhaust stream were mounted with the engine to measure fuel consumption, inlet air flow, and exhaust gas temperature (EGT), respectively. The setup was computer controlled and collected all measured parameters using LabVIEW software and saved the data to the computer for analysis.

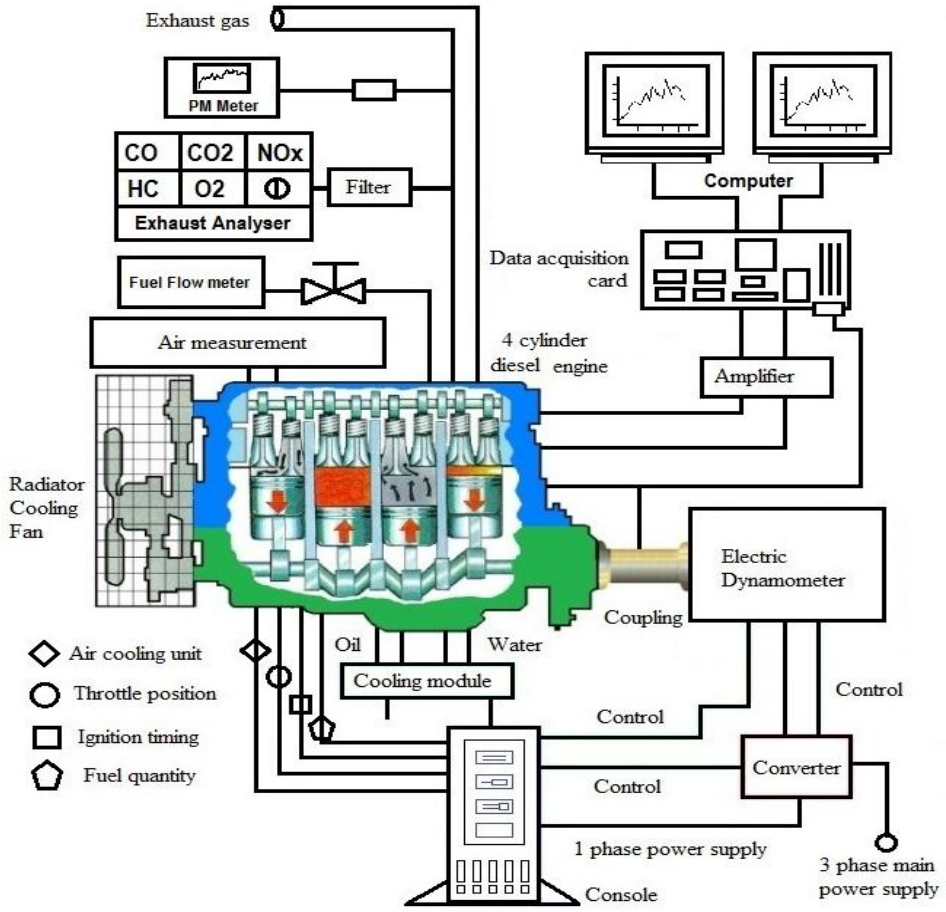

Figure 3.3: Schematic diagram of experimental setup

Table 3.1: Testbed engine specification

Items	Unit	Specifications
Type	-	Vertical, 4 stroke, liquid cooled
Bore × stroke	mm	98 × 110
No. of cylinders	-	4
Total displacement	L	3.32
Rated Torque	N. m/rpm	230/1400
Rated power output	kW/rpm	53.90/2400
Compression ratio	-	22.60:1
Fuel injection timing	-	16° before TDC
Injection pressure	MPa	13.73
Crank radius	mm	55.00
Connecting rod length	mm	170.00
Inlet valve (open / closed)	°CA	17° BTDC / 63° ABDC
Outlet valve (Open / closed)	°CA	51° BBDC / 28° ATDC

3.5.1. Emission analyser and particulate matter (PM) monitor

The exhaust gas emission analyser (Andros 6241A) was used to monitor harmful gas produced by combustion of the biodiesel. The analyser was capable of instantaneous readings of the exhaust gases including carbon monoxide (CO), carbon dioxide (CO_2), hydrocarbons (HC) using a non-dispersive infrared (NDIR) sensor. It can also measure excess oxygen (O_2) and nitrogen oxides (NO_x) using an electrochemical sensor. In this study, the particulate matter (PM) emission was monitored by a MAHA PM Meter for the range from less than 100 nanometers up to 10 microns. The detailed specification of the gas analyser and PM meter is presented in Table 3.2.

Table 3.2: Specification of the exhaust gas analyser and PM meter

Measured gas	Measurement		
	Range	Resolution	Accuracy
CO	0-15%	0.001%	±0.02% abs.
CO_2	0-20%	0.01%	±0.3% abs.
HC	0-30,000 ppm (n-Hexane)	1.00 ppm	±4 ppm abs.
NO_x	0-5,000 ppm	1.00 ppm	±20 ppm abs.
O_2	0-25%	0.01%	±0.1% abs.
PM	Particle size <100 nm to > 10 microns	Particle concentration range (0.1-> 700 mg/m^3)	Resolution ±0.1 mg/m^3

3.5.2. Combustion analyser (crank sensors and pressure sensors)

In combustion analysis, the in-cylinder pressure profile was monitored with respect to crank angle of the piston. Two independent devices were installed by TFX Engine Technology to monitor crank angle and cylinder pressure as shown in Figure 3.4. The crank sensor is mounted perpendicular to the crank trigger wheel which consists of 8 reflective and 8 non-reflective surfaces on the outer edge of the wheel to measure the crank angle of the engine. An Optrand H32218-GPA piezoelectric pressure sensor (pressure range: 0-3000 psi, install torque: 80 in-lbs, sensitivity: 1.29 mV/psi at 25°C and 1.26 mV/psi at 200°C) was mounted inside the cylinder head to measure in-cylinder pressure to evaluate the developed power of the engine. The pressure sensor used an optical fibre cable which is 1000 times faster than conventional pressure sensors. The mean values of a hundred consecutive combustion cycles of data for each

crank angle were recorded into the data acquisition and recording system for reliability of the data.

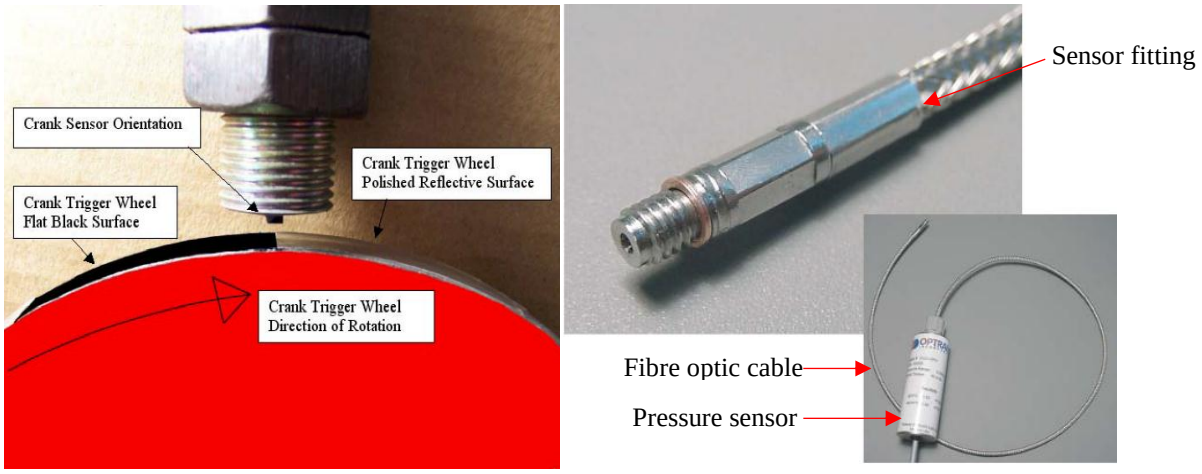

(a) (b)

Figure 3.4: Engine mounted (a) crank trigger and wheel, and (b) optical pressure sensor for cylinder pressure

The Heat Release Rate (HRR) was calculated using in-cylinder pressure data which was recorded by a highly sensitive high-speed pressure sensor as shown in Figure 3.4. HRR can be deduced from the first law of thermodynamics which is presented in Equation (3.10), assuming that no heat loss occurs from the system.

$$\frac{dQ}{d\theta} = \frac{V\frac{dP}{d\theta} + \gamma P\frac{dV}{d\theta}}{\gamma - 1} \tag{3.10}$$

where $\frac{dQ}{d\theta}$ is the heat release rate in J/°CA, V is the instantaneous cylinder volume in m^3, P is the instantaneous cylinder pressure in Pa (N.m), θ is the crank angle in °CA, and γ is the specific heat constant. It is reported in the literature that the value of γ is 1.35 (Sajjad et al., 2015). The values of V and $\frac{dV}{d\theta}$ are calculated using equations (3.11) and (3.12), respectively.

$$V = V_c + A.r\left[1 - \cos\left(\frac{\pi\theta}{180}\right) + \frac{1}{\lambda}\left\{1 - \sqrt{1 - \lambda^2 \sin^2\left(\frac{\pi\theta}{180}\right)}\right\}\right] \tag{3.11}$$

$$\frac{dV}{d\theta} = \left(\frac{\pi A}{180}\right) \times r \left\{ \sin\left(\frac{\pi\theta}{180}\right) + \frac{\lambda^2 \sin^2\left(\frac{\pi\theta}{180}\right)}{2 \times \sqrt{1 - \lambda^2 \sin^2\left(\frac{\pi\theta}{180}\right)}} \right\} \quad (3.12)$$

where V_c is the clearance volume, $\lambda = \frac{l}{r}$ where crank radius, $r = 0.50 \times stroke$ and l is the connecting rod length, and the area of the cylinder, $A = \frac{\pi D^2}{4}$ where D is the cylinder bore.

3.6. Uncertainty and Measurement Accuracy Analysis

The reliability of the measured data in the experiment can be verified by analysing the uncertainty of measuring equipment and the accuracy of the system. The uncertainties can be raised due to many causes such as instrument faults and calibration, test environment and condition (steady state or unsteady state), test strategy and plan, data reading and observation. The overall uncertainty implies the summation of individual uncertainties of the investigated parameters. The total percentage of uncertainty was calculated using the following equation.

Overall uncertainty = Square roof of [(uncertainty related to fuel consumption)^2 + (uncertainty of BP)^2 + (uncertainty of BTE)^2 + (uncertainty of HC emission)^2 + (uncertainty of CO_2 emission)^2 +(uncertainty of PM emission)^2 + (uncertainty of CO emission)^2 + (uncertainty of NO_x emission)^2 + (uncertainty of excess air factor λ)^2 + (uncertainty of EGT)^2 + (uncertainty of cylinder pressure)^2 + (uncertainty of crank trigger)^2 + (uncertainty of HRR)^2 + (uncertainty of friction coefficient)^2 + (uncertainty of wear scar diameter)^2]

= Square root of [$(0.10)^2$ + $(0.70)^2$ + $(0.90)^2$ + $(0.30)^2$ + $(0.02)^2$ + $(0.30)^2$ + $(0.80)^2$ + $(0.10)^2$ + $(0.40)^2$ + $(0.20)^2$ + $(0.90)^2$ + $(0.06)^2$ + $(0.05)^2$ + $(0.30)^2$ + $(1.50)^2$ + $(1.40)^2$]

= ± 2.73%

Hence, the total uncertainty of the experimental investigation was found to be ±2.73%. This could be acceptable because Sharma and Murugan (2015) and Mosarof et al. (2016b) calculated the total uncertainty of their experiments and found ±2.33%, ±4.48%, respectively.

3.7. Neural Network for the Experiment

An artificial neural network (ANN) is one of the prediction approaches that have been used to predict the performances of various thermodynamic systems. Recent progress shows that this technique is also used for modelling advanced thermodynamics systems in IC engine operation (Arcaklioğlu and Çelıkten, 2005). In particular, this approach is efficient for the prediction of engine performance and emissions characteristics of a diesel engine, specific fuel consumption, and air-fuel ration as well as in-cylinder combustion as reported by Canakci et al. (2006). Figure 3.5 illustrates the ANN for this experimental investigation.

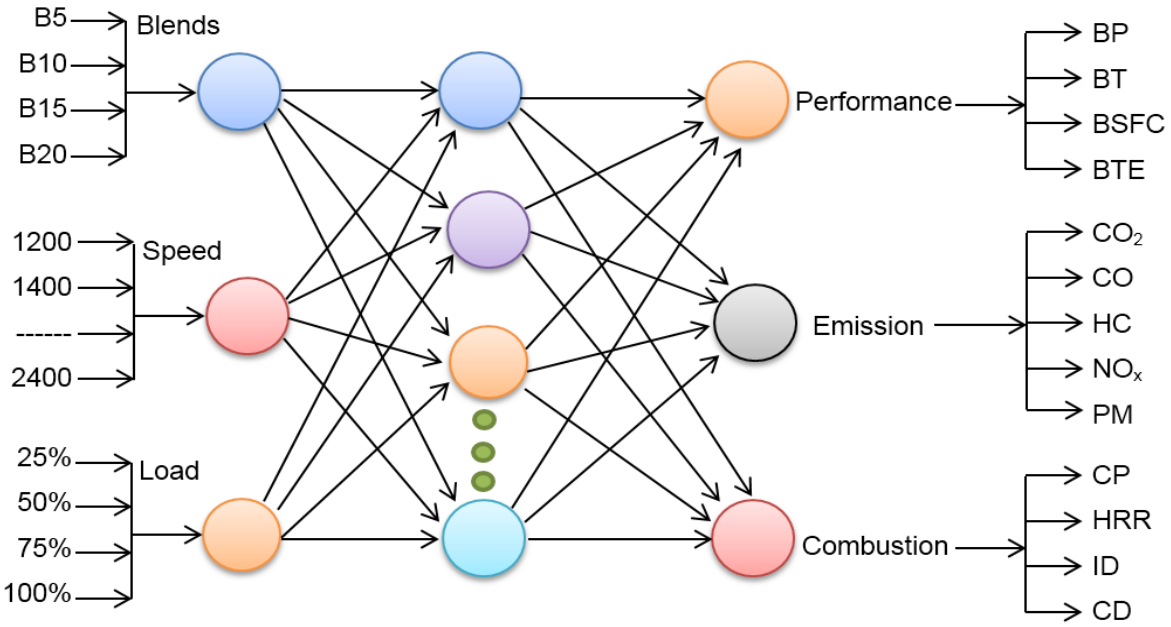

Figure 3.5: Neural network for the experimental test bed engine

The ANN was designed by considering three input variables of blend, speed, and load. For example, the fuel blend varies from B5 to B20 at particular speeds and loads. Then engine speed varies from 1200 rpm to 2400 rpm for a particular blend and load. Also, engine load varies from 25% to 100% at a particular speed for a particular blend. In short, when one variable varies then the other two were kept constant. For each case, performance parameter such as brake power (BP), brake torque (BT), brake specific fuel consumption (BSFC), break thermal efficiency (BTE) were measured. The emissions parameters of CO, CO_2, HC, PM and NO_x emissions were monitored by the exhaust gas analyser. In addition, combustion parameters including cylinder pressure (CP), HRR, ignition delay (ID) and combustion duration (CD) were measured and analysed in this study.

3.8. Tribological Study

The study aimed to analyse tribological characteristics of the tested fuels. The test was conducted with a four-ball tribotester (TR-30H) using the ASTM D4172 standard to obtain the friction and wear behaviour of the fuel. The test was conducted at 40 kg load and 1400 rpm at 75 °C speed for 1 hour. The friction coefficient can be expressed by Equation (3.20).

Coefficient of friction (COF), $$\mu = \frac{Torque(kg-mm)\times\sqrt{6}}{3\times Load(kg)\times Dis\tan ce(mm)} = \frac{T\sqrt{6}}{3Wr_c} \quad (3.20)$$

where T is friction torque in kg-mm, W is applied load in kg, r_c is the distance from the center of the lower ball contact surface to the axis of rotation in mm. The value of r_c = 3.67 mm was measured for the test setup. In addition, flash temperature parameter (FTP) is a critical flash temperature at which the fuel fails its lubricating properties. It can be expressed by a solitary number as calculated using Equation (3.21).

Flash temperature parameter, $$FTP = \frac{Load}{(WSD)^{1.4}} = \frac{W}{d^{1.4}} \quad (3.21)$$

where *d* is the wear scar diameter (WSD) in mm which is obtained from the optical microscope (model C2000, IKA, UK) with ±0.01mm resolution using ASTM D4172 method. The focal point on the surface of the ball can be adjusted to obtain a better quality of image for analysis. The WSD was calculated from the mean value of the wear diameter obtained from the image. Then the metal surface morphology of the tested balls was obtained using a scanning electron microscope (SEM) with energy dispersive X-ray (EDX) analysis. The images from the SEM/EDX test were analysed to obtain wear on the metal surface indicating the corrosive behaviour of the tested fuels. The assessment of the parameters mentioned above could help to improve engine health as well as the durability and total lifetime of the engine.

3.9. Chapter Conclusion

It can be concluded that the methodology followed in this study could be a pathway for evaluating new feedstocks for biodiesel production. The ANN could help in the efficient design of an experimental plan for investigation of performance, emissions and combustion parameters. The tribological study could help to investigate friction, wear and FTP properties of the fuel as well as metal surface morphology to assess engine health, durability and total lifetime.

Chapter 4

FUEL PROPERTIES AND BEHAVIOUR

This chapter deals with the fuel preparation, characterisation and behavior of the fuel. The vegetable oils were extracted by the n-hexane oil extraction method and converted to biodiesel by a transesterification reaction. In characterisation, fatty acid methyl esters were identified by the gas chromatography (GC) test using the AOCS Ce 1a-13 standard procedure. The fuel properties of the biodiesels and their mixture blends were tested and compared with fossil fuel and standard biodiesel using corresponding ASTM and EU standards. The behavior of the fuels was also investigated at various temperatures. The results are briefly discussed in this chapter.

4.1. Introduction

The study deals with six prospective feedstocks, namely Mandarin, Crambe, Tamanu, Borage, Avocado and Bush nut, for aviation bio-gasoline and biodiesel production. The vegetable oils were extracted from different parts of the species. For instance, the oil was extracted from peel or rind of Mandarin fruits, waste Avocado flesh (no oil found in seed), and Crambe, Tamanu, Borage, and Bush nut seeds. The Crambe and Borage oils were collected from Australian Wholesale Oils supplier in Australia. The seeds were collected from an Australian native plant supplier in Central Queensland, Australia. The waste Mandarin and Avocado fruits were collected from local farms at Central Queensland, Australia. The study found about 31% peel waste was obtained from fresh Mandarin fruits. The oil was extracted from the peel by mechanical cold pressing. The study found about a 1.03% oil yield from fresh Mandarin peel waste. The study also identified vegetable oil sourced from Mandarin seeds, but the feasibility of the oil and complexity of seed separation (an insignificant proportion of fresh seed content) from the waste makes it non-viable. This study conducted detailed analysis on peel or rind oil as there is a high possibility of producing aviation biofuel. This would help to manage the bulk green waste produced by juice factories in conjunction with extracting various by-products. For example, after oil extraction, the cake materials could be used as plant feed or green compost fertiliser.

Other oilseed feedstocks and waste Avocado flesh were prepared by extracting kernels and flesh, drying it, and determining the optimum moisture content to maximise oil yield as reported by Bhuiya et al. (2015c). The drying process was closely monitored at 60ºC for 24

hours by a smart incubator (IM550) to reach optimum moisture content as Bhuiya et al. (2015b) have done for other feedstocks. The study found 57.09% oil yield at 14.44% optimum moisture content for Tamanu, 73.08% oil yield at 13.34% optimum moisture content for Bush nut, and 65.21% oil yield for waste Avocado flesh by the n-hexane method. The study selected this chemical extraction for these three feedstocks due to their higher oil yields compared with mechanical extraction.

The extracted vegetable oils were converted to biodiesel by a transesterification reaction where triglycerides are converted to methyl esters and glycerine is removed (Ullah et al., 2015) as shown in Figure 4.1. It is important to check the acid value (AV) of the vegetable oils before proceeding to transesterification (Ghadge and Raheman, 2005). The AV of the crude oils were found to be less than one which indicates that single stage transesterification is needed for biodiesel conversion. The study followed the main steps shown in Chapter 3, Figure 3.2 for biodiesel conversion which is also illustrated as working steps in Figure 4.2. In the first step, the reactor setup was prepared with a three-necked glass reactor equipped with a Liebig condenser, thermometer (range 0-150ºC) and with a magnetic stirrer and heater (model: IKA C-MAG HS7). The conversion process was conducted in multiple batches (750 ml in each batch) to avoid any risk of saponification (the process that produces soap).

The conversion reaction was conducted in the presence of potassium methoxide ($KOCH_3$) as a catalyst with 6:1 methanol-oil molar ratio at 60°C temperature with 750 rpm stirring speed for 60 minutes. The $KOCH_3$ solution was prepared by adding 1%wt KOH pellets into methanol separately. After completion of the reaction, the glycerine was separated in three different steps of primary separation, secondary layer separation, and tertiary separation (by chilling and centrifuge machine at 7ºC and centrifuging at 5500 rpm for 20 minutes) as shown in Figure 4.2. Then the unreacted methanol or catalyst was removed by heating at 80°C for 1 hour and washing several times with warm demineralised water. The biodiesel was dried at 110°C for 45-60 minutes to remove moisture and residual water particles. After cooling to room temperature, a filtering process was conducted to remove impurities and ensure the excellent quality of the finished product. Finally, the finished product was stored in a closed container to avoid oxidation. The study followed the same procedure as for all biodiesel conversions. The properties of the biodiesel were tested and are discussed in the following section.

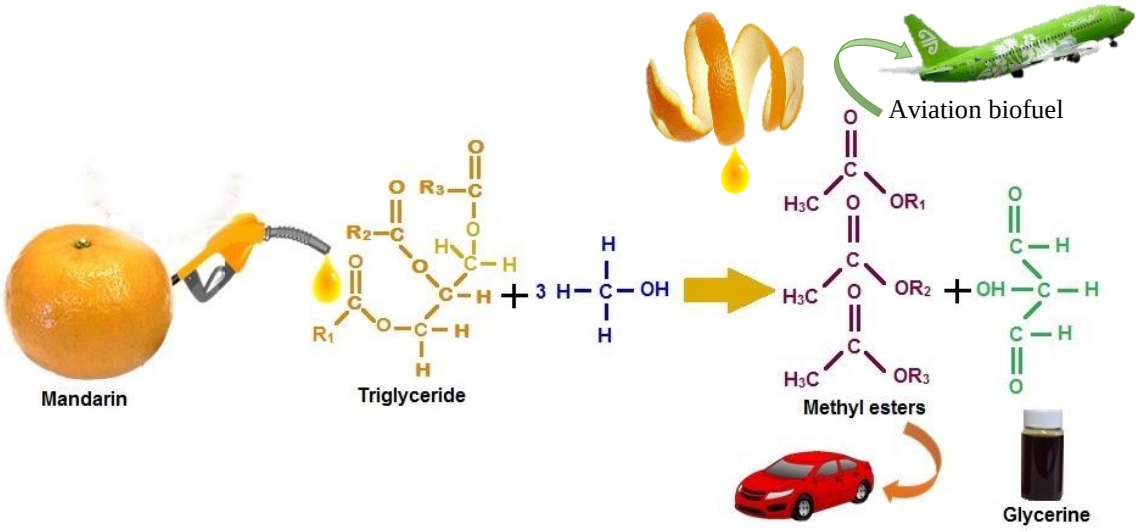

Figure 4.1: Transesterification reaction for biodiesel conversion

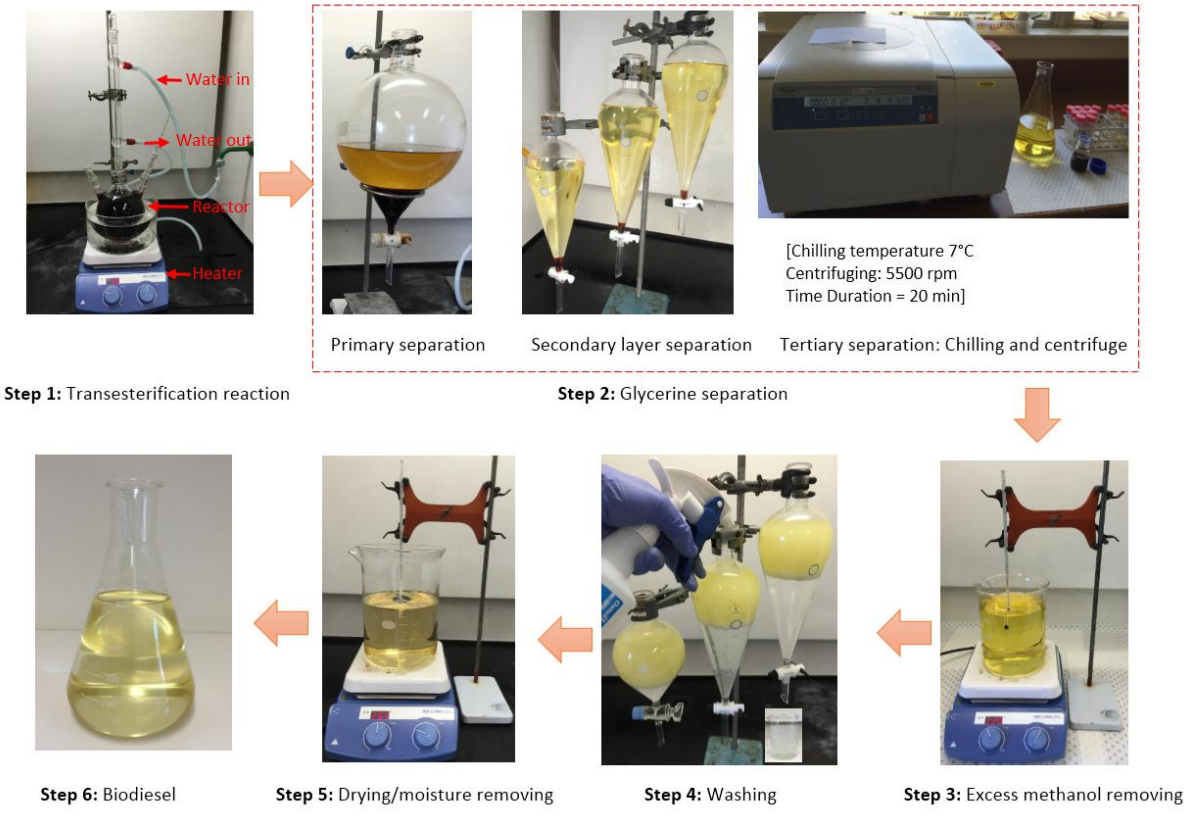

Figure 4.2: Biodiesel conversion steps for transesterification reaction

The optimisation of the conversion process was carried out by evaluating the effects of catalyst concentration, methanol-oil molar ratio, reaction temperature, and reaction time. The conversion yield was calculated using Equation 3.1. The study found conversion yields of 96.55% for Mandarin, 98.21% for Crambe, 86.72% for Tamanu, 97.79% for Borage, 98.37%

for Avocado and 95.11% for Bush nut at optimum reaction conditions. The conversion yield of Mandarin peel oil was calculated based on conversion mass only due to the very low ester content. The mass and energy balance was carried out using Equations (3.2) to (3.5) to identify the process loss of the conversion system. The CVs of the input and output materials were measured for the energy balance and to assess the fuel quality improvement which is presented in Table 4.1. The study found only 2% to 6% process loss for the crude oil to biodiesel conversion process. The study also identified that about 80% to 85% energy recovery is possible from biodiesel produced by this conversion technique.

Table 4.1: Gross heating value of the crude vegetable oils, biodiesels, and glycerine

Name of the product	CV (MJ/kg)					
	Mandarin	Crambe	Tamanu	Borage	Avocado	Bush nut
Crude oil	44.07	39.92	38.05	39.28	39.36	39.38
Biodiesel	44.66	40.63	38.54	39.94	40.00	39.88
Glycerine	23.92	22.35	20.67	21.74	25.02	24.50

4.2. Fatty Acid Methyl Esters (FAMEs) Composition

The analysis of FAMEs was conducted using a Shimadzu GC-2010 gas chromatograph (GC) equipped with 0.25mm × 25.00m inner diameter and 0.25μm film thickness capillary columns. The experiment was conducted using the AOCS Ce 1a-13 standard methods and the results are summarised in Table 4.2. The biodiesel samples were separated in the capillary gas-liquid chromatography column having a highly polar stationary phase, and analysed according to carbon chain length, the degree of unsaturation, plus the geometry and position of the double bonds present in the biodiesels. As seen from the table, there are three main types of fatty acids, namely saturated (Cn:0), monounsaturated (Cn:1) and polyunsaturated (Cn:2,3) which have two to three double bonds, which are identified in the biodiesels. On the contrary, the result also reveals that biodiesel contains an insignificant amount of arachidonic acid (C20:4) (0.03% vol. in Crambe and 0.07% vol. in Avocado) and eicosapentaenoic acid (C20:5) (0.22% vol. in Borage and 0.97% vol. in Bush nut) which have four and five double bonds, respectively. In addition, very low percentages of docosahexaenoic acid (C22:6) with hexa double bonds were identified in Mandarin (rind), Crambe, Borage, Avocado and Bush nut with about 0.16, 0.13, 0.09, 0.02, 0.02% by volume, respectively. The investigated biodiesels mostly contain a few fatty acids such as saturated palmitic acid (C16:0), monounsaturated oleic acid (C18:1), polyunsaturated linoleic (C18:2) and linolenic acid (C18:3) as highlighted (brown) in Table

4.2. In addition, saturated stearic acid (C18:0) and behenic acid (C22:0) are found to be 16.50% vol. in Tamanu and 57.69% vol. in Crambe, respectively. It should be noted that Avocado and Bush nut biodiesel contain about 70.43% vol. and 61.09% vol. of oleic acid, respectively which are much higher than the other biodiesels.

Table 4.2: FAMEs composition of the biodiesels tested by AOCS Ce 1a-13 standard methods

Fatty acid name	Lipid	Relative contents (% vol.) in biodiesel					
		Mandarin	Crambe	Tamanu	Borage	Avocado	Bush nut
Hexanoic acid	C6:0	0.08	-	-	-	-	-
Caprylic acid	C8:0	-	-	-	-	0.02	-
Capric acid	C10:0	0.04	-	-	-	-	-
Undecylic acid	C11:0	0.21	-	-	-	-	-
Lauric acid	C12:0	0.02	-	-	-	0.02	0.06
Myristic acid	C14:0	-	0.06	-	0.06	0.04	0.58
Tetradecenoic	C14:1	0.08	-	-	-	-	-
Pentadecylic acid	C15:0	0.74	-	0.10	-	0.02	-
Ginkgolic acid	C15:1	0.03	-	-	-	-	-
Palmitic acid	C16:0	**0.06**	**2.32**	**13.40**	**9.78**	**13.59**	**8.25**
Palmitoleic acid	C16:1	0.04	0.16	0.30	0.13	4.96	15.39
Margaric acid	C17:0	0.04	0.02	-	0.02	0.02	0.03
Ginkgolic acid	C17:1	0.02	0.04	-	-	0.11	0.08
Stearic acid	C18:0	-	0.89	**16.50**	-	-	3.55
Oleic acid	C18:1	**0.13**	**15.74**	**40.41**	**23.13**	**70.43**	**61.09**
Linoleic acid	C18:2	**0.21**	**10.15**	**26.22**	**36.53**	**9.18**	**1.86**
Linolenic acid	C18:3	**0.04**	**4.98**	**0.40**	**19.96**	**0.54**	**0.11**
Arachidic acid	C20:0	-	0.90	0.50	0.33	0.07	2.94
Eicosenoic acid	C20:1	-	1.06	0.30	4.07	0.22	2.55
Eicosadienoic	C20:2	-	0.18	-	0.16	-	0.06
Eicosatrienoic	C20:3	-	0.05	-	-	-	0.03
Arachidonic acid	C20:4	-	0.03	-	-	0.07	-
Eicosapentaenoic	C20:5	-	-	-	0.22	-	0.97
Heneicosylic acid	C21:0	-	0.05	-	-	-	-
Behenic acid	C22:0	0.02	**57.69**	0.20	2.61	0.07	0.04
Erucic acid	C22:1	0.03	0.65	-	0.02	0.02	0.16
Gadolenic acid	C22:2	-	0.04	-	0.03	-	0.13
Docosahexaenoic	C22:6	0.16	0.13	-	0.09	0.02	0.02
Tricosylic acid	C23:0	0.08	0.58	-	0.09	0.03	0.06
Lignoceric acid	C24:0	-	0.02	-	1.62	0.05	0.08
Nervonic acid	C24:1	-	-	-	0.12	0.14	0.13
Alpha pinene*		2.50	-	-	-	-	-
Limonene*		71.30	-	-	-	-	-
Gamma terpinene*		17.70	-	-	-	-	-

* Chemical composition measured by GC according to ISO 11024

The FAMEs results revealed that the fuel produced from Mandarin peel contains only 2.50% esters which has been identified using AOCS Ce 1a-13 standard methods. Further investigation was conducted to identify the total composition of the Mandarin fuel by applying different methods. Finally, the chemical composition was measured by GC using the ISO 11024 test procedure. The result revealed that it contains about 92% to 97% lighter hydrocarbons in the

range from C10 to C15. The chemical compositions are 2.50% alpha pinene, 71.30% limonene, and 17.70% gamma terpinene which are mainly $C_{10}H_{16}$ hydrocarbons with different carbon bonds and structures. The higher content of limonene indicates that it could have some other applications in the medical and cosmetics industries. Due to the higher content of the gasoline range hydrocarbons, this study predicted that the physio-chemical fuel properties are closer to aviation jet fuel which is briefly discussed in the following section. The study renamed the Mandarin rind biofuel as "Aviation Bio-Gasoline (ABG)". To present discussions in a simplified way, this aviation biofuel legend is referred to as "**Mandarin**" only throughout this thesis which will imply Mandarin ABG. To predict the fuel properties of the other synthesised biodiesels, the methyl esters of the tested fuels are presented in the triangular graph shown in Figure 4.3.

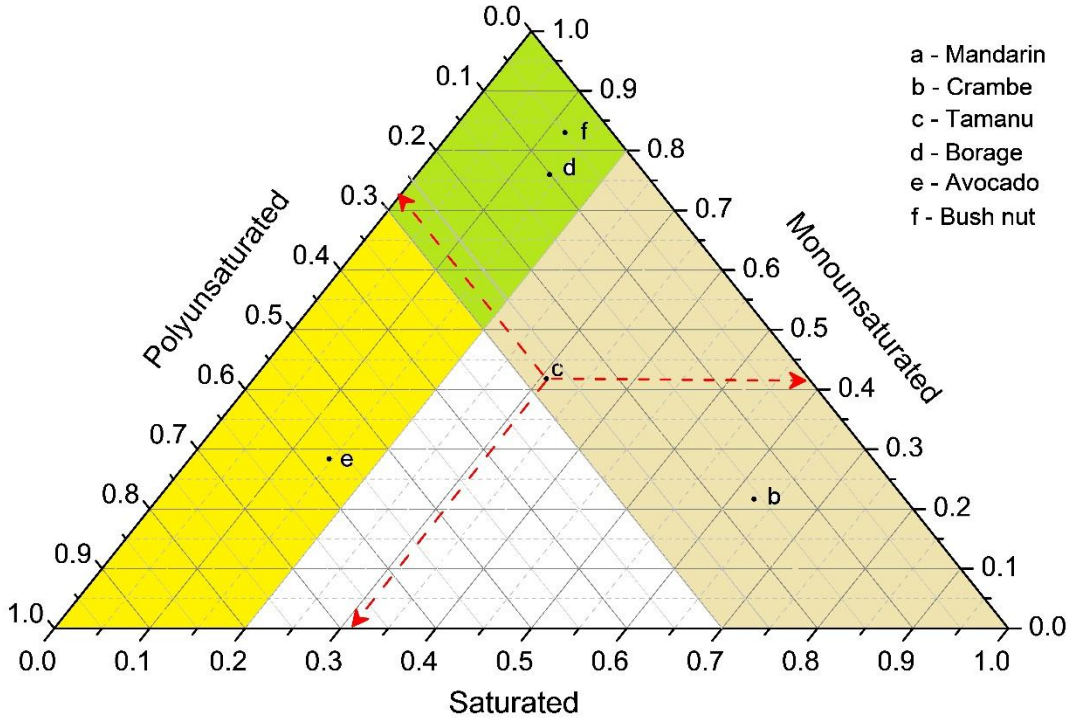

Figure 4.3: Triangular graph constructed with saturated, monounsaturated and polyunsaturated fatty acid content for tested biodiesels (coloured areas satisfy EN 14214)

The objective of Figure 4.3 is to illustrate biodiesels in groupings with similar properties and similar methyl esters content. In this graph, 0.1 denotes 10% and 1.0 denotes 100% in the scales for saturated, monounsaturated and polyunsaturated methyl esters. The coloured areas satisfy the parameters of the EN 14214 standard and indicate good CN values in the light brown area (on the right), good iodine values in yellow area (on the left) and good cold filter plugging

point (CFPP) values in the lime area (the overlap of brown and yellow areas) as reported by Ramos et al. (2009). The locations of the six chosen biodiesels are indicated by the points marked “a” to “f” as per the legend. By way of example, the dotted red arrows originate from point “c” which indicates the position of Tamanu biodiesel. As seen from Figure 4.3, all biodiesels are within the range of EN the 14214 standard except Mandarin which has disappeared from this figure due to its low esters content (about 2.5%). This also indicates that the Mandarin fuel properties are not compatible with standard biodiesel. It could be comparable with commercial jet fuel which is briefly discussed in the following section.

4.3. Fuel Properties

4.3.1. Aviation biofuel

The physio-chemical fuel properties of the produced aviation biofuel and biodiesels were measured using ASTM and EN standards. The results are presented in separate tables to compare Mandarin aviation biofuel with commercial jet fuel (Table 4.3) and other biodiesels with ULSD (Table 4.4). Table 4.3 demonstrates the important fuel properties of Mandarin aviation biofuel compared with those of commercial jet-A fuel as mentioned in World Jet Fuel Specifications by ExxonMobil (2016).

Table 4.3: Comparison of fuel properties of Mandarin aviation bio-gasoline and commercial jet-A fuel

Fuel properties	Unit	Mandarin aviation bio-gasoline	Commercial jet-A fuel*	Standard test method
Density (at 15ºC)	kg/m^3	838.00	775.00 - 840.00	ASTM D1298
Viscosity (at - 20ºC)	mm^2/s	2.13	Max 8.00	ASTM D445
Calorific value (CV)	MJ/kg	44.66	42.80	ASTM D4529
Flash point	ºC	52.00	Min 38.00	ASTM D56
Pour point	ºC	< - 27.00	Not defined	-
Cloud point	ºC	< - 40.00	Max-40 to-47	ASTM D4305
Acid value	mgKOH/g	0.22	0.10	ASTM D3242
Carbon residue	m/m	0.01	0.01	-
Sulphur content	Wt.%	0.00	Max 0.003	ASTM D1266
Oxygen content	%	11.65	0.00	-

* ExxonMobil aviation, World Jet Fuel Specification (ExxonMobil, 2016).

As seen from the table, the Mandarin aviation biofuel density is within the acceptable range and it has excellent viscosity. Its kinematic viscosity at -20 °C temperature was found to be 2.13 mm^2/s using the ASTM D445 standard which is about one-quarter of the maximum limit. Another fantastic finding is that this new fuel has about 4.34% higher CV (44.66 MJ/kg) compared to commercial jet-A fuel (42.80 MJ/kg). The study found the FP of the biofuel is 52 °C compared with the allowable minimum of 38 °C which indicates that Mandarin aviation biofuel is safer to handle and store compared to commercial jet fuel. The study found a slightly higher AV but it is not a big issue to neutralise the fuel. The result also revealed that it is a sulphur free fuel with 11.65% self-oxygenation compared to fossil jet fuel. The oxygen content in the aviation biofuel contributes to complete combustion and reduces emissions to minimise environmental pollution.

4.3.2. Biodiesels

4.3.2.1. Density

Table 4.4 shows the important physio-chemical properties of the biodiesels. The properties were measured using applicable ASTM and EN standards and the results are compared with ULSD and were found to be within the range of ASTM D6751 standard biodiesel. The density of the biodiesel was measured at 15ºC temperature using ASTM D1298 standard. The study found 832 kg/m^3 density for ULSD and 864 kg/m^3, 889 kg/m^3, 870 kg/m^3, 860 kg/m^3 and 868 kg/m^3 for Crambe, Tamanu, Borage, Avocado and Bush nut biodiesel, respectively. The results revealed that the biodiesel density is higher than ULSD but within the acceptable range (860 kg/m^3 to 890 kg/m^3) of the ASTM D6751 standard. The literature reported similar results for density; for instance, Rosa et al. (2014) found 872.0 kg/m^3 for Crambe, Atabani et al. (2014) measured Tamanu density of 877.4 kg/m^3 at 40°C temperature, Rachimoellah et al. (2010) measured 877.0 kg/m^3 for Avocado and Rahman et al. (2016a) found 859.0 kg/m^3 for Bush nut. This is an important property because higher density causes higher mass injection for the same volume at the same injection pressure as well as higher fuel consumption as reported by Ong et al. (2014). On the other hand, Saravanan et al. (2012) pointed out that higher density of biodiesel also increases NO_x emissions due to the following reasons:

- Higher density causes poor atomisation which results in larger fuel droplets which increase the physical delay between fuel injection and the start of combustion.
- The larger droplets also require a longer time for vaporisation of the fuel.

- The longer physical delay causes peak cylinder pressure rise as well as peak cylinder temperature increase which causes an increase in thermal NO_x emissions.

4.3.2.2. Viscosity

The kinematic viscosity is another impacting parameter for biodiesel combustion. Higher viscosity results in poor atomisation, vaporisation and uneven mixing which contribute to the incomplete combustion of the fuel as reported by Monirul et al. (2016). The kinematic viscosity was measured by an ARES rheometer at 40ºC temperature under the ASTM D445 standard. The results reveal that biodiesels have higher viscosity compared to ULSD and are within the acceptable range (3.50 to 5.00) of ASTM D6751 standard biodiesel except for Tamanu. The highest viscosity was measured at about 6.04 mm^2/s for Tamanu followed by 4.71 mm^2/s for Crambe, 4.57 mm^2/s for Bush nut, 4.35 mm^2/s for Avocado and the lowest viscosity of 3.65 mm^2/s for Borage biodiesel. The literature also reported similar results of viscosity for Tamanu of 5.74 mm^2/s measured by Atabani et al. (2014), Rosa et al. (2014) obtained a viscosity 6.00 mm^2/s for Crambe at 20 °C temperature, and Knothe (2013a) found 4.42 mm^2/s for Avocado biodiesel. The higher density and viscosity of the biodiesel is one of the reasons for their higher fuel consumption as discussed in Section 5.3 in Chapter 5.

4.3.2.3. Calorific value (CV)

The CV or gross heating value is one of the important fuel properties indicating the total amount of heat contained in the fuel. The study measured CV using an isoperibolic calorimeter (Parr 6400) with highly precise (0.10%) and 0.0001ºC temperature resolution in accordance with the ASTM D240 standard. The results reveal ULSD has the highest CV of about 45.67 MJ/kg compared with 40.63 MJ/kg, 38.54 MJ/kg, 39.94 MJ/kg, 40.00 MJ/kg and 39.88 MJ/kg for Crambe, Tamanu, Borage, Avocado and Bush nut biodiesel, respectively. Table 4.3 shows that the biodiesels have around 11.00% (Crambe), 15.60% (Tamanu), 12.50% (Borage), 12.40% (Avocado), and 12.70% (Bush nut) lower heat content compared to ULSD. A higher magnitude of CV implies better fuel efficiency. The literature reported that biodiesel should not have an energy content of less than 35.00 MJ/kg (Knothe 2010), however, neither ASTM nor EN standards have any specific limit. The CV of the fuel is also another key factor for total fuel consumption as reported in the literature (Monirul et al., 2016, Sajjad et al., 2015).

4.3.2.4. Cetane number (CN)

CN is a dimensionless number which quantifies the combustion quality of the fuel. Higher CN implies better combustion efficiency by shortening ignition delay as a result of prolonging combustion duration. Hence the ignition delay is inversely proportional to the CN as reported by Saravanan et al. (2012). The study measured CN in accordance with the ASTM D613 standard and found 44 for ULSD followed by 67 for Crambe, 53.0 for Tamanu, 51 for Borage, 61 for Avocado and 57 for Bush nut. All the chosen biodiesels satisfy the minimum CN limit of 47 in the ASTM D6751 standard. The results reveal that all the biodiesels have a CN higher than ULSD which has also been reported by many research groups in the literature (Knothe, 2014, Sánchez-Borroto et al., 2014).

4.3.2.5. Flash point (FP)

The FP implies the safety of the fuel for processing, handling, and storage. It is the temperature at which the oil starts to ignite in the presence of oxygen. The study measured the FP of the tested fuels using a flash point tester in accordance with the ASTM D93 standard. The results reveal that the FP temperature of 62 °C was found for ULSD whereas it varies from 52 °C to 96°C for conventional diesel. The study found higher FP temperatures for the biodiesels compared to ULSD, namely 190 °C for Crambe, 151° for Tamanu, 188 °C for Borage, 172 °C for Avocado and 135 °C for Bush nut. The biodiesel FPs all satisfy the minimum limit of 100 °C in the ASTM D6751 standard. The higher FP of biodiesel implies safer fuel compared to fossil fuel as has been reported in the literature (Rosa et al., 2014, Atabani et al., 2014).

4.3.2.6. Cold properties (pour point, cloud point, CFPP)

The physical behaviour of the fuel can be expressed by analysing density, viscosity and cold properties such as pour point, cloud point, and cold filter plugging point. These properties are important to analyse the behaviour of the fuel at different temperatures. The pour point indicates the minimum temperature at which the fuel loses its flow characteristics and becomes semi-solid. The pour point was measured using a pour point tester (TLC30) in accordance with the ASTM D97 standard and the results are presented in Table 4.4. The cloud point is the maximum temperature below which wax forms as a cloudy appearance in the fuel. The study measured cloud point with a cloud point analyser (PSA-70Xi) using the ASTM D5773 standard. The CFPP is a parameter which indicates the estimated lowest temperature at which the fuel gives trouble free flow under winter conditions. From Table 4.4, the biodiesels show

good cold properties except Tamanu. The results reveal 4.30 °C pour point, 13.20 °C cloud point and 10 °C CFPP for Tamanu which can be verified by the findings of Atabani et al. (2014). They found 11 °C pour point, 10 °C cloud point and 9 °C CFPP for Tamanu biodiesel. The other biodiesels can be used under any weather conditions.

4.3.2.7. Acid value (AV)

The AV of the fuel quantifies the total free fatty acid present in the biodiesel. Generally, it can be expressed as milligrams of potassium hydroxide (KOH) required to neutralise each gram of fuel. It is recommended that the AV of the biodiesel be lower than the maximum limit of 0.50 mgKOH/g set in the ASTD D6751 standard. The study measured the AV of the biodiesels using the ASTM D 664 standard method and found the AVs to be 0.13, 0.28, 0.09, 0.09 and 0.15 mgKOH/g for Crambe, Tamanu, Borage, Avocado and Bush nut, respectively. The low magnitude of the AV of the biodiesels implies that they are chemically stable fuels.

Table 4.4: Physio-chemical properties of biodiesel

Properties	Unit	ULSD	Crambe	Tamanu	Borage	Avocado	Bush nut	ASTM D6751
Density (at 15ºC)	kg/m^3	832.00	864.00	889.00	870.00	860.00	868.00	860-890
Viscosity (at 40ºC)	mm^2/s	4.10	4.71	6.04	3.65	4.35	4.57	3.5-5.0
Calorific value	MJ/kg	45.67	40.63	38.54	39.94	40.00	39.88	-
Cetane number	-	44.00	67.00	53.00	51.00	61.00	57.00	Min^m 47
Flash point	ºC	62.00	190.00	151.00	188.00	172.00	135.00	Min^m 100
Cloud point	ºC	-8.60	-2.00	13.20	- 1.00	-2.00	6.00	Report
Pour point	ºC	-15.00	0.00	4.30	- 6.00	- 6.00	-3.00	-
CFPP	ºC	-3.00	-5.00	10.00	-1.00	-1.00	-2.00	-
Acid value	mgKOH/g	-	0.13	0.28	0.09	0.09	0.15	Max^m 0.5
Carbon residue	m/m	0.01	0.01	-	0.01	0.01	0.01	Max^m 0.3
Ester content	%	-	95.75	98.96	99.62	99.64	98.21	Min^m 96.5
Free glycerol	Wt.%	0.00	0.003	0.01	0.00	0.00	0.00	Max^m 0.02
Total glycerol	Wt.%	0.00	0.08	0.11	0.09	0.05	0.13	Max^m 0.24
Saponification number	-	-	169.00	201.00	197.00	201.00	196.00	-
Iodine value	-	-	47.86	91.64	146.88	87.00	76.44	-
Degree of unsaturation	-	-	47.56	94.25	140.67	95.37	83.40	-
Fuel O_2 content	%	0.00	10.49	11.68	11.44	11.57	11.71	-

4.3.2.8. Ester content, free glycerol and total glycerol

The ester content in the biodiesels was measured in accordance with European Standard EN 14103. This study found 97.75% ester content in Crambe biodiesel, 98.96% for Tamanu, 99.62% for Borage, 99.64% for Avocado, and 98.21% for Bush nut. The biodiesels satisfy the

minimum ester content of 96.50% in EN 14214 standard biodiesel, however, no limit is defined in the ASTM D 6751 standard.

This study tried to remove glycerine by chilling at 7 °C temperature and centrifuging at 5500 rpm to remove glycerine completely. Then the study measured both free glycerine and total glycerine using the EN 14103 standard procedure to ensure higher quality biodiesel. The study found that the free glycerine was almost totally removed from each biodiesel except Tamanu. The latter contained about 0.01 wt.% free glycerine which is within the acceptable limit (Maximum 0.02 wt. %) of the ASTM D6751 standard. Further, total glycerine contents were 0.08%, 0.11%, 0.09%, 0.05% and 0.13% for Crambe, Tamanu, Borage, Avocado and Bush nut biodiesel, respectively. Total glycerine was found to be significantly lower compared to the maximum acceptable limit of 0.24% in ASTM D6751 standard biodiesel.

4.3.2.9. Saponification number (SN) or carbon chain length (CCL)

The SN is used to denote the CCL which indicates the mass of KOH required to saponify each gram of fatty acid methyl ester. The study calculated SN using Equation (3.6) and found about 169 for Crambe, 201 for Tamanu, 197 for Borage, 201 Avocado and 196 for Bush nut. Wang et al. (2016) reported that higher SN implies shorter CCL. In addition, Pham et al. (2013) pointed out that particulate matter (PM) emissions increase with the increase of carbon chain length. However, pollutant formation is also related to the number of double bonds present in the carbon chain which is briefly discussed below.

4.3.2.10. Degree of unsaturation (DU) and iodine value

The DU is an index of the number of double bonds present in the fatty acid chain of the biodiesel. The study calculated DU using Equation (3.9), and the results were verified by the iodine value which was also computed from Equation (3.7). The literature reported that iodine value can be used as an indicator of DU (Wang et al., 2016). Higher iodine values imply higher DU. In addition, higher DU denotes more double bonds present in the carbon chain. The study found iodine values of 47.86, 91.64, 146.88, 87.00, and 76.44 for Crambe, Tamanu, Borage, Avocado and Bush nut, respectively. The corresponding values of DU were found to be 47.56 for Crambe, 94.25 for Tamanu, 140.67 for Borage, 95.37 for Avocado and 83.40 for Bush nut. The results reveal that Borage biodiesel has a higher number of double bonds present in the CCL.

4.3.2.11. Molecular oxygen (O_2) concentration

As discussed above, biodiesel is mainly composed of long chain fatty acid methyl esters. This can be denoted by (-CHO-) whereas fossil fuel is denoted by (-CH-). It is clearly shown that the biodiesel molecule contains additional oxygen in the carbon chain whereas fossil fuel does not. For this reason, biodiesel is also called oxygenated fuel. This molecular O_2 is one of the reasons it is important to reduce emissions by enhancement of complete combustion. The study computed molecular O_2 concentrations from the FAMEs compositions of the biodiesels as presented in Table 4.2. The study found about 10.49% O_2 content in Crambe followed by 11.68% in Tamanu, 11.44% in Borage, 11.57% in Avocado and 11.71% in Bush nut biodiesel. It has also reported in the literature that the biodiesel contains about 10% to 12% more O_2 compared to fossil fuel (Silitonga et al., 2013a, Han et al., 2014).

4.4. Blend Sample Properties

The blends were prepared by mixing 5%, 10%, 15% and 20% of pure biodiesel into ULSD by volumetric ratio. The blending was conducted at an ambient temperature with a magnetic stirrer at 750 rpm for 20 min. The physio-chemical properties of the blends were extrapolated by numerical analysis of second order polynomial equations based on the measured data of pure biodiesel and ULSD. The results obtained by a curve fitting method were verified by randomly measured data to ensure the reliability of these results. This study considered the main fuel properties such as density, viscosity, CV and FP to assess the effect of biodiesel blend percentage on fuel properties. The results for biodiesel blends and the ternary mixture blends are presented in Table 4.5. As seen from the table, density and viscosity increase with the increase of biodiesel blends except for Mandarin. The viscosity and FP of the Mandarin blends decrease with the increase of blend proportion due to the lower viscosity and FP temperature of the Mandarin aviation biofuel compared to the other biodiesels as shown in Table 4.3. For those other biodiesels, CV decreases and FP increases with the increase of biodiesel blend percentages.

This study developed four ternary mixture blends described as ManCr_Pa, TaMan_Pa, BoMan_Pa and AvBn_Pa to closely match the CV of ULSD. The ternary blends are homogenous mixtures of two biodiesels (up to 5%) and paraffin (low density and viscosity with higher calorific value) as an additive (up to 4%). The density and viscosity of the mixture blends were kept as low as possible. This study was targeted to enhance combustion quality by

improving these two properties which directly impacted on combustion. The FP values of the mixture blends are slightly higher than ULSD which implies the blends are safer than ULSD. The physical behaviour of the developed biofuels at different temperatures were investigated which is briefly discussed in the following section.

Table 4.5: Physio-chemical properties of biodiesel blend and the mixture blends

Biodiesel	Blend	Density, kg/m^3	Viscosity, mm^2/s	CV, MJ/kg	FP, °C
Mandarin	B5	832.31	3.93	45.62	61.50
	B10	832.63	3.77	45.57	61.00
	B15	832.92	3.60	45.52	60.50
	B20	833.21	3.44	45.47	60.00
Crambe	B5	833.60	4.13	45.42	68.40
	B10	835.25	4.16	45.17	74.80
	B15	836.82	4.19	44.92	81.20
	B20	838.43	4.22	44.66	87.60
Tamanu	B5	834.84	4.19	45.31	66.50
	B10	837.71	4.29	44.96	70.90
	B15	840.57	4.39	44.60	75.40
	B20	843.42	4.49	44.24	79.80
Borage	B5	833.91	4.08	45.38	68.30
	B10	835.82	4.05	45.09	74.60
	B15	837.73	4.03	44.81	80.90
	B20	839.61	4.01	44.52	87.20
Avocado	B5	833.41	4.11	45.39	67.50
	B10	834.81	4.13	45.10	73.00
	B15	836.22	4.14	44.82	78.50
	B20	837.63	4.15	44.54	84.00
Bush nut	B5	833.84	4.12	45.38	65.70
	B10	835.61	4.15	45.09	69.30
	B15	837.42	4.17	44.80	72.90
	B20	839.22	4.19	44.51	76.60
Mixture blend					
ManCr_Pa		830.74	3.88	45.33	63.46
TaMan_Pa		831.88	3.89	45.29	62.71
BoMan_Pa		831.88	3.89	45.31	64.90
AvBn_Pa		831.48	4.01	45.28	65.96

4.5. Physical Behaviour of the Biodiesels at Various Temperatures

The study considered two properties which directly impact on combustion to assess the behaviour of the biodiesel at different temperatures. The physical behaviour means the variation of physical properties such as density and viscosity for different weather conditions throughout the year. For instance, a case study was done to identify the biodiesel behaviour for typical Australian seasonal weather conditions. According to the Australian Bureau of Meteorology (BoM), the average temperature range for winter is 8-15ºC, autumn is 15-23ºC, spring is 22-30ºC, and summer is 30-40ºC. Considering these temperature ranges, the study analysed the variation of density and kinematic viscosity of the aviation biofuel and biodiesel for the temperature range from 10ºC to 40ºC. These results are presented in Figures 4.4 and 4.5, respectively.

Figure 4.4 illustrates the close trend of density variation of Mandarin aviation biofuel with ULSD at different temperatures. As shown in Table 4.4, biodiesels have higher density compared to ULSD which is clearly presented in this figure where Tamanu biodiesel demonstrates high density compared to the other biodiesels. All the biodiesels show a similar trend of density variation with ULSD at various temperatures. According to the ASTM D1298 standard, Avocado biodiesel at 15ºC shows lower density and Tamanu shows higher density compared to the other biodiesels. Mandarin aviation biofuel shows a density close to ULSD from 20 °C to 30 °C temperature. The curves also imply that density decreases with increase in temperature. Hence, the derived biodiesels show similar behaviour to fossil fuel for typical Australian weather conditions.

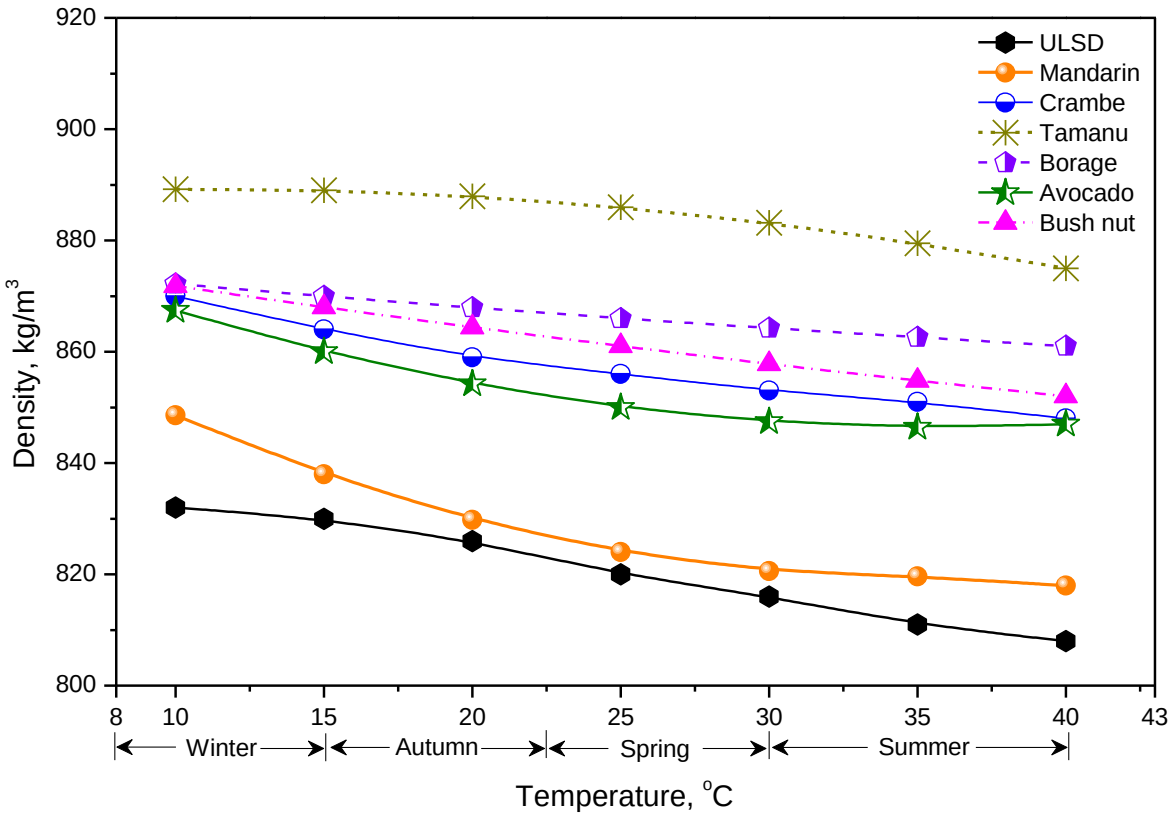

Figure 4.4: Variation of density with temperature

Figure 4.5 demonstrates the variation of kinematic viscosity with temperature from 10 °C to 40 °C. As seen from the figure, Mandarin aviation biofuel shows lower viscosity at each temperature compared to all the other fuels. However, it demonstrates a basically parallel trend with ULSD and their viscosity only slightly decreases with the increase of temperature. Generally, biodiesels show higher viscosity at a lower temperature which decreases with the increase in temperature. Borage and Avocado show close behaviour as do Crambe, and Bush nut over the full temperature range. The viscosity of Tamanu biodiesel is the highest throughout the entire temperature range. At 40 ºC temperature, the viscosity of Avocado and Bush nut is close to that of ULSD and Borage shows a slightly lower viscosity compared to ULSD. From this curve, it can be clearly seen that the biodiesels have a higher viscosity in winter compared with diesel fuel. It can be noted that the biodiesels behave very much like diesel in summer and the kinematic viscosity variation is within the range of 3.50 to 5.00 mm^2/s specified in the ASTM D6751 standard.

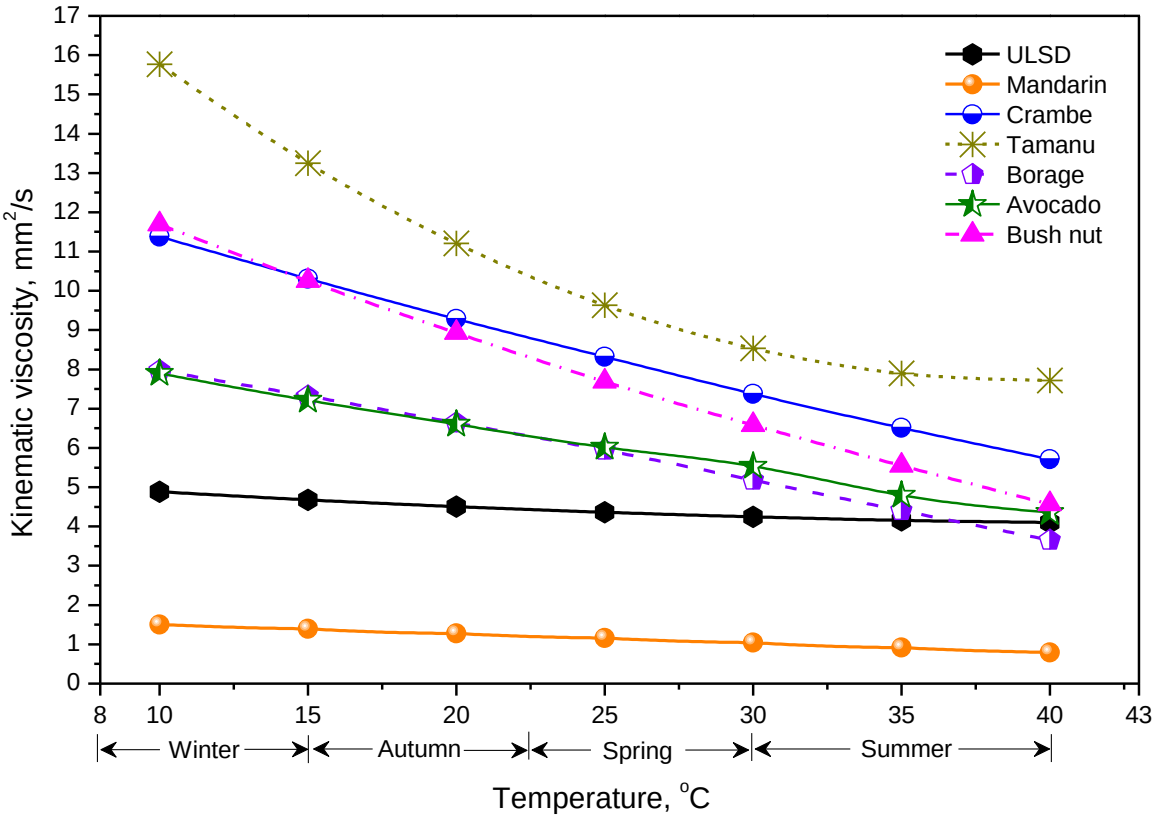

Figure 4.5: Variation of kinematic viscosity with temperature

4.6. Chapter Conclusion

The fatty acid composition of the biodiesels satisfies European standard EN 14214. The fuel properties of the newly developed aviation biofuel satisfy the requirements of commercial jet fuel. The biodiesels have satisfactory fuel properties within the acceptable range of the ASTM D6751 standard biodiesel. Their physical behaviours are similar to ULSD at a variety of temperatures. It can be concluded that the developed aviation biofuel from a new source could be one of the promising alternative jet fuels for the aviation sector in Australia. The biodiesels could be used as alternative fuels to meet the energy demand in the transport sector and minimise environmental pollution.

Chapter 5

ENGINE PERFORMANCE & EMISSIONS STUDY

This chapter deals with experimental results and discussion on engine performance and emissions of a 4-cylinder diesel test bed engine setup under ISO 8178-4 C1 engine testing procedure. The performance parameters such as brake power, brake torque, brake specific fuel consumption, brake thermal efficiency, etc. and emissions parameters such as CO, CO_2, HC, PM, NO_x, were investigated experimentally. The test parameters were measured by varying the biodiesel blend content (5% to 20%), and biodiesels-paraffin mixture blends in the engine speed range of 1200 rpm to 2400 rpm and engine loads in the range of 25% to 100%. The results are outlined and discussed in this chapter.

5.1. Introduction

The study investigated the effect of biodiesel blends on engine performance, emissions, and in-cylinder combustion. A Kubota V3300, 4-cylinder, 4-stroke, DI diesel test bed engine setup (Figure 3.3) was used in this study. The experiment was designed for a non-road steady state engine cycle using the ISO 8178 C1 test procedure to develop an experimental neural network (Figure 3.5) for optimising the investigated parameters. Utilising the neural network, three parameters of biodiesel blends (5% to 20%), engine speed (1200 rpm to 2400 rpm) and engine load (25% to 100%) were considered as input variables. For each case, output variables of performance, emissions, and combustion parameters were measured at steady state engine running conditions. In this chapter, the performance parameters of BP, BT, BSFC, and BTE are investigated. The emissions parameters, namely CO, CO_2, HC, PM and NO_x emissions, are discussed and compared between ULSD and the biodiesel blends. Combustion parameters of cylinder pressure, heat release rate, ignition delay and combustion duration etc. are outlined in Chapter 6.

Performance Analysis

5.2. Brake Power (BP)

5.2.1. Effect of biodiesel blends on BP

The BP is the usable final output power at the wheel of the engine. Figures 5.1 and 5.2 illustrate the variation of BP with biodiesel blends (B5, B10, B15, and B20 as well as biodiesels and

paraffin additive mixture blends) at the rated power (full load, 2400 rpm) and rated torque (full load, 1400 rpm) conditions, respectively. The mixture blends, namely ManCr_Pa, TaMan_Pa, BoMan_Pa and AvBn_Pa, were used to enhance performance and reduce emission as compared to B5 blends. The bar graphs are plotted for BP for better demonstration of the relative magnitude of the data between each pure blend as well as with the ternary biodiesel blends. The figures exhibit that the BP decreases with the increase in biodiesel blends (B5 to B20). The similar trend was also reported by Palash et al. (2015) and Abedin et al. (2014). The comparison of biodiesel BP with respect to ULSD is presented in Table 5.1. As is evident from the figures and tables, maximum BP reduction of about 2.6% to 6.2% and 0.8% to 2.1% (from B5 to B20) occurs for Tamanu biodiesel as compared to ULSD at rated power and rated torque conditions, respectively. On the contrary, minimum BP reduction of about 0.4% to 1.0% (B5 to B20) was found for Mandarin biodiesel and 0.4% to 0.9% for Borage biodiesel as compared to ULSD at rated torque and power conditions, respectively. The BP is reduced by the biodiesel blends due to their lower calorific value, higher density and viscosity as compared to ULSD as explained by Ong et al. (2014) and An et al. (2013). In this study, biodiesel blends were limited to a maximum of 20% because the literature reported that biodiesel can be blended up to 20% for use in a modern diesel engine without any major modification of the engine combustion system (Abedin et al., 2014, Ong et al., 2014).

The results also reveal that biodiesel-paraffin ternary mixture blends have insignificant BP reduction compared to ULSD for both test conditions. It can be seen from both figures that the mixture blends also yield better results [0.1% (Mandarin & Avocado), 0.2% (Crambe), 0.5% (Borage), 1.1% (Bush nut) and 2.0% (Tamanu) more BP] and 0.1 to 0.5% more BP as compared to each of the B5 blends at rated power and torque conditions, respectively. A noticeable BP improvement for the TaMan_Pa mixture blend (about 2.0% at rated power and 0.5% at rated torque condition) is observed for Tamanu biodiesel compared to Ta_B5 blend. This is due to the improvement of fuel properties such as lower density and viscosity of the mixture blend compared to the B5 blend. The mixture blends behave better with respect to in-cylinder combustion and their prolonged combustion durations are likely to increase BP. The study investigation on the variation of BP with different engine operating conditions (i.e. speed and load) is discussed as follows.

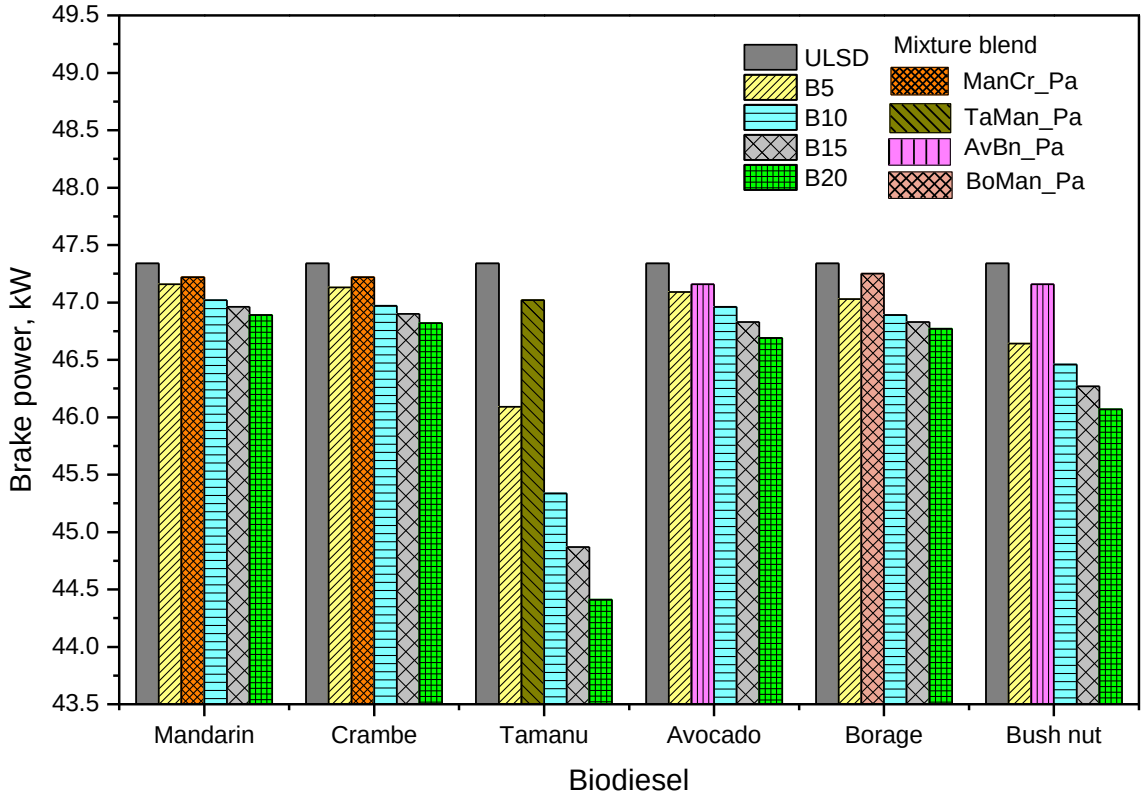

Figure 5.1: Effect of biodiesel blends on engine brake power at rated power condition at 2400 rpm

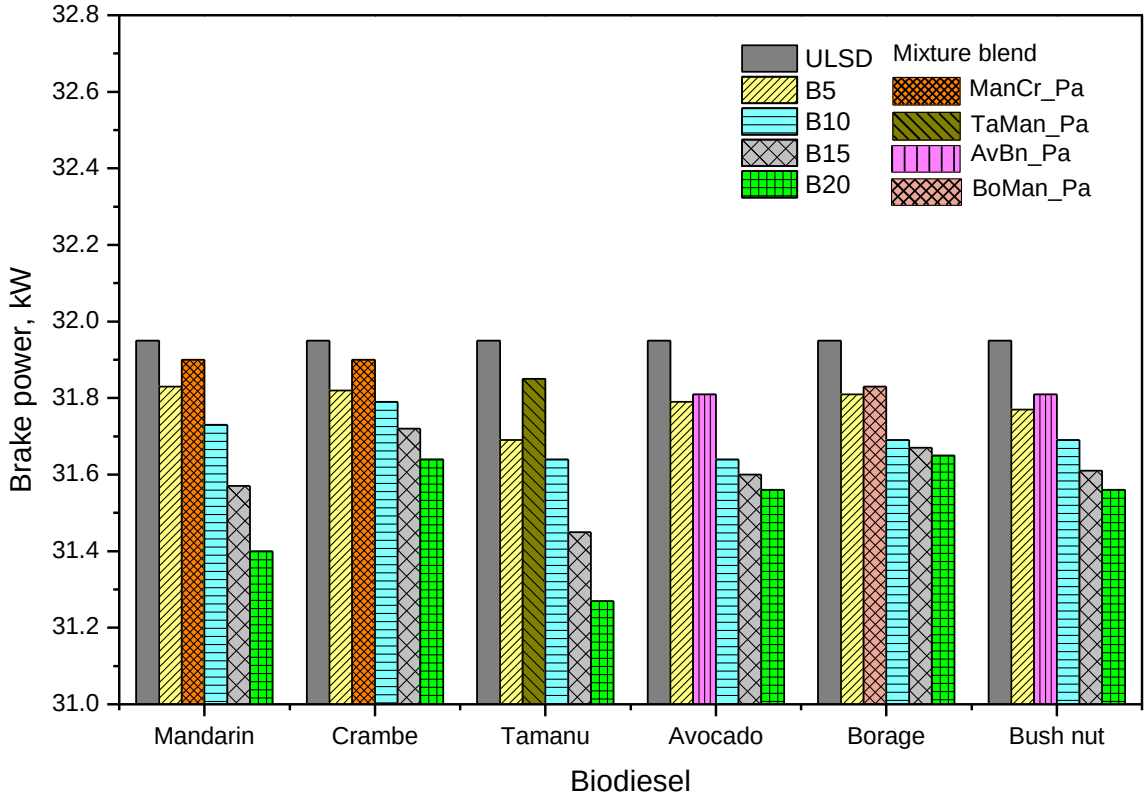

Figure 5.2: Effect of biodiesel blends on engine brake power at rated torque condition at 1400 rpm

Table 5.1: Summary of BP reduction by biodiesel blends as compared to ULSD

Biodiesel	Rated power				Rated torque			
	B5	B10	B15	B20	B5	B10	B15	B20
Mandarin	**-0.40**	-0.70	-0.80	-1.00	**-0.40**	-0.70	-1.20	-1.70
Crambe	**-0.40**	-0.80	-0.90	-1.10	**-0.40**	-0.50	-0.70	-1.00
Tamanu	-2.60	-4.20	-5.20	**-6.20**	-0.80	-1.00	-1.20	**-2.10**
Avocado	-0.50	-0.80	-1.10	-1.40	-0.50	-1.00	-1.10	-1.20
Borage	-0.70	-1.00	-1.10	-1.20	-0.40	-0.80	-0.90	-0.90
Bush nut	-1.50	-1.90	-2.30	-2.70	-0.60	-0.80	-1.10	-1.20

Note: *Negative sign (-) denotes reduction of BP. The minimum and maximum values are shown in bold.

5.2.2. Effect of engine speed on BP

Figure 5.3 shows the variation of BP at different engine speeds from 1200rpm to 2400rpm at full load condition for (a) Mandarin-Crambe, (b) Tamanu-Borage, (c) Avocado-Bush nut, and (d) biodiesels-paraffin mixture blends (B5, B20), respectively. The results reveal that the BP increases with the increase in engine speed which has also been pointed out by Buyukkaya (2010), and Aydın and Sayın (2014). The maximum BP was observed at rated speed of 2400 rpm for each fuel. ULSD shows the highest BP throughout the range of speed. The biodiesel blends follow the same trend with engine speed as ULSD. The trend implies that BP decreases with the increase in biodiesel blend percentage due to their lower heating value and unstable in-cylinder combustion behaviour as compared with ULSD (Ong et al., 2014, Muralidharan and Vasudevan, 2011). The summary of BP reduction compared to ULSD is shown in Table 5.2. As seen from the table and Figure 5.3 (a), Mandarin and Crambe biodiesel produced an average of 1.04% (B5) to 1.89% (B20) and 1.12% (B5) to 2.21% (B20) less BP compared with ULSD, respectively.

On the other hand, the ManCr_Pa mixture blend produced an average of 0.53% less BP as compared to ULSD, but 0.52% and 0.59% more BP than the Man_B5 and Cr_B5 blends, respectively. Figure 5.3 (b) demonstrates the maximum and minimum BP reduction by Tamanu and Borage biodiesel with an average of 1.75% (B5) to 3.71% (B20) and 0.69% (B5) to 2.27% (B20) compared to ULSD throughout the entire range of engine speed, respectively. In addition, the TaMan_Pa and BoMan_Pa mixtures produced about 0.67% and 0.31% higher BP as compared to Ta_B5 and Bo_B5, respectively. From Figure 5.3 (c), Avocado and Bush nut biodiesel produced an average of 1.21% (B5) to 3.11% (B20) and 1.99% (B5) to 3.37% (B20) less BP as compared with ULSD. Further, the AvBn_Pa mixture produced 0.90% and 1.69%

more BP as compared with Av_B5 and Bn_B5, respectively. Similar trends of BP variation were reported by Monirul et al. (2016) who did a comparative study on three different biodiesel blends with diesel at full load conditions. Figure 5.3 (d) presents the comparison of BP between mixture blends and ULSD. The results reveal that there are no noticeable differences between the mixture blends except for TaMan_Pa (about 1.0% less BP) as compared to ULSD throughout the entire range of engine speed. The study reveals better results for mixture blends due to their significant improvement of density and kinematic viscosity compared to B5 blends as discussed above.

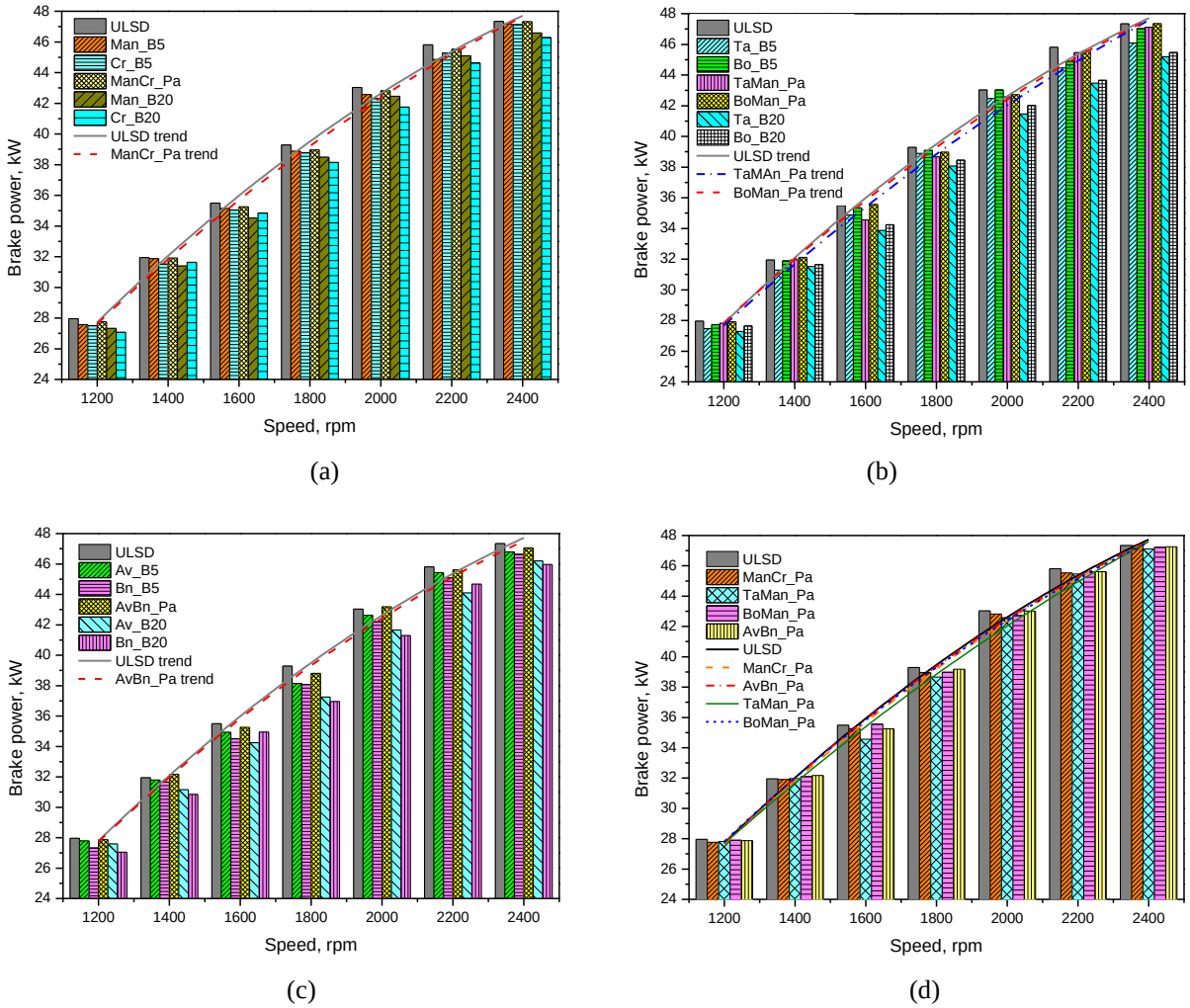

Figure 5.3: Variation of BP output at different engine speeds for (a) Mandarin-Crambe, (b) Tamanu-Borage, (C) Avocado-Bush nut, (d) Mixture biodiesels blends

Table 5.2: Summary of BP reduction (%) compared to ULSD throughout the entire range of engine speed

Compared with ULSD	Mandarin		Crambe		Tamanu		Borage		Avocado		Bush nut	
	B5	B20	B5	B20	B5	B20	B5	B20	B5	B20	B5	B20
	-1.04*	-1.89	-1.12	-2.21	-1.75	**-3.71**	-0.69	-2.27	-1.12	-2.79	-1.95	-3.02
Mixture name →		ManCr_Pa			TaMan_Pa		BoMan_Pa		AvBn_Pa			
Mixture/ULSD		-0.53			-1.07		**-0.37**		-0.44			
Mixture/B5		0.52**			0.67		0.31		0.68			

Note: *Negative sign (-) represents decrease and **positive sign (+) represents increase of BP.

5.2.3. Effect of engine load on BP

Figure 5.4 illustrates the comparison of BP at variable engine load conditions (25%, 50%, 75% and 100% at rated speed of 2400 rpm) for (a) Mandarin-Crambe, (b) Tamanu-Borage, (c) Avocado-Bush nut, and (d) biodiesels-paraffin mixture blends with ULSD. The trend implies that BP increases with the increase in engine load, but slightly decreases with the increase in biodiesel proportion (i.e. B5 to B20). A similar trend was also reported by Muralidharan et al. (2011) and An et al. (2013). ULSD produced elevated BPs of about 11.79 kW, 23.75 kW, 35.64 kW and 47.34 kW at 25%, 50%, 75% and 100% load, respectively. Table 5.3 demonstrates the summary of BP reduction by biodiesel blends as compared to ULSD. As seen from Figure 5.4 and Table 5.3, the maximum BP reduction occurs for Tamanu biodiesel with an average of 3.06% (B5) to 9.65% (B20) and the minimum reduction occurs for Borage 1.22% (B5) to 2.49% (B20) compared to ULSD throughout the entire range of engine load, respectively. Apparently, this BP reduction occurs due to the increase in density and viscosity and the decrease in calorific value associated with the increase in biodiesel blend. These findings are agreed with by many researchers in the literature (Ong et al., 2014, Monirul et al., 2016).

It is clearly seen in Figure 5.4 (d) that an insignificant variation of BP compared with ULSD was observed for mixture blends (average of 0.08% ManCr_Pa, 1.03% ManTa_Pa, 0.69% BoMan_Pa and 0.38% AvBn_Pa less BP) at variable engine load condition. On the other hand, the mixture blends enhanced BP as compared to each of their B5 blends. For instance, ManCr_Pa increased BP by about 1.61% compared to Man_B5, 2.11% (TaMan_Pa) in comparison to Ta_B5, 0.54% (BoMan_Pa) compared to Bo_B5 and 0.71% (AvBn_Pa) compared to Av_B5. This is due to the lower density and viscosity of all mixture blends as compared to each of their B5 blends (Chapter 4, Table 4.5), which promote enriched atomisation, vaporisation and mixing of the ternary mixture blends (Monirul et al., 2016). Due

to the improvement of these two fuel properties, mixture blends show shorter ignition delay and longer combustion duration as compared to both their B5 blends and ULSD which indicates better combustion behaviour of the mixture blends.

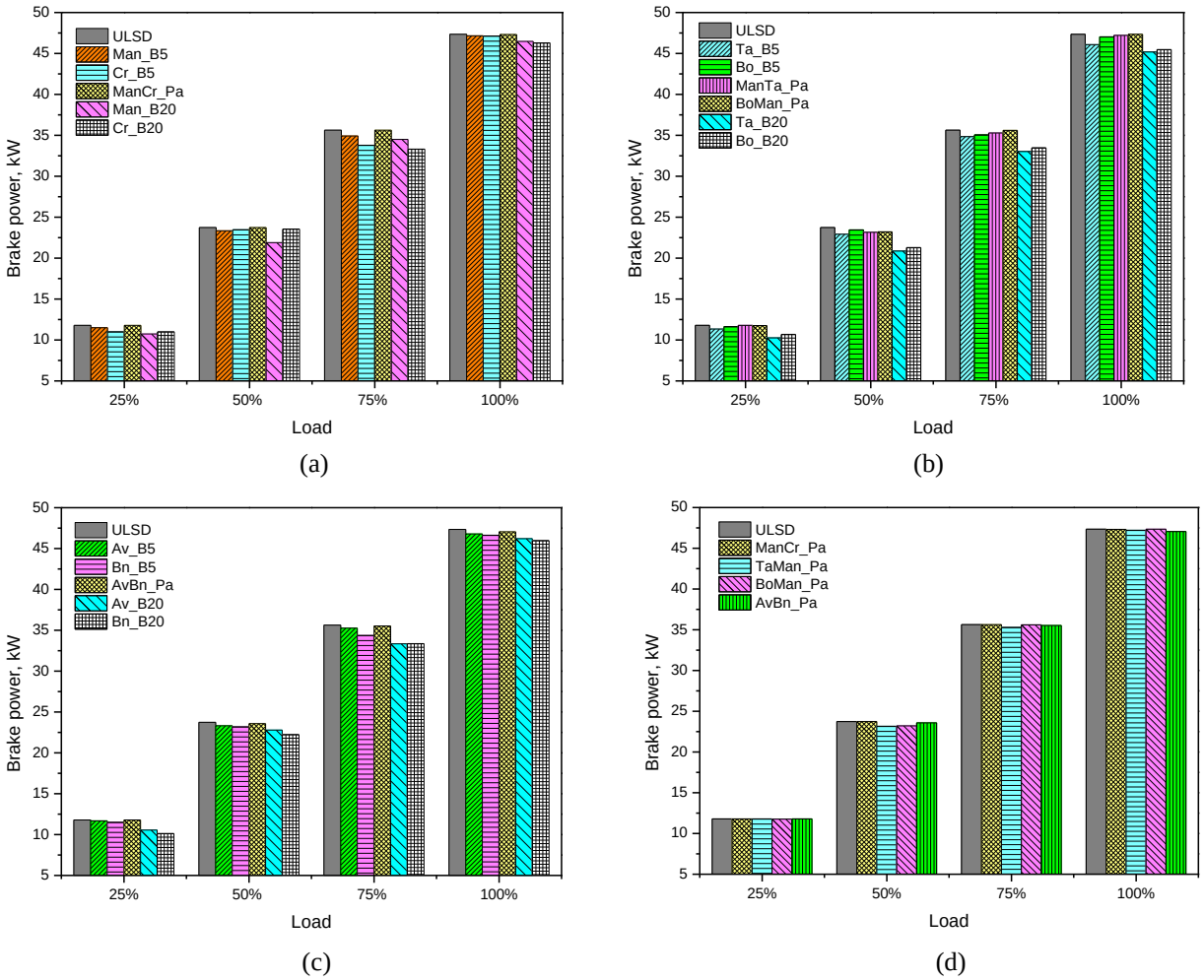

Figure 5.4: Variation of BP with engine load at rated power condition (2400 rpm) (a) Mandarin-Crambe, (b) Tamanu-Borage, (c) Avocado-Bush nut, and (d) Biodiesels-paraffin mixture blends

Table 5.3: Summary of BP reduction (%) compared with ULSD throughout the range of engine loads

Compared with ULSD	Mandarin		Crambe		Tamanu		Borage		Avocado		Bush nut	
	B5	B20	B5	B20	B5	B20	B5	B20	B5	B20	B5	B20
	-1.66*	-5.22	-3.37	-3.76	-3.06	**-9.65**	-1.22	-2.49	-1.08	-5.56	-2.44	-7.41
Mixture name →	ManCr_Pa				TaMan_Pa		BoMan_Pa		AvBn_Pa			
Mixture/ULSD	**-0.08**				-1.03		-0.69		-0.38			
Mixture/B5	1.61**				2.11		0.53		0.71			

Note: *Negative sign (-) represents decrease and **positive sign (+) represents increase of BP.

5.3. Brake Specific Fuel Consumption (BSFC)

5.3.1. Variation of BSFC with biodiesel blends

Figures 5.5 and 5.6 exhibit the variation of BSFC for biodiesel blends (B5, B10, B15, and B20) and biodiesels-paraffin mixture blends at rated power and rated torque conditions, respectively. The results reveal that BSFC increases with the increase in biodiesel blend. A similar trend was also reported by Ong et al. (2014), Aydın and Sayın (2014), and Sakthivel (2016). The increasing BSFC with biodiesel blends as compared to ULSD is summarised in Table 5.4. As seen from Table 5.4 and Figure 5.5, the maximum BSFC increase was found for Tamanu biodiesel and ranges from an average of 3.41% (B5) to 9.79 % (B20). The minimum BSFC was found for Avocado and ranges from an average of 0.83% (B5) to 3.97 % (B20) as compared to ULSD at rated power condition. The study also found that a significant increase in BSFC occurs at rated torque as compared to rated power condition for all biodiesels. For instance, the maximum BSFC at rated torque was found for Tamanu as being about 5.90% (B5), 8.61% (B10), 15.49% (B15) and 22.27% (B20) higher as compared to ULSD. On the other hand, the minimum increase of BSFC was found for Mandarin biodiesel as being about 4.10% (B5) to 7.61% (B20) higher than ULSD. This increasing BSFC trend is expected for biodiesel and could be due to a couple of main reasons: (a) the increase in density (kg/m^3), and (b) the decrease in calorific value with the increase of biodiesel blends. It is a known fact that the higher density biodiesel causes higher mass injection for the same volume at the same injection pressure as reported by Ong et al. (2014). The study found that the pure biodiesel (B100) contains about 10 to 15% less CV when compared with ULSD. In the literature, Roy et al. (2016) and Islam et al. (2015) reported about 12% and 15% less CV for canola and waste cooking biodiesel, respectively. This study experimentally investigated four ternary mixture blends to minimise the drawbacks as mentioned above. The density, viscosity and CV of the mixture blends are close to those of diesel. The results reveal that there is no noticeable (less than 1.00% except for Tamanu) variation of BSFC for the mixture blends as compared to ULSD at rated power conditions. However, the study identified about 1.36% (ManCr_Pa), 3.68% (TaMan_Pa), 2.25% (AvBn_Pa) and 2.97% (BoMan_Pa) higher BSFC as compared to ULSD at rated torque conditions. It can also be noticed that the mixture blends show about 2.63% (Man), 2.90% (Cr), 2.09% (Ta), 1.68% (Bo), 1.26%(Av) and 1.63% (Bn) lower BSFC as compared to each of their B5 blends due to the enhancement of the mixture blend properties.

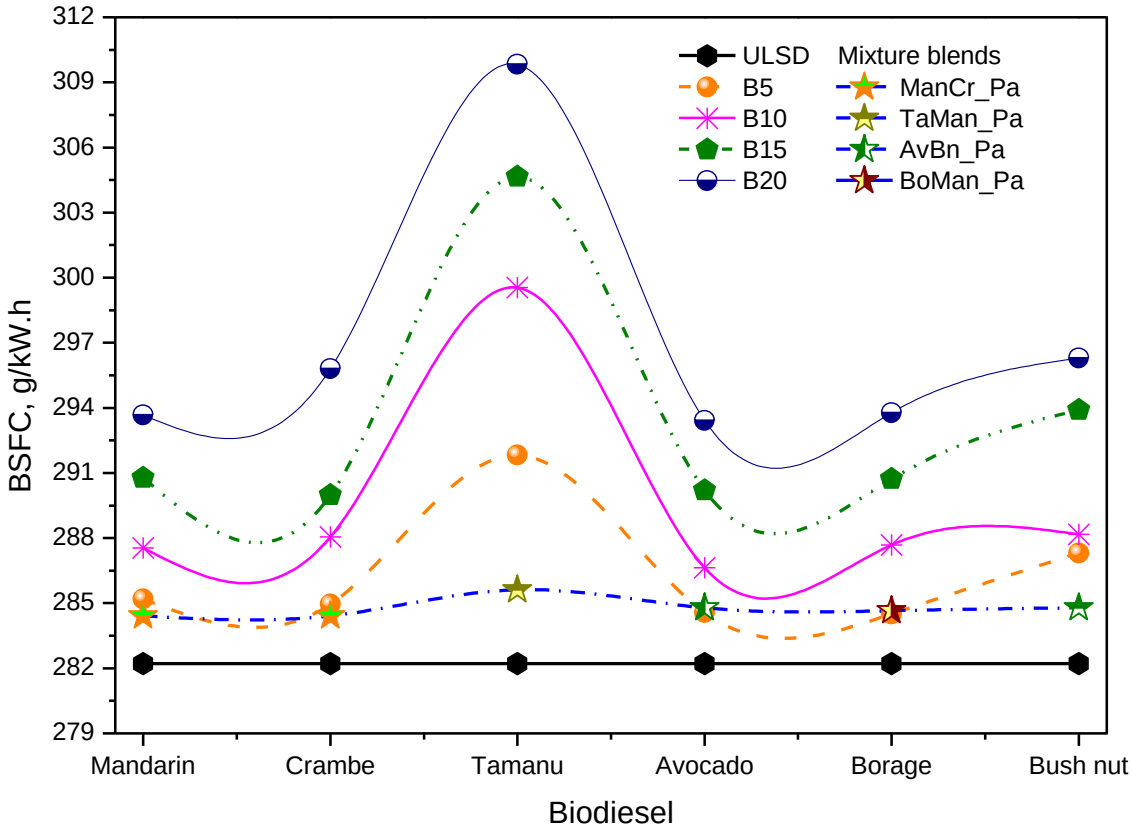

Figure 5.5: Variation of BSFC with biodiesel blends at rated power condition (full load, 2400 rpm)

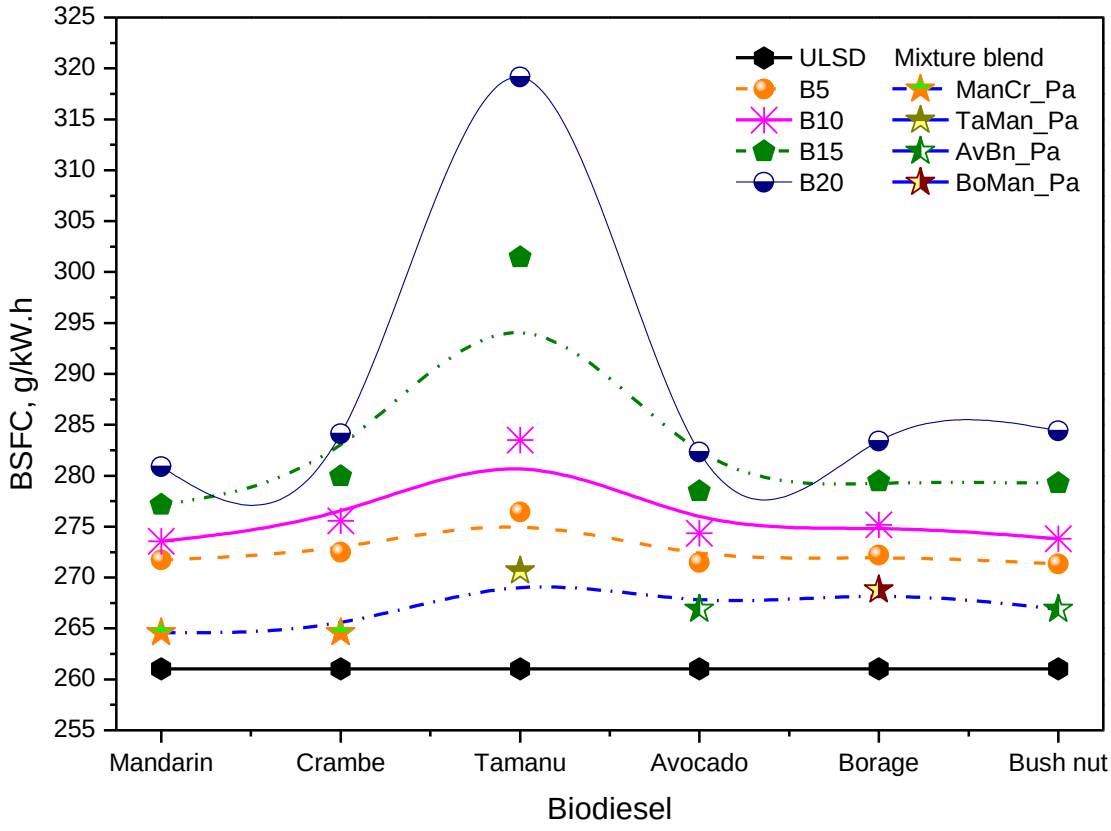

Figure 5.6: Variation of BSFC with biodiesel blends at rated torque condition (full load, 1400 rpm)

Table 5.4: Summary of BSFC increase by biodiesel blends as compared to ULSD

Biodiesel	Rated power				Rated torque			
	B5	B10	B15	B20	B5	B10	B15	B20
Mandarin	1.06*	1.89	3.04	4.06	4.10	4.80	6.18	7.61
Crambe	0.97	2.07	2.75	4.82	4.38	5.57	7.25	8.85
Tamanu	3.41	6.14	7.96	**9.79**	5.9	8.61	15.49	**23.25**
Avocado	0.83	1.57	2.83	3.97	4.00	5.10	6.69	8.16
Borage	**0.81**	1.94	3.02	4.10	4.05	5.42	7.05	8.57
Bush nut	1.81	2.11	4.15	4.99	**3.95**	4.90	6.99	8.95

Note: *Positive sign (+) represents increase of BSFC.

5.3.2. Variation of BSFC with engine speed

Figure 5.7 demonstrates the variation of BSFC at different engine speeds for (a) Mandarin-Crambe, (b) Tamanu-Borage, (c) Avocado-Bush nut, and (d) biodiesels-paraffin mixture blends (B5, B20), respectively. The results show that Crambe has slightly higher BSFC as compared to Mandarin (Figure 5.7 (a)), Tamanu has noticeably higher BSFC than Borage (Figure 5.7 (b)), and Avocado has a BSFC close to that of Bush nut (Figure 5.7 (c)) throughout the rage of engine speeds. The summary of average BSFC variation is presented in Table 5.5. The common phenomenon is that biodiesels have higher BSFC as compared to ULSD which increases with the increase in biodiesel blend (B5 to B20). It can be clearly noted from these figures that the fluctuation of BSFC is higher at lower engine speeds (i.e. 1200 rpm) as compared to higher engine speeds (i.e. 2400 rpm) for each case. This is due to the rich air-fuel mixture ($\lambda < 1.0$) at lower engine speed which contributes to incomplete combustion resulting in the engine consuming more fuel to produce high torque at low engine speeds. It can be noticed from the figure that all tested fuels at rated power show a similar behaviour due to the lean air-fuel mixture ($\lambda > 1.0$) which contributed to complete combustion at higher engine speed. The minimum BSFC was found from 1600rpm to 1800rpm for each tested fuel blend. On the other hand, B20 blends have higher BSFC compared to B5 blends throughout the engine speed range (Figure 5.7 (a) to (c)) as expected due to the higher density, viscosity and lower calorific value of the B20 blends as compared to B5 blends as confirmed by other studies (Monirul et al., 2016, Buyukkaya, 2010). These outcomes are also generally agreed with by many researchers in the literature (Tesfa et al., 2013, Sajjad et al., 2015). More specifically, Abedin et al. (2014) and Sanjid et al. (2014) studied palm and jatropha biodiesel by varying the engine speed and found similar trends of BSFC for biodiesel and attributed the findings to lower calorific value, higher density and viscosity.

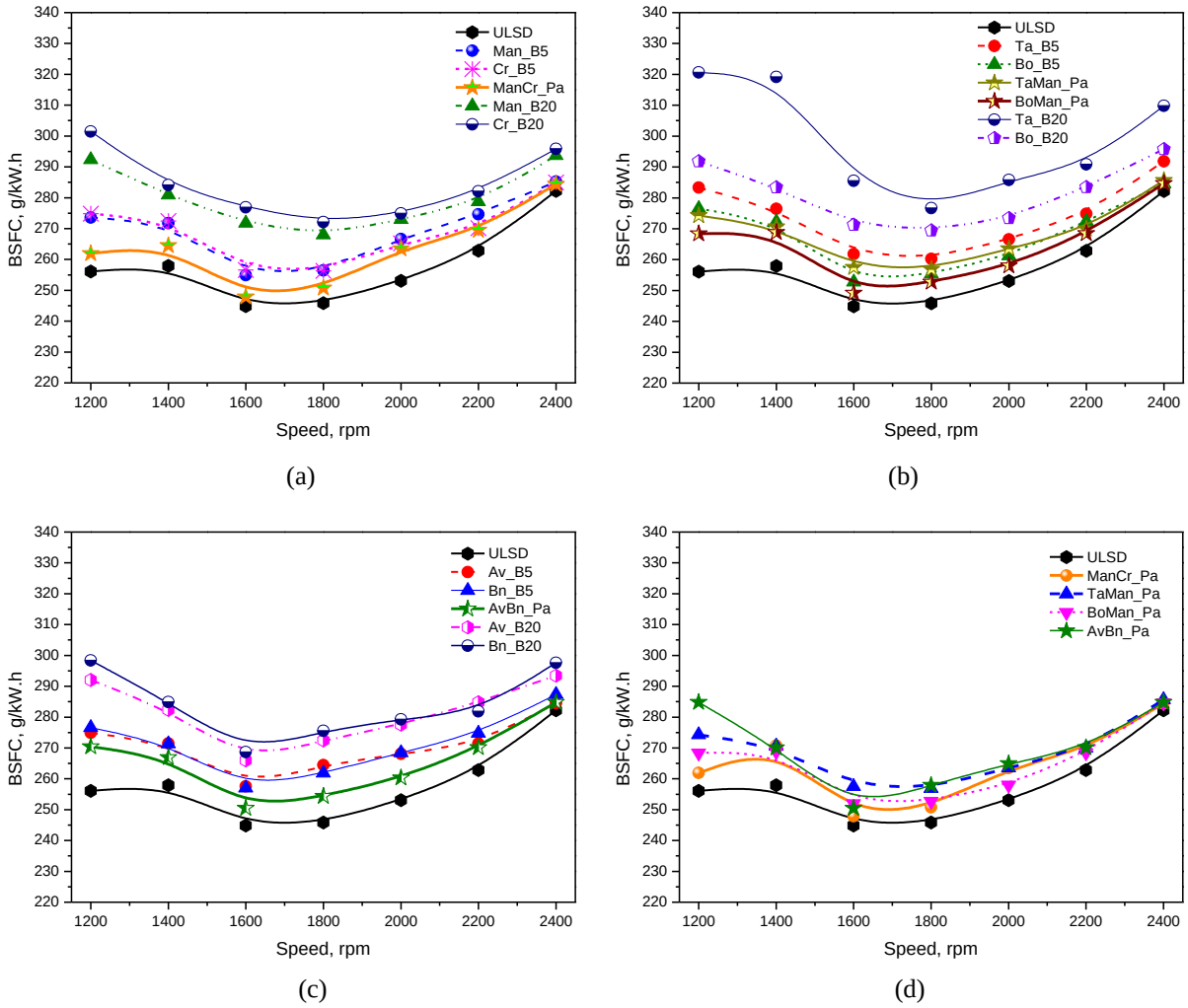

Figure 5.7: Variation of BSFC with engine speed at full load condition for (a) Mandarin-Crambe, (b) Tamanu-Borage, (c) Avocado-Bush nut, and (d) biodiesel-paraffin mixture blends

It was also found from the experiment that the mixture blends show lower BSFC as compared to each of their B5 blends but slightly higher than ULSD as seen from Table 5.5. For example, ManCr_Pa mixture blends show an average 2.20% lower BSFC compared to the Man_B5 blend which is about 2.21% higher compared to ULSD, respectively. Similar comparisons between B5 and ULSD for TaMan_Pa, BoMan_Pa and AvBn_Pa are presented in Table 5.5. As shown in the table, a significant improvement of engine performance has been recorded for the ManCr_Pa mixture blend as compared with Man_B5 blend due to a noticeable improvement of fuel properties. Figure 5.7 (d) illustrates a comparison of mixture blends with ULSD. The ManCr_Pa mixture blend shows the minimum BSFC with an average of 264.0 g/kWh and the TaMan_Pa blend shows the maximum BSFC with an average of 268.3 g/kWh

whereas the average BSFC for ULSD is 257.5 g/kWh. The effect of engine load on BSFC for tested fuels is briefly discussed below.

Table 5.5: Summary of average BSFC increase as compared to ULSD throughout the range of engine speeds

Compared with ULSD	Mandarin		Crambe		Tamanu		Borage		Avocado		Bush nut	
	B5	B20	B5	B20	B5	B20	B5	B20	B5	B20	B5	B20
	4.52*	8.71	4.36	10.34	6.27	**15.85**	4.00	9.17	5.06	9.28	5.31	10.25
Mixture name →	ManCr_Pa				TaMan_Pa		BoMan_Pa		AvBn_Pa			
Mixture/ULSD	**2.21**				4.24		2.64		3.06			
Mixture/B5	-2.20**				-1.90		-1.29		-1.89			

Note: *Positive sign (+) represents increase of BSFC and **Negative sign (-) represents decrease.

5.3.3. Variation of BSFC with engine load

Figure 5.8 illustrates the variation of BSFC at four engine loads (25%, 50%, 75% and 100%) at rated speed. The BSFC is the parameter quantifying fuel efficiency of the tested fuels. The figure shows that the BSFC decreases with the increase in engine load. Many researchers also found similar trends of BSFC with variable engine load (Agarwal et al., 2006, Muralidharan et al., 2011, Zhu et al., 2011). The results reveal that BSFC decreases from 378.29 g/kW.h to 282.21 g/kW.h for ULSD from lower to higher load as the brake mean effective pressure (BMEP) increases from 0.18 MPa to 0.71 MPa. This is due to the increase of brake thermal efficiency with the increase of engine load (Figure 5.12) as discussed by An et al. (2013). Another reason is likely to be the shorter combustion duration (CD) at lower engine loads which increases with the increase to higher engine loads. Shorter CD indicates major heat losses after combustion. This reason has also been explained by Sakthivel (2016) in page no 222 as "*the percent increase in fuel required to operate the engine is less than the percent increase in BP due to relatively less portion of the heat losses at higher load*".

The trend implies that the BSFC increases with the increase in biodiesel blend at variable engine load. This is mainly due to the increase in density and viscosity and the decrease in calorific value with the increase in biodiesel blend as discussed by Muralidharan et al. (2011). The results reveal that BSFC increases significantly at lower load (25%) conditions as compared to ULSD with an average of 5.37% (B5) to 16.67% (B20) for Mandarin, and 6.70% (B5) to 15.96% (B20) for Crambe, but only 1.79% for ManCr_Pa from Figure 5.8 (a); 14.09% (B5) to 30.37% (B20) for Tamanu, and 5.69% (B5) to 16.71% (B20) for Borage, but only

8.87% for TaMan_Pa and 1.60% for BoMan_Pa [Figure 5.8 (b)]. In addition, BSFC increases by about 6.14% (B5) to 19.41% (B20) for Avocado, 8.40% (B5) to 25.90% (B20) for Bush nut, but only 0.76% for AvBn_Pa from Figure 5.8 (c). At higher loads, BSFC variation is insignificant, being about 0.80 to 1.80% for all biodiesels B5 blends except Ta (3.40%) whereas B20 varies from 3.80 to 4.80% for all biodiesels except Ta (9.79%) as compared to ULSD. Figure 5.8 (d) shows the comparison between mixture blends with ULSD which reveals that BSFC decreases from 1.79% to 0.77% for ManCr_Pa, 8.87% to 1.21% for TaMan_Pa, 1.60% to 0.86% for BoMan_Pa and 1.76% to 0.91% for AvBn_Pa from low load (25%) to high load (100%), respectively. It can be noted that three mixture blends (the exception being TaMan_Pa) show very close BSFC as compared to diesel, however a significant improvement of BSFC has been recorded for the TaMan_Pa mixture blend as compared to the Ta_B5 blend.

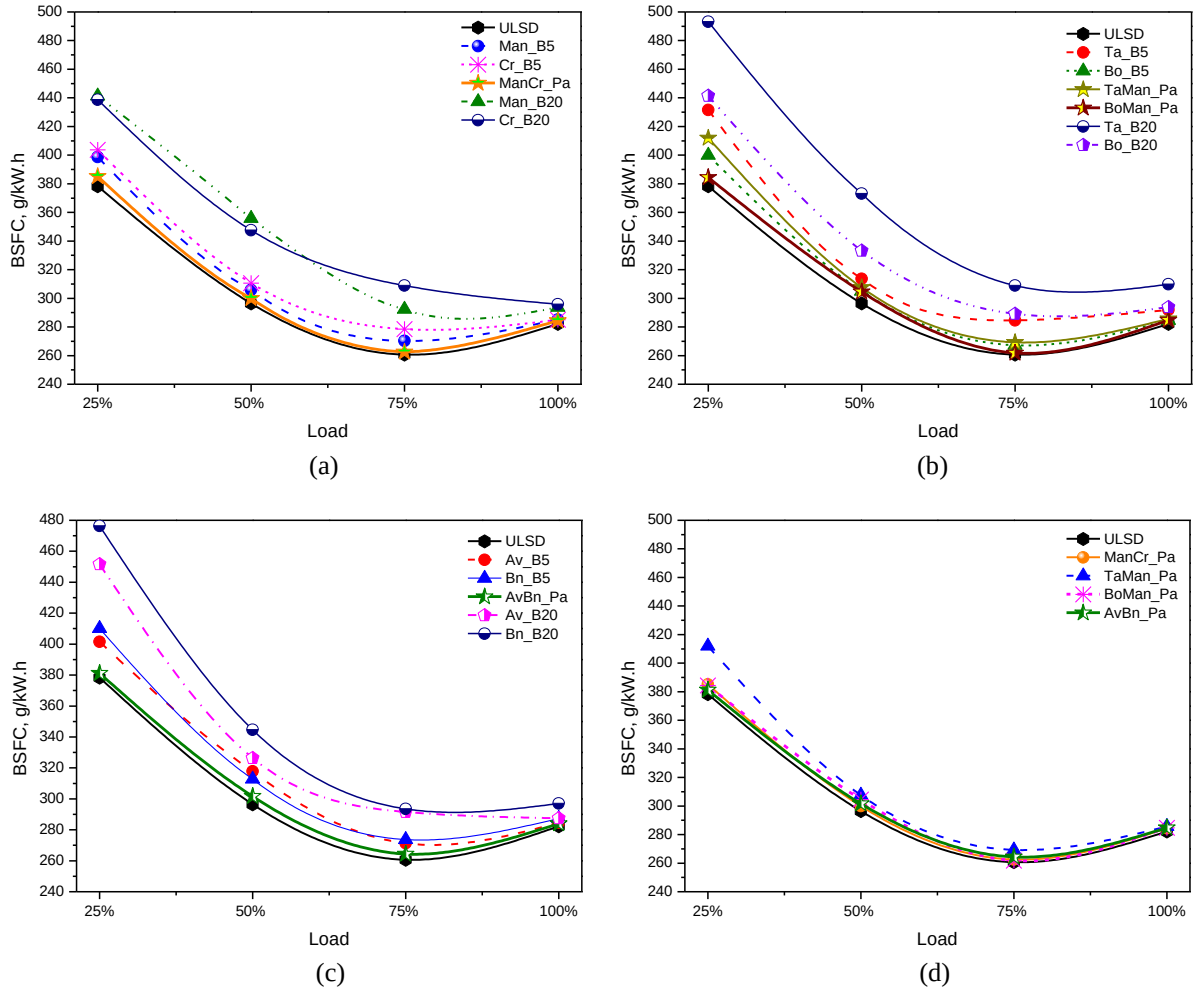

Figure 5.8: Variation of BSFC with engine loads at rated power condition (2400 rpm) for (a) Mandarin-Crambe, (b) Tamanu-Borage, (c) Avocado-Bush nut, and (d) biodiesel-paraffin mixture blends

The average augmentation of BSFC throughout the range of engine loads is summarised in Table 5.6. As seen from the table, the maximum BSFC occurred for Tamanu with an average of 8.11% (B5) to 21.13% (B20) and the minimum was for Borage with an average of about 2.97% (B5) to 11.05% (B20). Notably, the AvBn_Pa mixture blend shows relatively better performance at variable load conditions with a reduction of about 3.17% BSFC as compared to the Av_B5 blend.

Table 5.6: Summary of average BSFC increases compared to ULSD throughout the entire range of engine load

Compared with ULSD	Mandarin		Crambe		Tamanu		Borage		Avocado		Bush nut	
	B5	B20	B5	B20	B5	B20	B5	B20	B5	B20	B5	B20
	3.33*	13.21	4.82	14.14	8.11	**21.13**	2.97	11.05	4.57	11.33	5.18	15.05
Mixture name →	ManCr_Pa				TaMan_Pa		BoMan_Pa		AvBn_Pa			
Mixture/ULSD	**1.11**				4.28		1.41		1.20			
Mixture/B5	-2.13**				-3.50		-1.50		-3.17			

Note: *Positive sign (+) represents increase of BSFC and **Negative sign (-) represent decrease.

5.4. Brake Thermal Efficiency (BTE)

5.4.1. Variation of BTE with biodiesel blends

BTE quantifies the ability of the engine to transfer the chemical energy of the fuel into useful forms of mechanical energy at the engine shaft. Figures 5.9 and 5.10 indicate the variation of BTE with tested biodiesel blends (B5, B10, B15 and B20) and biodiesel-paraffin ternary mixture blends at rated power and rated torque conditions, respectively. Overall, the trend implies that an increase in biodiesel blends (B5 to B20) has an adverse effect on BTE which could be attributed to the lower calorific value, and higher density and viscosity of the biodiesel blends. These reasons were also pointed out by several researchers in the literature (Monirul et al., 2016, Sanjid et al., 2014). The summary of BTE reduction as compared to ULSD is presented in Table 5.7. The results reveal that there is no noticeable variation of BTE (average 0.04% and 0.73% less BTE) for mixture blends as compared to ULSD at rated power and rated torque conditions, respectively. As seen from Table 5.7 and Figure 5.9, biodiesel blends produced less BTE with an average of 0.57% (B5) to 2.08% (B20) for Man, 0.39% (B5) to 2.43% (B20) for Cr, 2.51% (B5) to 5.98% (B20) for Ta, 0.18% (B5) to 1.36% (B20) for Av, 0.18% (B5) to 1.47% (B20) for Bo, and 1.15% (B5) to 2.26% (B20) for Bn as compared to ULSD, respectively. For rated torque condition, Figure 5.10 indicates that BTE decreases as

compared to ULSD and the results are summarised in Table 5.7. The study identified more BTE reduction at rated torque as compared to rated power conditions because more fuel consumption has been recorded at rated torque condition (Figure 5.6). For both cases, Avocado biodiesel presents a better BTE as compared to other biodiesel blends and a minimum reduction of BTE with increase of biodiesel blend (B5 to B20). The study investigated the effect of engine speed and load on BTE which is briefly discussed below.

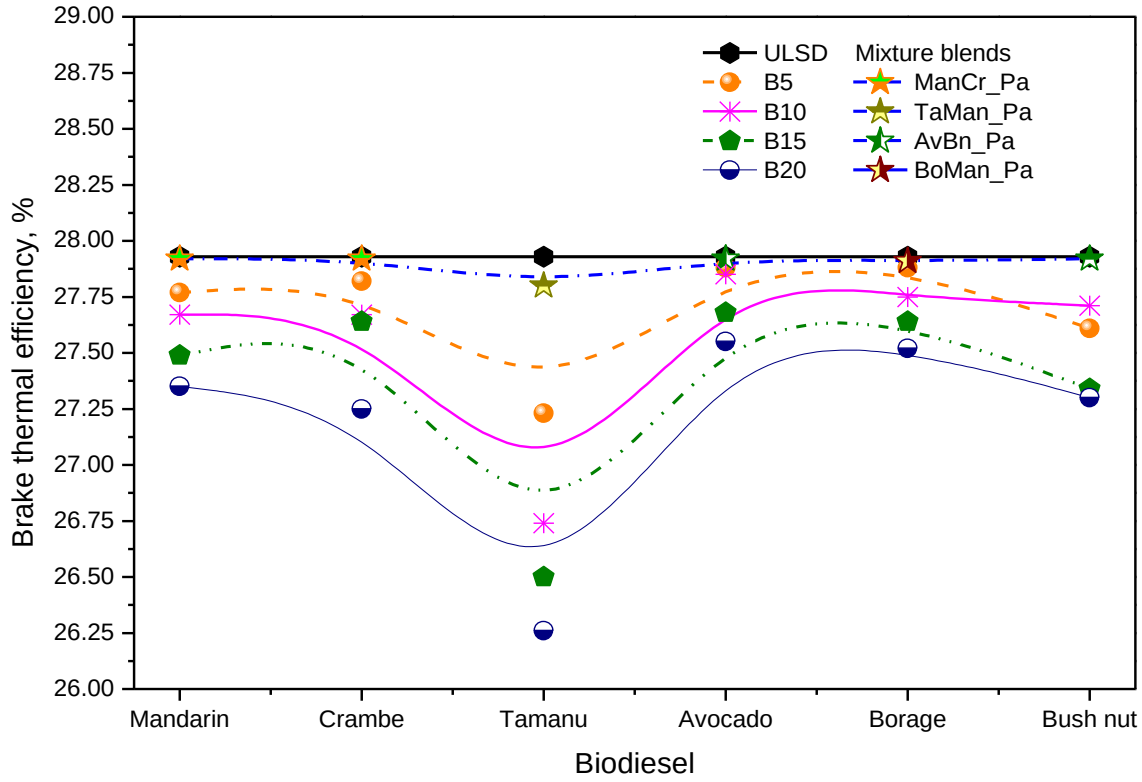

Figure 5.9: Variation of BTE with biodiesel blends (B5 to B20) at rated power condition (full load, 2400 rpm).

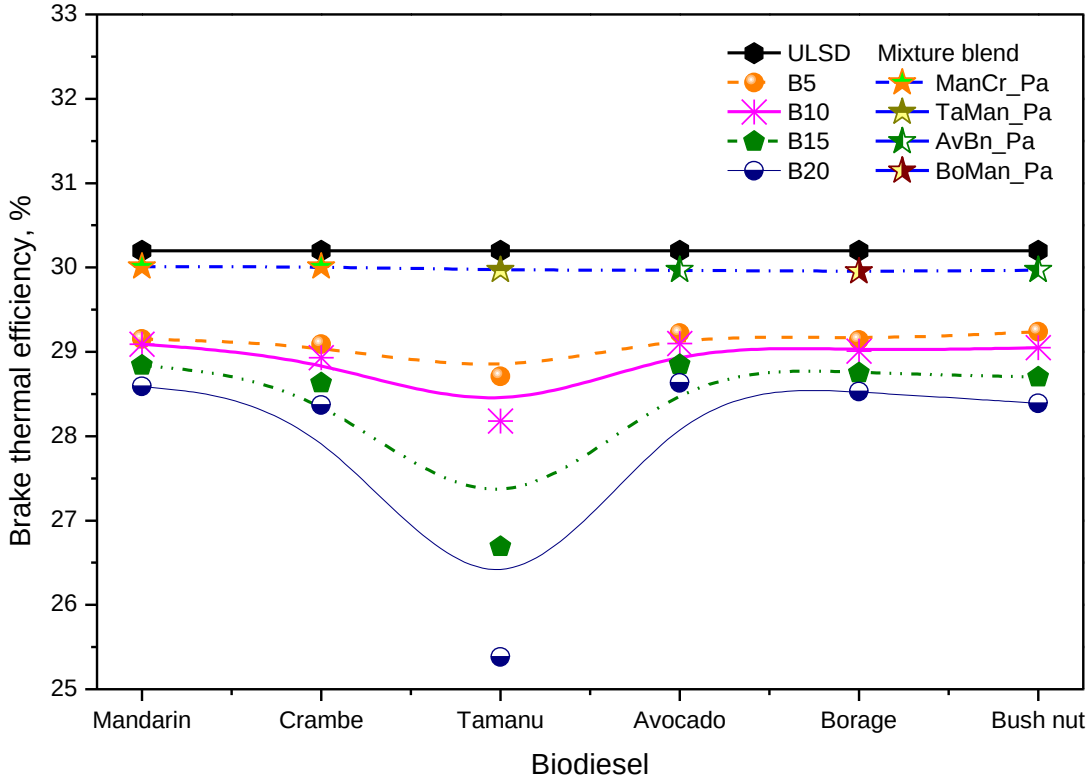

Figure 5.10: Variation of BTE with biodiesel blends (B5 to B20) at rated torque condition (1400 rpm)

Table 5.7: Summary of BTE decrease with biodiesel blends as compared to ULSD at rated power and torque

Biodiesel	Rated power				Rated torque			
	B5	B10	B15	B20	B5	B10	B15	B20
Mandarin	-0.57*	-0.93	-1.58	-2.08	-3.61	-3.68	-4.50	-5.33
Crambe	-0.39	-0.93	-1.04	-2.43	-3.68	-4.21	-5.20	-6.06
Tamanu	-2.51	-4.26	-5.12	**-5.98**	-4.93	-6.69	-11.62	**-16.62**
Avocado	**-0.18**	-0.29	-0.90	-1.36	-3.25	-3.64	-4.47	-5.20
Borage	**-0.18**	-0.64	-1.04	-1.47	-3.28	-3.94	-4.80	-5.53
Bush nut	-1.15	-0.79	-2.11	-2.26	**-3.18**	-3.81	-4.97	-5.99

Note: *Negative sign (-) represents reduction of BTE.

5.4.2. Variation of BTE with engine speed

Figure 5.11 illustrates the variation of BTE with engine speed from 1200 rpm to 2400 rpm at full load condition for tested biodiesel blends. The trend of the biodiesel blends follows a similar trend to ULSD which implies that BTE increases with engine speed until 1600 rpm (middle speed) and decreases until rated speed is reached. The maximum BTE of 32.20% was obtained for ULSD at 1600 rpm speed which attributes to the minimum BSFC at that particular speed (Figure 5.7). When engine speed increases to more than 1600 rpm, then BTE for all

tested fuels decreases simultaneously. This trend of BTE agrees with Monirul et al. (2016), Aydın and Sayın (2014), and Sanjid et al. (2014). Figures 5.11 (a) to (c) demonstrate that BTE decreases with the increase in biodiesel blend, which is expected due to the lower calorific value of the biodiesel compared to ULSD as discussed above. Further, higher density and viscosity of the biodiesel results in poor atomisation, vaporisation and mixing, contributing to the uneven combustion behaviour of the biodiesel blends compared to ULSD (Monirul et al., 2016).

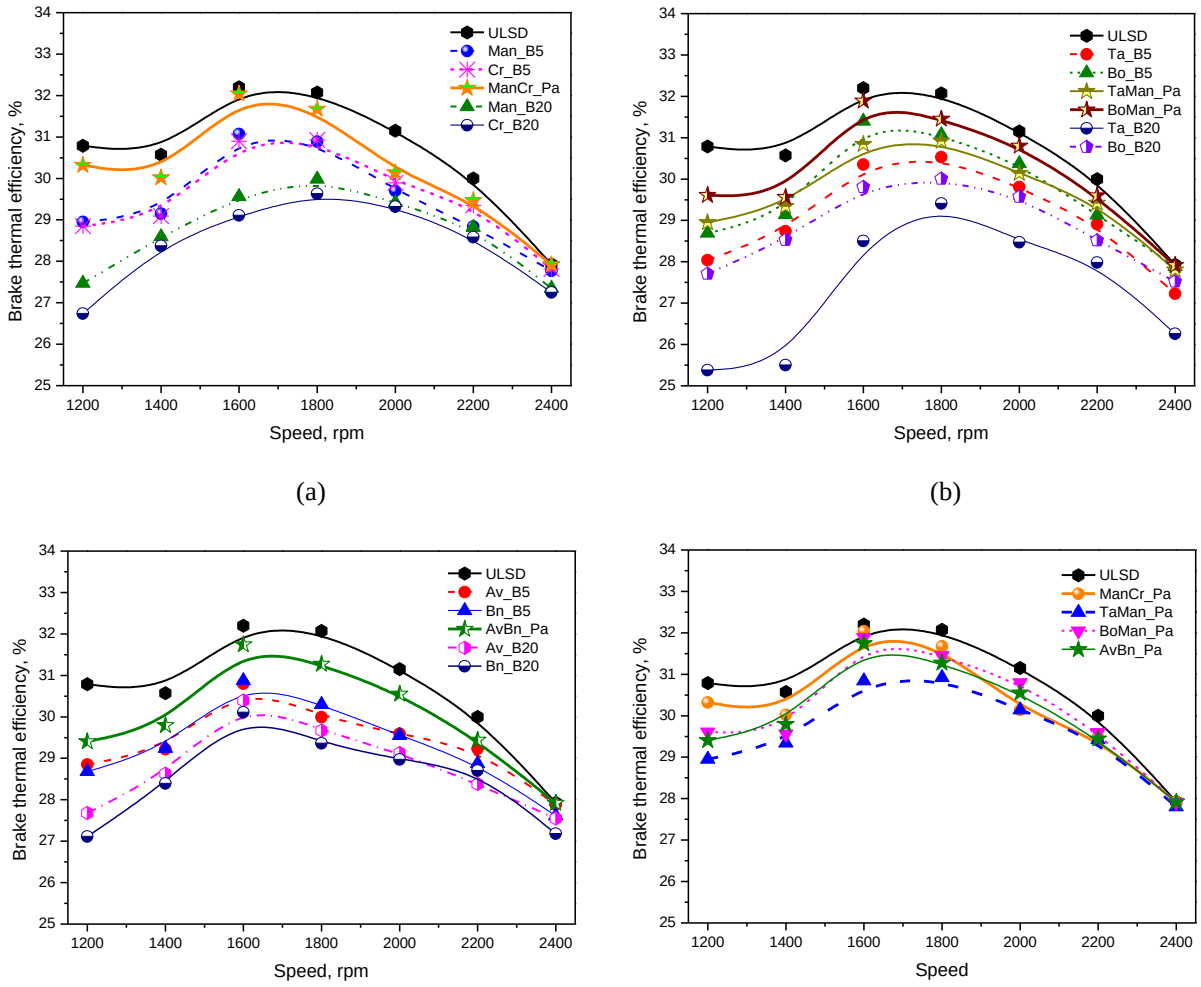

Figure 5.11: Variation of BTE with engine speed at full load condition for (a) Mandarin-Crambe, (b) Tamanu-Borage, (c) Avocado-Bush nut, and (d) biodiesel-paraffin mixture blends

It can also be noted that the fluctuation of BTE at low engine speeds is greater than at high engine speeds. This is due to the rich air-fuel mixture which deteriorates the combustion quality at low speeds and results in more fuel consumption (Figure 5.7) to produce higher torque (Appendix I, Figure 2). On the other hand, BTE shows a closer magnitude at high speeds due

to the proper combustion of the lean air-fuel mixture (where excess air factor, $\lambda > 1.0$). Table 5.8 summarises the average drops of BTE when compared with ULSD for tested fuels throughout the range of engine speeds. As seen from the table, maximum and minimum BTE drops occurred for Tamanu with an average of 5.13% (B5) to 10.70% (B20) and Borage 3.21% (B5) to 6.00% (B20) as compared to ULSD, respectively.

Table 5.8: Summary of average BTE variation to ULSD throughout the entire range of engine speed

Compared with ULSD	Mandarin		Crambe		Tamanu		Borage		Avocado		Bush nut	
	B5	B20	B5	B20	B5	B20	B5	B20	B5	B20	B5	B20
	-3.86*	-6.20	-3.62	-7.23	-5.13	**-10.7**	-3.21	-6.00	-4.19	-6.11	-4.42	-6.86
Mixture name →	ManCr_Pa				TaMan_Pa		BoMan_Pa		AvBn_Pa			
Mixture/ULSD	**-1.45**				-3.35		-1.79		-2.12			
Mixture/B5	2.53**				1.88		3.53		2.18			

Note: *Negative sign (-) represents decrease, ** Positive sign (+) represents increase of BSFC.

In each case, the mixture blends demonstrate better BTE when compared to each of their B5 blends. This could be attributed to the improvement of fuel properties (density and viscosity) of the mixture blend. For instance, the ternary mixture blends show less BTE decrease as compared to ULSD and enhanced BTE with an average of 2.53%, 1.88%, 3.53% and 2.18% for ManCr_Pa, TaMan_Pa, BoMan_Pa and AvBn_Pa mixture blends as compared to each of their B5 blends, respectively. The investigation into the effect of engine load on BTE is succinctly discussed in the following section.

5.4.3. Variation of BTE with engine load

Figure 5.12 depicts the variation of BTE with different engine loads (25%, 50%, 75% and 100%) at rated engine speeds for the tested fuels. The trend implies that BTE increases with the increase in engine loads up until 75% load, then decreases until full load. This is due to the reduction of heat loss and increase in BP with the increase in engine load (Figure 5.4) which agrees with Muralidharan et al. (2011) and Panwar et al. (2010). Contrariwise, BTE decreases with the increase of biodiesel blend. This can be ascribed to the collective effect of higher density and viscosity as well as the lower calorific value of the biodiesel blends. Many research groups have also pointed out these types of variation of BTE with biodiesel blends (Sajjad et al., 2015, Islam et al., 2015, Sakthivel, 2016). Figures 5.12 (a) to (d) imply that the variation of BTE at higher load (100%) is insignificant as compared to lower engine loads (25%) for all

fuels. This could be attributed to the high fuel injection pressure (as high as 235.4 bar) such that the viscosity effect of the fuels is negligible at full load condition (An et al., 2013). Due to this reason, the fine air-fuel mixture of the oxygenated biodiesel blends leads to proper combustion at full load condition.

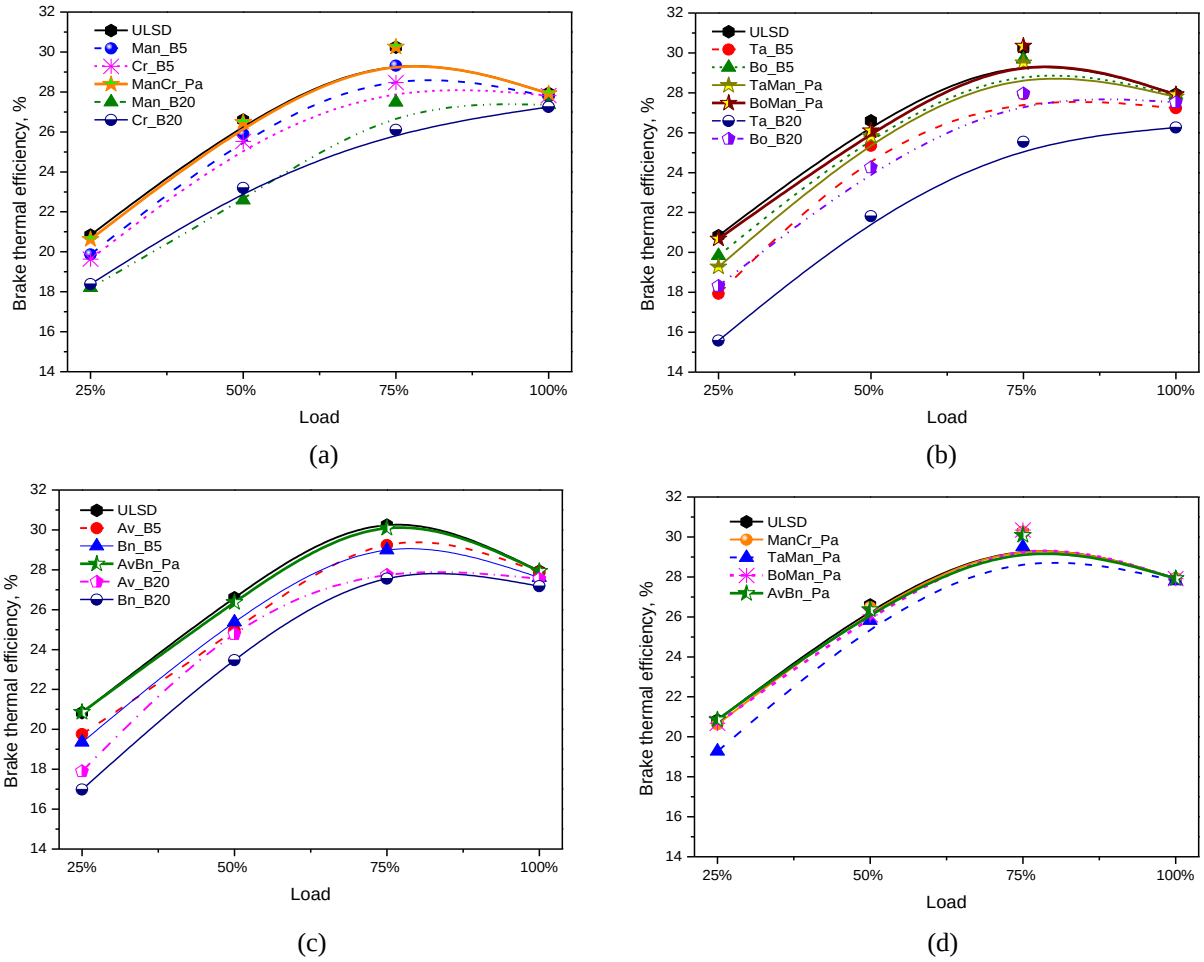

Figure 5.12: Variation of BTE with engine load at rated power condition (2400 rpm) for (a) Mandarin and Crambe, (b) Tamanu and Borage, (c) Avocado and Bush nut, and (d) biodiesel-paraffin mixture blends

The results reveal that BTE varies from 20.84% at lower load to 27.93% at higher load for ULSD. The maximum BTE was achieved at 75% load for all tested fuels. This is because of the higher heat release rate at 75% load as compared to full load for all fuels. For instance, a BTE increase was obtained of about 30.35% for the BoMan_Pa mixture blend, whereas 30.24%, 30.25%, 30.08% and 29.50% BTE increases were recorded for ULSD, ManCr_Pa, BoMan_Pa, AvBn_Pa and TaMan_Pa, respectively. This is due to the oxygen enriched mixture blend with higher cetane number (for example, about 73 for the Borage biodiesel) that enhanced the quality of combustion. The summary of average BTE variation is presented in

Table 5.9. As seen from the table and Figure 5.12(b), maximum and minimum BTE drops occurred for Tamanu with an average of 6.64% (B5) to 14.43% (B20) and Borage with about 2.25% (B5) to 7.47% (B20), respectively as compared to ULSD. Figure 5.12 (d) compares the BTE variation for all mixture blends and found BTE values very close to those of ULSD. For instance, the ManCr_Pa mixture blend had a 2.45% higher BTE as compared to the Mandarin B5 blend, while the drop in BTE is only 0.38% for the ManCr_Pa mixture blend compared to ULSD. On the contrary, BoMan_Pa and AvBn_Pa mixture blends show an average of 6.62% and 3.54% higher BTE values when compared with Borage and Avocado B5 blends, respectively. The highest BTE decline occurred for the TaMan_Pa mixture blend which shows about a 3.34% drop compared to ULSD.

Table 5.9: Summary of average BTE variation compared to ULSD throughout the entire range of engine load

Compared with ULSD	Mandarin		Crambe		Tamanu		Borage		Avocado		Bush nut	
	B5	B20	B5	B20	B5	B20	B5	B20	B5	B20	B5	B20
	-2.74*	-9.70	-4.02	-10.2	-6.64	-14.43	-2.25	-7.47	-3.70	-7.66	-4.26	-10.5
Mixture name →	ManCr_Pa				TaMan_Pa		BoMan_Pa		AvBn_Pa			
Mixture/ULSD	-0.38				-3.34		-0.59		**-0.34**			
Mixture/B5	2.45**				3.58		6.62		3.54			

Note: * Negative sign (-) represents decrease, and **Positive sign (+) represents increase of BSFC.

Emission Analysis

5.5. Carbon Monoxide (CO) and Carbon Dioxide (CO_2) Emissions

5.5.1. Reduction of CO emissions with biodiesel blends

CO is an odourless, colourless and highly toxic gas formed before complete combustion when fuel reacts with the oxidiser. CO oxidation can lag behind in the presence of enough oxygen (O_2) due to its slow oxidation rate. The oxidation of CO with the help of hydroxyl (OH) is a highly exothermic reaction which implies complete combustion as well as higher heat releasing rate of the fuel (Equation 5.1). However, OH formation is highly temperature dependent which causes the CO oxidation reaction to freeze when the in-cylinder temperature falls below 1400 K. It is reported in the literature that an in-cylinder temperature of about 1500 K is required for OH formation and the complete oxidation of CO then follows the below chemical reaction (Bagal et al., 2009).

$$CO + OH \rightarrow CO_2 + H \quad \Delta \text{ (heat)} \tag{5.1}$$

Figures 5.13 and 5.14 illustrate the variation of CO emissions reduction for different biodiesel blends at rated power and torque conditions, respectively. It has been found that all fuel blends show lower CO emissions compared to ULSD. For instance, the tested Man, Cr, Ta, Av, Bo and Bn fuel blends (B5 to B20) reduced CO emissions by about 10.00 to 50.00%, 6.67 to 50.00%, 16.67 to 36.67%, 16.70 to 50.00%, 16.60 to 48.33% and 5.00 to 46.67%, respectively at rated power (Figure 5.13). On the other hand, significant reduction of CO in progressing from B5 to B20 blends was recorded at rated torque condition (Figure 5.14) by about 30.10 to 41.00%, 27.95 to 50.60%, 22.40 to 56.50%, 31.90 to 46.90%, 11.20 to 35.40% and 12.70 to 32.91% compared to ULSD for Man, Cr, Ta, Av, Bo and Bn, respectively. It can be noted from both figures that the mixture blends reduced CO by about 33.33% (for ManCr_Pa and AvBn_Pa), 25.00% (for TaMan_Pa), and 28.33% (for BoMan_Pa) compared to ULSD at rated power condition, and 37.60% (for ManCr_Pa), 35.10% (for TaMan_Pa), 39.75% (for AvBn_Pa), and 26.10% (for BoMan_Pa) as compared to ULSD at rated torque condition, respectively.

The mixture blends also have lower CO emissions compared to each of their B5 blends. The trends imply that CO emissions decrease with the increase in biodiesel blends due to the prolonged combustion duration and oxygen enriched fuel. Similar trends were also pointed out in the literature (Sajjad et al., 2015, Aydın and Sayın, 2014). To cite an example, Buyukkaya (2010) examined B5 to B100 rapeseed biodiesel and found about 12% to 35% CO reduction in his experimental study. Further, after oxidation of CO, a reduction in biodiesel blend percentage leads to an increase in CO_2 emissions which indicates the complete combustion of the fuel. This study found that CO_2 increases with the increase in biodiesel blends due to higher oxygen content in the higher biodiesel blends contributing to the conversion of CO to CO_2 (Figure 3.15 and 3.16). The factors that influence CO emissions are engine speed, air-fuel ratio, injection pressure and timing etc. which are briefly discussed below.

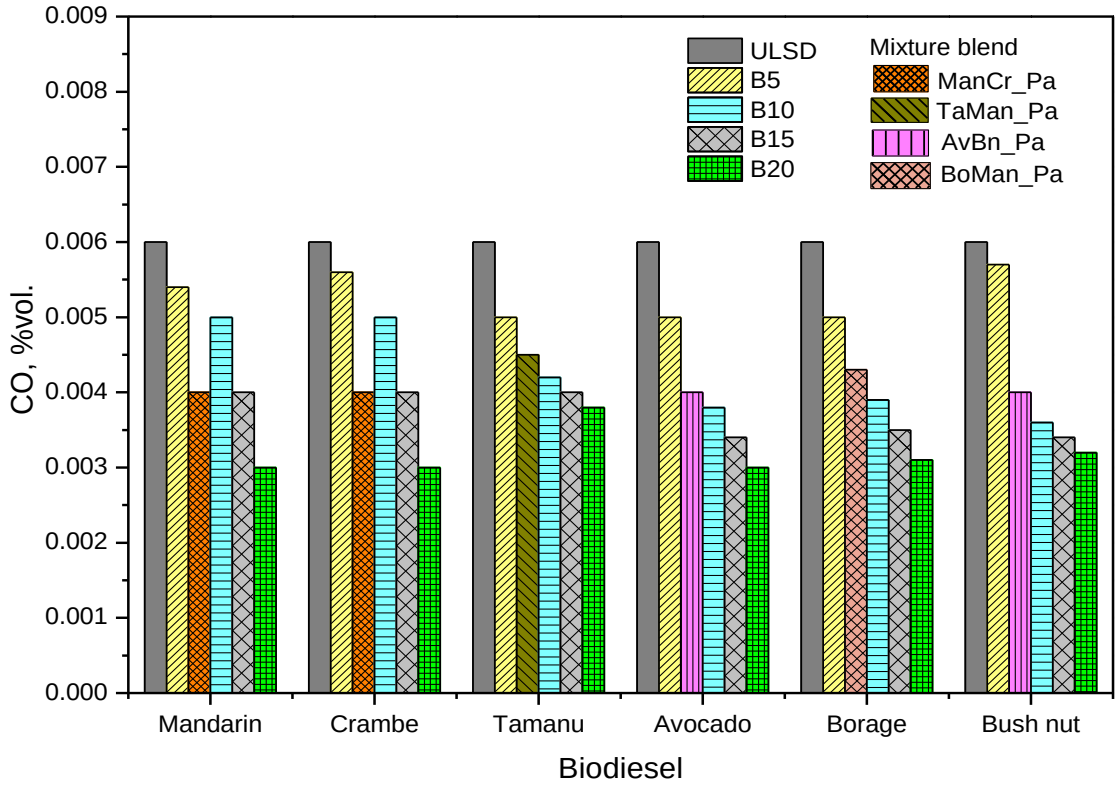

Figure 5.13: Variation of CO emissions reduction with biodiesel blends (B5 to B20) at rated power condition (full load, 2400 rpm)

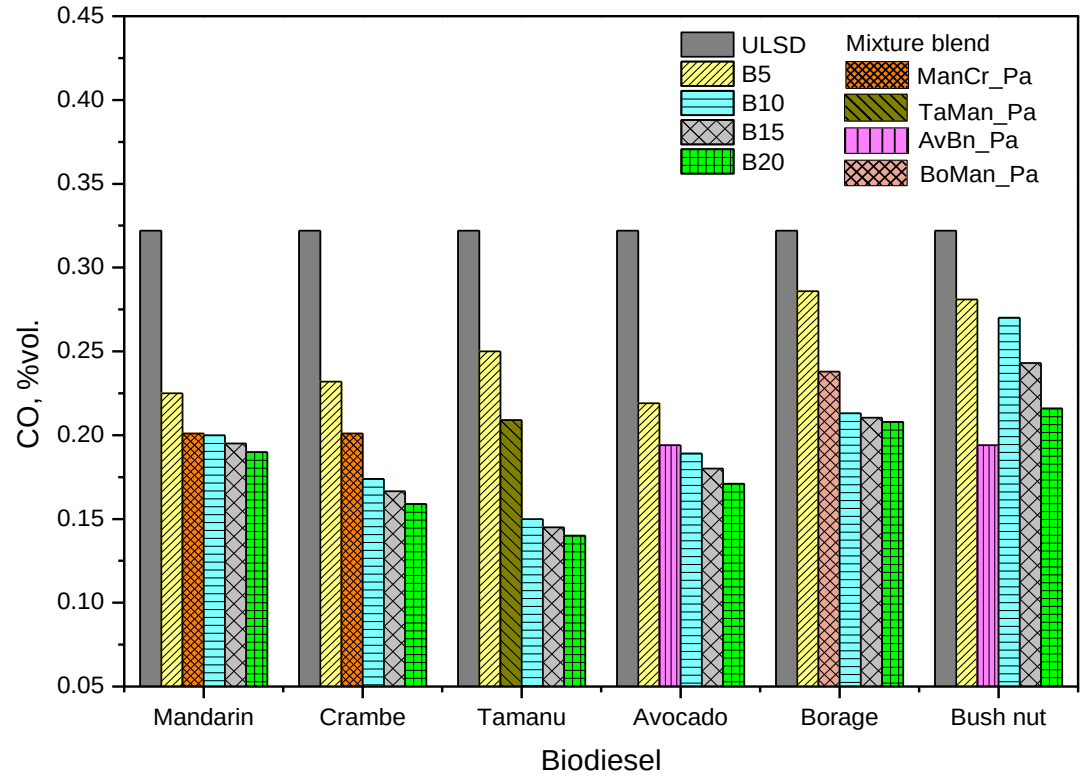

Figure 5.14: Comparison of CO emissions reduction with biodiesel blends at rated torque condition (full load, 1400 rpm)

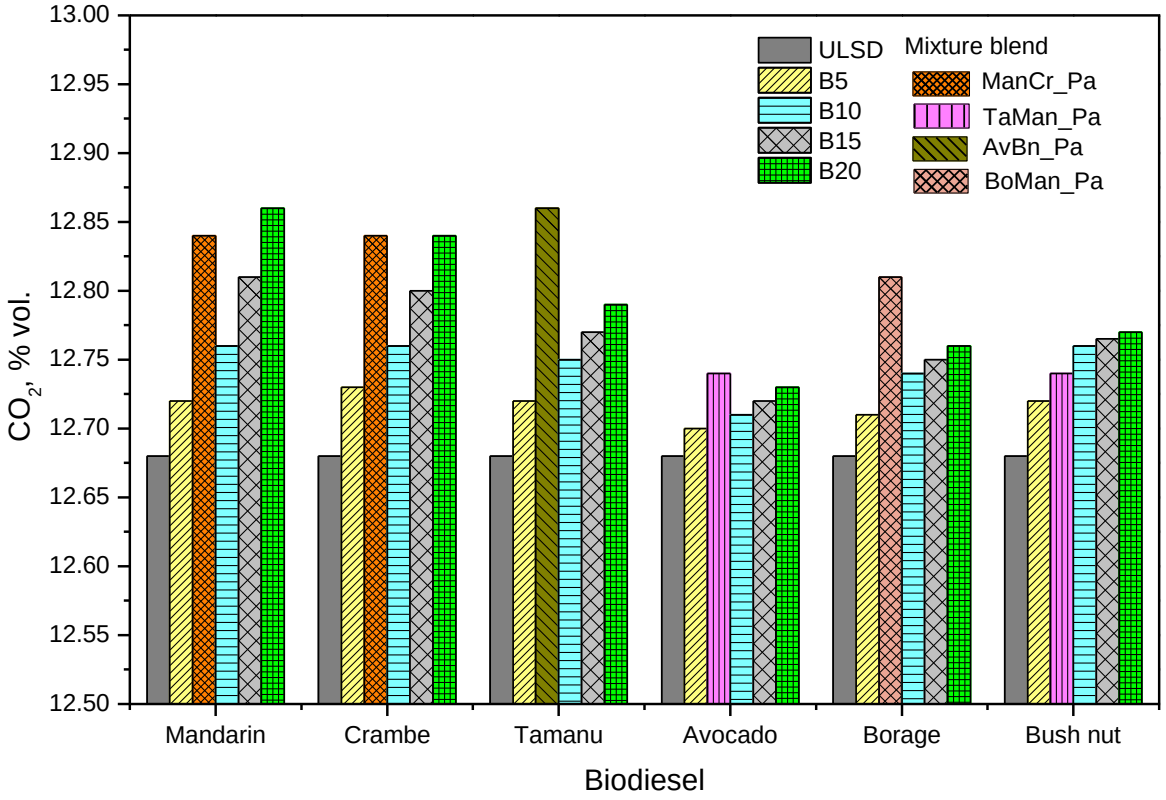

Figure 5.15: Variation of CO_2 emissions with biodiesel blends (B5 to B20) at rated power condition (full load, 2400 rpm)

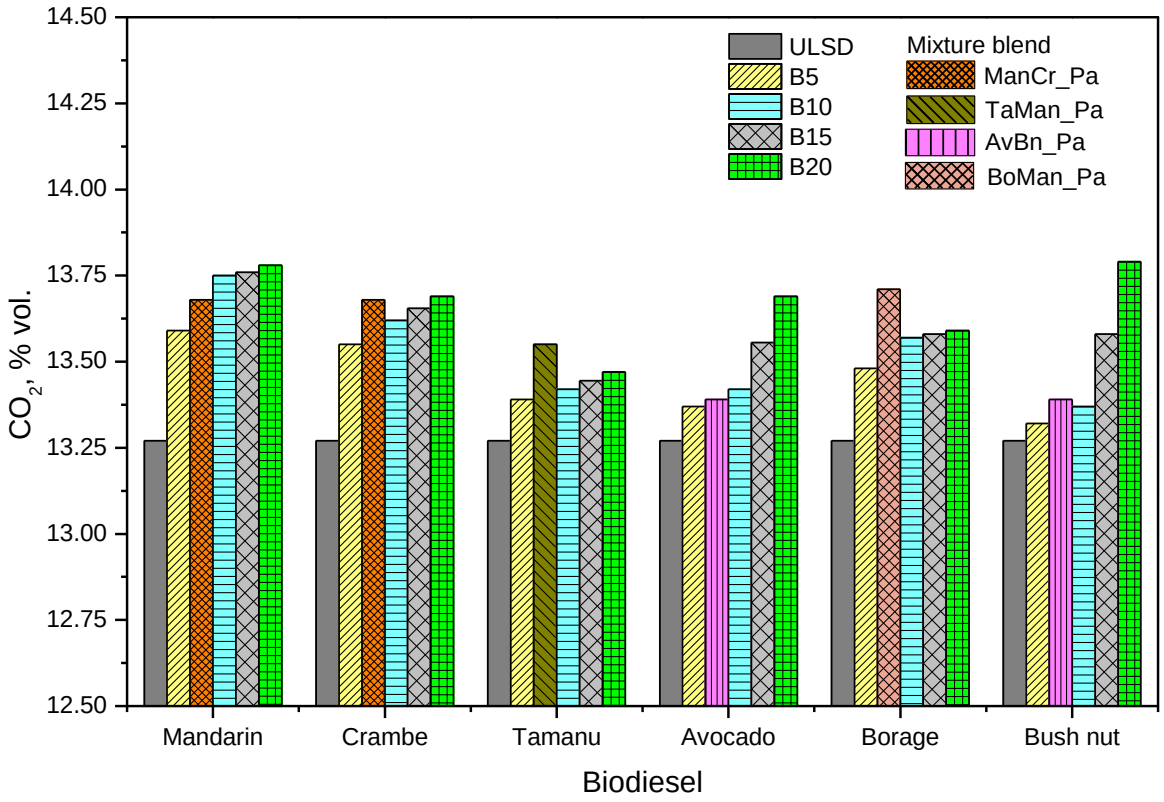

Figure 5.16: Comparison of CO_2 emissions with biodiesel blends at rated torque condition (full load, 1400 rpm)

5.5.2. Parameter effects on CO, CO_2 formation i.e. speed, lambda (λ)

Figure 5.17 illustrates the variation of CO emissions with excess air factor (lambda, λ) at different engine speeds for (a) Mandarin-Crambe, (b) Tamanu-Borage, (c) Avocado-Bush nut, and (d) biodiesels-paraffin mixture blends at full load condition. The results reveal that CO decreases with the increase of engine speed. The biodiesel blends follow trends very much like ULSD which also implies that CO decreases with the increase in biodiesel blends. This is due to the combined effect of higher cetane number and higher oxygen content in biodiesel which enhance combustion quality by shortening ignition delay and prolonging combustion duration. This finding also agrees with other studies (Palash et al., 2015, Buyukkaya et al., 2013). Over the entire range of engine speed, significant reductions of CO emissions were recorded for mixture blends with an average of 38.97%, 22.74%, 30.14% and 35.19% for ManCr_Pa, TaMan_Pa, BoMan_Pa, and AvBn_Pa, respectively. The maximum reduction of CO was recorded for ManCr_Pa (Figure 5.17 (d)).

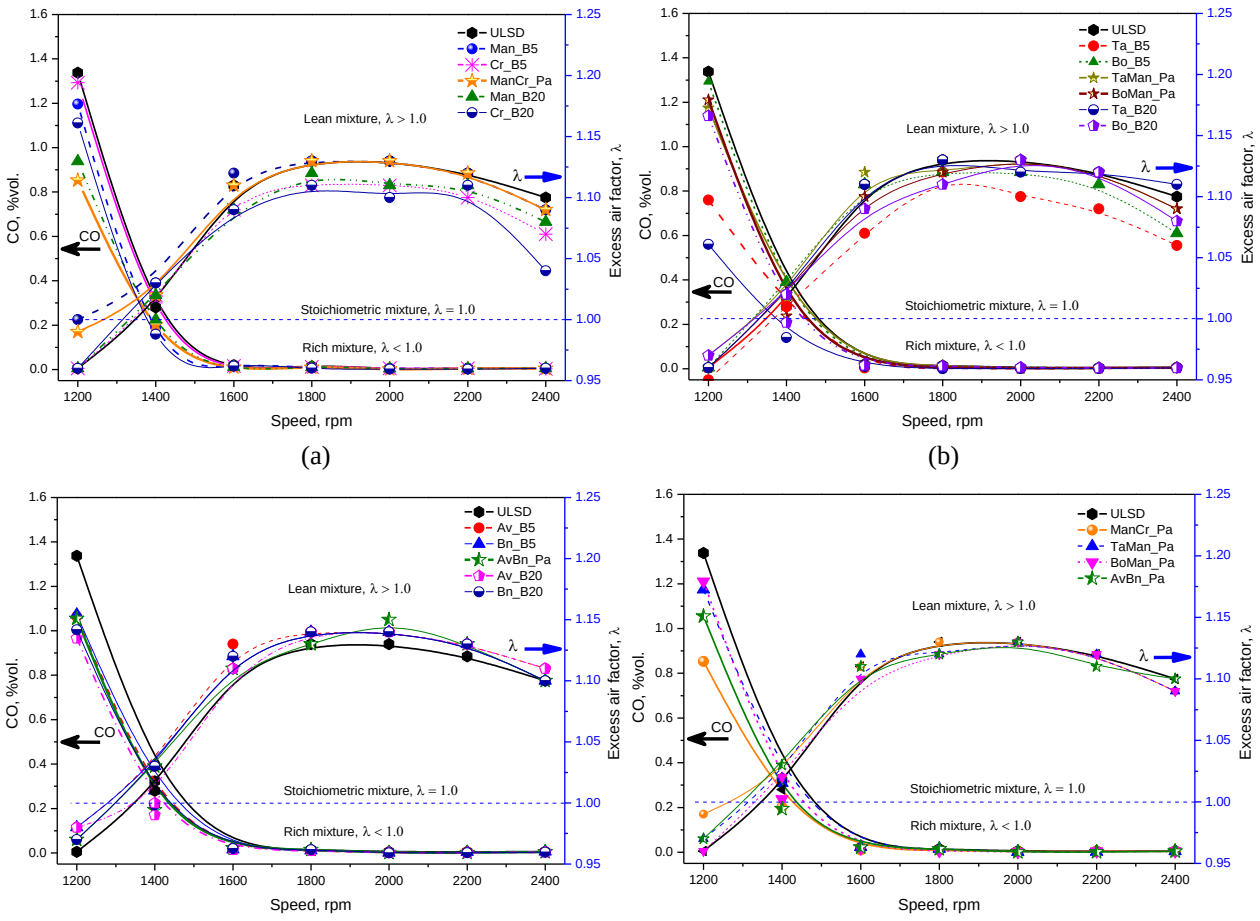

Figure 5.17: Variation of CO and lambda (λ) with engine speed at full load condition for (a) Mandarin-Crambe, (b) Tamanu-Borage, (c) Avocado-Bush nut, and (d) biodiesel-paraffin mixture blends

Figure 5.17 also demonstrates that CO emissions at low engine speeds are significant compared to high engine speeds. From 1600 rpm until 2400 rpm, CO emissions were found to be near to zero. So engine speed definitely has a great impact on CO emissions. This is due to the rich air-fuel mixture at low engine speeds which can be expressed by the excess air factor (λ). For better understanding the effect of λ on CO emissions, the figures are divided into three main mixture regions of rich mixture (λ < 1.0), stoichiometric mixture (λ = 1.0), and lean mixture (λ > 1.0) (Reşitoğlu et al., 2015). The highest CO emissions occurred at lower speeds due to the lack of the required air in the rich fuel mixture (λ < 1.0) which contributes to incomplete combustion of the fuel as well as lower in-cylinder temperature (Wu et al., 2004, Abedin et al., 2014). Further, no noticeable CO emissions were recorded at high engine speeds due to the complete combustion of the fuel with the lean air-fuel mixture (λ > 1.0). This is expected because diesel engines are lean combustion engines which emit lower CO as compared to gasoline engines as reported by Reşitoğlu et al. (2015). Figure 5.18 illustrates the variation of CO_2 emissions with variable engine speed at full load condition.

The key parameter of combustion efficiency is the level of CO_2 emissions. Figure 5.18 implies that CO_2 increases with the increase in biodiesel blends, However, CO_2 also increases with the increase in engine speed up until 1400 rpm, then decreases until 2200 rpm and again increases up to 2400 rpm. Similar trends of CO_2 emissions are observed for other biodiesels by various research groups (Sakthivel, 2016, Palash et al., 2015, Muralidharan and Vasudevan, 2011). The study found that, over the entire range of engine speed, Mandarin biodiesel CO emissions declined by an average of 18.00% (B5) to 26.00% (B20) which leads to about 0.70% (B5) to 1.44% (B20) CO_2 emissions as compared to ULSD [Figure 5.17 (a) and Figure 5.18 (a)]. Similarly, Crambe CO emissions decrease by about 7.00% (B5) to 39.00% (B20) which leads to CO_2 emissions of about 0.65% (B5) to 1.64% (B20). Avocado reduces CO emissions by about 31.00% (B5) to 49.00% (B20) which leads to CO_2 emissions of about 0.65% (B5) to 1.33% (B20). Borage emits about 15.00% (B5) to 22.00% (B20) CO that leads to about 0.37% (B5) to 0.77% (B20) CO_2 emission. Bush nut emits about 26.00% (B5) to 40.00% (B20) CO which leads to about 0.47% (B5) to 1.41% (B20) CO_2 emission as compared to ULSD. The results also reveal that the mixture blends significantly reduce CO by an average of 38.00% (ManCr_Pa), 22.00% (TaMan_Pa), 30.00% (BoMan_Pa), and 35.00% (AvBn_Pa) which enhances CO_2 emissions by about 1.50%, 1.34%, 1.70% and 0.94% respectively over the entire range of engine speed. The mixture blends reduce two times CO emissions and emit bit more CO_2 as compared to each of their B5 blends which implies better combustion of blends.

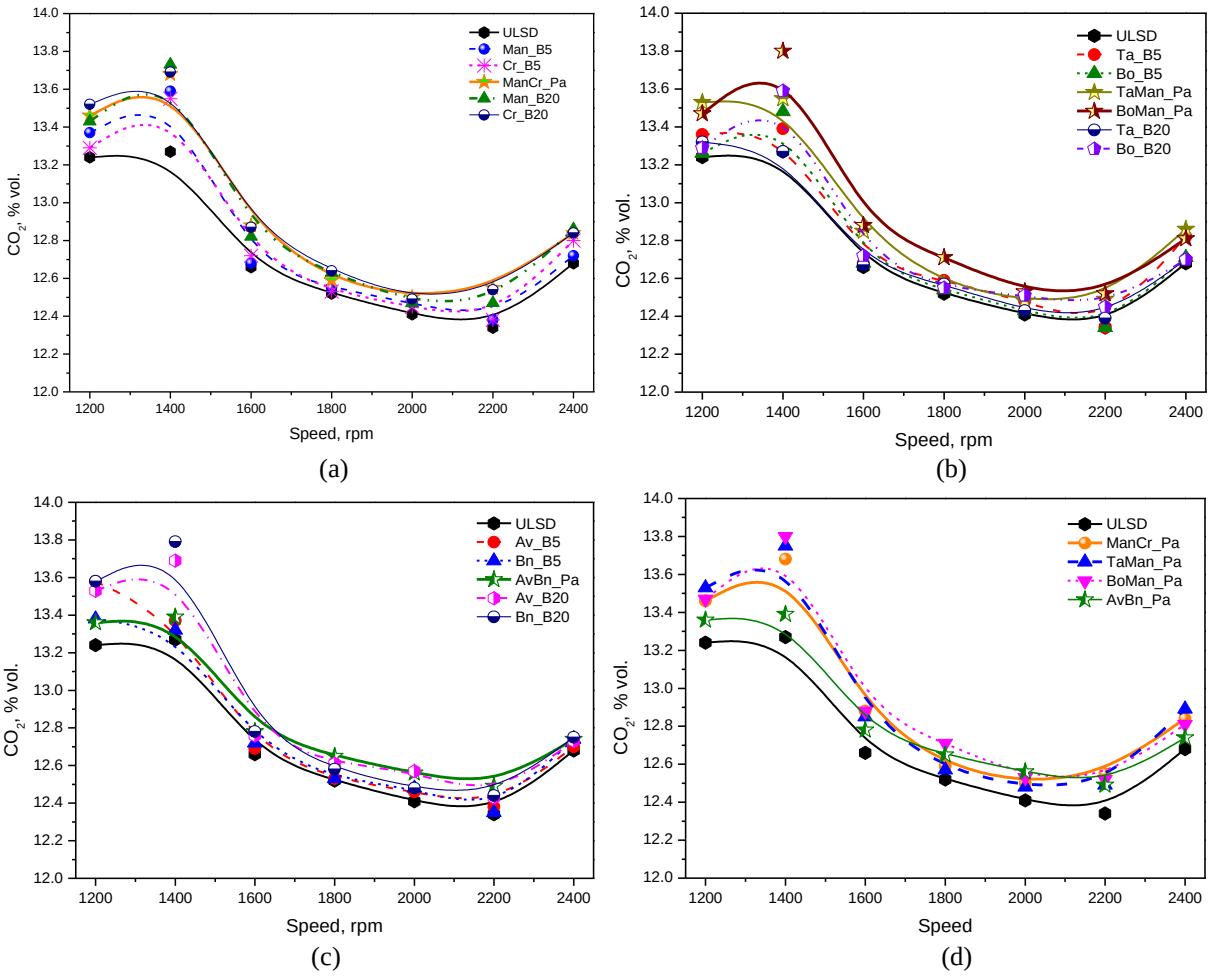

Figure 5.18: Variation of CO_2 and lambda (λ) with engine speed at full load condition for (a) Mandarin-Crambe, (b) Tamanu-Borage, (c) Avocado-Bush nut, and (d) biodiesel-paraffin mixture blends

5.5.3. Variation of CO and CO_2 emissions with engine load

Figure 5.19 demonstrates the variation of CO and λ with engine load (25%, 50%, 75% and 100%) at rated engine speed for (a) Mandarin-Crambe, (b) Tamanu-Borage, (c) Avocado-Bush nut, and (d) biodiesels-paraffin mixtures blends, respectively. The trend implies that CO emissions decrease with the increase in engine load up until 75% load, then remains approximately stable until full load (Palash et al., 2015, Buyukkaya et al., 2013). On the other hand, CO_2 emissions increase with the increase in engine load (Figure 5.20). Similar trends were also found by Sanjid et al. (2014). This is due to the high temperature rise in the combustion chamber when the engine runs over 50% load (Sakthivel, 2016). This higher temperature is the main reason for the generation of more hydroxyl (OH) that oxidises CO (Equation 5.1), hence the reduction in CO emissions. Another reason for the reduction in CO

is likely to be the shorter ignition delay and longer combustion duration at higher load condition. As reported by Reşitoğlu et al. (2015), the oxidation rate of CO is slow. It requires a longer time to complete the oxidation reaction. So, the longer combustion duration at higher engine load allows enough time to oxidise CO and convert it to CO_2. This conversion is clearly reflected in Figure 5.20 which shows that CO_2 increases from when progressing from lower load to higher load whereas CO decreases with the increase in engine load. At lower loads, CO generation is higher due to the over-lean mixture of air-fuel ($\lambda \approx 2.0$). At over-lean conditions, the air-fuel mixture is too lean to auto ignite and the droplets are too large to initiate adequate turbulence or swirl to support a propagating flame which results in higher CO emissions (Abedin et al., 2014, Reşitoğlu et al., 2015). On the other hand, at full load condition the air-fuel mixture becomes stoichiometric ($\lambda = 1.0$) (Figure 5.15) which results in higher combustion efficiency and leads to lower CO emissions. Due to similar reasons, CO_2 emissions increase with the increase in engine load as shown in Figure 5.20.

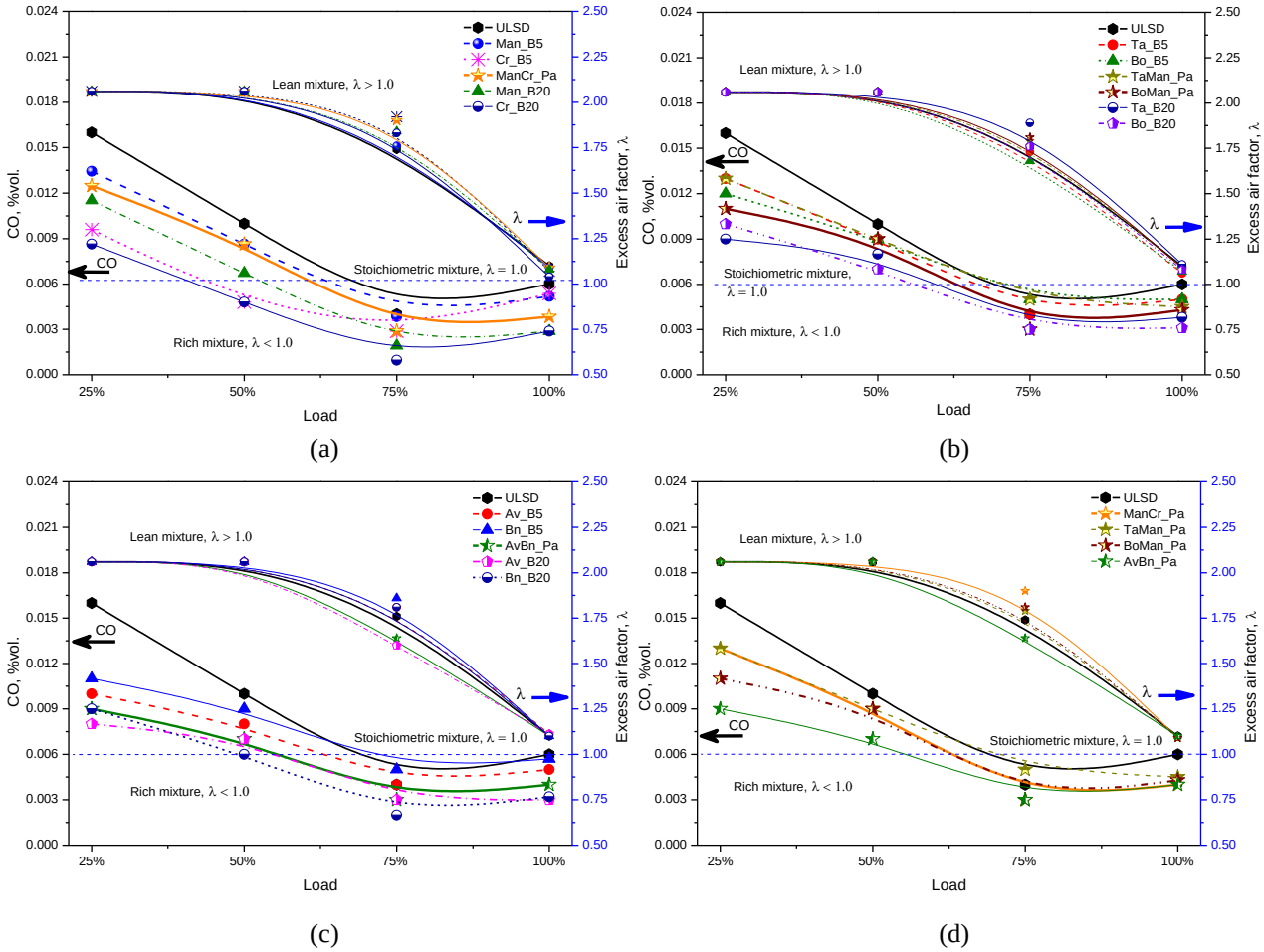

Figure 5.19: Variation of CO and lambda (λ) with engine load at rated power condition for (a) Mandarin-Crambe, (b) Tamanu-Borage, (c) Avocado-Bush nut, and (d) biodiesel-paraffin mixture blend

Figure 5.20 shows CO_2 emissions increase with increase in engine load and biodiesel blend due to oxidised CO being converted to CO_2. A noticeable drop of CO emissions was recorded for mixture blends due to the improvement in fuel properties. For instance, ManCr_Pa reduced CO by about 7.14% to 25.93% from low load (25%) to high load (100%) as compared to Man_B5; TaMan_Pa drops CO up to 10.00% at higher load as compared to Ta_B5; BoMan_Pa decreases CO emissions about 8.33% to 14.00% from low load to high load as compared to Bo_B5; and the AvBn_Pa mixture blend reduces CO emissions by about 10.00% to 20.00% from low load at high load as compared to Av_B5. This can be attributed to the lower density and viscosity of the mixture blends as compared to each of their B5 blends. The properties of the mixture blends enhance the fine spray and atomisation quality with sufficient turbulence or swirl, resulting in a decline in CO emissions. These results also agree with previous studies conducted by Reşitoğlu et al. (2015) and Abedin et al. (2014).

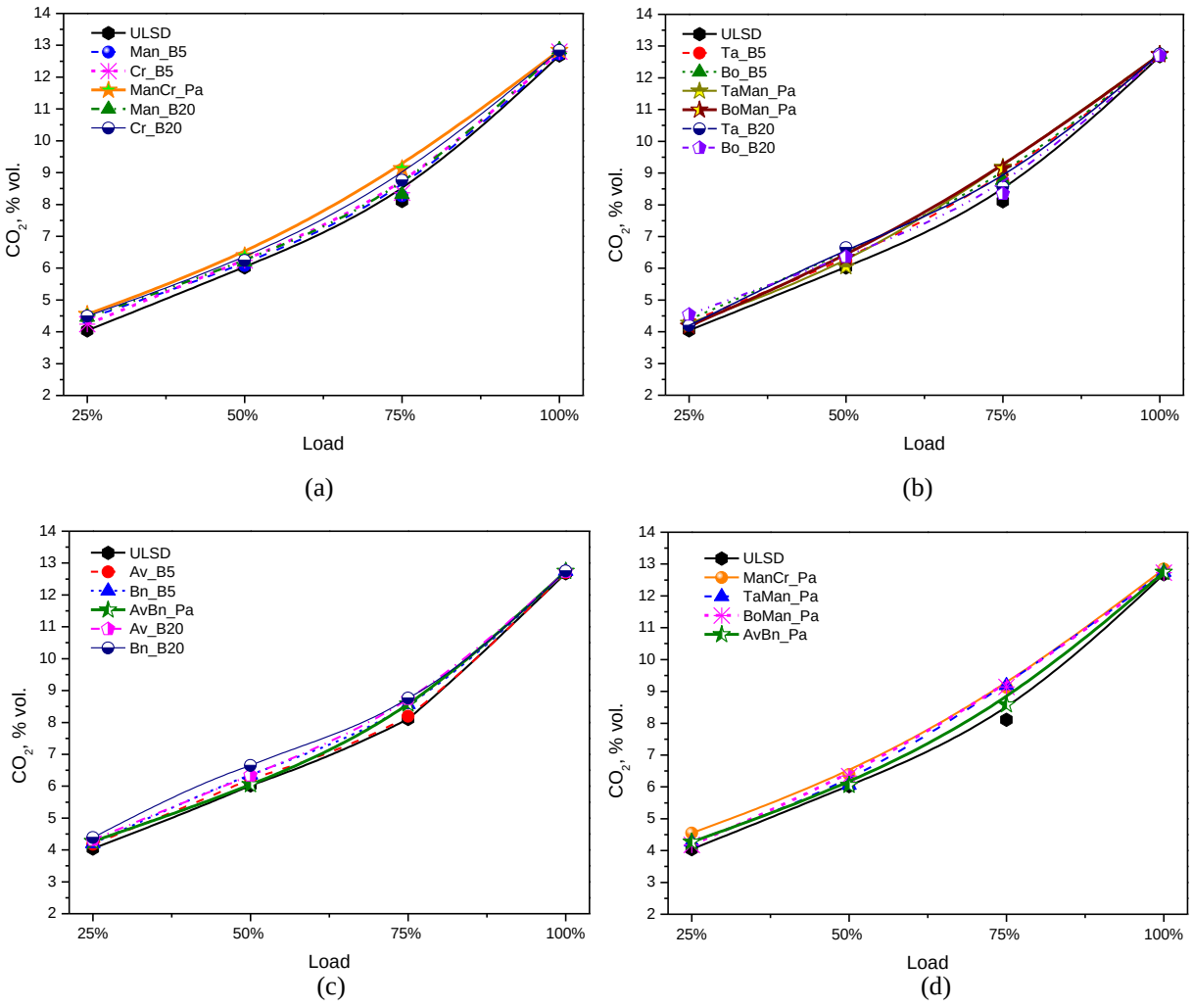

Figure 5.20: Variation of CO_2 emissions with engine load at full load condition for (a) Mandarin-Crambe, (b) Tamanu-Borage, (c) Avocado-Bush nut, and (d) biodiesel-paraffin mixture blends

5.6. Hydrocarbon (HC) Emissions

5.6.1. Variation of HC emissions with biodiesel blends

Hydrocarbon (HC) is one of the organic compounds composed of unburned fuels which form due to incomplete combustion. It is reported in the literature that HC consists of many species including alkanes, alkenes and aromatics etc. which is generally denoted as an equivalent CH_4 content (Reşitoğlu et al., 2015, Yamada et al., 2011). The prime reasons for HC emissions in CI engines are over lean or over rich air-fuel mixtures, cylinder temperature, operating conditions, fuel properties, untidy injection and improper mixing (Sajjad et al., 2015, Reşitoğlu et al., 2015). During combustion, HC formation occurs near the cylinder wall due to the significantly low temperatures as compared to the centre core of the combustion chamber as shown in Figure 5.21 (Machado Corrêa and Arbilla, 2008).

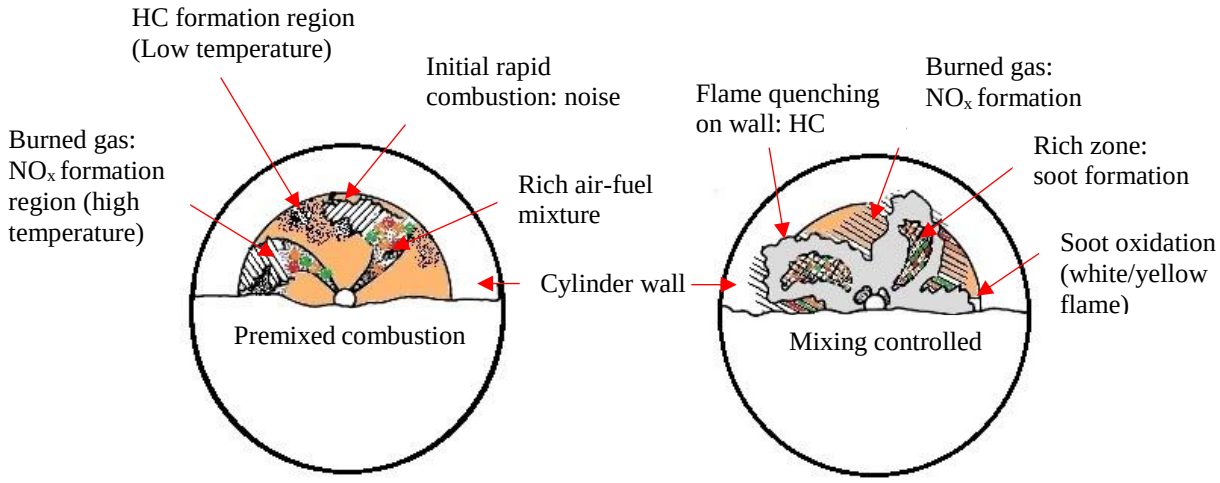

Figure 5.21: Pollutant formation mechanisms inside the cylinder

Figures 5.22 and 5.23 illustrate a comparison of HC emissions for tested biodiesel blends and ULSD at rated power and rated torque conditions, respectively. The trend of the curves implies that oxygen enriched biodiesel blends reduce HC emissions compared to ULSD. HC emissions decrease with the increase in biodiesel blends for both conditions which has also been reported by Abedin et al. (2014). For example, the maximum reductions of HC were recorded for mixture blends at rated torque to rated power condition by about 63% to 73% for ManCr_Pa, 36% to 40% for TaMan_Pa, 26% to 33% for AvBn_Pa, and 20% to 26% for BoMan_Pa respectively compared to ULSD. The results also reveal that the mixture blends reduce the HC emissions more compared to each of their B5 blends mainly due to the improvement of fuel

properties as compared to the B5 blends. The summary of HC reductions for biodiesel blends compared to ULSD is illustrated in Table 5.10. As seen from the table, the Crambe biodiesel achieves the maximum reduction in HC emissions compared to ULSD, with an average of 33.0% (B5) to 46.7% (B20) at rated power (Figure 5.22) and 26.0% (B5) to 36.8% (B20) at rated torque condition (Figure 5.23), respectively. The least reduction occurred for both Mandarin and Bush nut with an average of 6.0% (B5) to 33.0% to 40.0% (B20) at rated power and 5.0% to 10.0% (B5) to 26.0% to 31.0% (B20) at rated torque condition, respectively. This is due to the availability of more oxygen contents in the biodiesel blends which enhances the combustion quality i.e. reduced HC emission.

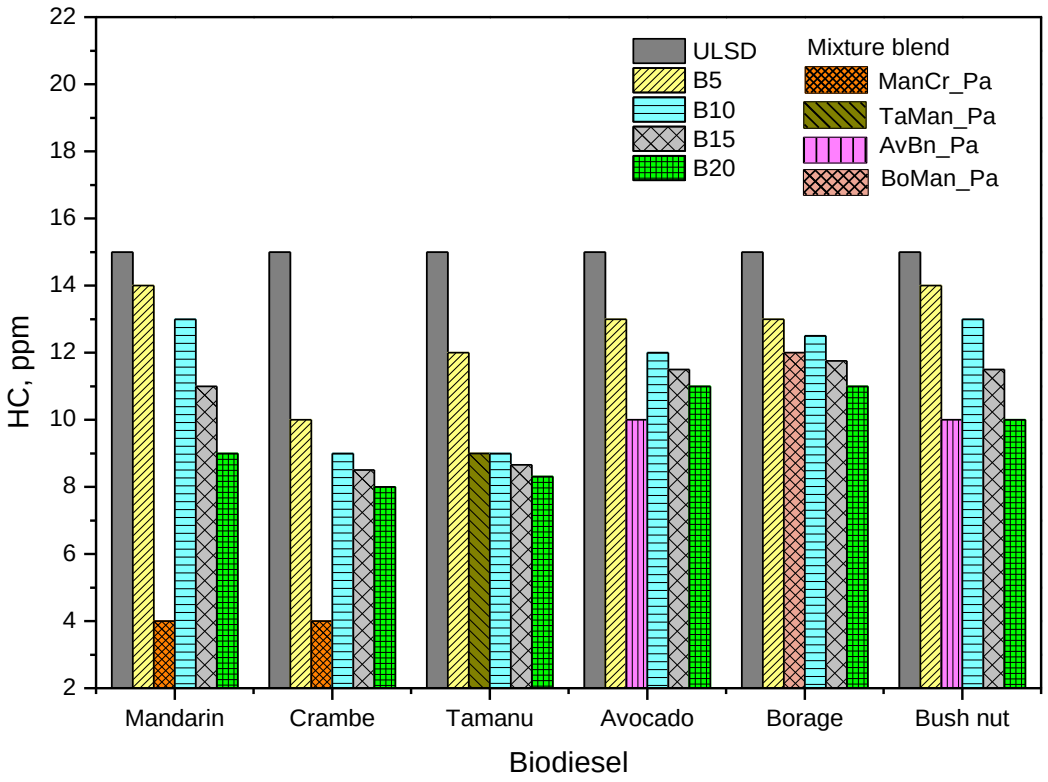

Figure 5.22: Variation of HC emissions reduction with biodiesel blends (B5 to B20) at rated power condition

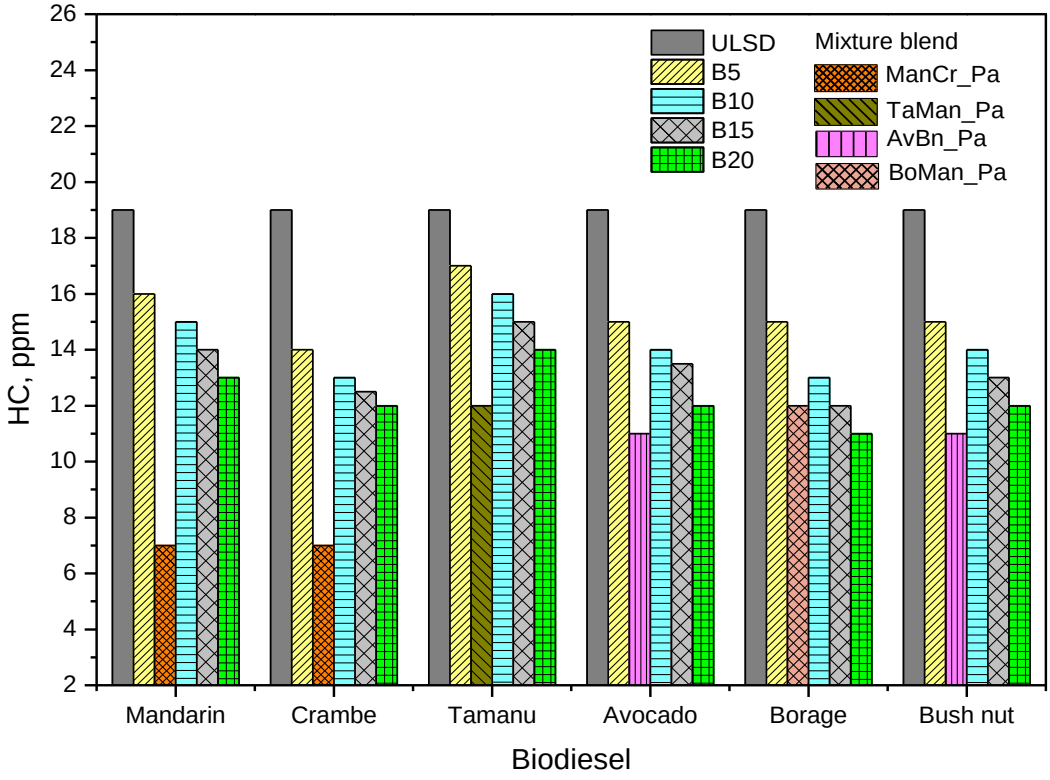

Figure 5.23: Comparison of HC emissions reduction with biodiesel blends at rated torque condition

Table 5.10: Comparison (%) of HC reduction by biodiesel blends compared to ULSD

Biodiesel	Rated power, 2400 rpm				Rated torque, 1400 rpm			
	B5	B10	B15	B20	B5	B10	B15	B20
Mandarin	-6.67*	-13.33	-26.67	-40.00	-15.79	-21.05	-26.32	-31.58
Crambe	-33.33	-40.00	-43.33	-46.67	-26.32	-31.58	-34.21	-36.84
Tamanu	-20.00	-40.00	-42.30	-44.60	-10.53	-15.79	-21.05	-26.32
Avocado	-13.33	-20.00	-23.33	-26.67	-21.05	-26.32	-28.95	-36.84
Borage	-13.33	-16.67	-21.67	-26.67	-21.05	-31.58	-36.84	-42.11
Bush nut	-6.67	-13.33	-23.33	-33.33	-21.05	-26.32	-31.58	-36.84

Note: *Negative sign (-) represents reduction of HC.

5.6.2. Reduction of HC emissions with engine speed

Figure 5.24 shows the variation of HC emissions with engine speed at full load condition for tested fuels. The results reveal that HC decreases with the increase of engine speed. A similar trend was also reported by various research groups (Monirul et al., 2016, Aydın and Sayın, 2014, Palash et al., 2015). At lower engine speed, more HC emissions occurred due to the over rich air-fuel mixture ($\lambda < 1.0$) (Figure 5.17) resulting in incomplete combustion and lower cylinder temperature which indicates lower EGT (Figure 5.33). On the other hand, lower HC

emissions are expected at higher engine speed which can be explained by the stoichiometric air-fuel mixture (λ = 1.0) (Figure 5.17) and shorter ignition delay resulting in higher combustion temperature by cleaner combustion of fuels. The study found that, over the entire range of engine speed, mixture blends show significant reduction in HC emissions with an average of 61%, 38%, 25%, and 30% by ManCr_Pa, TaMan_Pa, BoMan_Pa and AvBn_Pa compared to ULSD, respectively [Figure 5.24 (a) to (c)]. This is primarily due to the oxygenated biodiesels mixed with additives to improve fuel quality by reducing density and viscosity of the mixture blends. These can be attributed to the fine spray (enhanced air-fuel mixture quality) containing more oxygen which is essential for good combustion characteristics (An et al., 2013). Figure 5.24 (d) demonstrates the comparison of mixture blends with ULSD which indicates that the ManCr_Pa mixture blend cuts more HC emissions compared to other mixture blends.

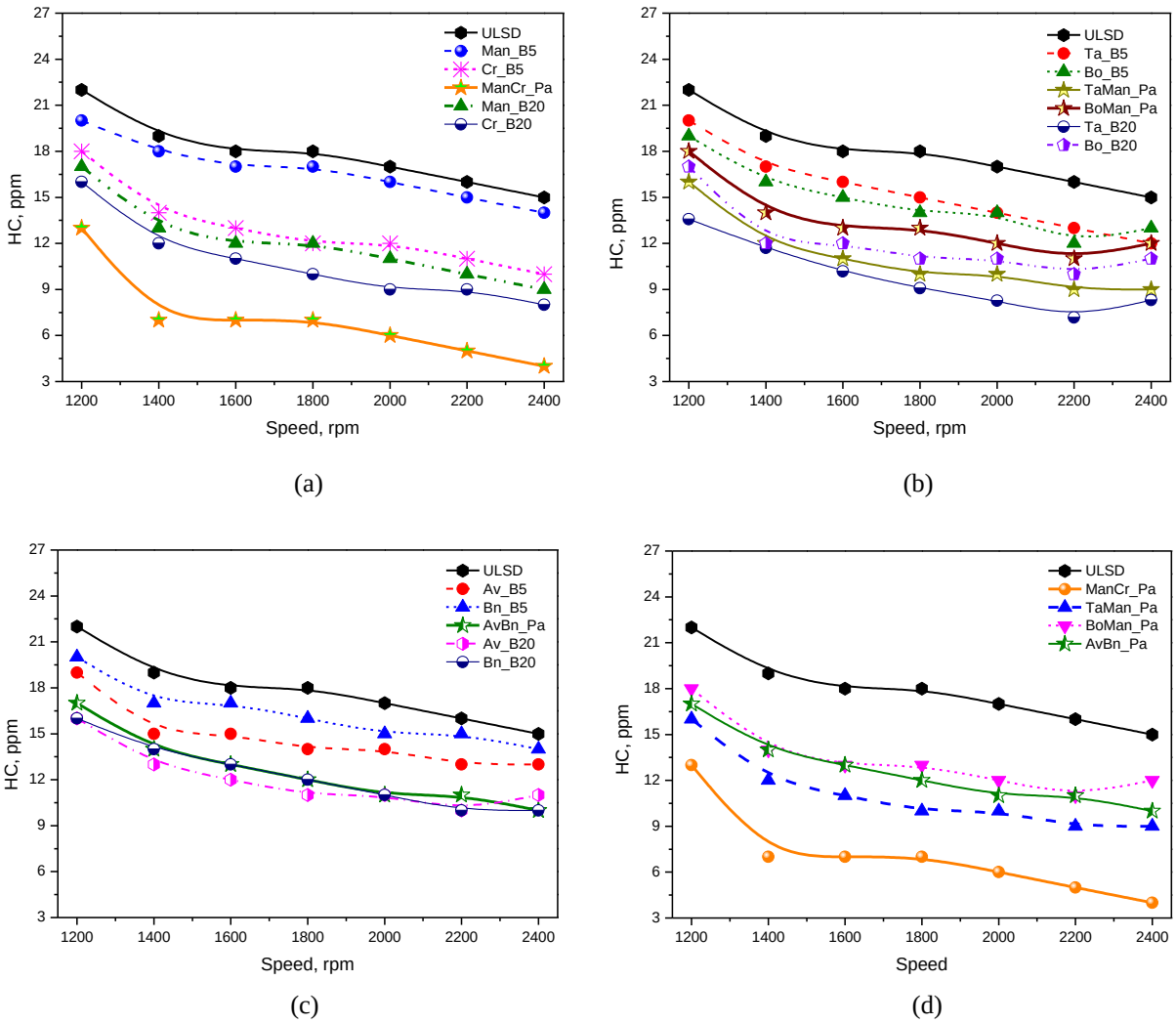

Figure 5.24: Variation of HC emissions with engine speed at full load condition for (a) Mandarin-Crambe, (b) Tamanu-Borage, (c) Avocado-Bush nut, and (d) biodiesel-paraffin mixture blends

Table 5.11 provides the summary of HC reductions for the biodiesel blends compared with ULSD as well as for the mixture blends compared to ULSD and the B5 blends. As seen from the table, over the entire range of engine speed, Mandarin biodiesel reduces HC emissions by about 6% to 33% (B5 to B20), Crambe by about 28% to 40% (B5 to B20), Tamanu by about 41% to 45% Avocado by about 17% to 33% (B5 to B20), Borage by about 8% to 33% (B5 to B20) and Bush nut by about 8% to 31% (B5 to B20) compared to ULSD, respectively. Thus, Tamanu biodiesel shows better performance with respect to HC emissions reduction. The study investigation on HC emissions at different engine loads are briefly discussed below.

Table 5.11: Summary of HC reduction (%) compared to ULSD throughout the entire range of engine speed

Compared with ULSD	Mandarin		Crambe		Tamanu		Borage		Avocado		Bush nut	
	B5	B20	B5	B20	B5	B20	B5	B20	B5	B20	B5	B20
	-6.4*	-33.4	-28.5	-40.7	-14.8	-45.8	-17.7	-33.0	-17.6	-32.9	-8.7	-31.5
Mixture name →	ManCr_Pa				TaMan_Pa		BoMan_Pa		AvBn_Pa			
Mixture/ULSD	**-61.9**				-38.9		-25.8		-30.0			
Mixture/B5	-59.2				-28.3		-34.3		-8.7			

Note: *Negative sign (-) represents decrease of HC emissions.

5.6.3. Effect of engine load on HC emissions

Figure 5.25 depicts the variation of HC emissions of the tested biodiesels at different engine speeds for (a) Mandarin-Crambe, (b) Tamanu-Borage, (c) Avocado-Bush nut, and (d) biodiesel-paraffin mixture blends. The trend of the curves implies that HC emissions decrease with the increase in engine load. This is mainly because of the very lean air-fuel mixture at lower engine loads (Figure 5.19) which leads to higher HC emissions as discussed above. This reason was also pointed out by (Sajjad et al., 2015). In addition, higher HC emissions at lower load condition can also be attributed to the poor fuel distribution, longer ignition delay and inadequate air-fuel mixture due to the insufficient turbulence or swirl (Sakthivel, 2016). Another major reason is the occurrence of wall quenching of flames due to the impingement of fuel spray into the lower temperature region on the peripheral areas of the cylinder (Sajjad et al., 2015). Nevertheless, when an engine runs over half load, it overcomes those drawbacks leading to efficient combustion. This could also be identified by higher EGT at higher engine loads (Figure 5.34) which implies a near complete combustion profile and hence HC emissions reduce (Roy et al., 2016).

The results also reveal that HC emissions decrease with the increase in biodiesel blends at different engine load conditions, which is expected. The summary of HC reductions compared to ULSD is presented in Table 5.12. As seen from the table, Mandarin reduces HC emissions by an average of 5.10% (B5) to 32.80% (B20), Crambe reduces about 17.80% (B5) to 38.20% (B20), Tamanu reduces about 13.10% (B5) to 47.70% (B20), Borage reduces by 13.20% (B5) to 31.80% (B20), Avocado reduces about 14.20% (B5) to 32.80% (B20), and Bush nut reduces about 12.90% (B5) to 24.90% (B20) compared to ULSD. It can be noted that the mixture blends show HC reductions compared to ULSD as well as to each of their B5 blends. Figure 5.25 (a) and (d) imply that the ManCr_Pa mixture blend reduced HC emissions by an average of 52% compared to the Man_B5 blend. On the other hand, TaMan_Pa, BoMan_Pa and AvBn_Pa mixture blends reduced HC emissions by an average of 22%, 15%, and 20% over the entire range of engine load compared to Ta_B5, Bo_B5 and Av_B5, respectively.

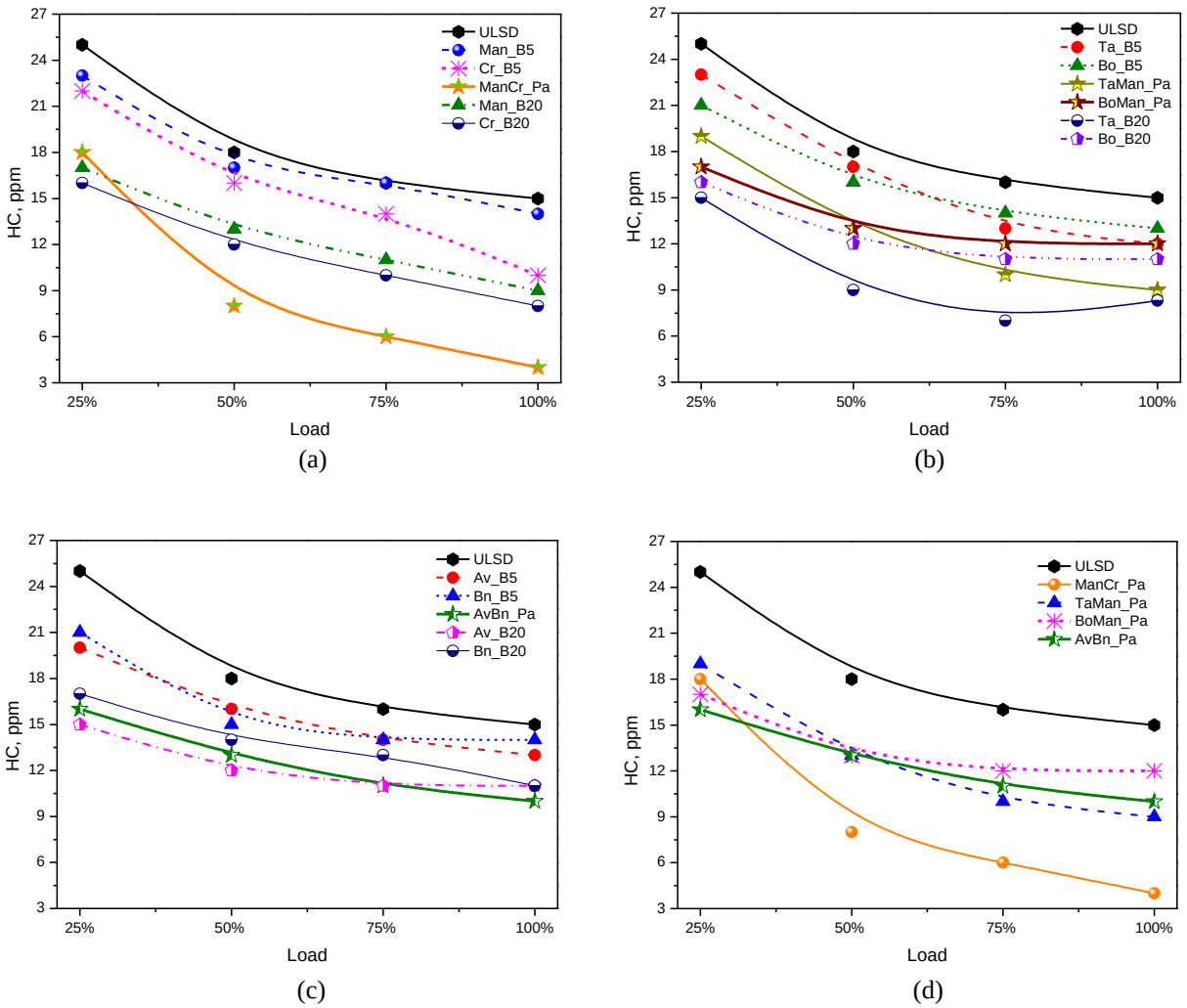

Figure 5.25: Variation of HC emissions with engine load at rated power condition for (a) Mandarin-Crambe, (b) Tamanu-Borage, (c) Avocado-Bush nut, and (d) biodiesel-paraffin mixture blend

Table 5.12: Summary of HC reduction (%) compared to ULSD throughout the entire range of engine load

Compared with ULSD	Mandarin		Crambe		Tamanu		Borage		Avocado		Bush nut	
	B5	B20	B5	B20	B5	B20	B5	B20	B5	B20	B5	B20
	-5.1*	-32.8	-17.2	-38.4	-13.1	-47.7	-13.2	-31.8	-14.2	-32.8	-12.9	-24.9
Mixture name →	ManCr_Pa				TaMan_Pa		BoMan_Pa		AvBn_Pa			
Mixture/ULSD	**-54.9**				-32.3		-26.2		-32.1			
Mixture/B5	-52.2				-22.3		-14.9		-20.8			

Note: *Negative sign (-) represents decrease of HC emissions.

5.7. Particulate Matter (PM) Emissions

PM formation in the combustion process is a complex and inter-linked phenomenon. As seen in Figure 5.26, it initially forms as soot which is sprouted by the agglomeration of tiny particles of partially oxidised fuel and lube oil, ash, sulphates and water vapour. Agarwal (2007) investigated PM composition and identified about 31% elemental carbon, 7% unburnt fuel, 40% unburnt lube oil, 14% sulphur and moisture with the remainder likely to be the ash, metal (Zn, P, Cu are in lube oil and biodiesel) and other substances. In this study, the tested fuels are ultra-low sulphur diesel (maximum 15 ppm sulphur content) and sulphur free biodiesel which may cause insignificant PM formation due to sulphur content in the fuel.

Figure 5.26 also demonstrates that the PM formation process is initiated as nucleation, surface growth, agglomeration and adsorption/condensation. The first three steps occur inside the cylinder due to the dehydrogenation or oxidation process with time and the fourth step (adsorption or condensation) occurs in the exhaust stream in the atmosphere. In the combustion process, carbon particles start nucleating initially then some semi-volatile and low-volatile organic components condense on the surface of the carbon (known as surface growth) and start growing. The agglomeration of all particles together to form the extreme tiny particles during expansion and exhaust stroke is known as PM (Wang et al., 2016). It is reported in the literature that PM spheres are typically about 15 to 40 nm while about 90% of particles are less than 1μm in diameter (Reşitoğlu et al., 2015). The study investigated the particle size < 100 nm to > 10 microns in the exhaust emissions for the tested fuels. The formation of PM by combustion of diesel and biodiesel blends depends on many factors which are briefly discussed below.

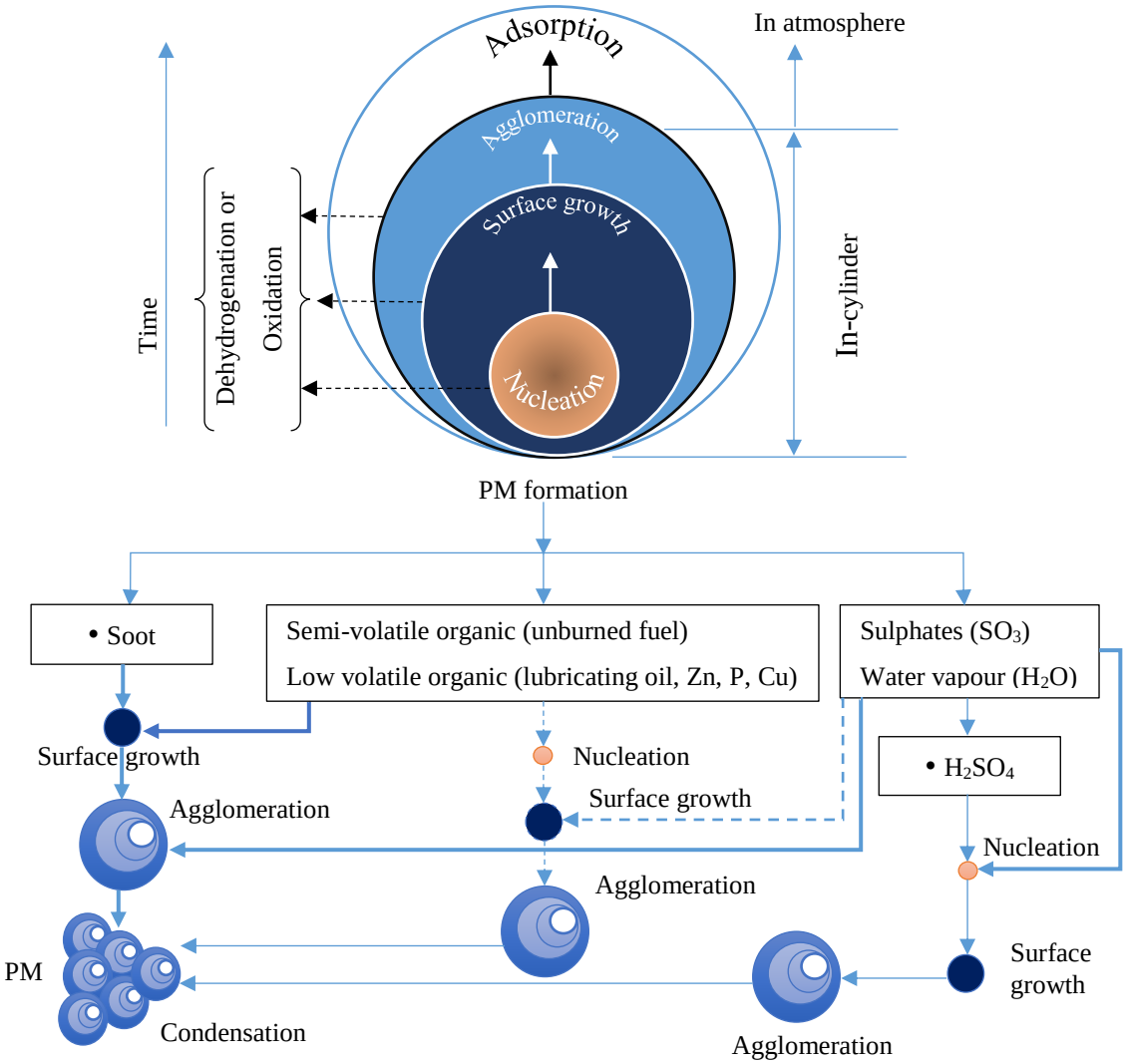

Figure 5.26: PM formation process

5.7.1. Variation of PM emissions with biodiesel blends

Figures 5.27 and 5.28 illustrate the variation of PM emissions in the exhaust gases with biodiesel blends at rated power and torque condition, respectively. The results reveal that higher PM emissions were recorded for ULSD. On the other hand, PM emissions declined for the ternary mixture blends (ManCr_Pa, TaMan_Pa, AvBn_Pa, BoMan_Pa) by about 17.79%, 41.93%, 31.59%, 38.75% and 32.44%, 11.57%, 40.03%, 53.96%, 40.03% as compared to ULSD at rated power and rated torque condition, respectively. The comparisons of PM reduction by binary (biodiesel) blends are presented in a tabular form in Table 5.13 for both test conditions. As seen from the table, the maximum and minimum reductions are obtained for Tamanu biodiesel with 23.54% (B5) to 60.16% (B20) and Mandarin biodiesel with about

3.82% (B5) to 14.29% (B20) at rated power condition, respectively. Further, the maximum and minimum PM reductions occurred for Borage biodiesel with about 52.00% (B5) to 57.00% (B20) and Tamanu biodiesel with 2.75% (B5) to 14.62% (B20) at rated torque condition, respectively. The study investigated the reasons for significant PM reductions at rated torque condition for Borage biodiesel. It was identified as being due to the prolonged combustion duration and higher heat release rate (HRR) at the diffusion (or mixing controlled) phase which helps soot oxidation and hence reduces PM formation. In addition, the higher rate of the late combustion phase is also identified as contributing to the reduced PM emissions due to the greater oxidation period of semi-volatile or low volatile organics and metals for the Avocado, Borage and mixture blends. In the same way, less PM reduction was observed for Avocado biodiesel and mixture blends (compared to ULSD and each B5 blend). In contrast, higher viscosity is responsible for poor atomisation and mixing of air and fuel as well as higher BSFC for Tamanu (Figure 5.6) which results in flame quenching on the cylinder wall. Due to this reason, higher un-burnt or partially burnt HC formation occurs (Figure 5.19) during the diffusion combustion phase. The higher HC formation helps to agglomerate more PM formation during combustion.

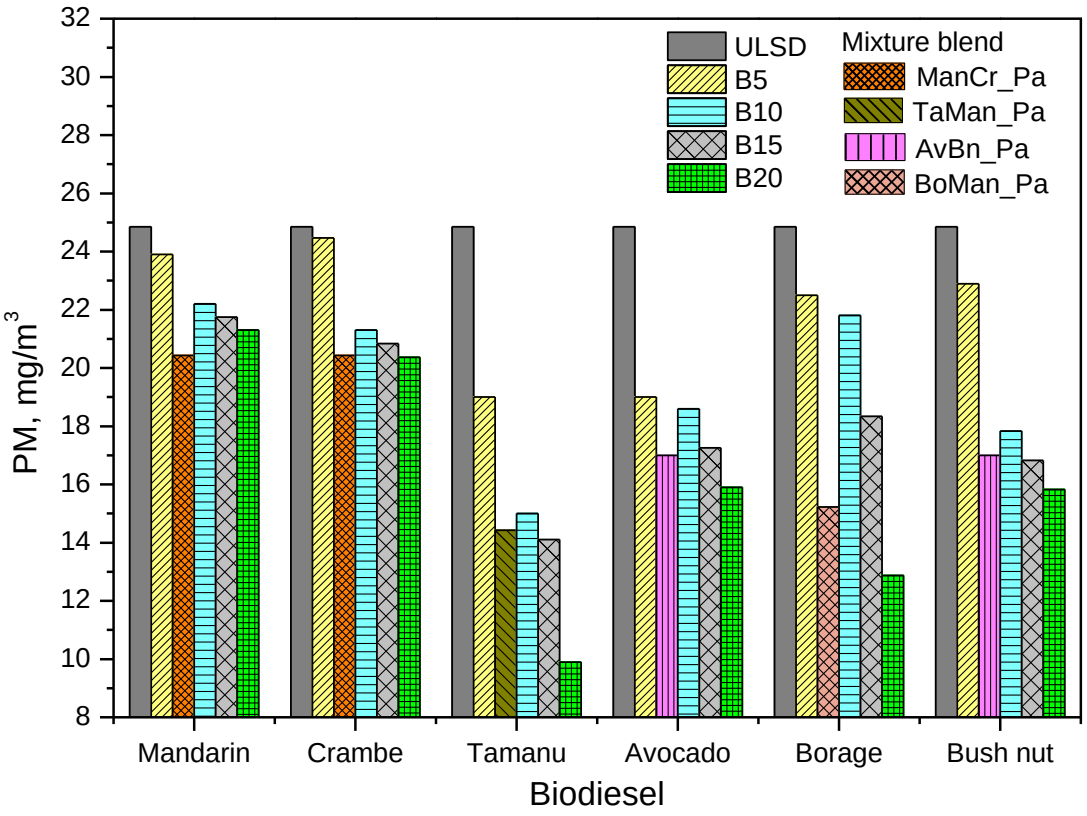

Figure 5.27: Variation of PM emissions reduction with biodiesel blends (B5 to B20) at rated power condition (full load, 2400 rpm)

The overall trends of these curves imply that PM decreases with the increase in biodiesel blends due to the enriched combustion quality of the oxygenated biodiesel blends. The study also found that the biodiesel blends have shorter ignition delay and prolonged combustion duration due to the higher cetane number of the biodiesel compared to ULSD. A similar trend was also reported by Magno et al. (2016) and Lapuerta et al. (2008b). Figure 5.28 shows that higher PM emissions occurred for Tamanu and lower emissions for Borage. This could happen for many reasons such as Tamanu having a higher number of double bonds, a higher content of ash and foreign metals (i.e. Z_n, P, and C_u etc.) and lower cetane number compared to other biodiesels. On the contrary, Borage has a higher cetane number (about 72) and a lower number of double bonds in the carbon chain compared to Tamanu. Due to the better combustion quality of Borage, soot oxidation occurred properly which helped to reduce PM emissions. By comparing these two figures, it could be clearly noted that PM emissions at rated power are insignificant compared to rated torque condition. So engine speed has a great impact on PM emissions as discussed in the following section.

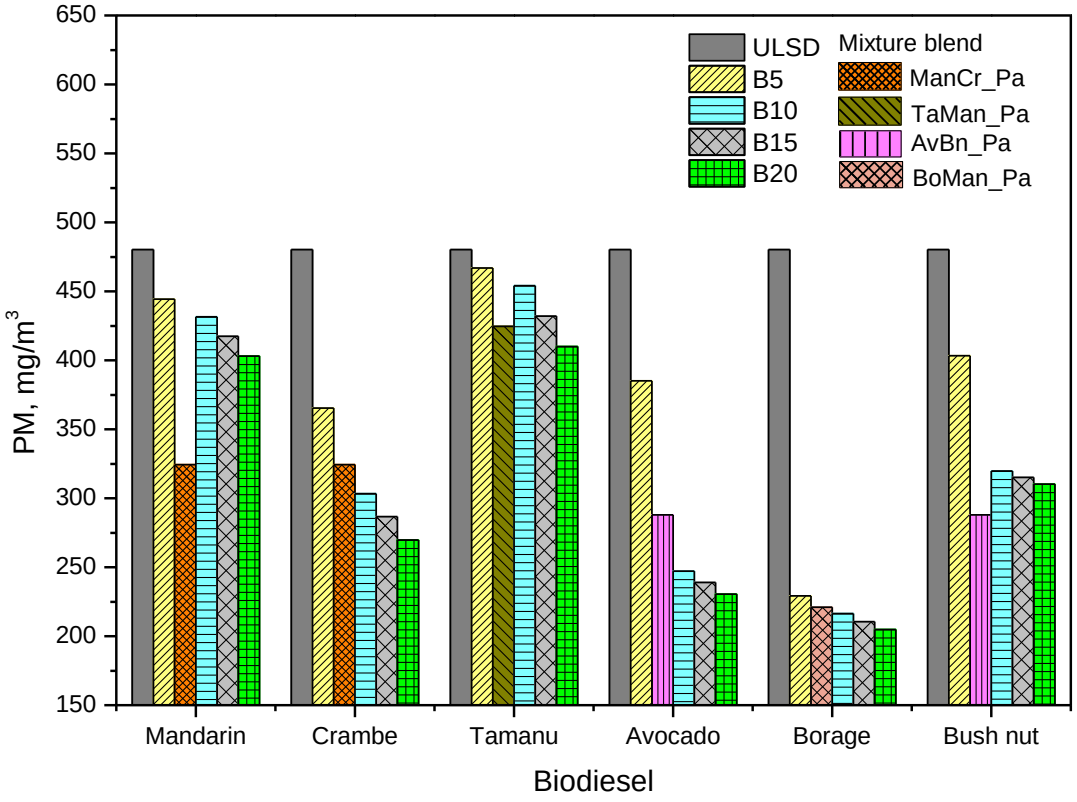

Figure 5.28: Comparison of PM emissions reduction with biodiesel blends at rated torque condition (1400 rpm)

Table 5.13: Comparison (%) of PM reduction by biodiesel blends from ULSD

Biodiesel	Rated power condition				Rated torque condition			
	B5	B10	B15	B20	B5	B10	B15	B20
Mandarin	-3.82*	-10.66	-12.47	-14.29	-7.45	-10.14	-13.09	-16.05
Crambe	**-1.53**	-14.29	-16.16	-18.03	-23.93	-36.83	-40.31	-43.85
Tamanu	-23.54	-39.64	-43.26	**-60.16**	**-2.75**	-5.46	-10.04	-14.62
Avocado	-23.54	-25.15	-30.58	-36.02	-19.78	-48.52	-50.25	-51.99
Borage	-9.46	-12.23	-26.20	-48.21	-52.26	-54.96	-56.16	**-57.36**
Bush nut	-7.89	-28.21	-32.27	-36.30	-16.00	-33.42	-34.40	-35.38

Note: *Negative sign (-) represents reduction of PM.

5.7.2. Effect of engine speed on PM emissions

Figure 5.29 demonstrates the effect of engine speed on PM emissions for tested fuels. The trends imply that PM emissions decrease with the increase in engine speed (Sajjad et al., 2015, Aydın and Sayın, 2014). The maximum PM emissions occur at lower engine speeds. This is due to the rich air-fuel mixture ($\lambda < 1.0$) (Figure 5.17) and higher ignition delay at lower engine

speeds which cause incomplete combustion. For this reason, PM formation occurs due to higher HC and soot formation at the diffusion combustion phase. It can also be noted that the trend lines for PM emissions become straight after 2000 rpm for each case due to the lean air-fuel mixture enhancing HC and soot oxidation and apparently reducing PM formation. There are many other factors that could also directly or indirectly influence PM emissions. Some of these factors are related to fuel properties, carbon chain length and the number of double bond present, fuel oxygen content, fuel quality (i.e. ash, aromatic, and sulphur content), lubricating oil quality and operating conditions (Reşitoğlu et al., 2015).

Table 5.14 compares the PM reductions with ULSD for the entire range of engine speeds. As seen from the table, the maximum PM reduction occurred with Borage biodiesel with an average of 29% (B5) to 52% (B20) compared to ULSD. This is due to the higher cetane number (about 73), lower number of double bonds in the carbon chain and adequate self-oxygen content (about 11.44%) compared to other tested biodiesels. The minimum PM reduction was found for Mandarin with about 12% (B5) to 19% (B20) compared to ULSD throughout the range of engine speeds. This lower reduction is mainly due to lower CN (about 49) and higher number of double bonds in the carbon chain (i.e. higher degree of unsaturation). The result also reveals that the biodiesel-paraffin ternary mixture blends show better performance in PM reduction compared to each of their B5 blends [Figure 5.29 (a)-(c)]. Figure 5.29 (d) compares the PM reduction of each mixture blend. It was found that the reduction of PM is highest for BoMan_Pa with about 44% and 19% (Table 5.14) as compared to ULSD and its B5 blend, respectively, whereas the TaMan_Pa mixture blend reduces PM emissions by an average of 15% and 3% compared to ULSD and the Ta_B5 blend, respectively. This is due to the higher fuel density and viscosity which causes poor atomisation, vaporisation and mixing that results in flame quenching on the cylinder wall likely to promote higher soot formation during combustion (Sharma and Murugan, 2015). The study also investigated the effect of engine load on PM formation which is briefly discussed in the following section.

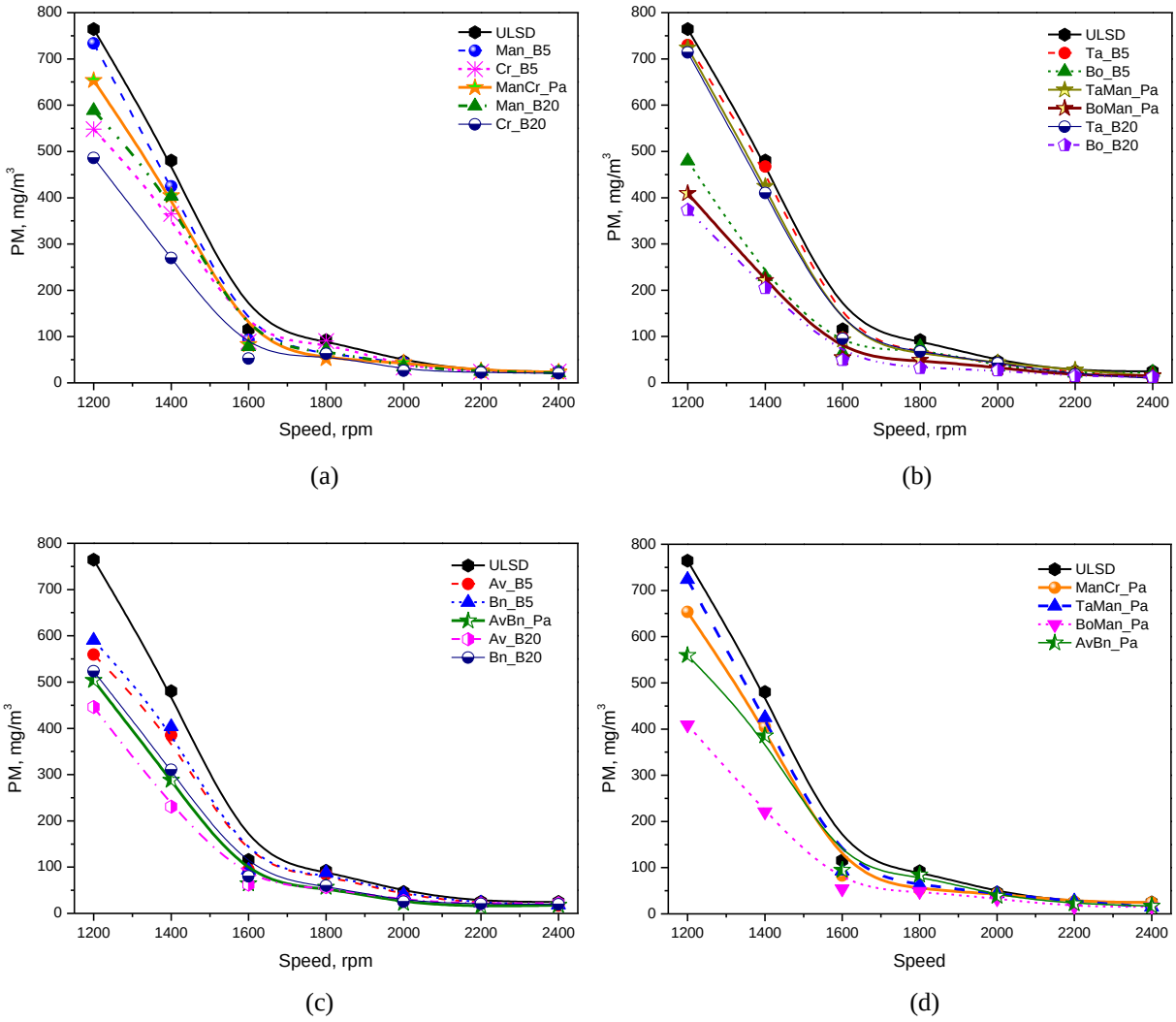

Figure 5.29: Variation of PM emissions with engine speed at full load condition for (a) Mandarin-Crambe, (b) Tamanu-Borage, (c) Avocado-Bush nut, and (d) biodiesel-paraffin mixture blends

Table 5.14: Summary of PM reduction (%) compared to ULSD throughout the entire range of engine speed

Compared with ULSD	Mandarin		Crambe		Tamanu		Borage		Avocado		Bush nut	
	B5	B20	B5	B20	B5	B20	B5	B20	B5	B20	B5	B20
	-12.7*	-19.3	-16.0	-34.2	-13.5	-23.7	-29.1	-52.5	-16.3	-39.2	-15.5	-33.1
Mixture name →	ManCr_Pa		TaMan_Pa		BoMan_Pa		AvBn_Pa					
Mixture/ULSD	-20.8		-15.5		**-44.1**		-39.9					
Mixture/B5	-9.5		-2.8		-19.1		-27.8					

Note: *Negative sign (-) represents reduction.

5.7.3. Variation of PM emissions with engine load

Figure 5.30 depicts the effect of engine load on PM formation at rated power condition for tested fuels. The trend implies that PM emissions increase with the increase in engine load. Similar trends were also reported by Zhu et al. (2016), Sharma and Murugan (2015) and Wang et al. (2016). It can also be noticed that engine loads up to 75% have insignificant impact on PM formation, but full engine load (100% load) has a great impact on PM formation. This is due to the large quantity of fuel injection (decreased λ in Figure 5.19) at full load which creates numerous fuel-rich zones in the combustion chamber. The fuel-rich zone creates uneven temperature distribution and lower oxygen concentration in the combustion chamber which causes more soot formation. In addition, the oxygen content in biodiesels could be one of the dominating factors for soot reduction at higher engine loads. As reported in the literature, soot formation decreases with the increase of oxygen concentration (Wang et al., 2016). This could be explained by Figures 5.30 (a) to (c) which indicate that PM emissions decrease with the increase in biodiesel blends. Besides, at lower load condition, the viscosity becomes a dominating factor for higher PM formation because the fuel self-oxygen becomes less advantageous at lean air-fuel mixtures.

The results reveal that, up to 75% load, Mandarin and Borage reduce PM by an average of 11% (B5) to 31% (B20) and 23% (B5) to 35% (B20) compared to ULSD, respectively due to their lower viscosity (Chapter 4, Table 4.4). On the other hand, maximum PM reduction is obtained for Tamanu and Bush nut with about 37% (B5) to 48% (B20) and 38% (B5) to 51% (B20) compared to ULSD, respectively. This is due to the higher oxygen content of about 11.68% (Tamanu) and 11.71% (Bush nut) in the biodiesels and it is evident that the higher oxygen content has a noticeable controlling impact on soot formation during combustion. Higher soot oxidation in fuel-rich zone results in lower PM formation. The summary of the PM reductions throughout the range of engine loads is presented in Table 5.15. As seen from the table, maximum PM reduction occurred for Bush nut with about 25% (B5) to 45% (B20) and the minimum reduction was for Crambe with about 5% (B5) to 9% (B20) compared to ULSD. Further, BoMan_Pa and AvBn_Pa mixture blends show very similar results due to their lower viscosity and higher oxygen content as compared to other fuels.

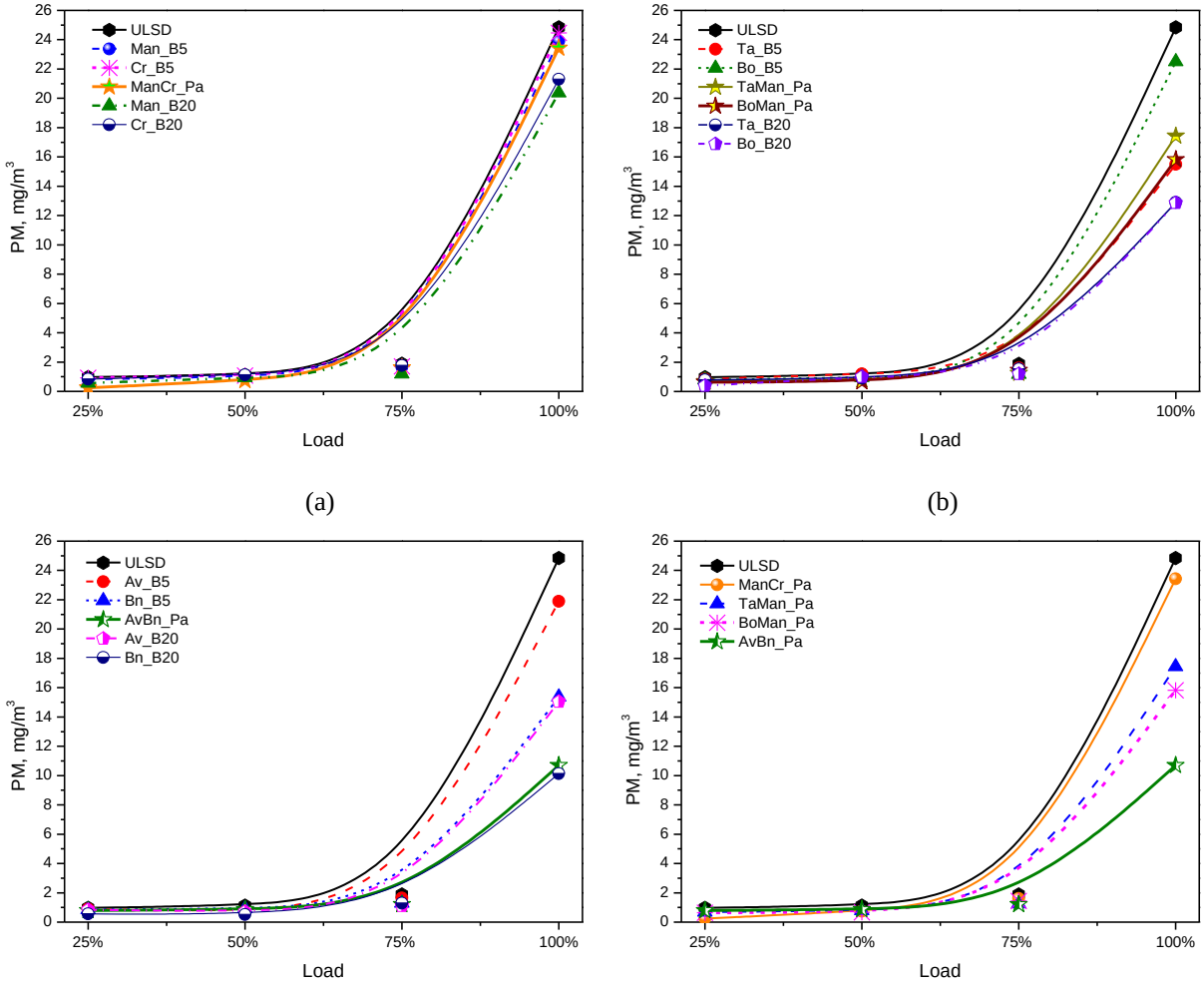

Figure 5.30: Variation of PM emissions with engine load at rated power condition (2400 rpm) for (a) Mandarin-Crambe, (b) Tamanu-Borage, (c) Avocado-Bush nut, and (d) biodiesel-paraffin mixture blend

Table 5.15: Summary of PM reduction (%) compared to ULSD throughout the entire range of engine load

Compared with ULSD	Mandarin		Crambe		Tamanu		Borage		Avocado		Bush nut	
	B5	B20	B5	B20	B5	B20	B5	B20	B5	B20	B5	B20
	-10.8*	-28.5	**-4.8**	-8.9	-14.4	-26.4	-20.3	-38.6	-17.9	-32.9	-25.3	-46.9
Mixture name →		ManCr_Pa			TaMan_Pa		BoMan_Pa		AvBn_Pa			
Mixture/ULSD		-31.9			-30.7		-33.6		**-33.7**			
Mixture/B5		-24.7			-15.9		-16.8		-16.9			

Note: *Negative sign (-) represents reduction.

5.8. Nitrogen Oxides (NO_x) Emissions and Exhaust Gas Temperature (EGT)

Nitrogen oxides emissions by combustion of biodiesels in CI engines are one of the main concerns for environmental sustainability. These are formed due to the chemical reaction of ambient nitrogen and oxygen at high temperature during combustion (Hill and Douglas Smoot, 2000). The main constituents are 85 to 95% NO and 10 to 20% NO_2 which is generally denoted as NO_x (Reşitoğlu et al., 2015). The NO_x formation can be expressed by extended Zeldovich mechanism as in the following chemical equations (Saravanan et al., 2012, Magno et al., 2016).

$$N_2 + O \leftrightarrow NO + N \quad (5.2)$$

$$N + O_2 \leftrightarrow NO + O \quad (5.3)$$

$$N + OH \leftrightarrow NO + H \quad (5.4)$$

The locally generated high temperature equilibrium at the premixed combustion phase is favourable for NO formation. However, NO_2 is formed due to the quenching of the formation of NO by mixing with excess air. This can be expressed by the following equations.

$$NO + HO_2 \leftrightarrow NO_2 + OH \quad (5.5)$$

$$NO_2 + O \leftrightarrow NO + O_2 \quad (5.6)$$

5.8.1. Variation of NO_x emissions with biodiesel blends

Figures 5.31 and 5.32 illustrate the variation of NO_x emissions with biodiesel blends (B5 to B20) and mixture blends at rated power and torque condition, respectively. The results reveal that NO_x emissions increase with the increase in biodiesel blends which has also been reported by Monirul et al. (2016), Palash et al. (2015) and Sanjid et al. (2014). This is due to the higher combustion temperature as represented by the EGTs in Figure 5.33 and the biodiesel oxygen content (Chapter 4, Table 4.4) which contributes to higher NO_x emissions. The trend also implies that biodiesel-paraffin mixture blends show comparatively lower NO_x emissions for ManCr_Pa and AvBn_Pa of about 1.80%, 3.79% and 1.03%, 6.65% compared to Man_B5 and Av_B5 at rated power and torque, respectively due to the reduction of in-cylinder peak temperatures. The summary of NO_x emissions compared to ULSD for all tested fuels is presented in Table 5.16. As seen from the table, higher percentages of NO_x emissions are recorded for Mandarin, Crambe and Avocado for both tested conditions. Mandarin and Avocado biodiesels have higher numbers of double bonds (higher DU) in the carbon chain and

Crambe has a long CCL both of which promoter higher NO_x emissions. Further, Tamanu shows lower NO_x emissions as compared to other biodiesels due to the lower cylinder peak temperature at the premixed combustion phase. NO_x emissions are highly sensitive to cylinder temperature which can be represented by EGT. The effect of EGT on NO_x emissions with variable engine speed and load is further discussed in brief below.

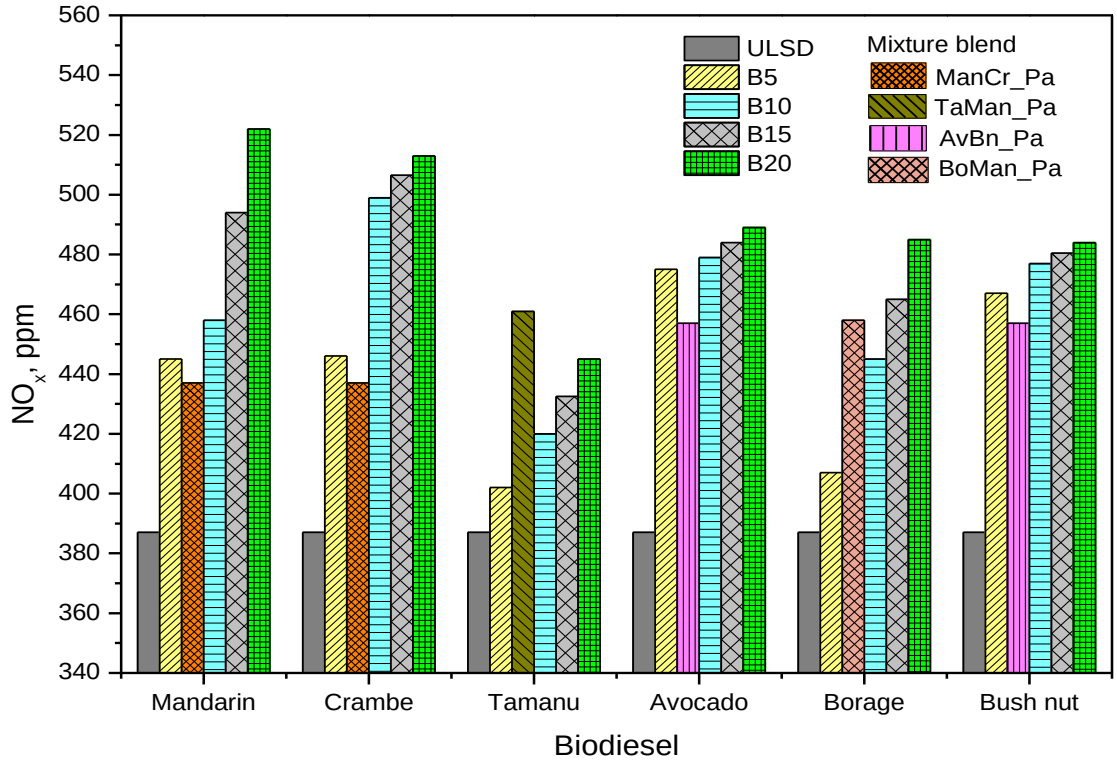

Figure 5.31: Variation of NO_x emissions with biodiesel blends (B5 to B20) at rated power condition (at full load)

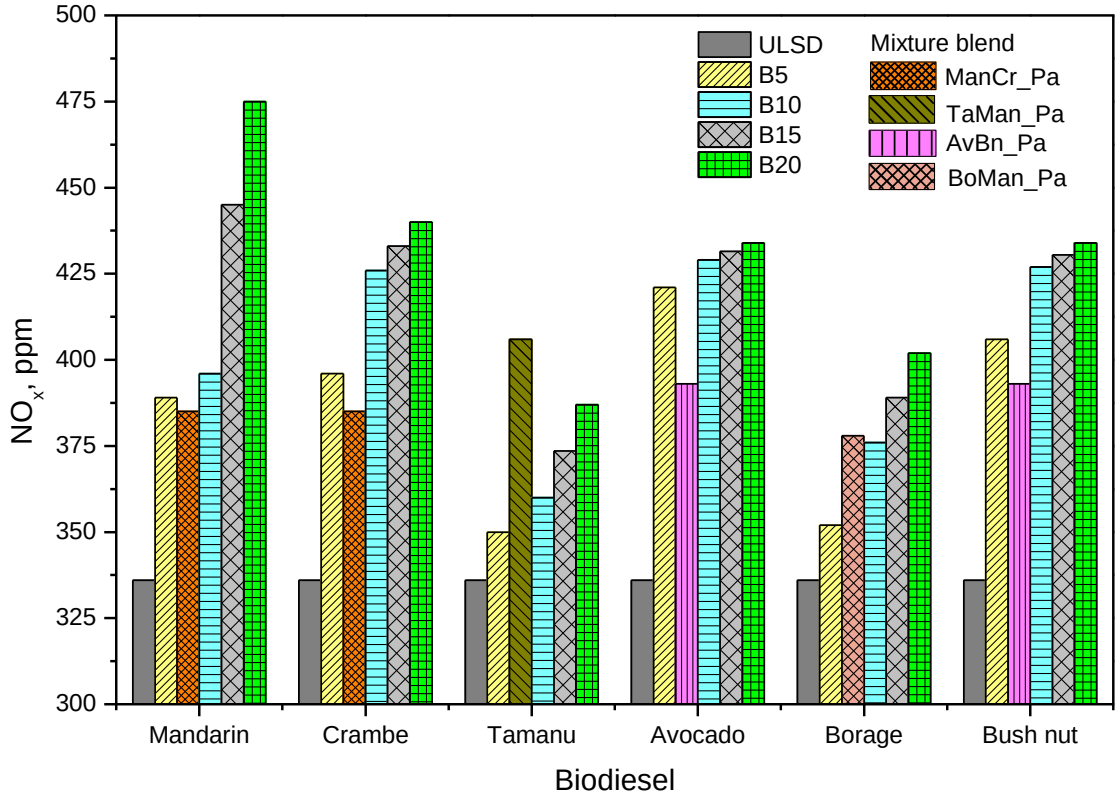

Figure 5.32: Variation of NO_x emissions with biodiesel blends at rated torque condition (at full load)

Table 5.16: Summary of NOx emissions by biodiesel blends compared to ULSD

Biodiesel	Rated power, 2400 rpm				Rated torque, 1400 rpm			
	B5	B10	B15	B20	B5	B10	B15	B20
Mandarin	14.99*	18.35	27.65	34.88	11.31	17.86	32.44	**41.37**
Crambe	15.25	28.94	**30.88**	32.56	17.86	26.79	28.87	30.95
Tamanu	**3.88**	8.53	11.76	14.99	**4.17**	7.14	11.16	15.18
Avocado	22.74	23.77	25.06	26.36	25.30	27.68	28.42	29.17
Borage	5.17	14.99	20.16	25.32	4.76	11.90	15.77	19.64
Bush nut	20.67	23.26	24.16	25.06	20.83	27.08	28.13	29.17

Note: *Positive sign (+) represents increase.

5.8.2. Effect of EGT on NOx emissions with engine speed

Figure 5.33 exhibits the effect of EGT on NO_x emissions with engine speed at full load condition for (a) Mandarin-Crambe, (b) Tamanu-Borage, (c) Avocado-Bush nut, and (d) biodiesel-paraffin mixture blends, respectively. The trend implies that both EGT and NO_x emissions increase with the increase in engine speed which have also been reported by Monirul et al. (2016) and Abedin et al. (2014). This is due to the rich air-fuel mixture ($\lambda < 1.0$) at lower engine speeds as shown in Figure 5.15 and has been ascribed to incomplete combustion

resulting in lower cylinder temperatures (Figure 5.33). On the contrary, the engine reaches lean air-fuel mixtures at higher engine speed whereas the excess air factor λ varies from 1.05 to 1.15 giving cleaner combustion with higher flame temperatures which causes higher NO_x emissions. The summary of NO_x emissions compared to ULSD is presented in Table 5.17. The results reveal that average NO_x emissions increase from B5 to B20 blends by about 13% to 30%, 15% to 26%, 15% to 27%, 21% to 24%, 27% to 27.6% and 22% to 27% throughout the entire range of engine speed for Mandarin, Crambe, Tamanu, Borage, Avocado and Bush nut, respectively.

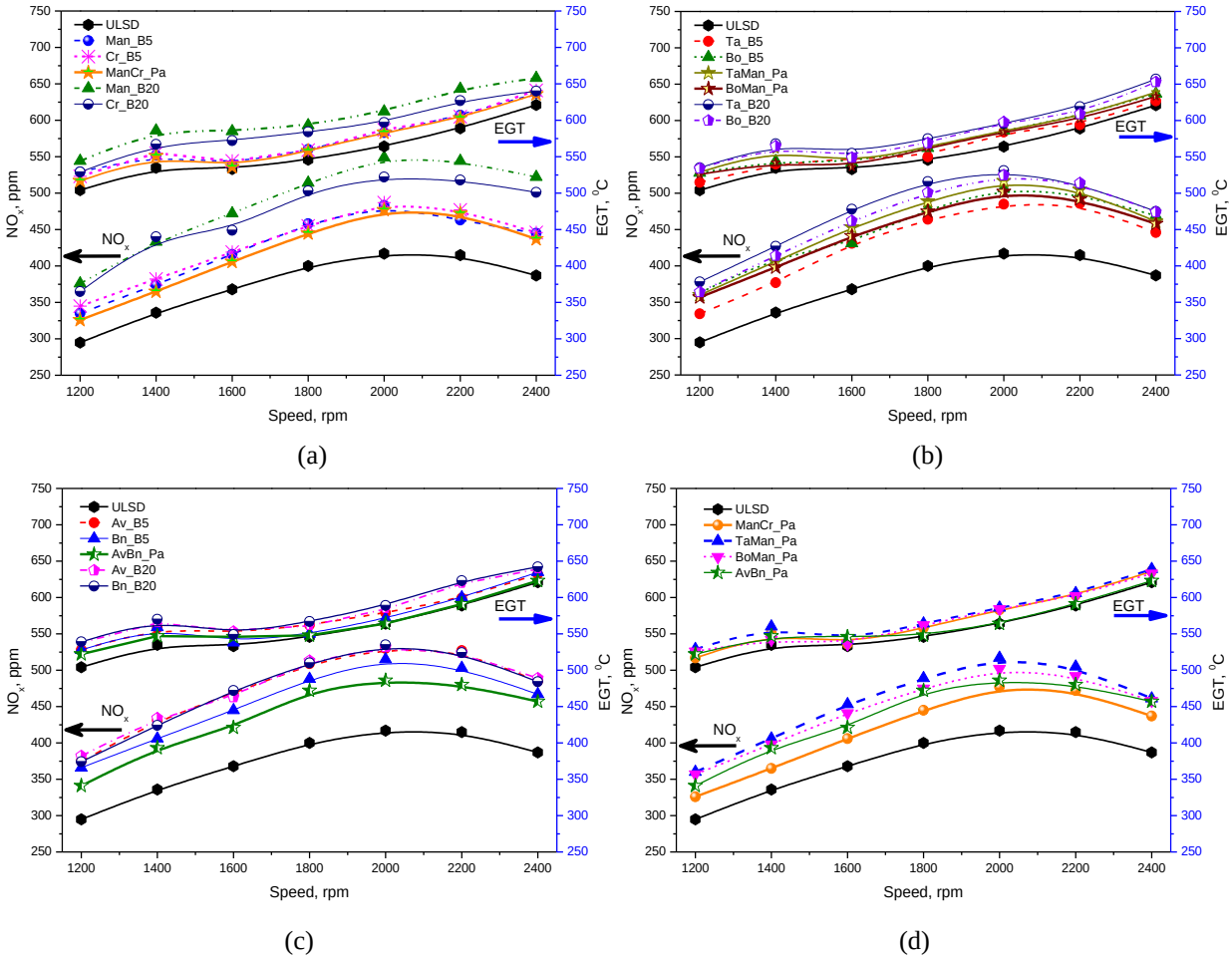

Figure 5.33: Variation of EGT and NO_x emissions with engine speed at full load condition for (a) Mandarin-Crambe, (b) Tamanu-Borage, (c) Avocado-Bush nut, and (d) biodiesel-paraffin mixture blends

The biodiesel-paraffin ternary mixture blends (except TaMan_Pa) show better performance at diminishing NOx emissions as compared to B5 blends due to the improvement of fuel properties. Lower density and viscosity of the mixture blends contribute to fine atomisation, vaporisation and proper mixing of the fuel into the air. For this reason, enhanced combustion quality and prolonged combustion durations help to reduce flame temperature resulting in

lower NO_x emissions. For instance, ManCr_Pa mixture blends emit 11.70% higher NO_x as compared to ULSD which is about 1.60% lower emissions compared to the Man_B5 blend. Similarly, BoMan_Pa and AvBn_Pa mixture blends result in an average of 19.30% and 16.5 higher NO_x emissions throughout the range of engine speed compared to ULSD which is about 1.20% and 8.30% lower NO_x emissions compared to Bo_B5 and Av_B5 blends, respectively. Figure 5.33 (d) portrays the comparison of the mixture blends which shows that ManCr_Pa has lower NO_x emissions compared to other blends due to the lower oxygen content in that biodiesel. The study extends to an investigation on the effect of engine load on NO_x emissions as is briefly discussed below.

Table 5.17: Summary of NO_x emissions compared to ULSD throughout the entire range of engine speed

Compared with ULSD	Mandarin		Crambe		Tamanu		Borage		Avocado		Bush nut	
	B5	B20	B5	B20	B5	B20	B5	B20	B5	B20	B5	B20
	13.5*	**30.1**	15.0	26.0	15.5	26.8	20.8	24.2	27.0	27.6	21.8	26.9
Mixture name →	ManCr_Pa		TaMan_Pa		BoMan_Pa		AvBn_Pa					
Mixture/ULSD	**11.7**		21.8		19.3		16.5					
Mixture/B5	-1.6**		5.7		-1.2		-8.3					

Note: *Positive sign (+) represents increase; **Negative sign (-) represents reduction.

5.8.3. Effect of engine load on NO_x emissions

Figure 5.34 demonstrates the effect of engine load on NO_x emissions and EGT variation at rated engine speed for (a) Mandarin-Crambe, (b) Tamanu-Borage, (c) Avocado-Bush nut, and (d) biodiesels-paraffin mixtures blends, respectively. The figure depicts that the EGT increases with the increase in engine load as well as with increased biodiesel proportion. On the other hand, NOx emissions increase with the increase in EGT as lean air-fuel mixtures persist at partial load. It is reported in the literature that NO_x emissions increase three fold with every 100 °C temperature increase (Reşitoğlu et al., 2015, Lee et al., 2013). Furthermore, the figure also illustrates that NO_x emissions increase with the increase in engine load which is also reported by Saravanan et al. (2012). Similar trends were also reported by Muralidharan et al. (2011) and Reşitoğlu et al. (2015). At full load, NO_x emissions slightly decrease for ULSD due to the decreased air supply as presented in Figure 5.16. However, biodiesels have higher NO_x emissions as compared to ULSD at full load condition due to the dominating effect of fuel oxygen content. This is because the fuel oxygen content has an insignificant effect in lean air-fuel mixtures at lower load condition but a significant effect in rich air-fuel mixtures at higher

loads. The summary of NO_x emissions for tested fuels compared to ULSD is presented in Table 5.18. As seen from the table, maximum NO_x emissions occurred for Bush nut biodiesel with an average of 27.80% (B5) to 37.00% (B20) due to the higher oxygen content (about 11.71%) in the biodiesel and the comparatively lower number of double bonds present in the carbon chain. The minimum NO_x emissions were for Tamanu at about 10.00% (B5) to 19.00% (B20) due to the reduced peak cylinder temperature as discussed above. On the contrary, the mixture blends of ManCr_Pa, BoMan_Pa and AvBn_Pa emit about 13.0%, 19.0% and 20.0% more NOx compared to ULSD which is about 2.2%, 1.7% and 6.7% lower emissions compared to Mandarin, Borage and Avocado B5 blends, respectively.

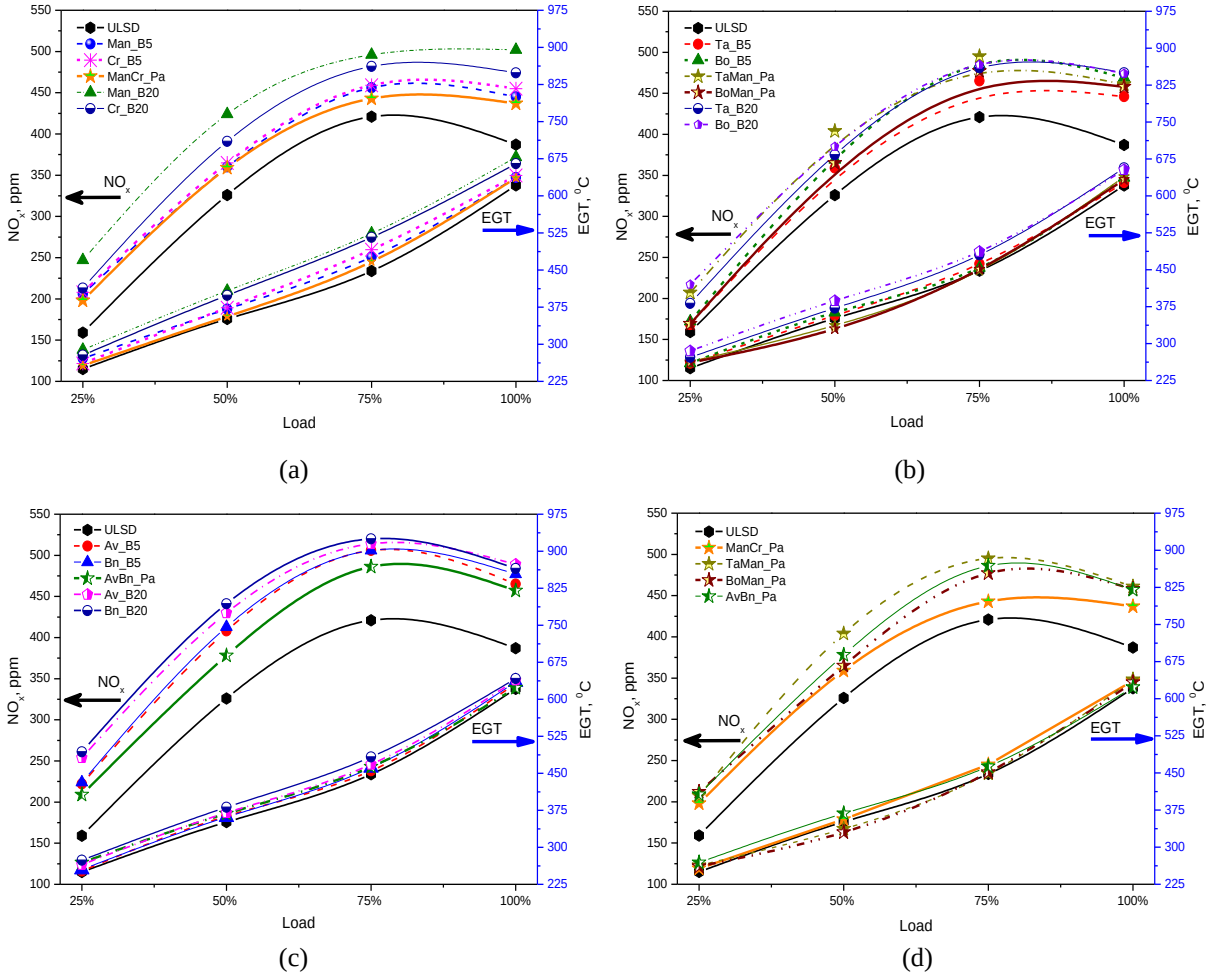

Figure 5.34: Variation of EGT and NO_x emissions with engine load at rated power condition (2400 rpm) for (a) Mandarin-Crambe, (b) Tamanu-Borage, (c) Avocado-Bush nut, and (d) biodiesel-paraffin mixture blend

Table 5.18: Summary of NO_x emissions compared to ULSD throughout the entire range of engine speed

Compared with ULSD	Mandarin		Crambe		Tamanu		Borage		Avocado		Bush nut	
	B5	B20	B5	B20	B5	B20	B5	B20	B5	B20	B5	B20
	15.8*	33.2	17.3	22.7	10.4	18.5	14.5	23.1	26.3	35.0	27.8	37.0
Mixture name →	ManCr_Pa				TaMan_Pa		BoMan_Pa		AvBn_Pa			
Mixture/ULSD	13.2				22.7		19.2		20.2			
Mixture/B5	-2.2**				11.4		-1.7		-4.7			

Note: *Positive sign (+) represents increase; **Negative sign (-) represents reduction of NO_x emissions.

5.9. Chapter Conclusion

This chapter presented the experimental investigation of DI diesel engine performance and emissions for tested biodiesel blends at different engine operating conditions. The experiments were conducted on steady state engine operating conditions by varying biodiesel blend proportion, engine speed, and engine load. The study reveals that Mandarin, Crambe, Avocado, Borage and Bush nut biodiesel blends show similar behavior throughout the range of engine test conditions. However, Tamanu biodiesel demonstrates poor performance as compared to ULSD and other biodiesel blends, mainly due to the higher density and viscosity and lower calorific value of the fuel. The other possibility could be that a higher degree of unsaturation implies a higher number of double bonds present in the carbon chain of Tamanu resulting in poor performance. Overall, BP increases with the increase in engine speed and load, but decreases with the increase of biodiesel blends. BSFC increases with the increase of biodiesel blends and decreases with the increase of engine load due to the lower calorific value of the biodiesel. Comparing with ULSD and other biodiesels, Mandarin and Borage show close BP and BSFC at variable engine speeds and load conditions, but Borage demonstrates better BTE compared to other biodiesel blends. The trend implies that BTE drops with the rise of biodiesel blend and that maximum BTE is achieved at 1600 rpm. Further, BTE increases with the increase of engine load. Among the other three biodiesels, Avocado shows better BTE as compared to Crambe and Bush nut biodiesel. This is due to better fuel properties including higher heating value and lower density and viscosity which enhance the combustion efficiency of the Avocado biodiesel.

The study also revealed that biodiesel reduces toxic gas emissions of CO, HC, and PM compared to ULSD or conventional diesel. These gas emissions occur at lower engine speeds and loads due to the rich air-fuel mixture (where excess air factor $\lambda < 1.0$). These gas emissions

are insignificant above 1600 rpm due to the lean air-fuel mixture. There is also evidence that overall engine emissions drop with increase in biodiesel blend proportion due to the self-oxygenated biodiesel enhancing the combustion efficiency of the fuel. The higher cylinder temperature indicated by higher EGT causes higher NO_x emissions because NO_x formation is highly sensitive to temperature. In other words, NO_x emissions increase with the increase of biodiesel blends due to higher cylinder peak temperatures.

Among biodiesel blends, B5 blends demonstrate better performance as compared to B10, B15, and B20 blends. On the other hand, B20 blends show a higher reduction of exhaust emissions compared to B5 blends. The new biodiesel-paraffin ternary mixture blends developed in this study show better performance compared to B5 blends and higher emissions reductions. Figure 3.35 illustrates the comparison of performance and emissions of the mixture blends with ULSD and each of their B5 blends at full load condition throughout the entire range of engine speeds. The figure clearly shows that the mixture blends slightly drop BP and BTE and increase BSFC compared to ULSD. However, they increase BP and BTE and decrease BSFC compared to each of their B5 blends. On the other hand, the mixture blends significantly reduce CO, HC, and PM emissions compared to both ULSD and B5 blends (except CO emissions which are increased by TaMan_Pa compared to the Tamanu B5 blend). However, the mixture blends slightly increase CO_2 emissions compared to ULSD and each of their B5 blends as a result of oxidation of CO that is converted to CO_2 which implies proper combustion of the fuel. One of the main findings of this study is the reduction of NO_x emissions (by about 1.2% to 8.8%) by mixture blends as compared to B5 blends by reducing the cylinder peak temperature, however; it emits about 10.0% to 20.0% more NO_x as compared to ULSD. By comparing the performance and emission parameters, the study concluded that ManCr_Pa and AvBn_Pa mixture blends are selected as economically and environmentally sustainable blends from the tested fuels. The study recommends further analysis (i.e. CP, HRR, ID, CD, and CFD modeling) of these two blends and their comparison with ULSD.

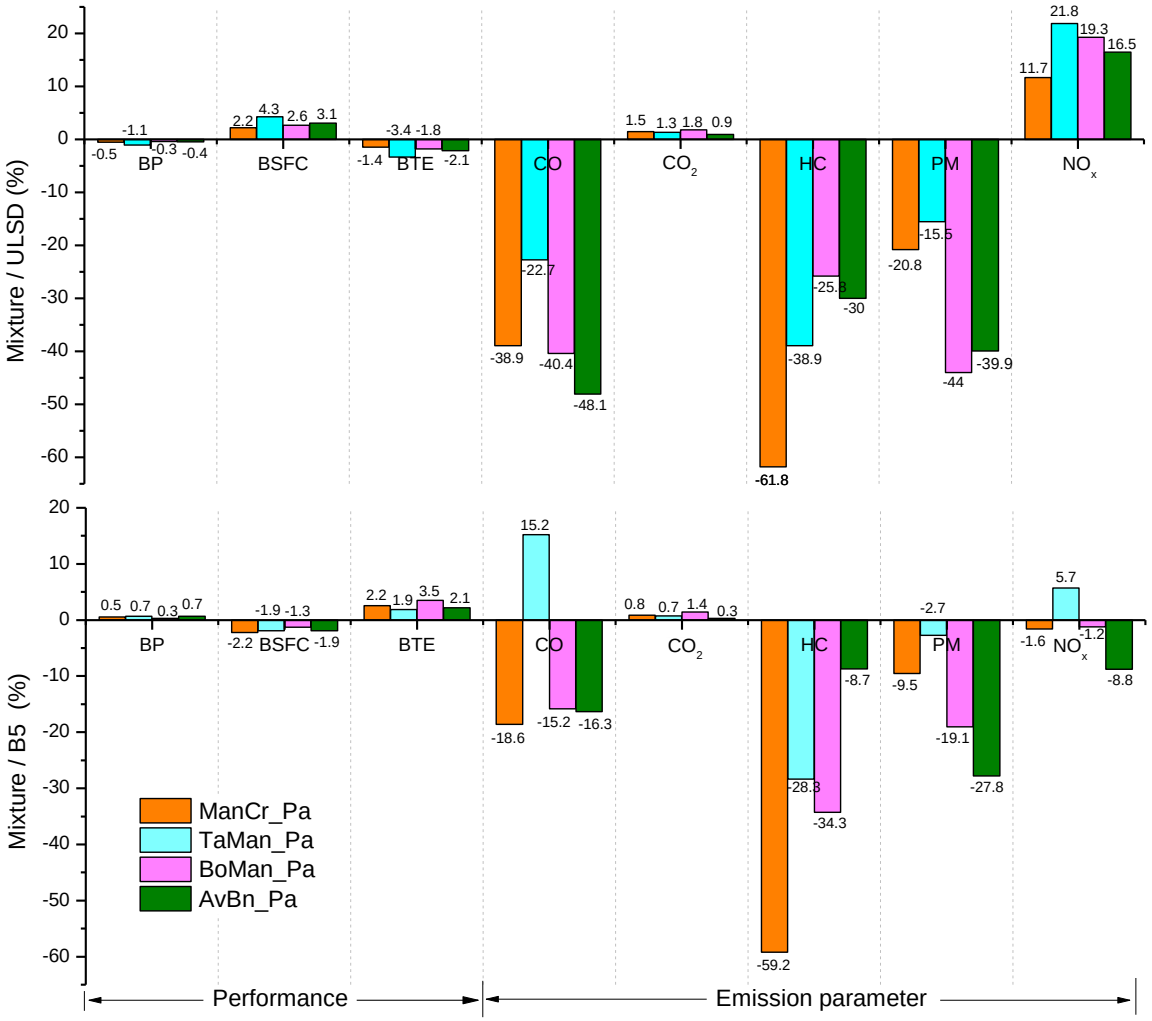

Figure 5.35: Comparison of mixture blends with ULSD and B5 blends

Chapter 6

COMBUSTION STUDY

This chapter deals with the combustion analysis of the better performing fuels identified in Chapter 5, namely ULSD, ManCr_Pa, and AvBn_Pa blends. The combustion parameters of cylinder pressure (CP), heat release rate (HRR), ignition delay (ID), combustion duration (CD), etc. are analysed from experimental data. The investigated parameters were measured from 0 to 720°CA (crank angle) with variable engine speed and load for full engine cycle investigation. The results are outlined and discussed in this chapter.

6.1. Introduction

Biodiesel is an oxygenated, alternative fuel which has many environmental benefits because it performs complete combustion with higher volumetric efficiency in a CI engine. Biodiesel combustion in a CI engine comprises highly complex and interlinked phenomena combined with a thermochemical reaction, fluid dynamics, heat transfer and the mechanical system. Combustion analysis is crucial for predicting the formation of pollutants and behavior of the combustion process which could give important information to modify engine designs for improving efficiency (Gogoi and Baruah, 2011). To target these issues, the experimental setup was equipped with a highly sensitive optical pressure sensor and a crank sensor with a data acquisition and recording system to investigate the combustion phenomena. The data were recorded from the mean values of hundreds of consecutive combustion cycles for each crank angle (CA) to eliminate error and improve the sensitivity of the analysis. The combustion analysis system for this experimental study was installed and calibrated by TFX Engine Technology Inc. (Canada). The combustion analysis was only conducted on the better performing fuel blends of ManCr_Pa and AvBn_Pa, and also on ULSD as concluded in Chapter 5. The study investigated the combustion parameters of cylinder pressure (CP), heat release rate (HRR), ignition delay (ID), and combustion duration (CD) by varying engine speeds and loads. The study examined the parameters at 1400 rpm (for rated torque), 1600 rpm (for maximum efficiency) and 2400 rpm (for rated power) engine speed at full load condition. The speeds were selected based on the performance of the engine as discussed in Chapter 5. The study also investigated the variation of combustion behavior with varying engine loads of 25%, 50%, 75% and 100% at rated engine speed. The key findings are briefly discussed here.

6.2. Cylinder Pressure

6.2.1. Variation of cylinder pressure with engine speed

The in-cylinder pressure profiles have been illustrated in Figures 6.1 (a) as a front view, and Figure 6.1 (b) as contour colour maps (top view) for the tested fuels at 1400 rpm, 1600 rpm, and 2400 rpm at full load conditions. As seen from Figure 6.1(a), the peak CP at 1400 rpm is obtained close to 63.90 bar, 65.70 bar, and 66.00 bar at 3° ATDC (or 363 °CA) for ULSD, ManCr_Pa, and AvBn_Pa, respectively. At 1600 rpm, maximum pressure is found to be about 64.05 bar at 1 °ATDC for ULSD and 64.80 bar at 2 °ATDC for both ManCr_Pa and AvBn_Pa blends. The pressure at 2400 rpm was found to be 65.85 bar, 66.63 bar and 66.55 bar at TDC (360 °CA) of the cylinder for ULSD, ManCr_Pa and AvBn_Pa mixture blends, respectively. The results reveal that CP increases with the increase in engine speed which has also been reported by Sajjad et al. (2015) and Awad et al. (2016). This is due to the lean air-fuel mixture at higher engine speeds causing the complete combustion of the fuel. Figure 6.1(b) illustrates the contour colour maps for in-cylinder pressure variation in bar at different combustion phases with various engine speeds. The figure clearly demonstrates the substantial diminution of the premixed combustion zone at 2400 rpm due to the shorter ignition delay as discussed later at Section 6.4. Prolonged cylinder pressures of over 60 bar appeared at the lower engine speed zone as shown in Figure 6.1(b) due to the insignificant difference of peak CP during premixed and diffusion combustion phases. Further, a shorter diffusion phase occurred at the lower engine speed which also indicates incomplete combustion resulting in higher CO, HC and PM emissions. For more detailed analysis, the in-cylinder pressure profiles have been zoomed out from 300 °CA (before fuel injection) to 480 °CA (exhaust valve opening, EVO) which is briefly discussed below.

Figures 6.2 to 6.4 depict the variation of CP with full engine load at 1400 rpm, 1600 rpm and 2400 rpm, respectively. As seen from these figures, ManCr_Pa, and AvBn_Pa mixture blends demonstrate higher CP compared to ULSD due to the combined effects of higher CN, BSFC and O_2 content of the biodiesel contributing to the complete combustion of the fuels (Ozsezen and Canakci, 2011, Imtenan et al., 2014a). Figure 6.2 portrays the higher CP summits which are an average 1.07% (ManCr_Pa) and 2.89% (AvBn_Pa) higher compared to ULSD. The pressure variation at higher speed is insignificant as demonstrated in Figures 6.4 due to sufficient air being present during combustion and hence resulting in reduced emissions.

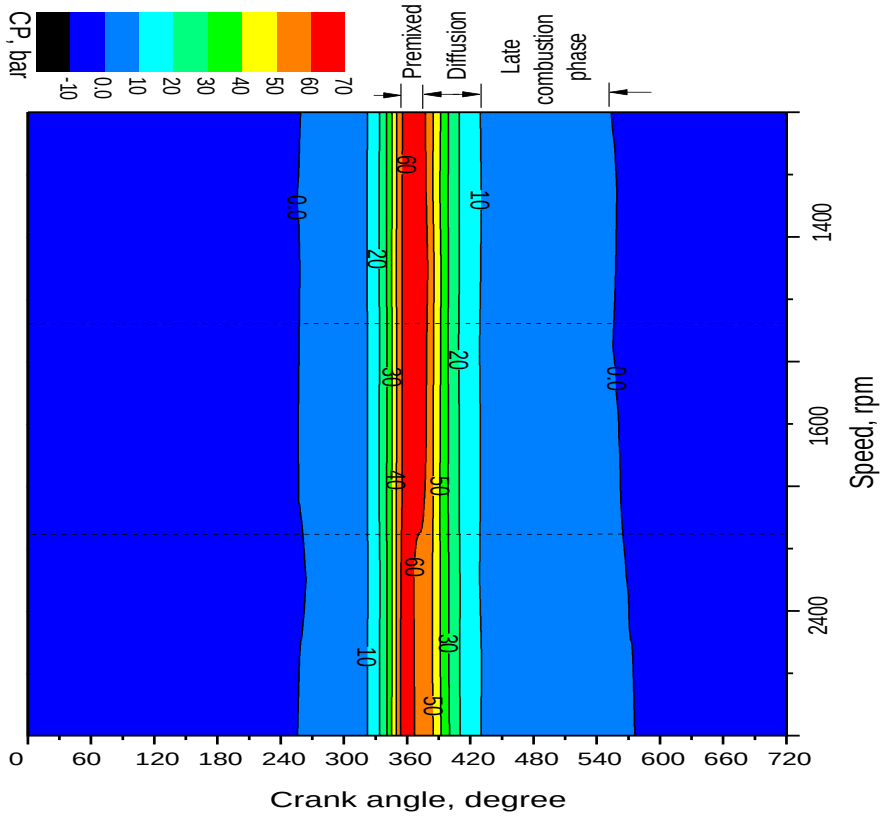

(b) Contour surface colour maps of the cylinder pressure (top view)

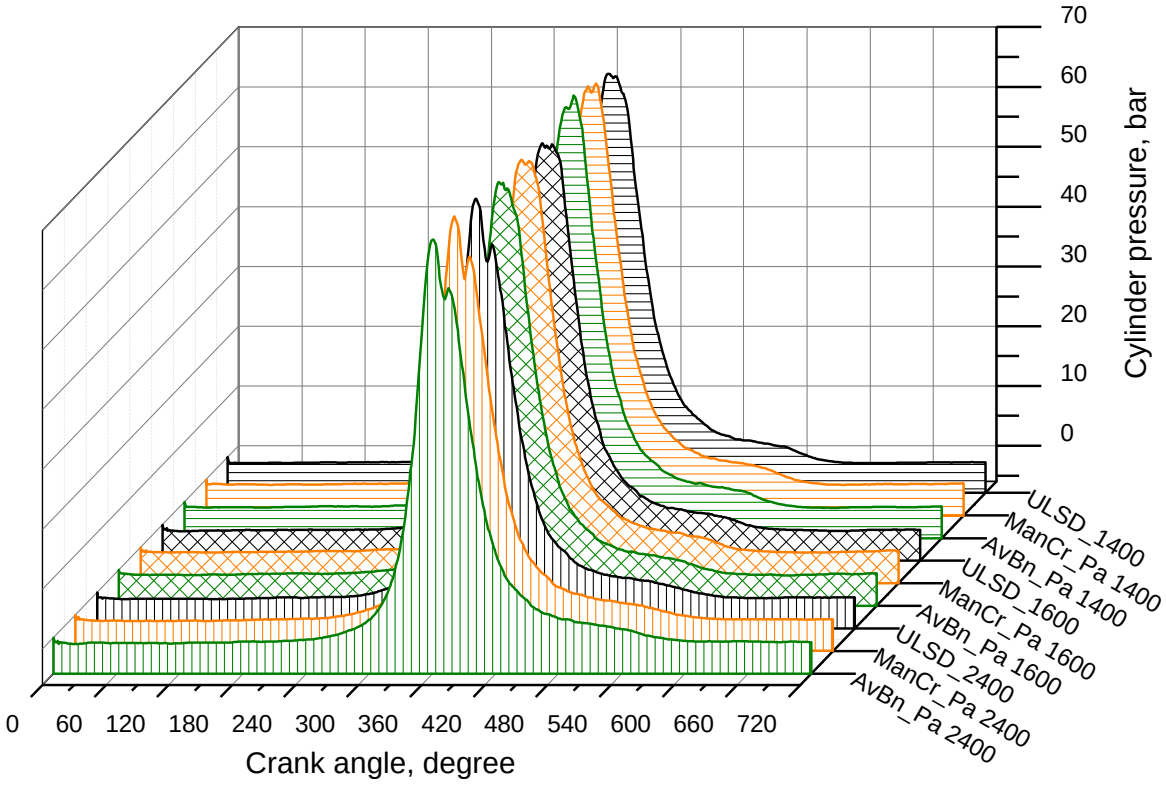

(a) Cylinder pressure profile (front view)

Figure 6.1: (a) Cylinder pressure variation with the crank angle, and (b) Contour colour maps from the top of the profile for tested fuels at 1400 rpm, 1600 rpm, and 2400 rpm at full load condition

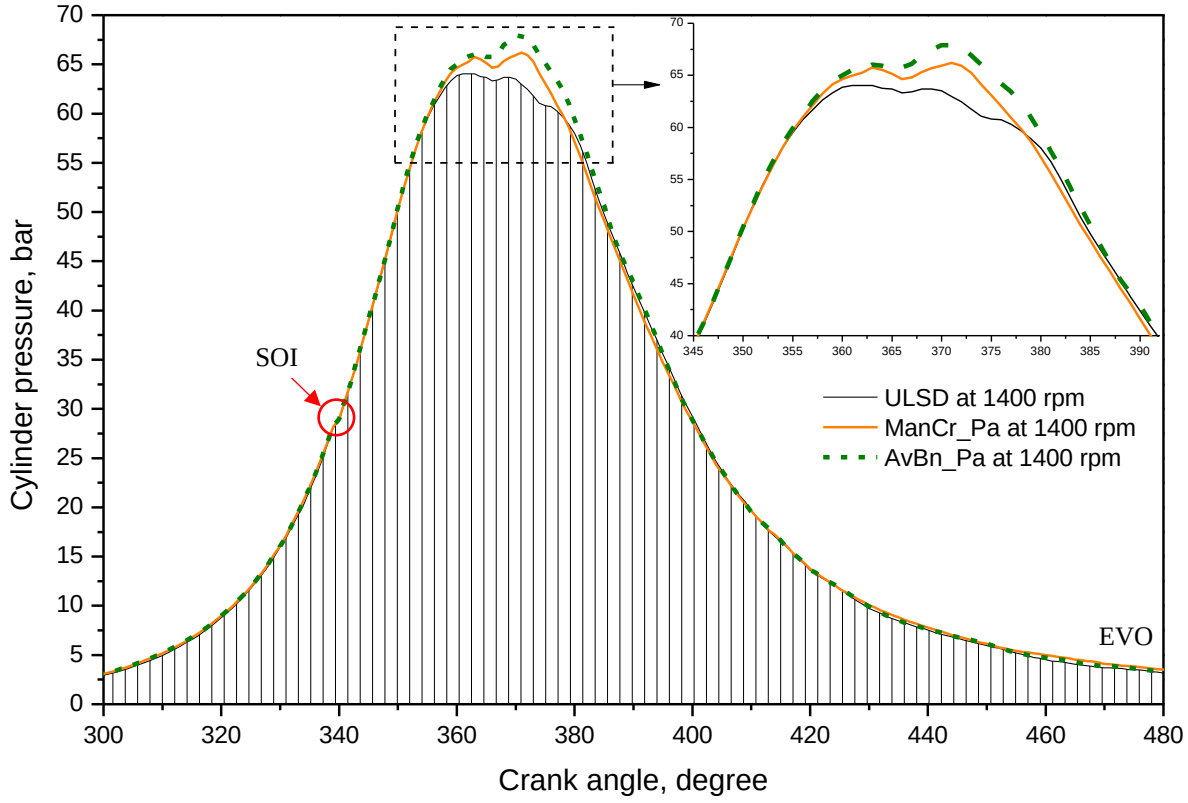

Figure 6.2: Comparison of in-cylinder pressure profiles for tested fuels at 1400 rpm and full engine load

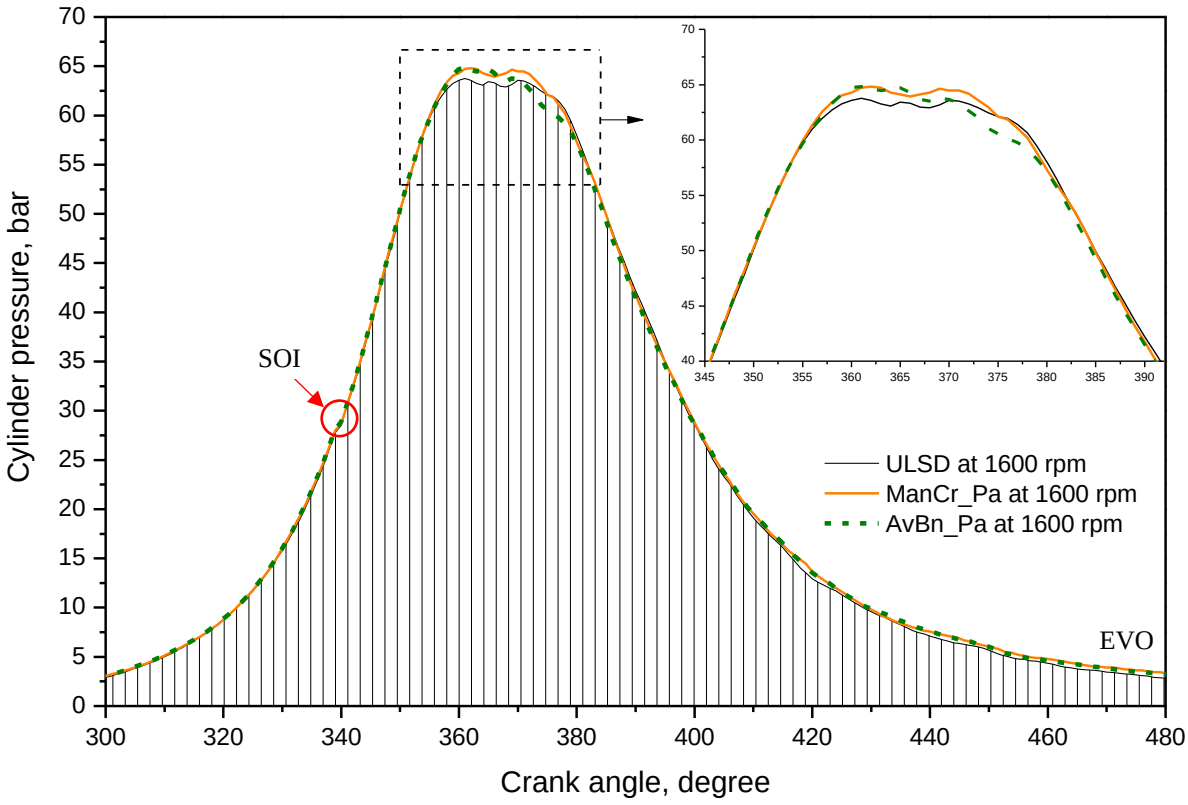

Figure 6.3: Comparison of in-cylinder pressure profiles for tested fuels at 1600 rpm and full engine load

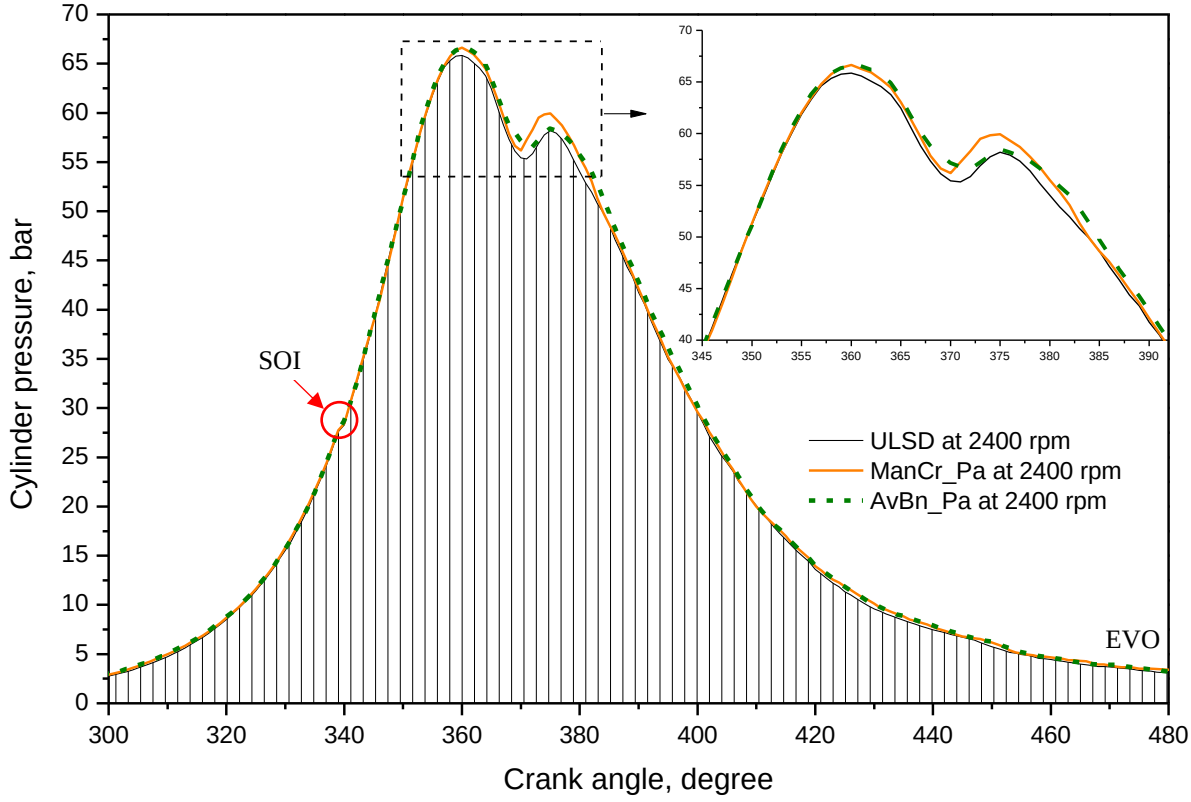

Figure 6.4: Comparison of in-cylinder pressure profiles for tested fuels at 2400 rpm and full engine load

From the study it is identified that the main reason for the in-cylinder pressure rise at 1400 rpm (Figure 6.2) is fuel oxygen content. The mixture blends contain about 0.56% (ManCr_Pa) and 0.58% (AvBn_Pa) more oxygen (O_2) as compared to ULSD. The AvBn_Pa blend shows higher CP because it contains about 3.78% more O_2 compared to ManCr_Pa blends. This fuel O_2 has a significant effect on combustion in rich air-fuel mixtures at the lower speed as shown in Figure 5.17 of Chapter 5. However, the fuel O_2 has no noticeable effect in lean air-fuel mixtures at the higher speed as has been agreed by Reşitoğlu et al. (2015). On the other hand, the higher BSFC of the mixture blends compared to ULSD (Chapter 5, Table 5.5) also contributes to higher CP as compared to ULSD. The CP apex is directly related to the enhancement of HRR as reported by Rajendra Prasath et al. (2010) and Vallinayagam et al. (2014). For better understanding, the relationship between CP and HRR with °CA is presented in Figures 6.5, 6.6 and 6.7. In these figures, black dots represent the cylinder pressure data points, and different colour codes represent corresponding HRRs at particular °CA. The figures clearly demonstrate the variation of HRR with CP which indicates higher CP and HRR occurred at TDC for each fuel. ULSD shows high HRRs above 190.90 J/°CA for a short durations, but the mixture blends show HRRs of about 156.80 J/°CA (ManCr_Pa) and 155.90 J/°CA (AvBn_Pa) for longer CD

with complete combustion resulting in higher CPs as well as higher BPs as shown in Figure 5.3 (d) in Chapter 5.

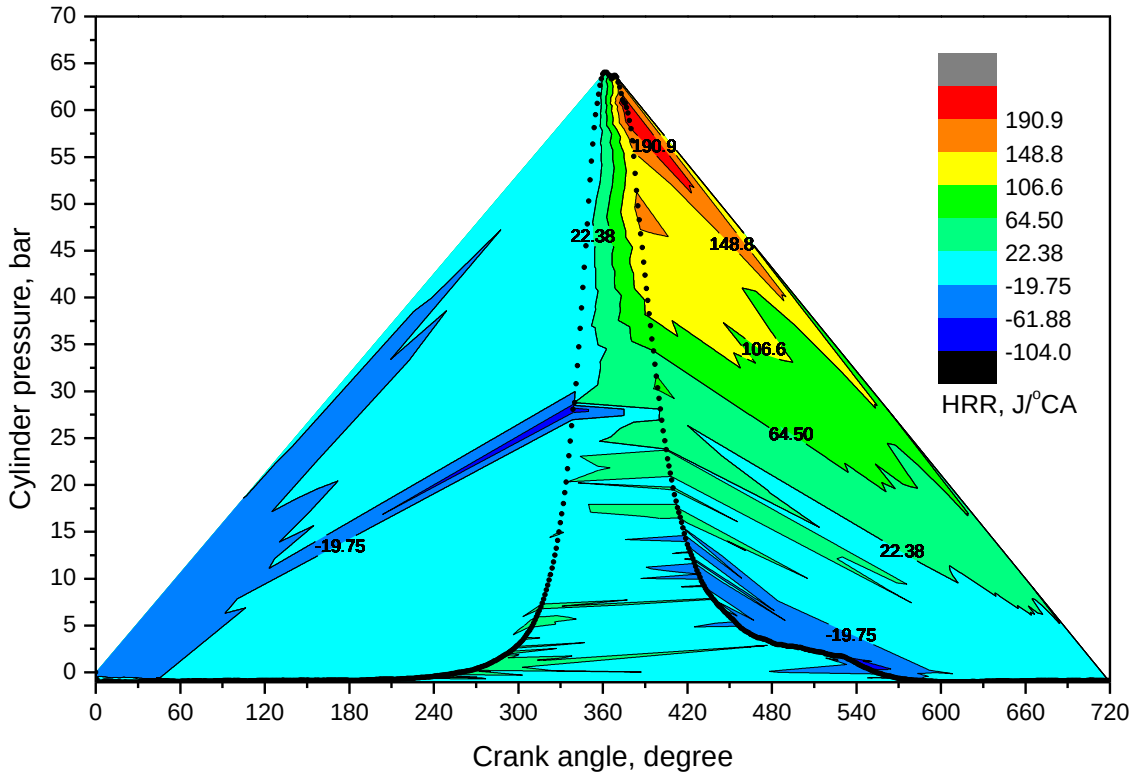

Figure 6.5: Relationship of CP and HRR at full engine cycle for ULSD at 1400 rpm and full load

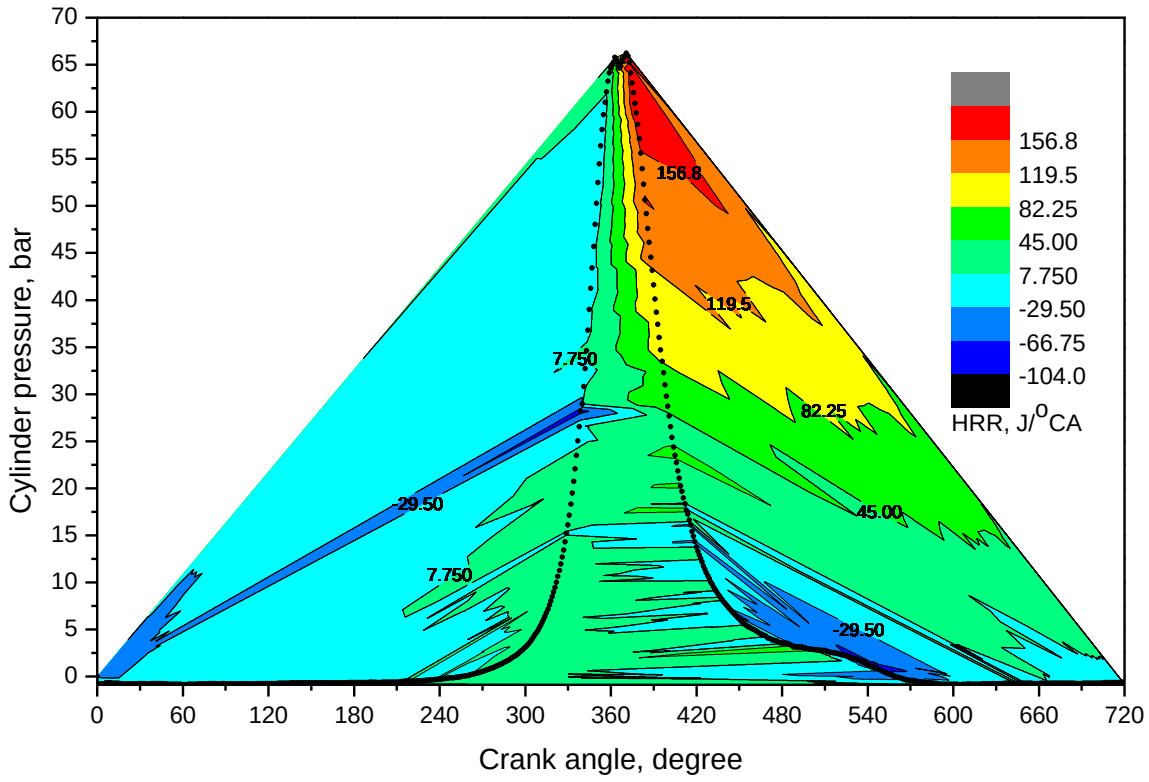

Figure 6.6: Relationship of CP and HRR at full engine cycle for ManCr_Pa blend at 1400 rpm

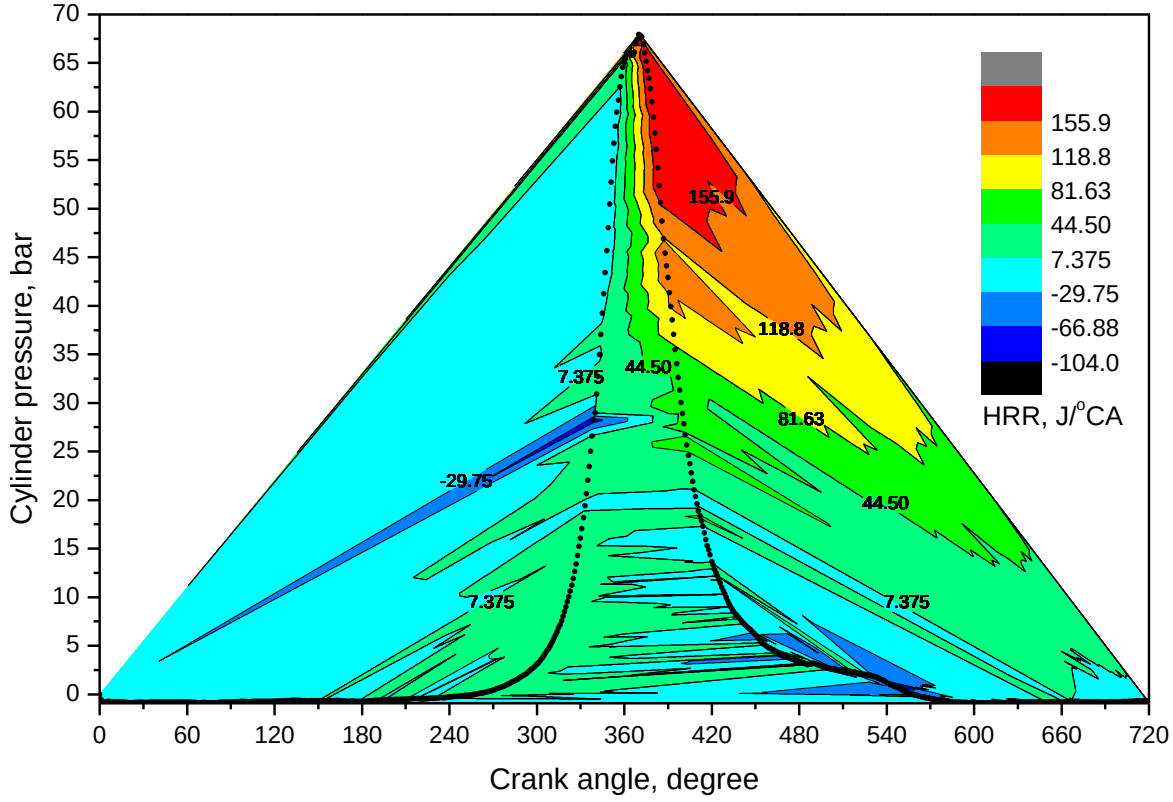

Figure 6.7: Relationship of CP and HRR at full cycle for AvBn_Pa mixture blend at 1400 rpm and full load

6.2.2. Variation of cylinder pressure at variable engine load

Figure 6.8 (a) illustrates the CP variation at power stroke for tested fuels at variable engine loads. Figure 6.8 (b) demonstrates the contour colour maps for a top view of the CP profile for a better understanding and exhibition of CP comparisons at variable engine load at rated speed. The mixture blends show slightly higher CP compared to ULSD throughout the investigated CA at power stroke in Figure 6.8 (a). Figure 6.8 (b) clearly exhibits the shorter combustion durations at lower load condition which indicates incomplete combustion resulting in higher CO and HC emissions. However, mixture blends demonstrate higher CP compared to ULSD at lower load due to the self-oxygen content. Another reason is the improvement of spray and atomisation characteristics of the mixture blends which occurs due to the lower density and viscosity of the blends as compared to ULSD (Vallinayagam et al., 2014). Also, a fine dispersion of fuel droplets can be achieved by including low viscous paraffin as an additive in the Mandarin-Crambe and Avocado-Bush nut biodiesels mixture blends which promotes CP enhancement. These facts were also verified by the studies conducted by Zhu et al. (2011), and Hulwan and Joshi (2011) who experimented on ethanol-diesel mixture blends.

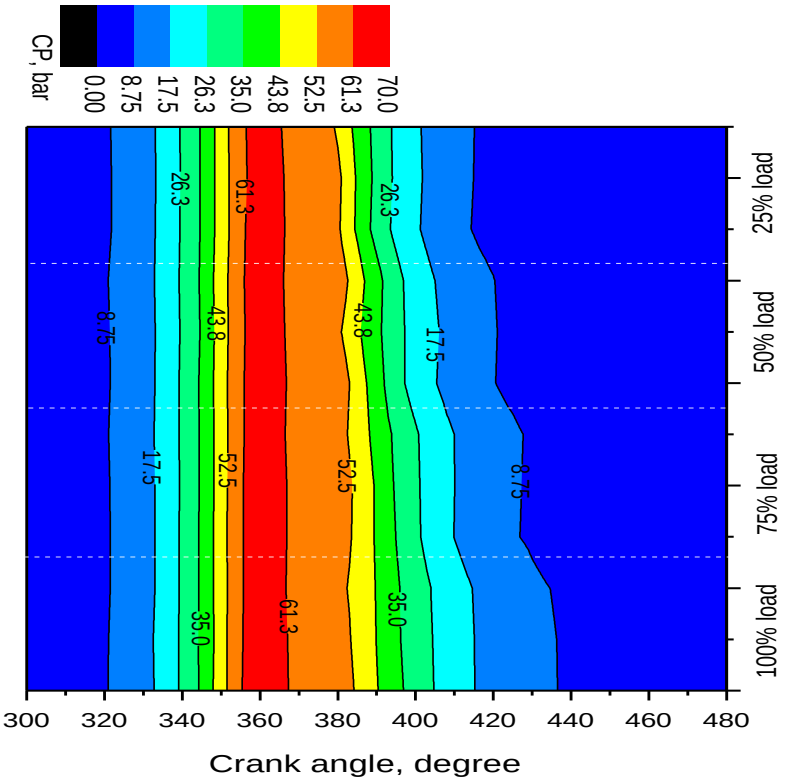

(b) Contour colour maps (top view of the CP profile)

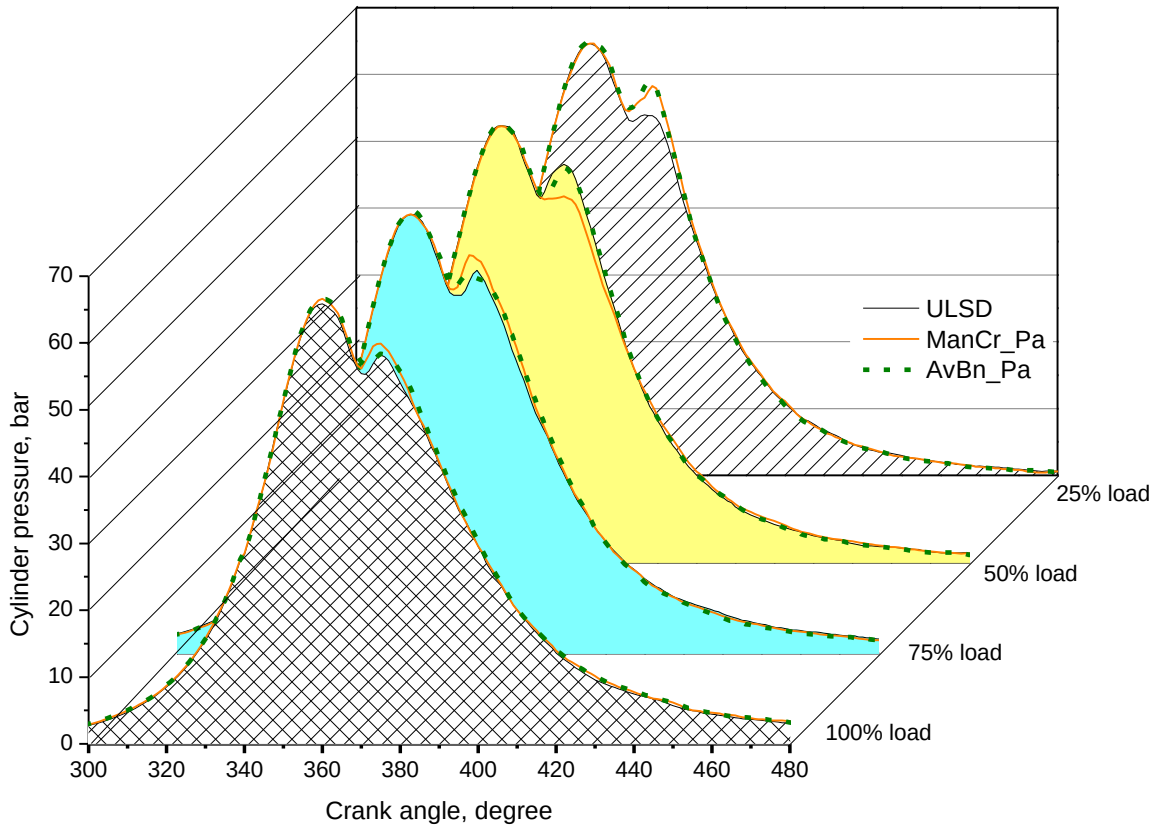

(a) CP profile at variable engine load (front view)

Figure 6.8: (a) CP variation during power stroke, and (b) contour colour maps (top view) of the CP profile at different engine loads

Figure 6.9 depicts the variation of CP at 25% load to 100% load for tested fuels. The results reveal that CP increases with the increase in engine load. Similar results were also reported by Gogoi and Baruah (2011) and Islam et al. (2015). At 25% load, a lower CP was found because of incomplete combustion due to the very lean air-fuel mixture (Chapter 5, Figure 5.19) and shorter CD as shown in Figure 6.8(b). As a result of incomplete combustion and lower EGT, the PM and NO_x emissions are reduced at lower loads. On the other hand, higher CP was found at full load condition due to the prolonged CD and stoichiometric air-fuel mixture which result in the complete combustion of the fuel. From Figure 6.8(b), it can be clearly identified that an insignificant CP variation exists at the premixed combustion phase for each fuel. However, a noticeable CP variation with the engine load was observed at the mixing-controlled combustion phase whereas the formation of pollutants and oxidation occurred at a strong combustion phase. The study found that the mixture blends gives better combustion performance as compared to ULSD through the entire range of engine loads. Also, the AvBn_Pa ternary mixture blend demonstrates higher CP and smoother combustion behavior as compared to the other fuels which are explained by HRR in the following section.

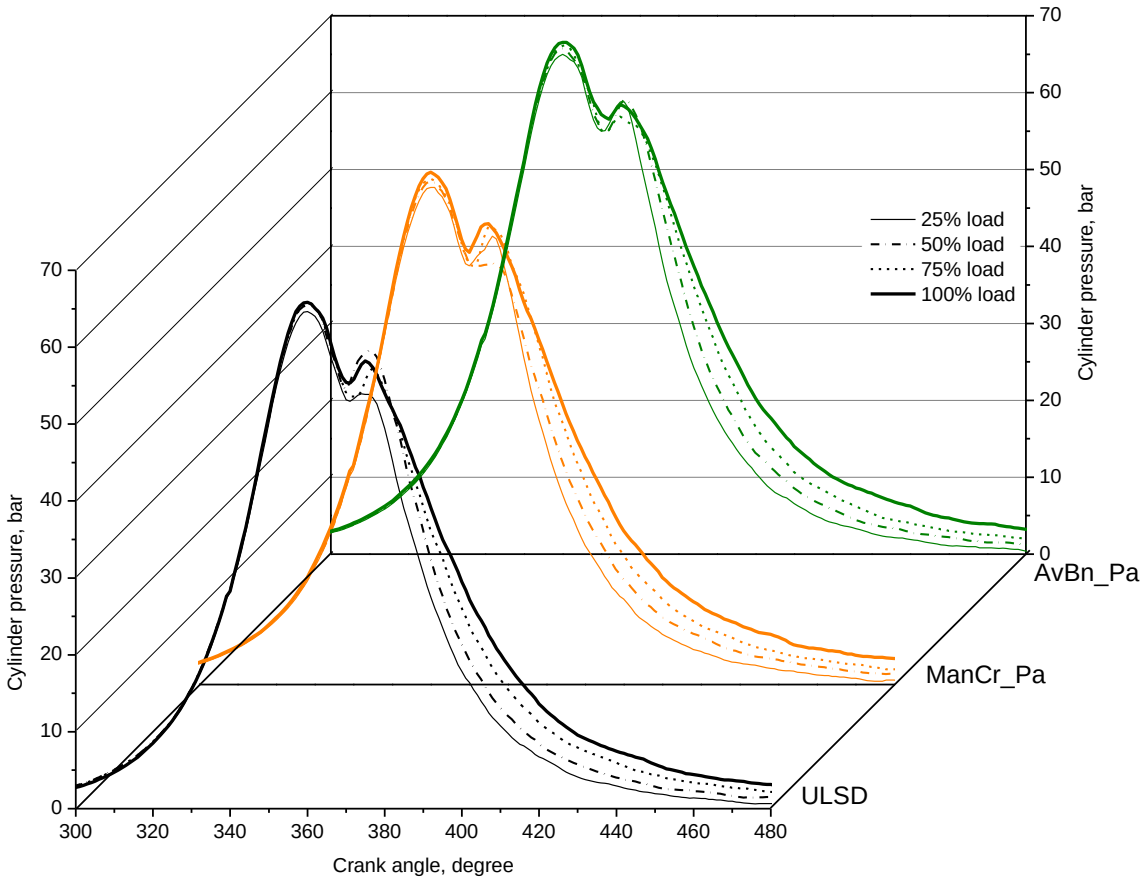

Figure 6.9: Comparison of CP variation at different loads for ULSD, and ManCr_Pa and AvBn_Pa blends

6.3. Heat Release Rate (HRR)

6.3.1. Variation of HRR with engine speed

HRR is one of the important parameters to illustrate in-cylinder combustion phenomena of the CI engine. For a better understanding of the combustion phenomena in this study, the power stroke is sub-divided into three main combustion phases as shown in Figure 6.10. Here, b to c represents the premixed combustion phase, c to d is the diffusion (or mixing-controlled) combustion phase, and d to e is the late combustion phase. The ignition delay (ID) period is indicated as a to b, hence "a" implies start of injection (SOI) and "b" denotes the start of combustion (SOC). Figures 6.10 to 6.12 illustrate the variation of HRR with respect to °CA from 300 to 480 degree at full load condition. These figures also show the excellent comparison of combustion behavior for ManCr_Pa and AvBn_Pa mixture blends compared with ULSD at 1400 rpm, 1600 rpm, and 2400 rpm engine speeds, respectively. The results reveal that all tested fuels exhibit prompt HRR at the premixed combustion phase at each operating condition leading towards the diffusion combustion phase (Sajjad et al., 2015). As seen from these Figures, ULSD demonstrates the highest magnitude of peak HRR due to its higher calorific value, and the late SOC causes the lower cetane number (CN) as compared to mixture blends (Vallinayagam et al., 2014, Lapuerta et al., 2008a, Arul Mozhi Selvan et al., 2009). In this study, the SOI was fixed at 344 °CA or -16° BTDC for all tested fuels to identify the ID period for all fuels. It can be noted from the HRR diagrams that biodiesel mixture blends show earlier SOC and lower HRR compared to ULSD due to the higher CN and shorter ID. These characteristics of the blends reduce the mass of injected fuel and the rate of evaporation of the fuel and these result in a lower burning rate and less HRR during the premixed combustion phase as pointed out by Sajjad et al. (2015). The variation of ID and CD is also discussed in following section.

The study also reveals the pollutant formation mechanism at different combustion phases as shown in Figure 6.10 which indicates ManCr_Pa and AvBn_Pa blends have a sharper but more prolonged HRR profile (Figures 6.13 to 6.15) at the premixed combustion phase as compared to ULSD which indicates their higher cylinder peak pressure and temperature. The relationship between HRR and CP is illustrated in Figures 6.13 to 6.18 by colour maps which reflect this statement. This higher cylinder temperature contributes to the formation of more thermal NO_x at rich air-fuel mixing zones at the premixed combustion phase. Besides, the hydroxyl (OH)

formation is highly temperature sensitive which requires temperatures above 1500 °K at the premixed combustion phase. This OH is required for CO oxidation by the highly exothermic reaction at the next combustion phase. The extra heat generated by the CO oxidation reaction strengthens and reinforces HRR during the diffusion combustion phase. On the other hand, due to the slow oxidation rate of CO, the longer combustion duration of biodiesel blends allows more CO oxidation which contributes to higher EGT and CO_2 emissions. Soot and HC are formed during combustion due to the uneven temperature distribution between the cylinder core and walls. Unburnt hydrocarbons form near the cylinder wall due to flame quenching at low temperature compared to the cylinder core which contributes to the soot surface growth and agglomeration to form PM. The oxidation of soot and HC depends on the behavior of the diffusion combustion phase. Figures 6.10 to 6.12 also illustrate higher HRR at diffusion and late combustion phases for mixture blends due to their lower density and viscosity contributing to prompt vaporisation and mixing. As a result, faster diffusion combustion and higher HRR is observed as compared to ULSD. Their longer combustion duration allows more oxidation of pollutants which reduces emissions and enhances cleaner combustion of the biodiesel mixture blends.

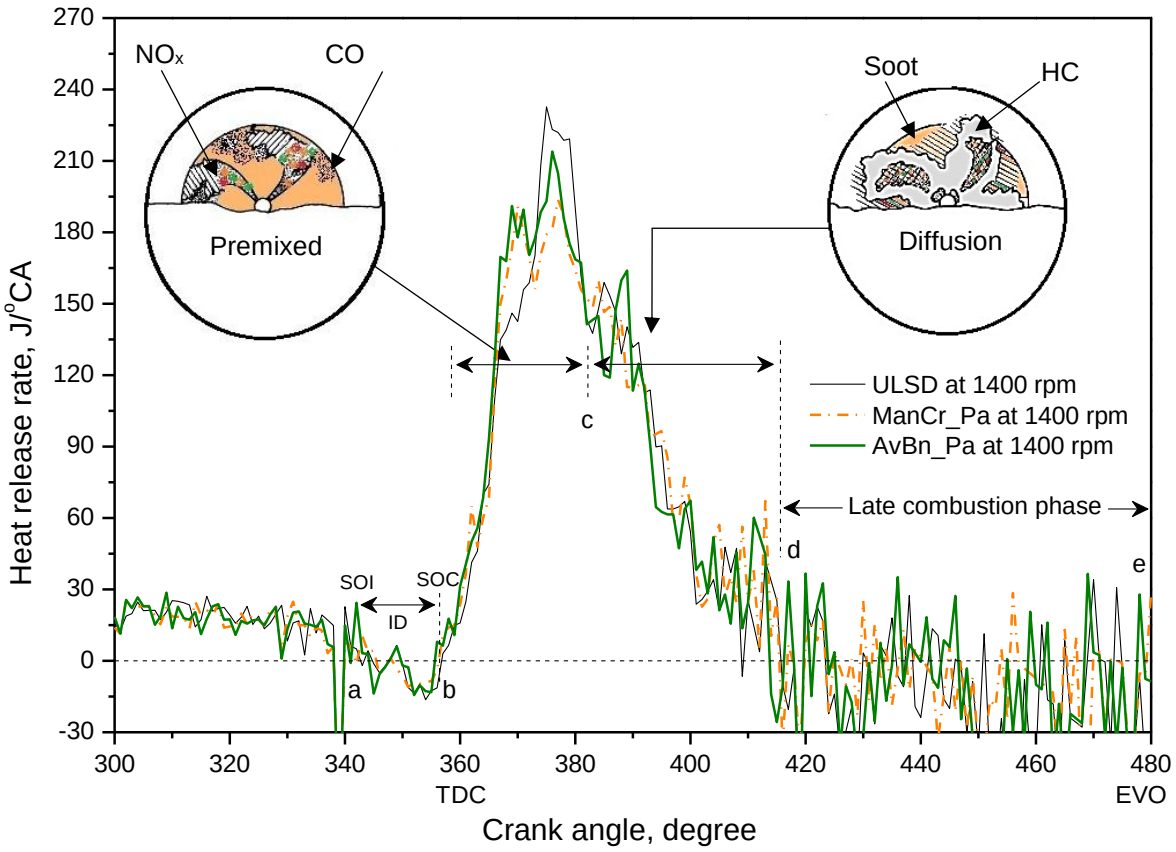

Figure 6.10: Variation of heat release rate with the crank angle for tested fuels at full load with 1400 rpm speed

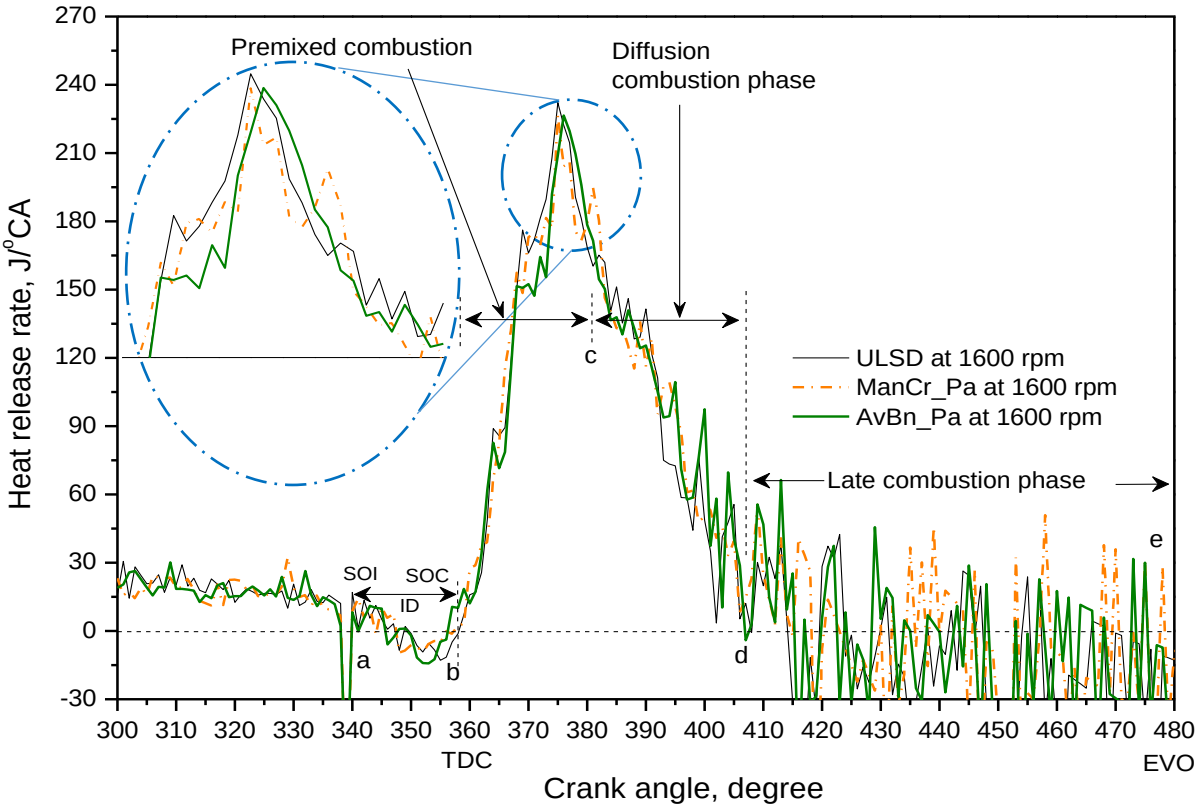

Figure 6.11: Variation of heat release rate with the crank angle for tested fuels at full load with 1600 rpm speed

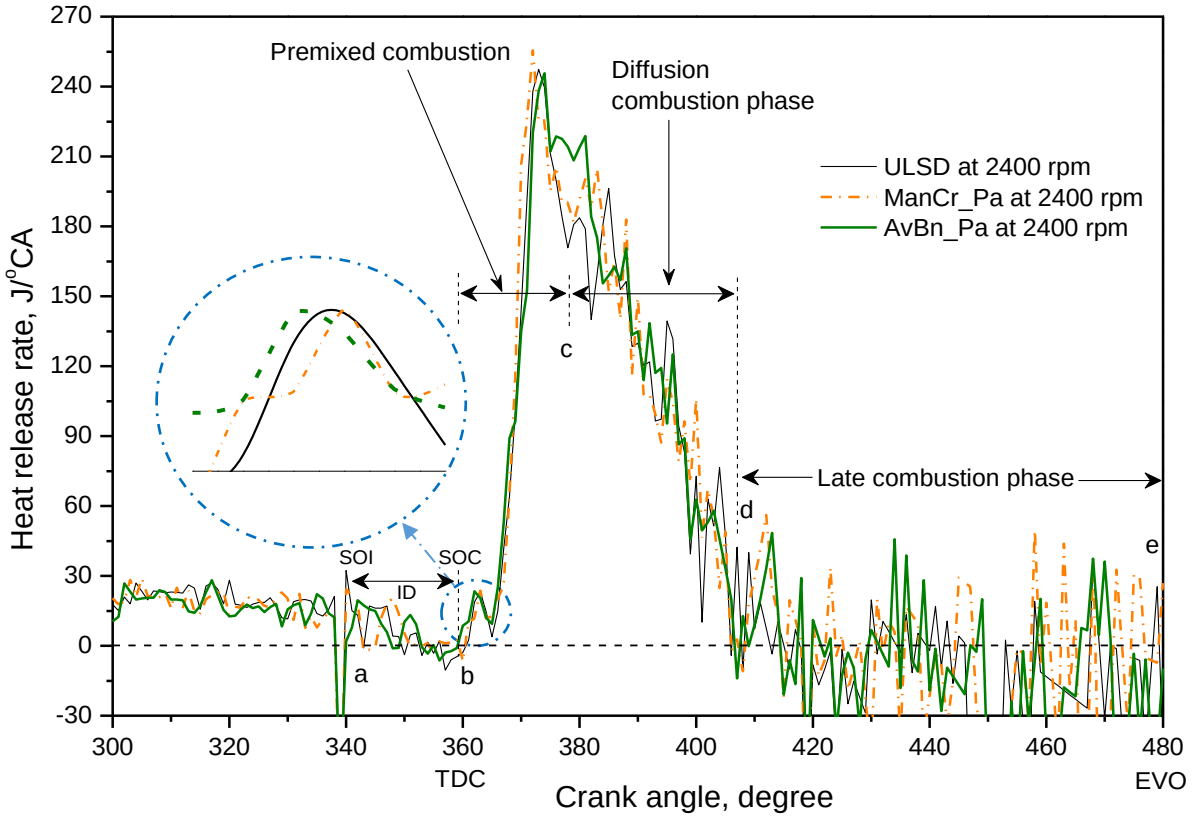

Figure 6.12: Variation of heat release rate with the crank angle for tested fuels at full load with 2400 rpm speed

It can be seen from Figure 6.11 that the blends show similar combustion behavior to ULSD at 1600 rpm. Although the diffusion phase is similar to ULSD at 2400 rpm (Figure 6.12), the premixed phase shows only a small variation from the lower speed (1400 rpm) which can be explained by Figures 6.13 to 6.18. The study shows the relationship between HRR and CP which is presented in those figures. As seen from the figures, the magnitude of maximum HRR at 1400 rpm is lower than that at 2400 rpm. Further, the longer duration of the premixed combustion phase with high CP results in more CO_2, HC, and PM emissions and the shorter diffusion combustion phase contributes to higher CO emissions at 1400 rpm compared to 2400 rpm. On the other hand, a significant difference of combustion behavior evidencing higher HRR with shorter duration of peak CP at TDC is identified at 2400 rpm for all tested fuels as shown by Figures 6.16 to 6.18. The study also reveals another important characteristic of complete combustion which is that the prolonged and stronger diffusion phase results in lower emissions. It is reported in the literature that the diffusion phase exhibits more energy than the premixed combustion phase (Sajjad et al., 2015). From Figure 6.17, a certain level of undesirably high CP rise indicates knocking associated with the ManCr_Pa blend at 2400 rpm. On the other hand, AvBn_Pa shows a smooth and cleaner combustion as compared to other fuels. The study investigated the effect of engine load on combustion which is discussed briefly in the following section.

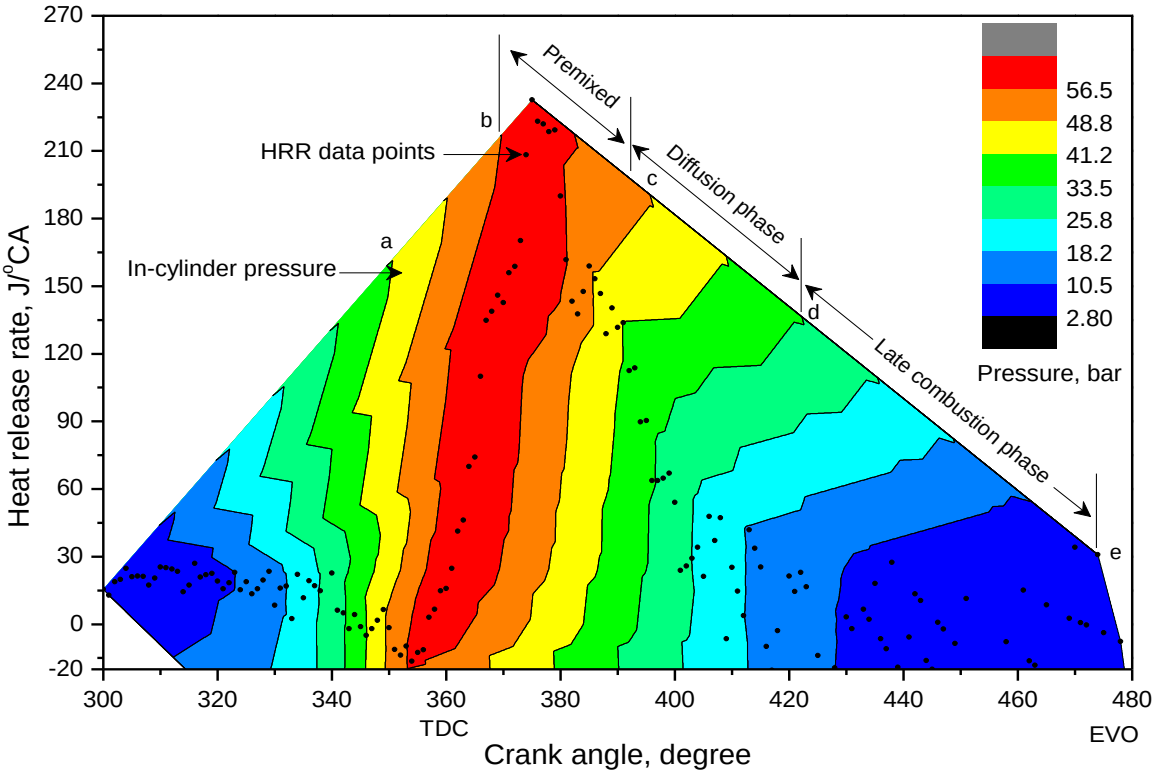

Figure 6.13: Correlation of HRR and CP at combustion phase for ULSD at 1400 rpm engine speed

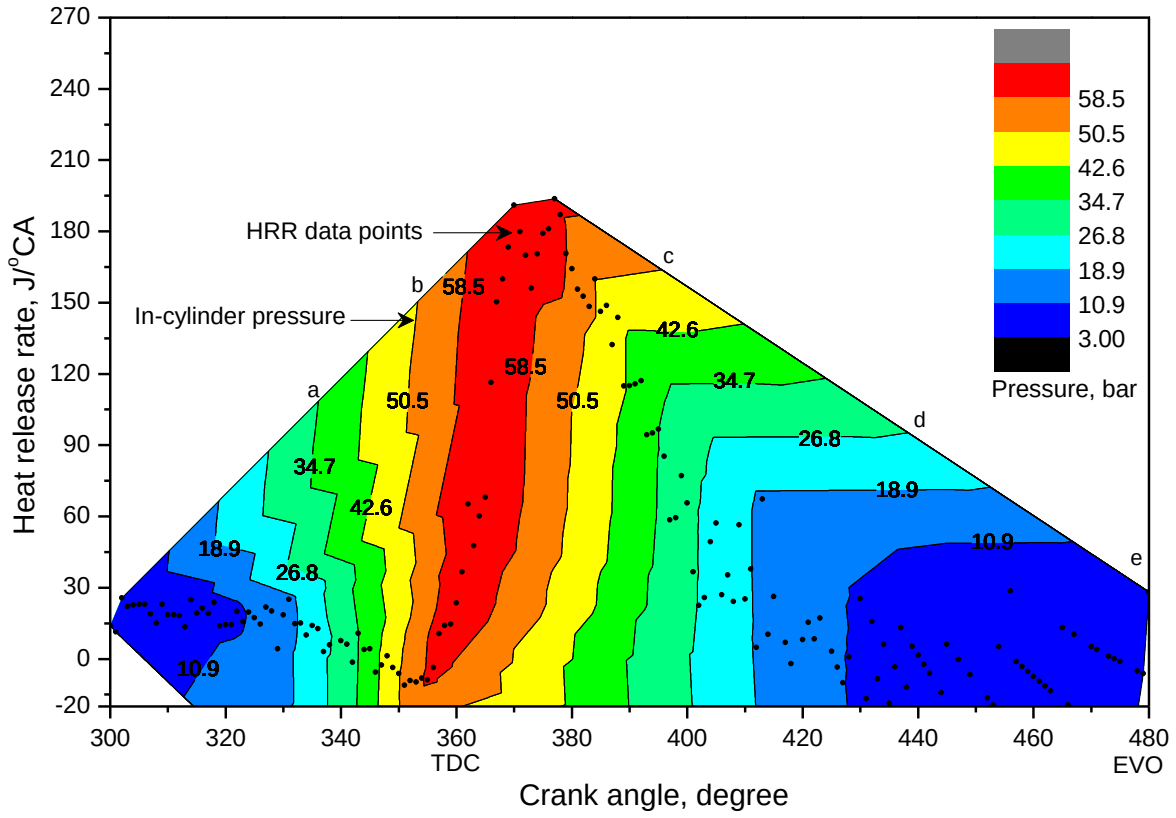

Figure 6.14: Correlation of HRR and CP at combustion phase for ManCr_Pa at full load and 1400 rpm speed

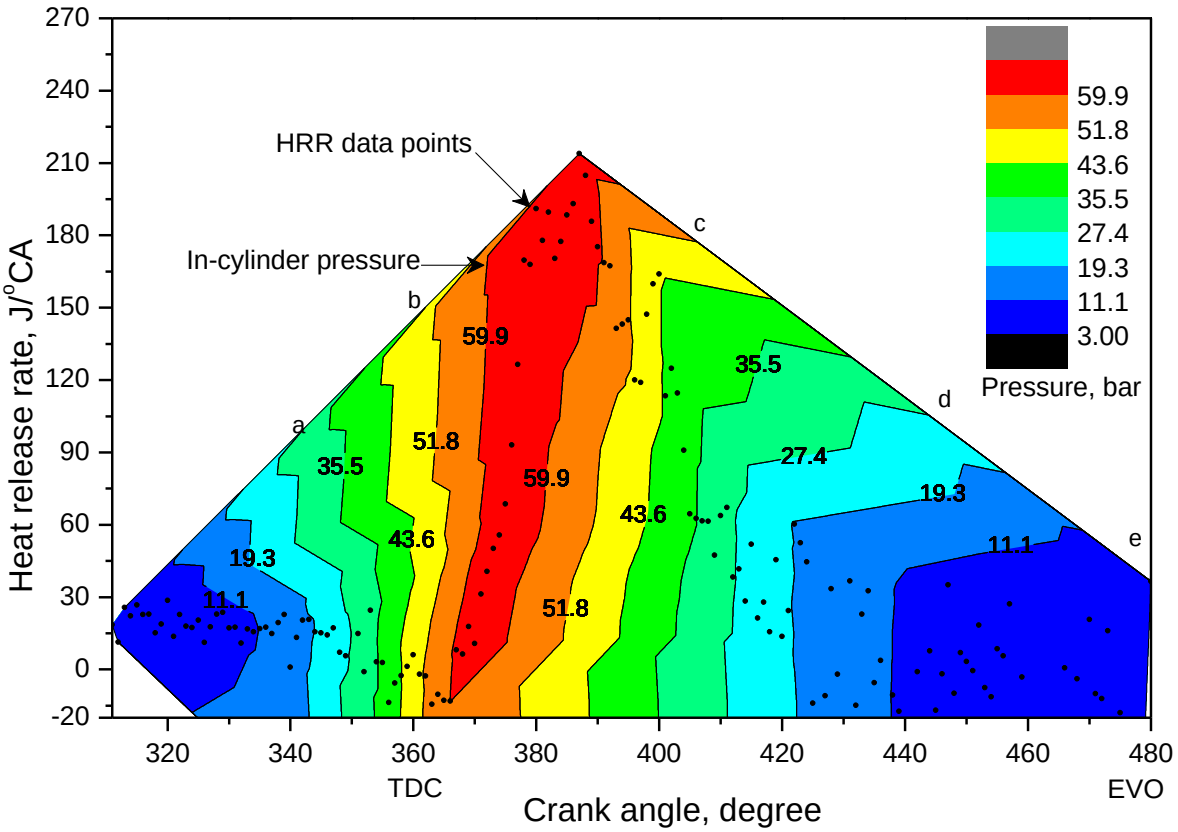

Figure 6.15: Correlation of HRR and CP at combustion phase for AvBn_Pa at full load and 1400 rpm speed

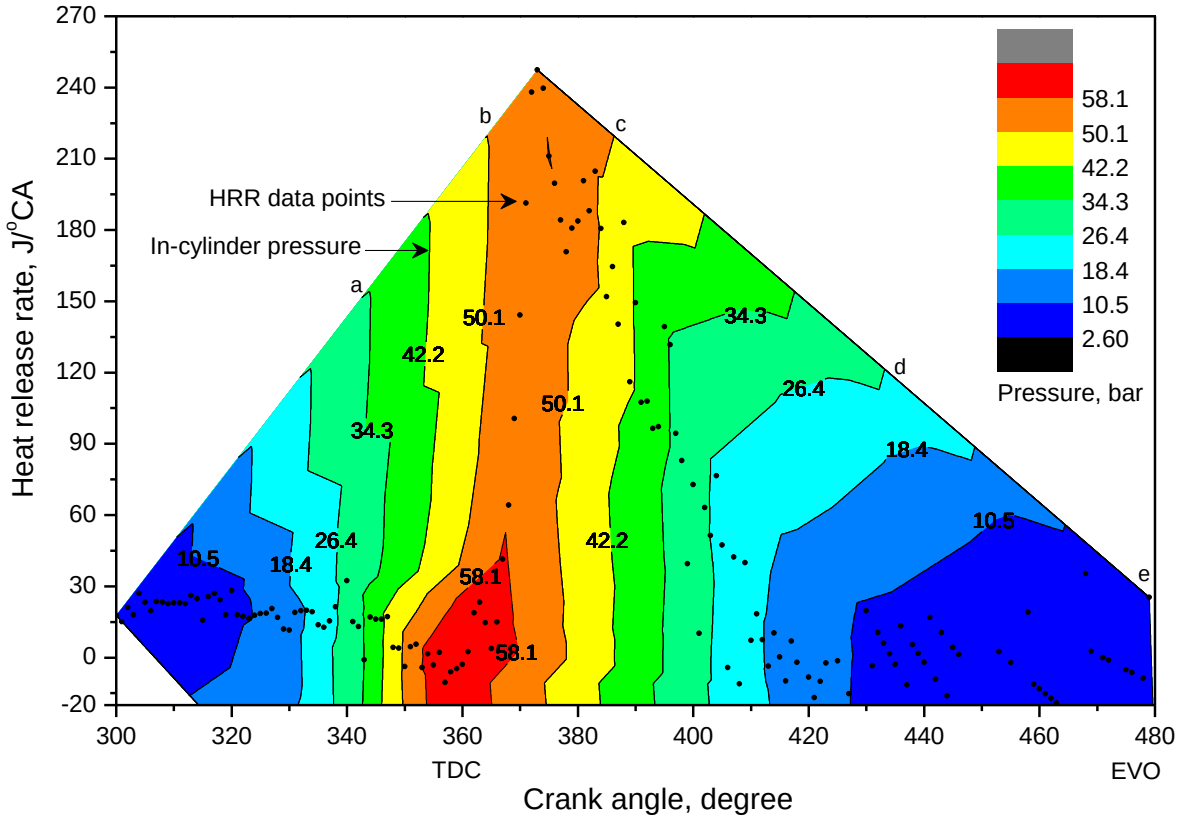

Figure 6.16: Correlation of HRR and CP at combustion phase for ULSD at full load and 2400 rpm engine speed

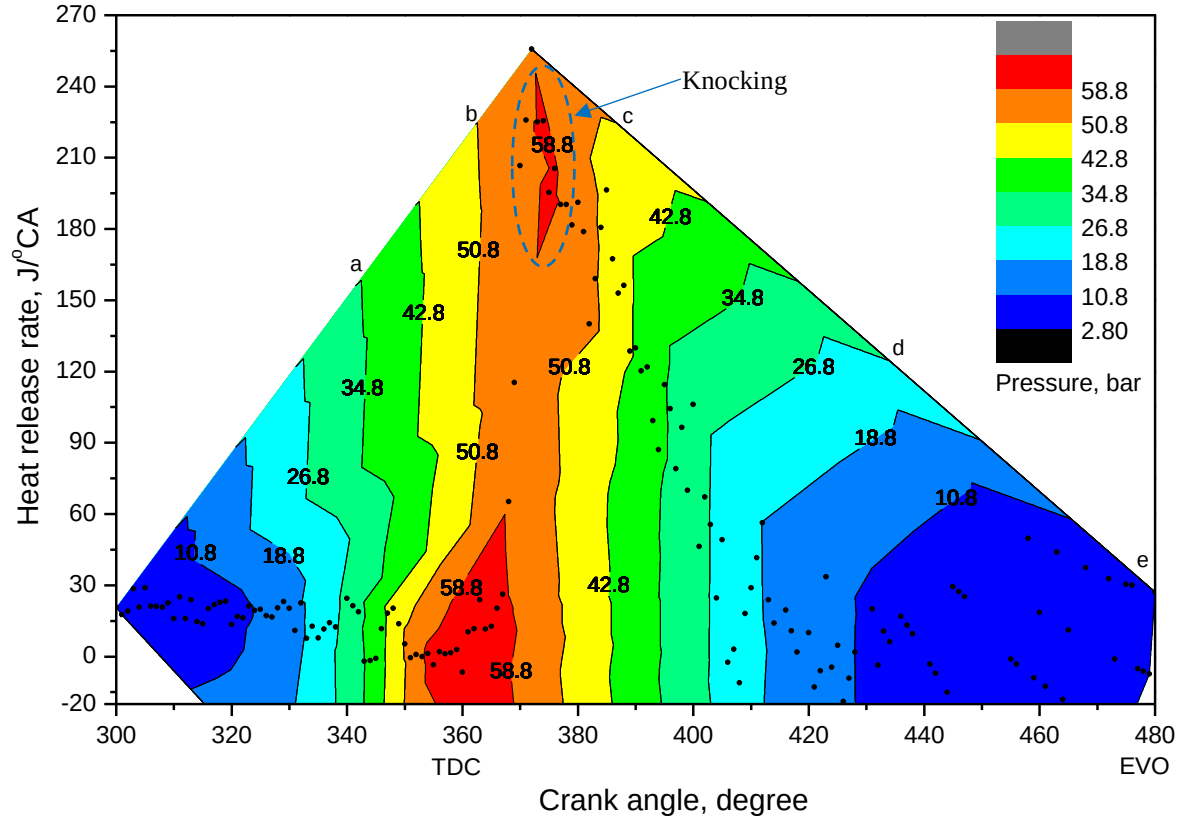

Figure 6.17: Correlation of HRR and CP at combustion phase for ManCr_Pa at full load and 2400 rpm engine speed

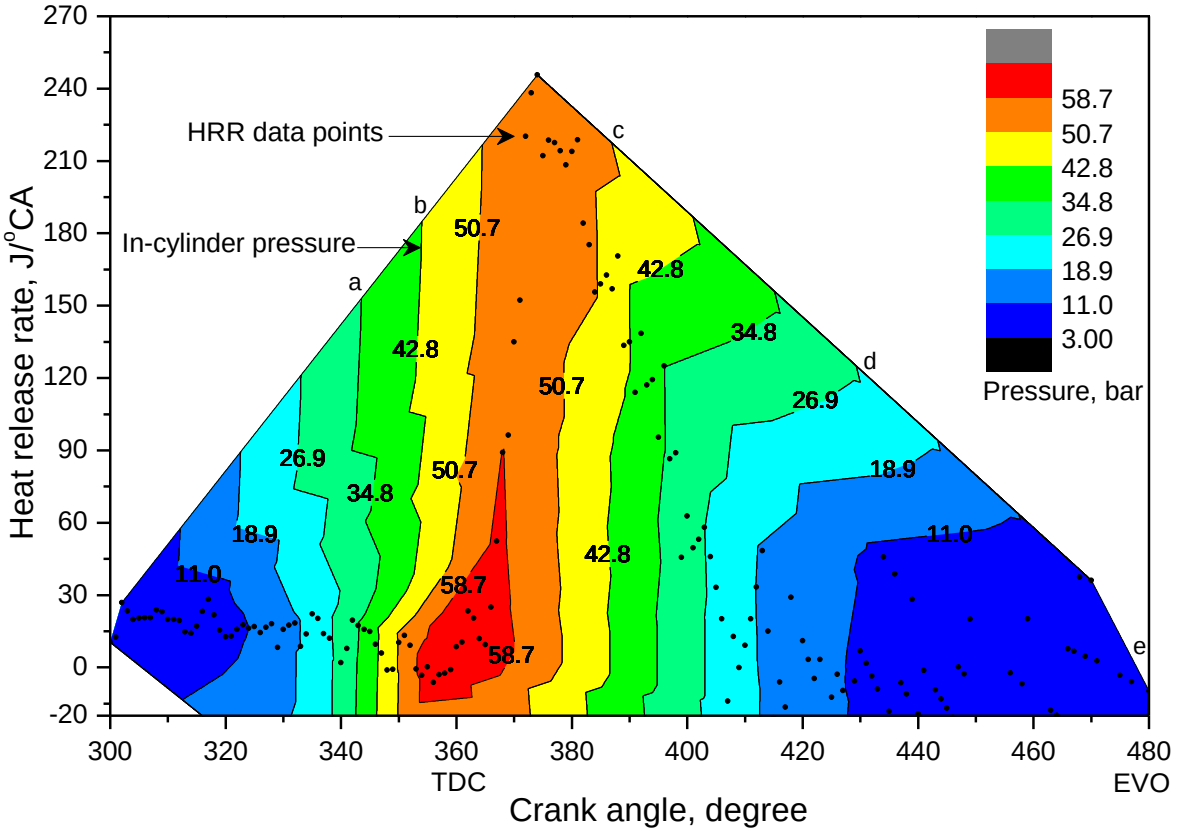

Figure 6.18: Correlation of HRR and CP at combustion phase for AvBn_Pa at full load and 2400 rpm speed

6.3.2. Variation of HRR with engine load

Figures 6.19 to 6.22 illustrate the comparison of HRR between ULSD, ManCr_Pa and AvBn_Pa, respectively, at power stroke with 25%, 50%, 75%, and 100% engine loads at 2400 rpm. For better visual presentation, the HRR diagram is zoomed out from 340 °CA to 420 °CA to consider only the premixed and diffusion combustion phases as late combustion is less important. The combustion behavior at partial load is unpredictable due to the lean air-fuel mixture as shown in Figure 5.19 (d). The excess air factor (λ) is almost doubled for 75% load. In the presence of excess air, mixture blends show better combustion and higher HRR compared to ULSD at partial load along with reduced emissions due to the improvement of fuel properties. Contradictory conclusions were drawn by Islam et al. (2015) and Hossain and Davies (2012). They found lower HRR at partial load due to the higher viscosity of the biodiesel. Further, the lean mixture at lower load contributes to higher HC emissions and lower NO_x emissions due to the shorter CD, along with lower in-cylinder temperature as compared to higher load. In Figures 6.20 and 6.21, ManCr_Pa and AvBn_Pa show lower HRR at the premixed phase but higher HRR at the diffusion phase, respectively. This is due to the prompt vaporisation, and faster diffusion mixing which results in a higher rate of diffusion combustion

(Sajjad et al., 2015). Knocking behavior due to the very sharp premixed phase is identified for ManCr_Pa as shown in Figure 6.22.

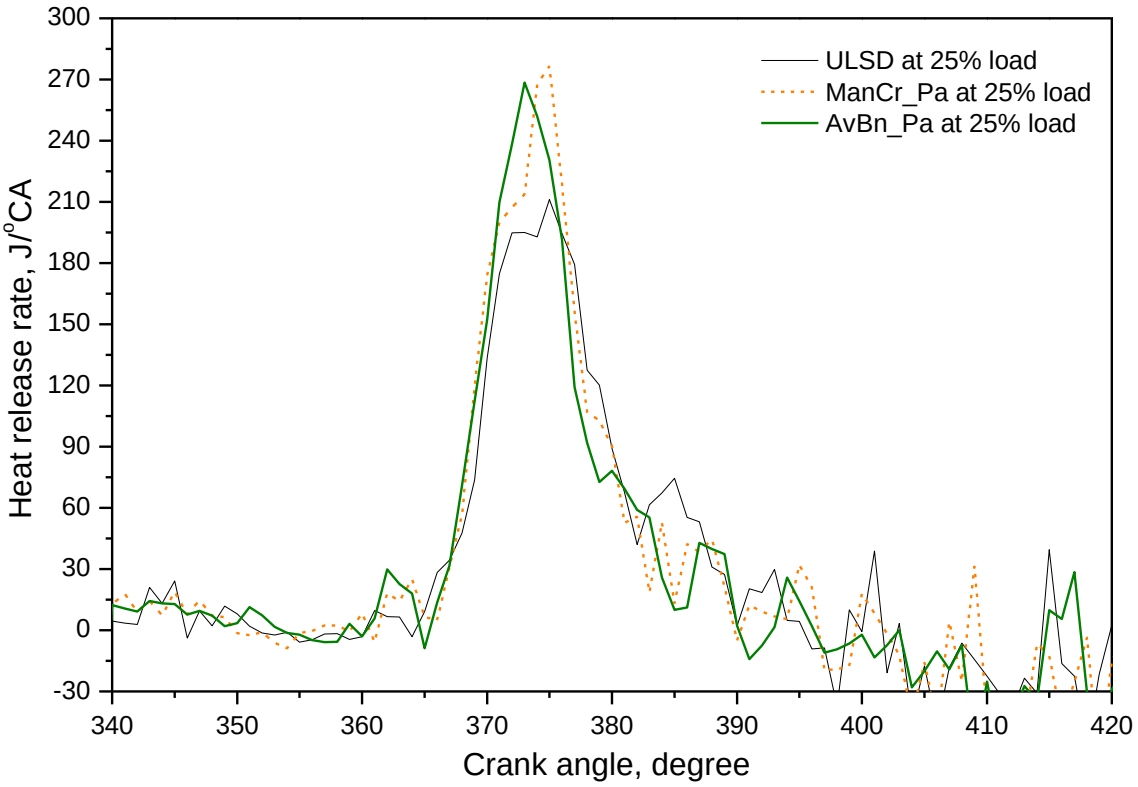

Figure 6.19: Variation of HRR with °CA at power stroke for all tested fuels at 25% load and 2400 rpm speed

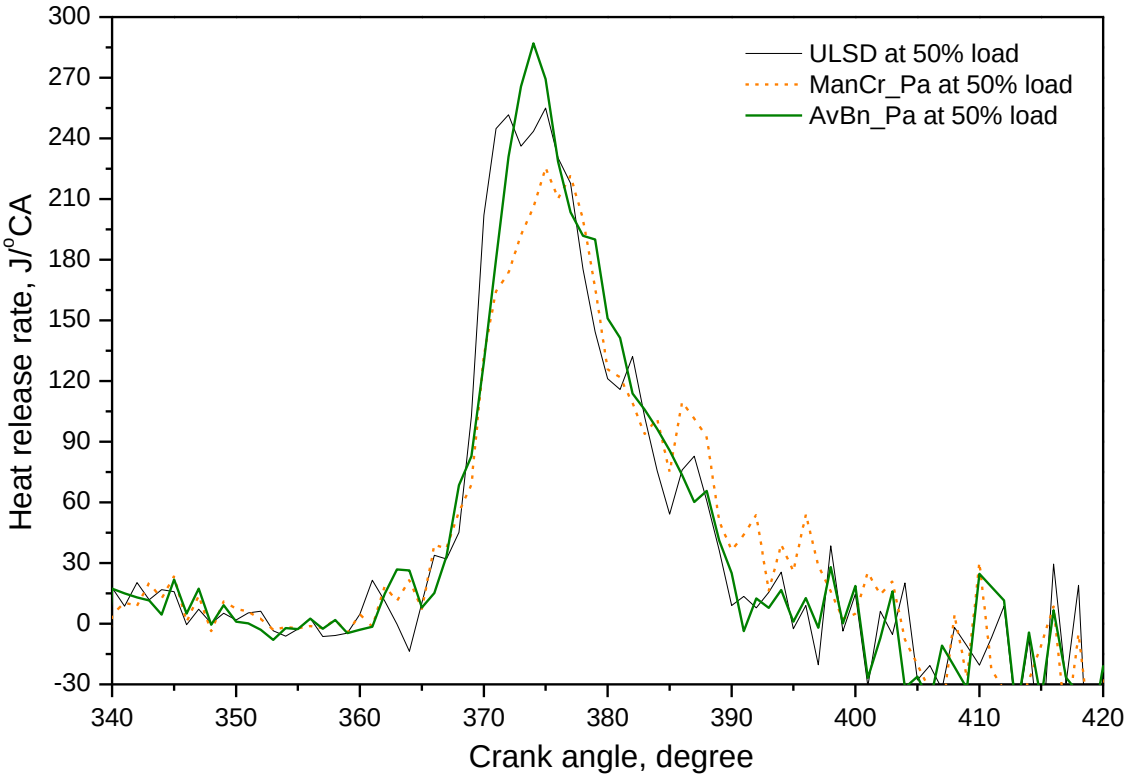

Figure 6.20: Variation of HRR with °CA at power stroke for all tested fuels at 50% load and 2400 rpm speed

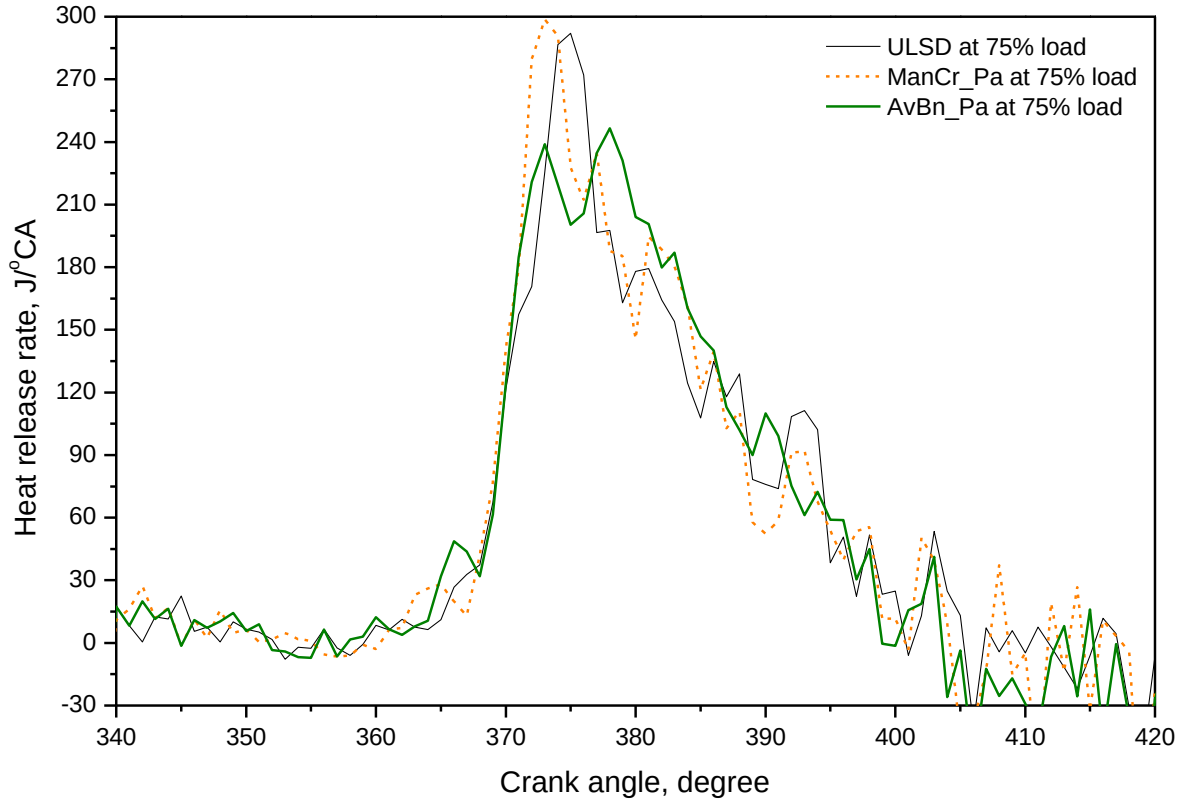

Figure 6.21: Variation of HRR with °CA at power stroke for all tested fuels at 75% load and 2400 rpm speed

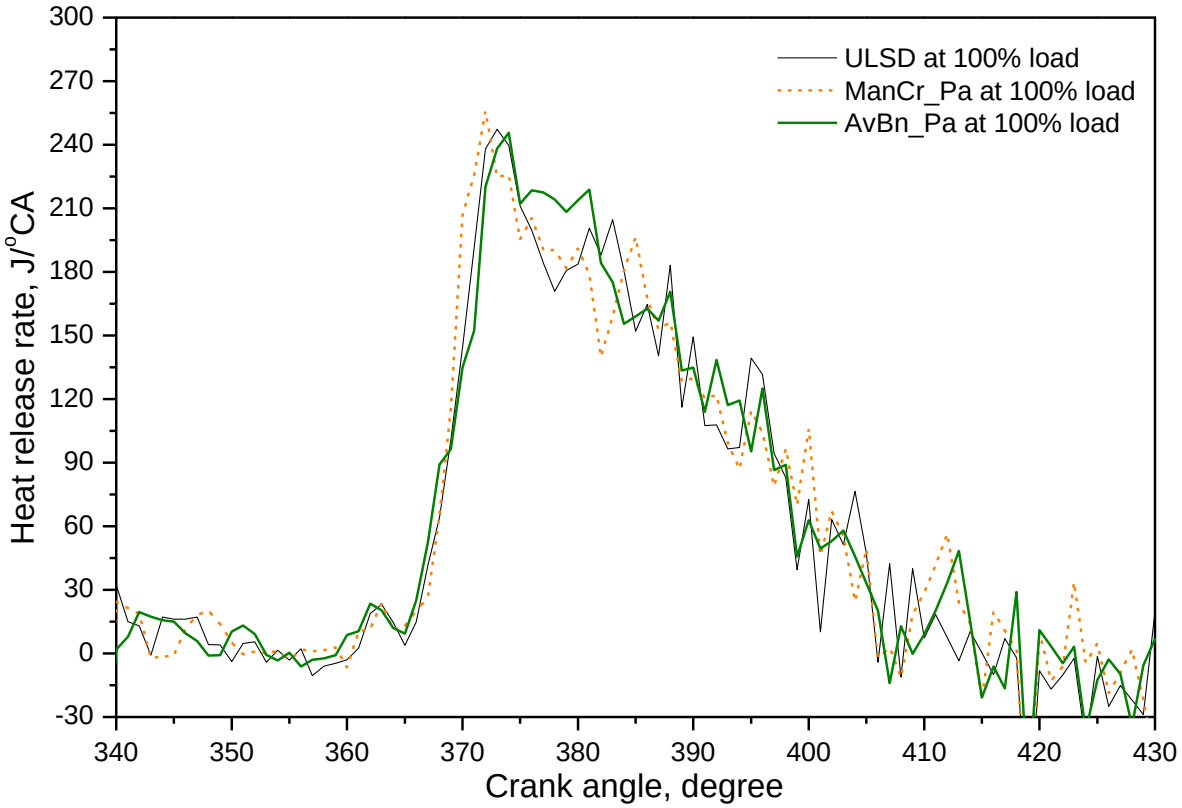

Figure 6.22: Variation of HRR with °CA at power stroke for all tested fuels at full load and 2400 rpm speed

6.4. Ignition Delay (ID)

The period between the start of injection (SOI) and the start of combustion (SOC) is known as ignition delay (Awad et al., 2016). The study calculated ID in crank angle and converted this to milliseconds using Equation 6.1.

$$t(ms) = \frac{CA}{N \times \left(\frac{\min}{60}\right) \times \left(\frac{360}{rev}\right)} \times 1000 \tag{6.1}$$

where CA is crank angle in degrees, N is speed in rpm and t is ignition delay in milliseconds (ms).

Figures 6.23 compares the ID for tested fuels at 1400 rpm, 1600 rpm, and 2400 rpm. The results reveal that biodiesel blends show shorter ID as compared to ULSD due to their higher CN. Similar results were obtained by many researchers in the literature (Gogoi and Baruah, 2011, Saravanan et al., 2010, Sahoo and Das, 2009). The high molecular weight of the methyl esters breaks down into lighter components by thermal cracking due to rapid and pre-flame chemical reaction at high temperatures as pointed out by Gogoi and Baruah (2011). In addition, biodiesel contains mostly saturated and unsaturated fatty acids. A higher DU of the biodiesel causes enhanced oxidation instability which leads to prompt oxidation during combustion. As seen from Figure 6.23, ID decreases with the increase in engine speed due to the rich air-fuel mixture at lower speeds. Figure 6.24 portrays the variation of ID with variable engine load. The figure shows that ID also decreases with the increase in engine load. Biodiesel mixture blends also show less ID at each load condition due to the inadequate turbulence and mixing of very lean air-fuel mixtures at lower load conditions. At higher load, a large quantity of fuel is burnt per cycle which implies higher cylinder temperatures that help to decrease the chemical delay period and hence result in a reduced ID. For both cases, the AvBn_Pa blend shows less ID as compared to ManCr_Pa and ULSD. This is due to its higher CN and self-oxygen content as well as the shorter carbon chain length of the AvBn_Pa ternary mixture blend.

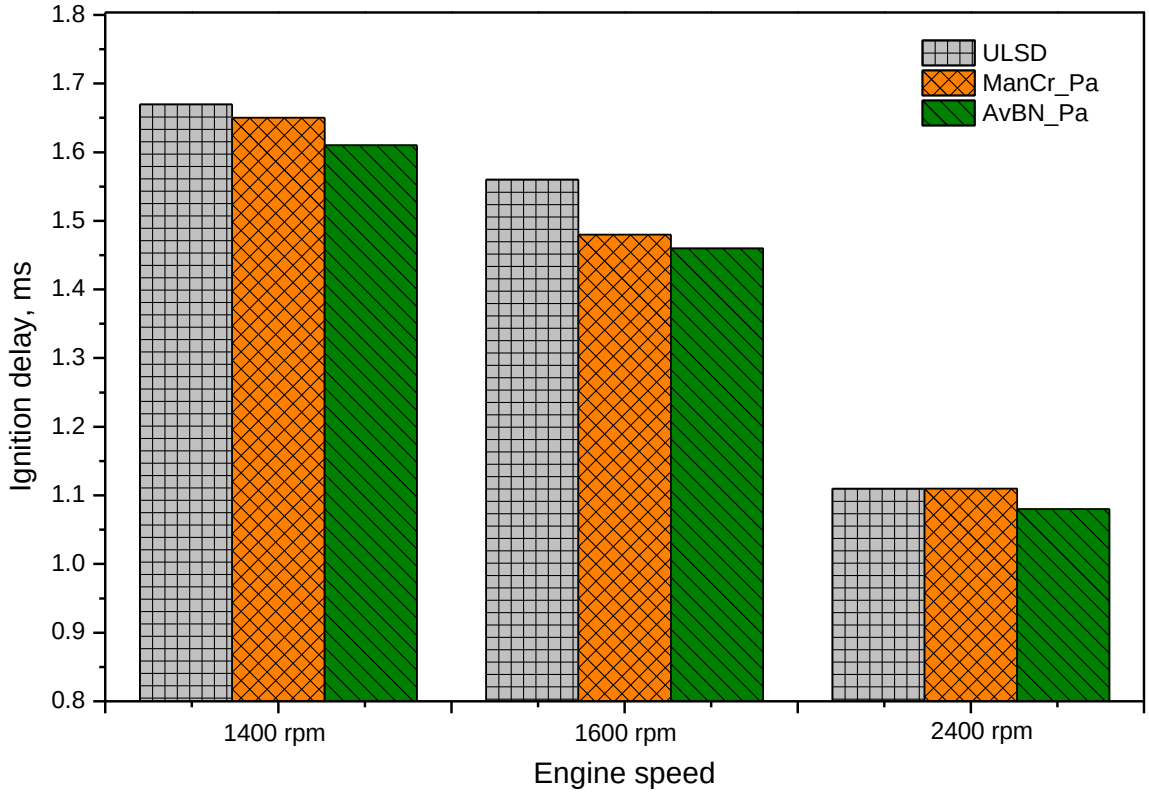

Figure 6.23: Variation of ignition delay with engine speed at full load for tested fuels

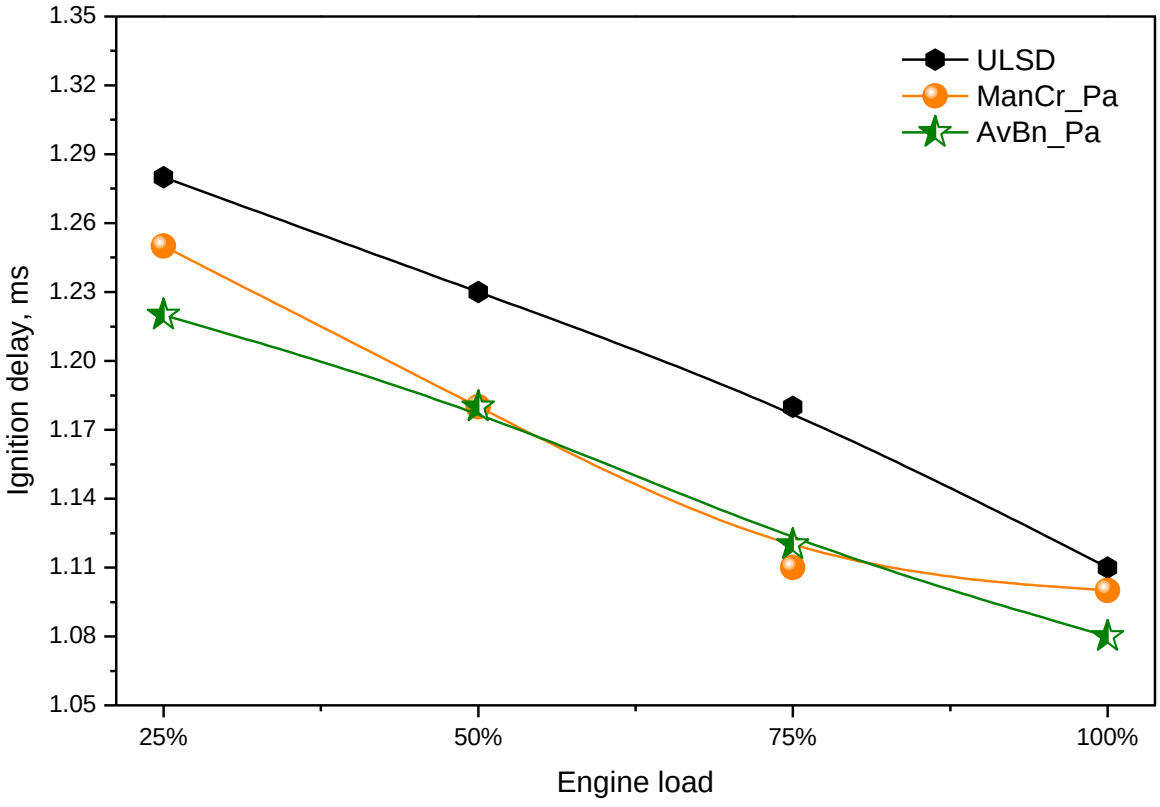

Figure 6.24: Variation of ignition delay with engine load at rated power for tested fuels

6.5. Combustion Duration (CD)

Combustion duration (CD) is the period between the start of heat release to the end of heat release (Sahoo and Das, 2009). As discussed above, there are three combustion phases that comprise the total CD. Due to this reason, it is difficult to identify the end of combustion. However, different research groups have their individual opinions. It is well justified in the literature that 90% cumulative heat release could be considered as indicating the end of combustion (Gogoi and Baruah, 2011, Banapurmath et al., 2008b). The study followed this method to calculate total CD. Figure 6.25 illustrates the variation of CD for tested fuels for full load at 1400 rpm, 1600 rpm, and 2400 rpm. The trend implies that CD decreases with the increase in engine speed for all tested fuels. This is due to the rich air-fuel mixture, and lower cylinder temperature and pressure which slows down the oxidation rate and thermal decomposition of the fuel at the lower engine.

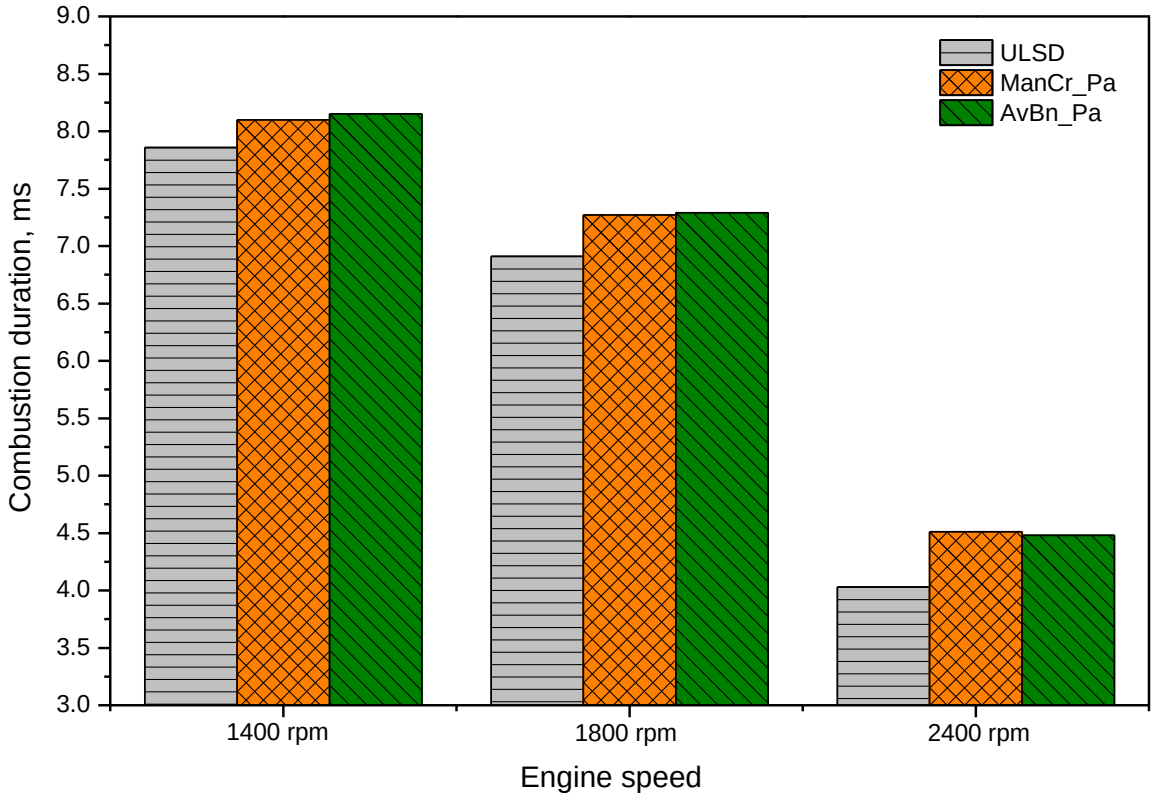

Figure 6.25: Variation of combustion duration with engine speed at full load for tested fuels

Figure 6.26 demonstrates the variation of CD at variable engine load which implies that CD increases with the increase in engine load. As seen from the figure, the maximum CD was found at full load condition for each fuel. At lower load, the air-fuel mixture was too lean and the combustion was not completed which contributes to the lower cylinder pressure and

temperature. The diffusion combustion phases could be shortened due to the inadequate combustion environment and poor atomisation and mixing of air-fuel at partial load. It could be noted from Figure 6.26 that ManCr_Pa and AvBn_Pa mixture blends demonstrate longer combustion duration compared to ULSD. In addition, the higher fuel consumption of biodiesel blends leads to longer combustion duration, and the higher CN results in smoother combustion and higher HRR at the diffusion phase. The prolonged CD and self-oxygen content are the main reasons why combustion of biodiesel in CI engines reduces emissions.

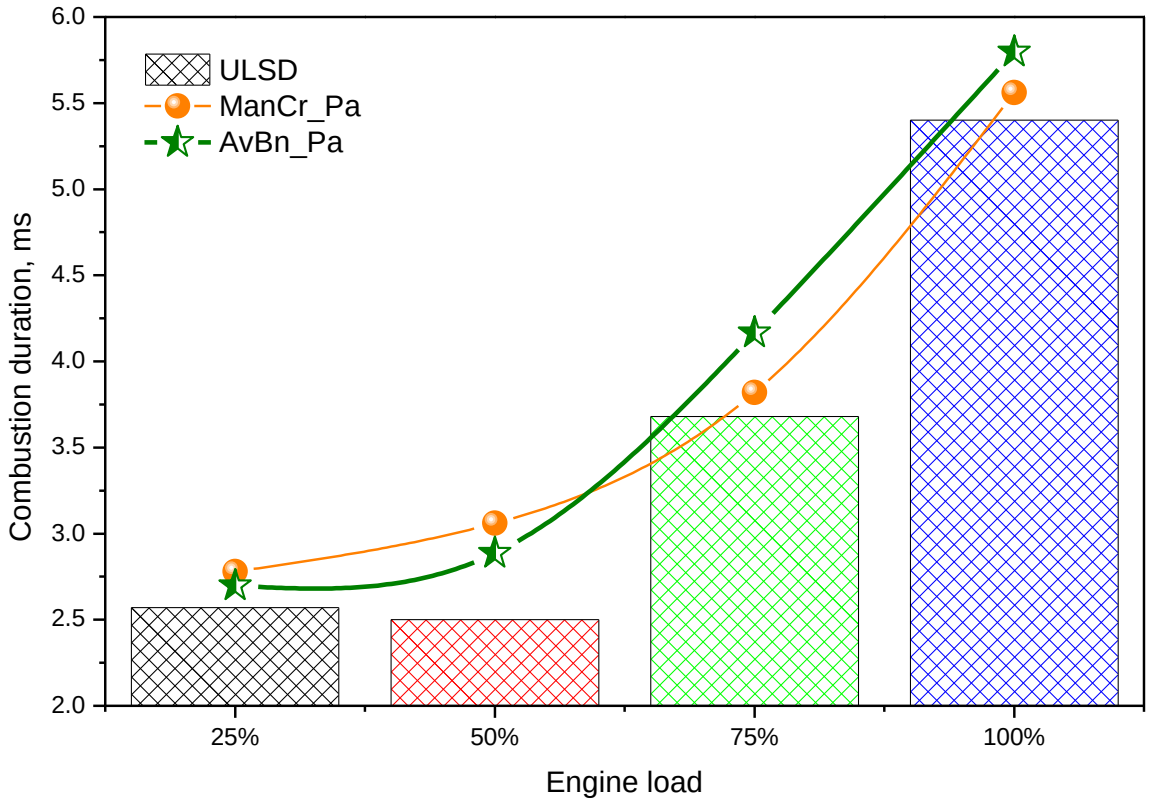

Figure 6.26: Variation of combustion duration with engine load at rated power for tested fuels

6.6. Chapter Conclusion

In this chapter, combustion analysis was conducted on the better performing fuel blends to analyse CP, HRR, ID and CD at power stroke. The mixture blends demonstrate higher CP as compared to ULSD at each operating condition (i.e. both variable speed and load conditions). The study presented an excellent relationship between CP and HRR to describe the combustion phenomena of the tested fuels which shows CP increases with the increase in engine speed and load. ULSD exhibits higher peak HRR at the rapid premixed combustion phase at variable speed. The ManCr_Pa and AvBn_Pa mixture blends show higher HRR with longer combustion

duration at the diffusion combustion phase which is the most powerful phase in combustion. The mixture blends demonstrate combustion behaviour close to that of ULSD at full load and higher HRR at partial load. A knocking characteristic is identified for the ManCr_Pa blend at full load condition. When comparing the two mixture blends, AvBn_Pa demonstrates better combustion behaviour as compared to the ManCr_Pa blend mainly due to the higher oxygen content, shorter ID and longer CD.

Chapter 7

TRIBOLOGICAL STUDY

This chapter deals with the tribological characteristics of the better performing fuels, namely ULSD, ManCr_Pa and AvBn_Pa, as identified in Chapters 5 and 6. Tribological parameters of friction, wear, and lubrication stability were measured to assess the impact of these fuels on engine health. The tests were conducted on a four-ball tribotester using the ASTM D4172 standard; friction coefficient and wear scar diameter for the fuels were measured. The wear scar surface morphology of the ball metals was evaluated by a high-performance scanning electron microscope with energy dispersive x-ray SEM/EDX analysis. The corrosive behaviour of the fuels was also assessed by evaluating images from the SEM/EDX tests. Finally, the engine health, reliability, and longevity were also evaluated based on the measured tribological parameters.

7.1. Introduction

The tribological aspects of IC engine combustion systems mainly deal with the cylinder and the piston in a reciprocating motion. When the engine runs, the piston slides on the inner surface of the cylinder, and friction is produced between the mating surfaces which gives rise to wear of both the surfaces. Thus the energy produced by combustion of fuel is partially consumed to overcome friction which reduces the engine efficiency by up to 20% as reported by Nagar and Miers (2011). Clearances are increased due to wear of cylinder and piston, giving rise to blow-by of gases which also contributes to reducing the efficiency. Lubrication of piston and cylinder surfaces occurs mainly as a boundary lubrication regime, and a very thin film of normally less than a micron is formed in the contact zone giving a lambda ratio (λ_l) between 1 and 1.5. It is the ratio between the film thickness and composite roughness of the two surfaces. The lubrication is used to minimise the friction and wear by creating a very thin layer between the metal surfaces. However, it involves additional cost and the additive constituents such as Fe, Cr, P, Zn, etc. into the lubricating oil causes more PM formation when they are mixed with the exhaust gases near the cylinder wall as discussed in Chapter 5. It is also reported in the literature that adding additives in a lubricating oil causes environmental pollution due to higher contents of sulphur and phosphorus (Mosarof et al., 2016c). Therefore, lubrication is important for not only conserving energy but also for safe running of engines as reported by Tung and McMillan (2004). Mosarof et al. (2016a) also reported that about 33% of total energy losses are due to the friction of the moving parts in passenger cars (Holmberg et al., 2012). However,

there are some other techniques such as coating, texturing and application of lighter metal that have also been used to minimise friction (Mosarof et al., 2016c).

Biodiesel can be used to minimise environmental pollution and also the dependency on lubricating oil due to its excellent self-lubricating properties (Habibullah et al., 2015b). The literature also reported that vegetable oils such as soybean, sunflower, coconut, corn, and rice bran oils can be used as bio-lubricant in CI engines (Mosarof et al., 2016a). The lubricating property of the biodiesel depends on the dynamic viscosity of the fuel which is related to its density and the kinematic viscosity for a given operating temperature. Other research reveals that the wear and friction decrease with the increase in biodiesel blend percentage as investigated by Fazal et al. (2013). On the other hand, Haseeb et al. (2010) experimented on the variation of wear and friction of a biodiesel drive with palm oil at temperatures of 30 °C, 45 °C, 60 °C, and 75 °C. They found that both wear and friction increase with the increase of cylinder wall temperature. Mosarof et al. (2016b) and Habibullah et al. (2015b) investigated the tribological characteristics of biodiesel produced from *Calophyllum inophyllum* under different load conditions in a CI engine. Their results revealed that wear and friction increase with an increase in applied load, but decrease with the increase of biodiesel blends at constant load. Many other researchers used a four-ball triobotester to analyse the tribological behaviour of different biodiesels as reported in the literature (Habibullah et al., 2015b, Mosarof et al., 2016c, Haseeb et al., 2010). Four-ball testers are widely used by lubricant manufacturers in research and development (R&D) of new lubricants and characterising their friction and wear behaviour.

This study performed tribological testing using a four-ball tribotester in accordance with the ASTM D4172 standard whereby friction coefficient (FC) and wear scar diameter (WSD) were measured for the tested fuels. The wear scar surface morphology of the ball metals was further evaluated by a high-performance scanning electron microscope (SEM) with energy dispersive x-ray (EDX) analysis.

7.2. Tribology Test by Four-Ball Tribotester

In this study, a four-ball (TR-30H, DUCOM) test rig was used to assess the tribological characteristics of the tested fuels as illustrated in Figure 7.1. The test rig consists of four balls, three of which are stationary balls (Nos. 1, 2, and 3) sitting in a cup and submerged into the

tested fuel with one rotating ball (No. 4) resting on the stationary balls and held by a spindle rotating at a constant speed at 1200 rpm. The specification of the tested ball materials and test conditions are presented in Table 7.1. The test was conducted using the ASTM D 4172 standard method. Initially, the setup was prepared by washing the tested balls with *n*-heptane solution and wiping with soft tissue paper to dry. The oil cup was also cleaned and dried before being used for each test. The three balls were placed into the cup using tweezers, and the cup was filled with 10 ml of the fuel sample being tested which comes to about 3mm over the stationary balls. During the test, the axial load of 40 kg was applied to the stationary balls by the loading arm according to the ASTM D4172 standard method. The friction torque (FT) was measured by the calibrated torque arm which is assembled with a friction recording device. This test was conducted at a nominal 75 °C temperature which was controlled between 75 °C to 80 °C during the study using a thermostated bath. After completion of the test, the stationary balls were cleaned to laboratory standards. A high-resolution microscopy was performed on these balls using a high-resolution optical microscope in accordance with the ASTM D4172 standard. Finally, SEM/EDX analysis was conducted to evaluate the metal surface morphology of the tested balls. The FC and flash temperature parameter (FTP) were obtained using Equations (3.18) and (3.19), respectively as discussed in Chapter 3.

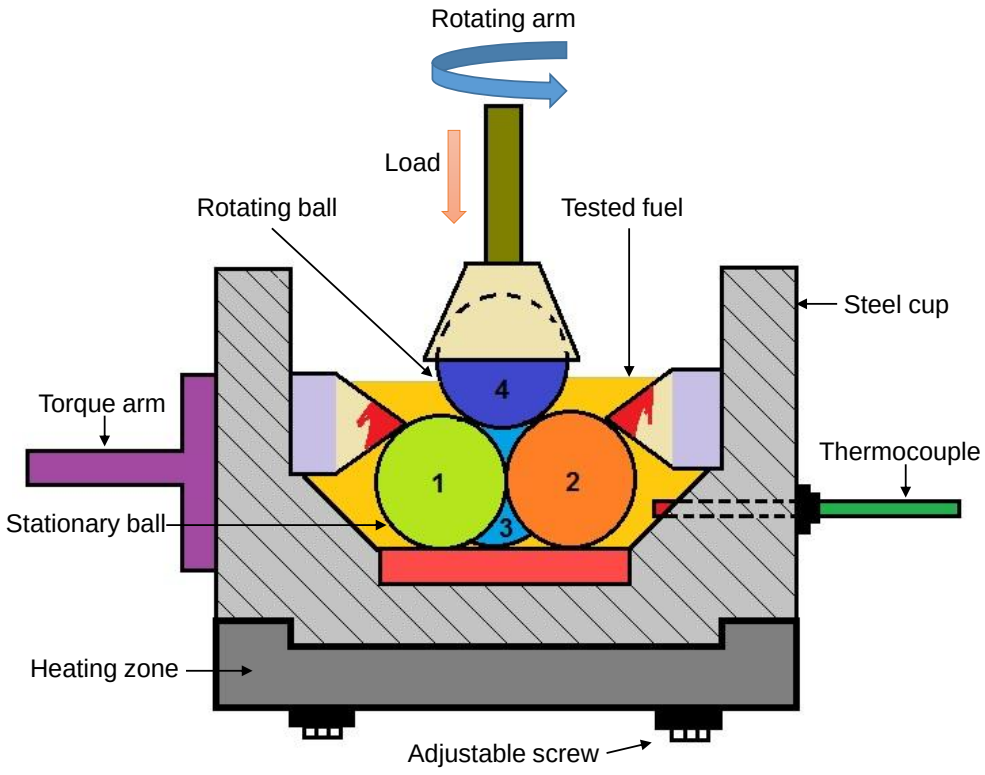

Figure 7.1: Schematic diagram of four-ball tribotester (TR-30H)

Table 7.1: Setup specification and experimental test condition

Items	Parameters	Description
Specification	Speed range	300 to 3000 rpm
	Temperature range	25 to 1000 °C
	Axial applied load	Maximum 1020 kg
	Scar range	100 to 4000 micron
	Drive motor power	1.50 kW
Test condition	Applied load	40 kg
	Rotation	1200 rpm
	Test duration	3600 sec
Testing ball specification	Diameter of the ball	12.70 mm
	Materials	Carbon-chromium alloy steel
	Metal composition	85.05% Fe, 10.26% C, 2.13% Zn, 1.44% Cr, 0.43% Si, 0.44% Mn, 0.09% S, 0.13% P, and 0.06% Ni
	Hardness of the metal	62 HRc
	Surface roughness	0.10μm (C.L.A)
	Density	7.87 gm/cm^3
	Tensile strength	325,000 psi
	Yield strength	295,000 psi

The uncertainty or error analysis was conducted to ensure the reliability of the test results. Mosarof et al. (2016a) reported that a high degree of uncertainty could occur due to instrument faults, test conditions, test environment, wrong test procedure and observation. The overall uncertainty of the whole experiment was discussed in Chapter 3. More specifically, the uncertainty related to the tribological test as conducted is summarised in Table 7.2. The test was repeated three times to minimise the error of the result. Overall uncertainty related to wear and friction was found to be about 3.68% for this experiment which was well within the acceptable limits as verified by Mosarof et al. (2016a) and Habibullah et al. (2015b).

Table 7.2: Summary of uncertainty related to different parameters

Measurements	FC		WSD	FTP
	Run-in period	Steady state		
Accuracy	±0.50	±0.50	±0.01 mm	±0.50
Relative error	±2.54	±1.27	±1.51	±2.76

7.3. Friction Behaviour Analysis

The friction behaviour of the tested fuels was evaluated for 3600 seconds to the ASTM D4172 standard. The results reveal that, at the beginning of the test (0 to 10 sec), the FC exhibited a higher magnitude and unstable conditions which is denoted as the run-in period. The FC variation soon became stable and followed a steady state condition until the end of the test. This is due to several reasons as reported by Fazal et al. (2013). After the run-in period, the contact surface of the tested balls became smoother and prominent asperities were flattened or removed. Figure 7.2 illustrates the variation of FC during the run-in period for all tested fuels. The ManCr_Pa mixture blend demonstrates the highest FC with a shorter run-in period compared to other fuels. This is due to the lower (about 5.25%) dynamic viscosity of ManCr_Pa (3.23 mPa.s) compared to ULSD (3.41 mPa.s) which is one of the key parameters of lubrication properties as discussed above (Mosarof et al., 2016c). ULSD exhibits a higher FC compared to the AvBn_Pa blend with a longer run-in period. The results reveal that the AvBn_Pa mixture blend shows lower FC with shorter run-in duration compared to other fuels which implies the capability of biodiesel to prompt a change of unsteady state to steady state condition of FC for reducing friction.

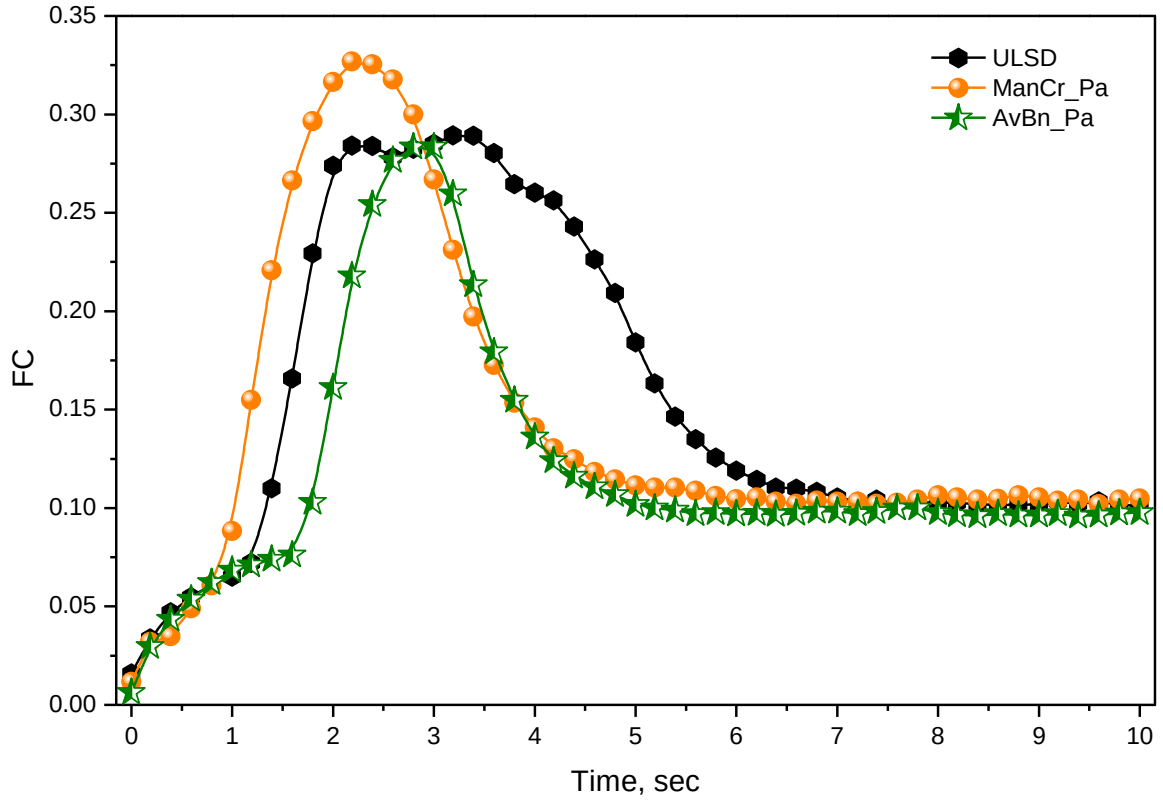

Figure 7.2: Variation of FC with time during run-in period

Figure 7.3 illustrates the variation of FC at steady state conditions for ULSD, ManCr_Pa and AvBn_Pa. The figure shows that the fluctuation of FC for ULSD is higher than for the other fuels which implies more friction occurred for fossil fuel compared to biodiesel. Similar results were also found by Mosarof et al. (2016c), Habibullah et al. (2015b) and Haseeb et al. (2010). The ManCr_Pa blend demonstrates minimal fluctuation of FC and a lower average FC compared to ULSD at steady state conditions. However, it shows higher FC during run–in conditions and transitioned to a steady state quickly as shown in Figure 7.2. This study found a significant reduction of FC for the AvBn_Pa blend in both the run-in period and the steady state period due to the long chain fatty acid content in this fuel. The FC reduction evidenced by the biodiesel blends implies that the ester molecules act as surfactants by creating a thin layer between the contact surfaces of the metals (Habibullah et al., 2015b, Fazal et al., 2013). The results reveal that ManCr_Pa and AvBn_Pa blends reduced FC by about 6.5% and 20.9% compared to ULSD at steady state conditions, respectively. This study conducted an in–depth analysis of the lubricating behaviour of these fuels by showing a correlation between FT and FC which is presented in Figures 7.4 to 7.6.

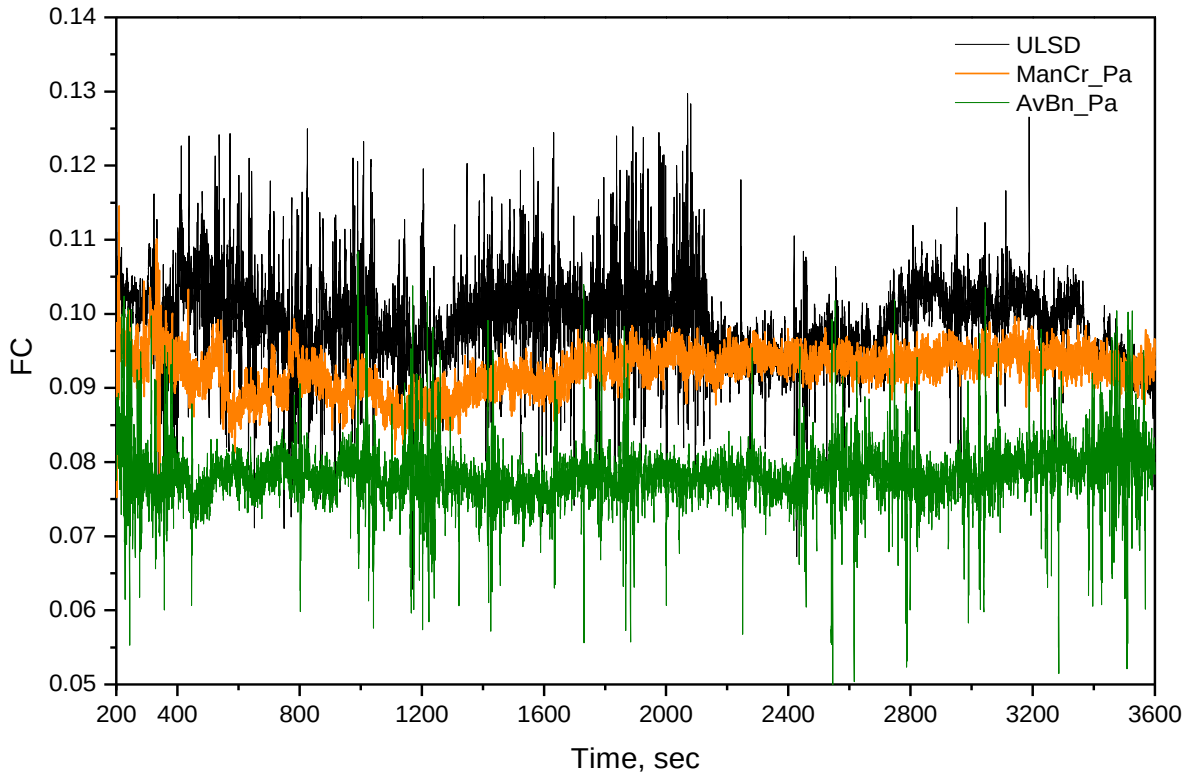

Figure 7.3: Variation of FC with time at steady state condition for ULSD, ManCr_Pa and AvBn_Pa

Figures 7.4, 7.5 and 7.6 illustrate the correlation of FT and FC at steady state conditions for tested fuels. The figures show the variation of FC and FT with time at steady state conditions

by black dot points and contour colour maps, respectively. More FT implies more energy loss due to friction which causes more wear on the metal surfaces as reported by Mosarof et al. (2016b). Figure 7.4 demonstrates that the average FC value for ULSD varies between 0.09 and 0.11 within the range of 0.17 N.m to 0.19 N.m FT. However, this study found some higher values of FC at FT values above 0.22 N.m which implies significant energy loss due to friction and higher wear on the metal surfaces (Zulkifli et al., 2013). Figure 7.5 demonstrates an average FC variation for ManCr_Pa between 0.09 and 0.97 within the range of 0.17 N.m to 0.79 N.m FT. It also shows higher values of FC at FT values above 0.18 N.m which is lower than for ULSD. Figure 7.6 demonstrates better tribological behaviour by AvBn_Pa with a reduced FC average ranging from 0.07 to 0.09 within the minimal FT range of 0.13 N.m to 0.15 N.m. This fuel shows an insignificant number of FC values at FT values above 0.173 N.m. The results reveal that AvBn_Pa reduces FT by 23.70% compared to ULSD which implies lower frictional energy loss and minimum wear on the metal surfaces contributing to sustainable engine health and improved engine reliability compared to fossil fuel. The wear analysis is briefly discussed in the following section.

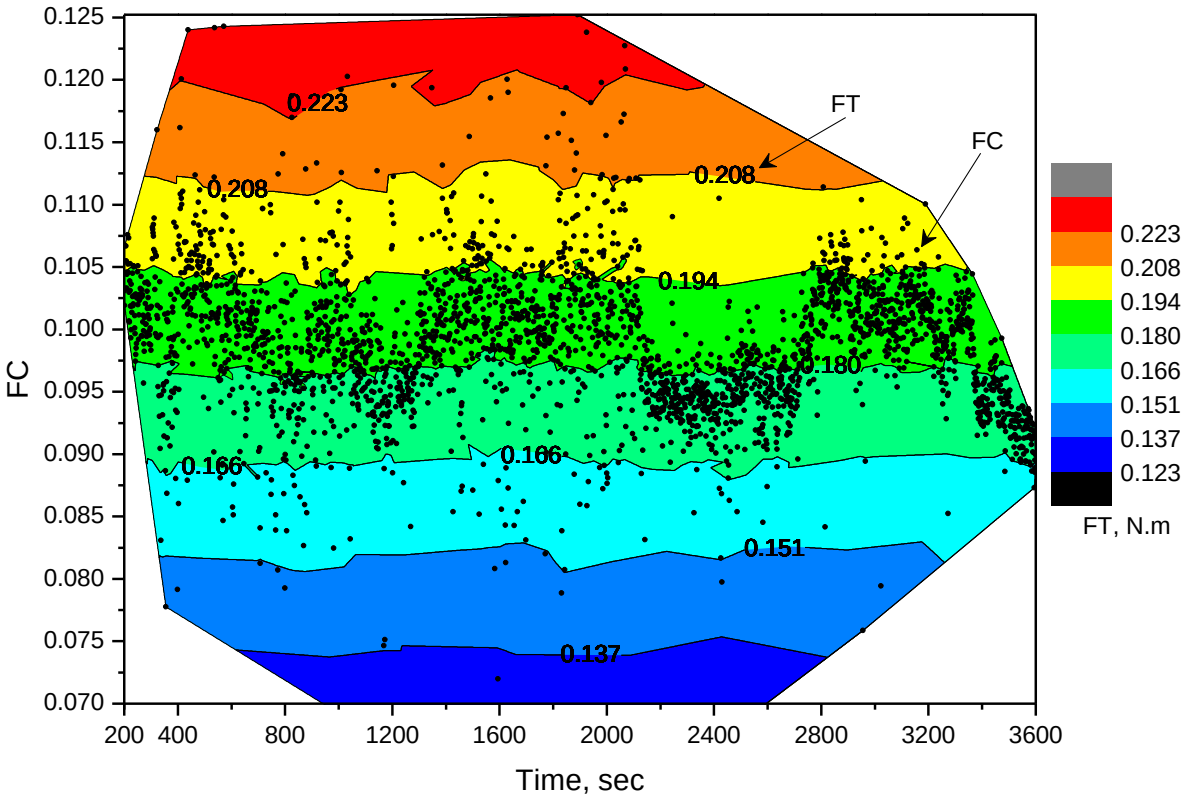

Figure 7.4: Correlation of FT and FC at steady state condition for ULSD

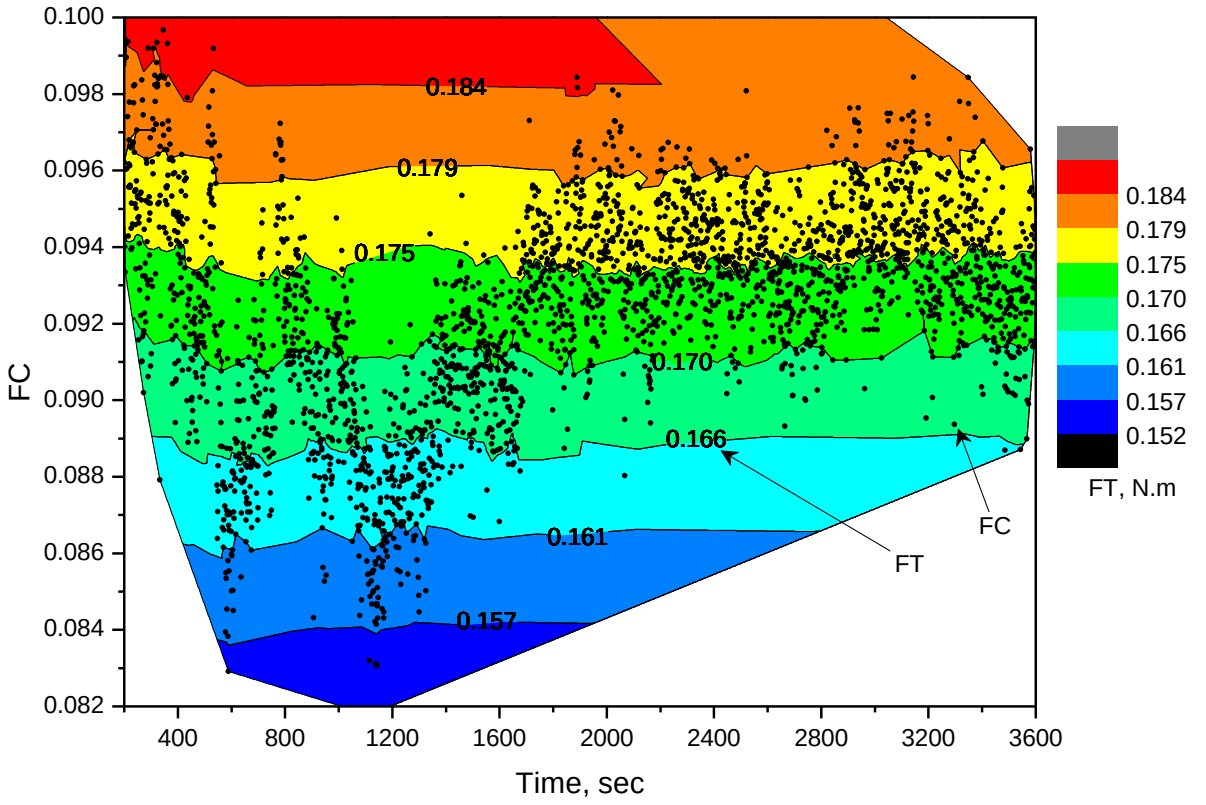

Figure 7.5: Correlation of FT and FC at steady state condition for ManCr_Pa mixture blend

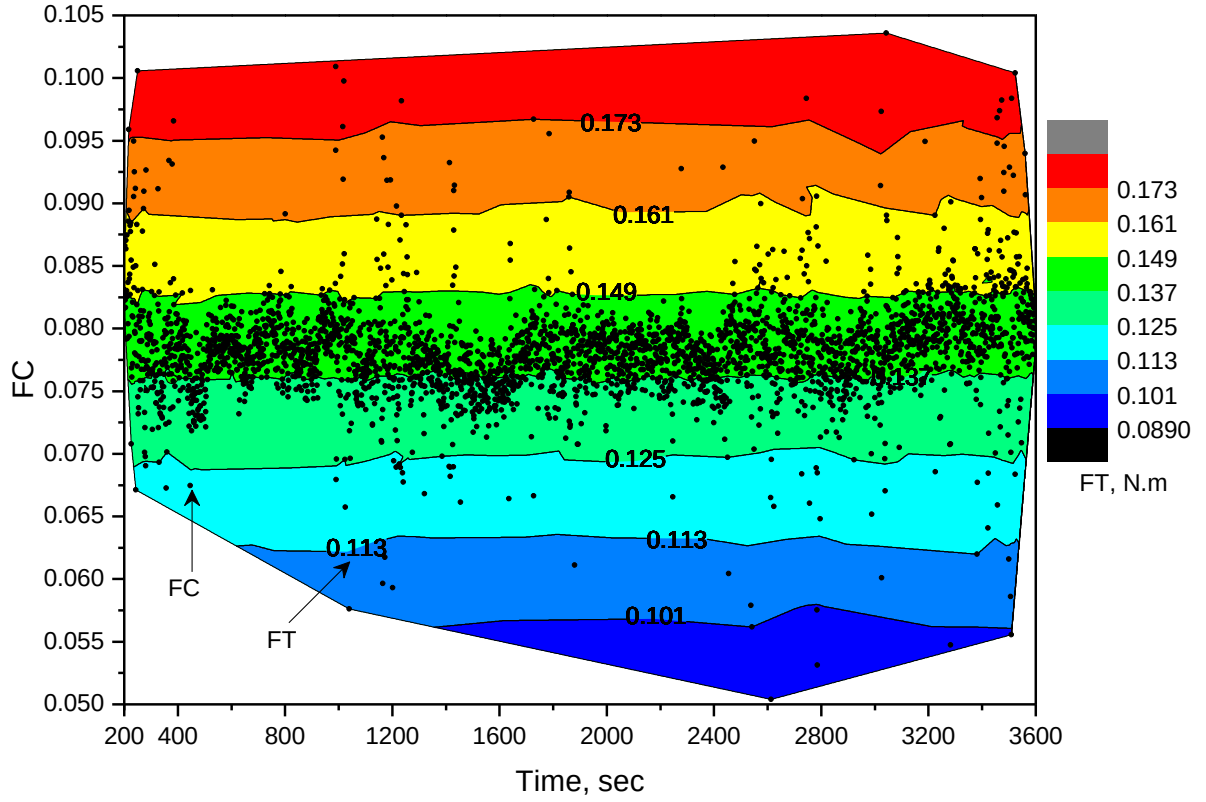

Figure 7.6: Correlation of FT and FC at steady state condition for AvBn_Pa mixture blend

7.4. Wear Characteristics

Figure 7.7 demonstrates the mean WSD of the stationary balls used in the four-ball tribotester in this study. The balls were scanned by an optical microscope to assess the wear characteristics of ULSD, ManCr_Pa and AvBn_Pa blends at a constant speed, load and temperature condition. The major, minor and mean WSD and wear areas for each ball are summarised in Table 7.3. The results reveal that the highest WSD was found for ULSD and the lowest for AvBn_Pa blend under the same test conditions. As seen from Figure 7.7 and Table 7.3, the mean WSD was found to be 0.630 mm for ULSD which is 3.90% and 23.80% higher than for the ManCr_Pa and AvBn_Pa blends, respectively.

The WSD also depends on various operating conditions such as speed, load, temperature and oil compositions, etc. as reported by Maleque et al. (2000). For instance, Mosarof et al. (2016c) investigated the WSD of two biodiesels at different temperatures and loads with constant speed. They reported an increasing trend of WSD with both an increase in temperature and applied load. On the contrary, Fazal et al. (2013) experimented by palm biodiesel at constant temperature and load but for varying speeds from 600 rpm to 1500 rpm. They pointed out that WSD increased with increased speed but decreased for higher biodiesel blend proportions. There are some other reasons for improving lubricity which involve the FAMEs composition of the biodiesel. Hu et al. (2005) reported that the presence of mono and di-glycerides and free fatty acids in the biodiesel enhance the lubricity of the fuel. In addition, Fazal et al. (2013) and Geller and Goodrum (2004) have pointed out that the higher DU and longer CCL can play an important role to enhance lubrication properties of fuel.

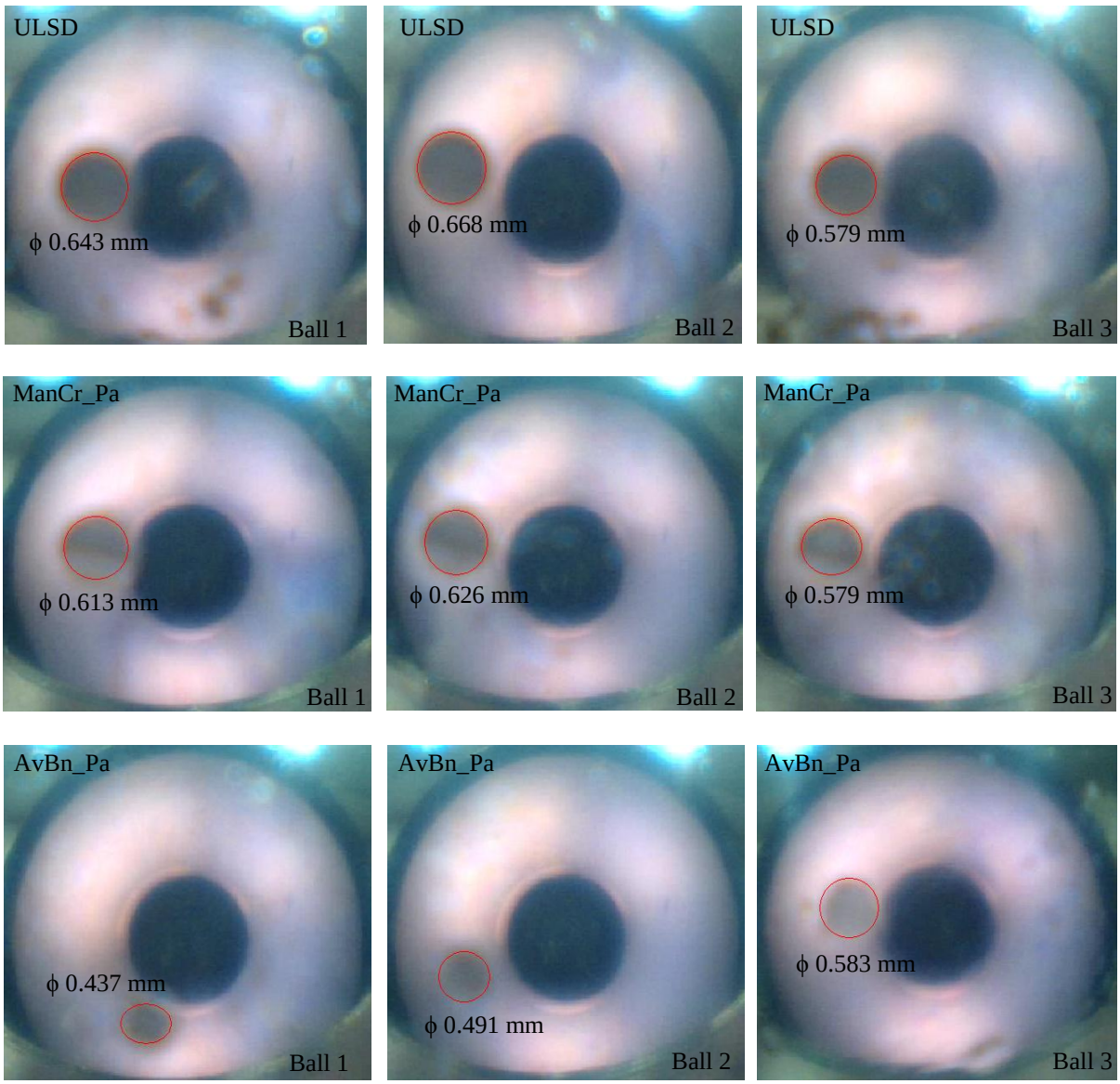

Figure 7.7: Optical microscope scanning image for WSD of the three stationary balls

Table 7.3: Summary of wear characteristics of the tested fuels

Tested balls	ULSD				ManCr_Pa				AvBn_Pa			
	Major WSD mm	Minor WSD mm	Mean WSD mm	Area mm^2	Major WSD mm	Minor WSD mm	Mean WSD mm	Area mm^2	Major WSD mm	Minor WSD mm	Mean WSD mm	Area mm^2
Ball 1	0.65	0.64	0.64	0.32	0.63	0.60	0.61	0.30	0.50	0.37	0.44	0.15
Ball 2	0.68	0.66	0.67	0.35	0.63	0.62	0.63	0.31	0.51	0.47	0.49	0.19
Ball 3	0.60	0.56	0.58	0.26	0.61	0.55	0.58	0.26	0.61	0.60	0.58	0.28
	Mean WSD =		0.63 mm		Mean WSD =		0.61 mm		Mean WSD =		0.51 mm	

This study found a mean WSD of 0.61 mm for ManCr_Pa and 0.51 mm for AvBn_Pa biodiesel blends. The results reveal that the AvBn_Pa blend shows excellent wear reduction (about 19.20%) characteristics compared to ULSD, whereas the ManCr_Pa blend demonstrates only 3.80% less WSD compared to ULSD. This could be due to the higher content of aliphatic acid ($C_nH_{2n+1}COOH$) in the AvBn_Pa blend enhancing the lubricating properties to reduce friction and wear by creating a thin lubricating film between the metal surfaces. This has already been agreed by many researchers such as Habibullah et al. (2015b), Fazal et al. (2013) and Syahrullail et al. (2013). In addition, the longer CCL of biodiesel contributes to thickening of the lubricating film which creates a more protected surface area on the metal contact surface as reported by Havet et al. (2001). In this study, Avocado and Bush nut biodiesels have a high saponification number of about 200.90 and 196.23, respectively which implies longer CCL compared to other biodiesels as discussed in Chapter 4. The mean wear scan area for AvBn_Pa is 0.21 mm^2 whereas it is 0.31 mm^2 for ULSD and 0.28 mm^2 for ManCr_Pa which implies AvBn_Pa has provided more protection to the contact surfaces (about 32.20% more compared to ULSD).

7.5. Flash Temperature Parameter (FTP) Analysis

The FTP is the minimum temperature below which the fuels can sustain their lubricating properties which implies the capability of the fuel to create a lubricating film on the metal contact surface. The higher magnitude of FTP denotes a lower potential for the scuffing phenomenon which occurs at high temperature at TDC (top dead centre) due to inadequate lubrication. The engine performance significantly decreases due to this effect as reported by Shuster et al. (2000). It also implies the stability of the lubrication properties and the lower potential for film breakdown at variuos operating conditions as reported by Habibullah et al. (2015a). The FTP values of the tested fuels were calculated using Equation (3.21). Figure 7.8 illustrates the correlation of FTP and WSD of the tested fuels. The figure shows FTPs of 76.38 °C for ULSD, 80.61 °C for ManCr_Pa and 102.96 °C for AvBn_Pa. The results reveal that FTP increases with the decrease of WSD of the fuel. The FTP value of 102.96 °C for AvBn_Pa implies that the fuel is capable of sustaining its lubricating properties below this temperature. This higher magnitude of FTP indicates about 35% more lubricating film reliability by the AvBn_Pa blend compared to ULSD which could enhance the sustainability of the engine health. Thus AvBn_Pa can withstand higher temperatures before scuffing takes place and the lubricating film breaks down in the contact.

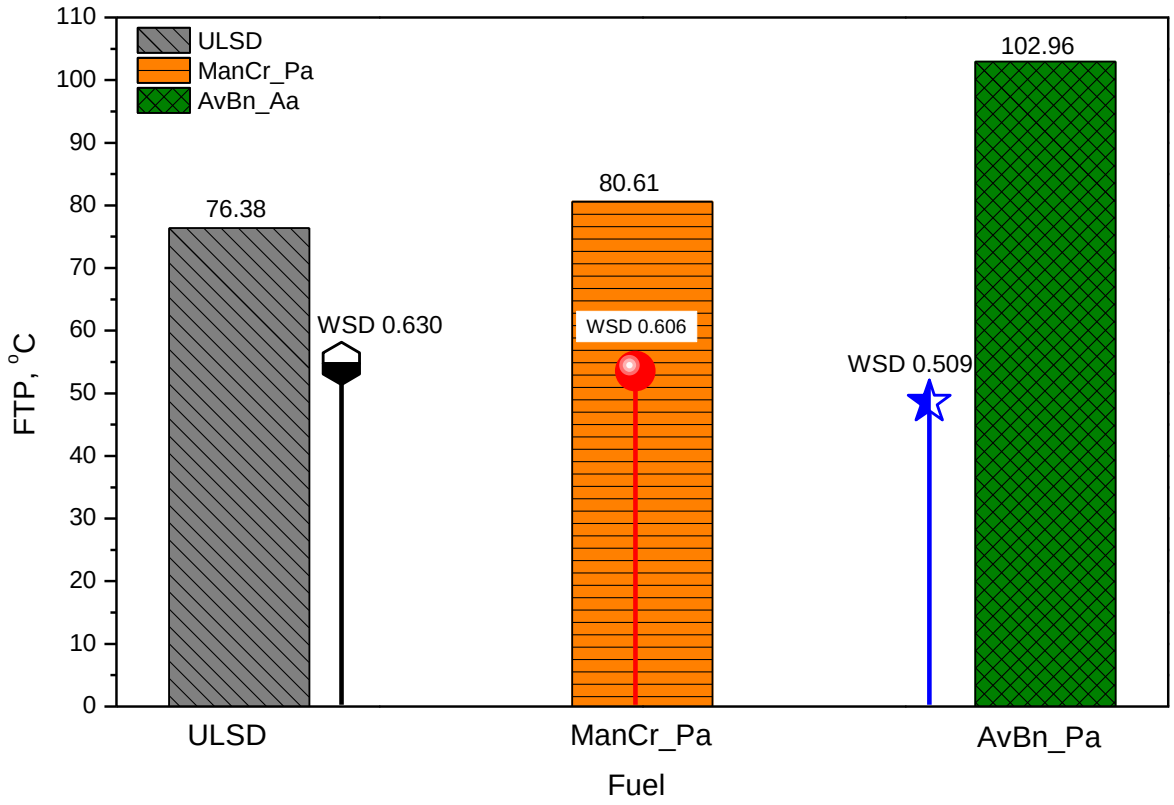

Figure 7.8: Correlation of FTP and WSD of the tested fuels

7.6. Wear Debris and Surface Morphology by SEM/EDX

7.6.1. Evaluation of filtered wear debris by SEM/EDX

Wear debris analysis is one of the key techniques to evaluate wear particle counts and measure their sizes for the tested fuels. This study was conducted using the wear debris analysis by SEM/EDX on the filtered metal debris samples which were collected by filtering the oil from the four-ball tribotester. In the analysis of different spots on the filter paper, mainly iron (Fe), chromium (Cr), silicon (Si), carbon (C) and oxygen (O) were found and recorded in average percentages of weight and atomic concentration. The results of the wear debris analysis in this experiment are presented in Table 7.4 and Figure 7.9. The results reveal that the maximum particle concentration was found for ULSD and the minimum was for the AvBn_Pa. This indicates that highest friction and wear occurred for ULSD and these were the lowest for AvBn_Pa. The average particle size of the wear debris was measured for each fuel. The particle sizes found were in the ranges of about 1.75 to 13.70 µm for ULSD, 1.71 to 15.50 µm for ManCr_Pa and 3.57 to 13.00 µm for AvBn_Pa (Figure 7.10). The larger particle sizes of the

wear debris can break down the lubricant film and cause adhesive wear on the metal surfaces which has also been reported by Habibullah et al. (2015b).

Table 7.4: Wear debris analysis of the filtering particles by SEM/EDX

Element	ULSD		ManCr_Pa		AvBn_Pa	
	Weight %	Atomic %	Weight %	Atomic %	Weight %	Atomic %
Fe	22.90	6.74	16.57	4.44	8.97	2.27
C	64.87	81.98	66.11	79.85	65.24	75.26
O	12.03	11.21	17.23	15.65	25.84	22.47
Cr	0.59	0.21	-	-	-	-
Si	-	-	0.27	0.14	-	-
Particle size, µm	1.75-13.70		1.41-15.50		3.57-13.00	

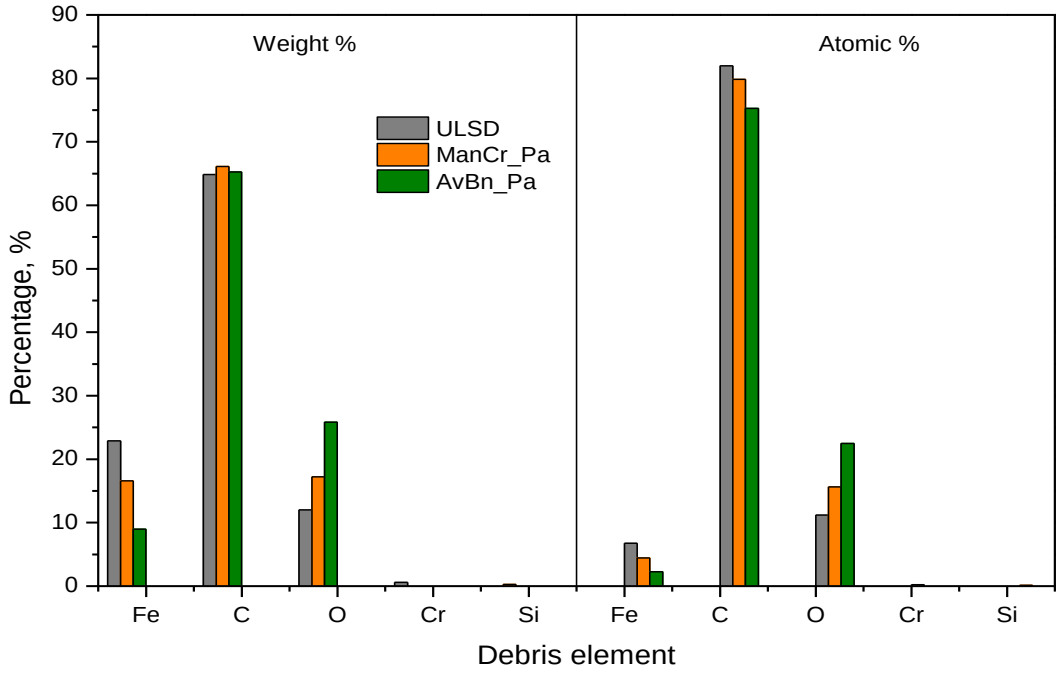

Figure 7.9: Filtered wear debris analysis by SEM/EDX

Figure 7.9 illustrates the particle concentrations in both weight and atomic percentage from the SEM/EDX analysis. The figure shows that higher Fe and lower C and O concentrations were found for ULSD compared to the other fuels which implies ULSD caused more metal surface wear. On the other hand, C and O concentrations were found to be higher for the biodiesels compared to ULSD. In addition, about 0.59% wt. Cr and 0.27% wt. Si were identified for ULSD and ManCr_Pa, respectively. Similar results were also reported by Mosarof et al. (2016c) and Habibullah et al. (2015b). The results reveal that the higher O concentration in AvBn_Pa blend produced more oxides on the metal surfaces which enhanced the lubricity of the fuel as agreed by Lu et al. (2005).

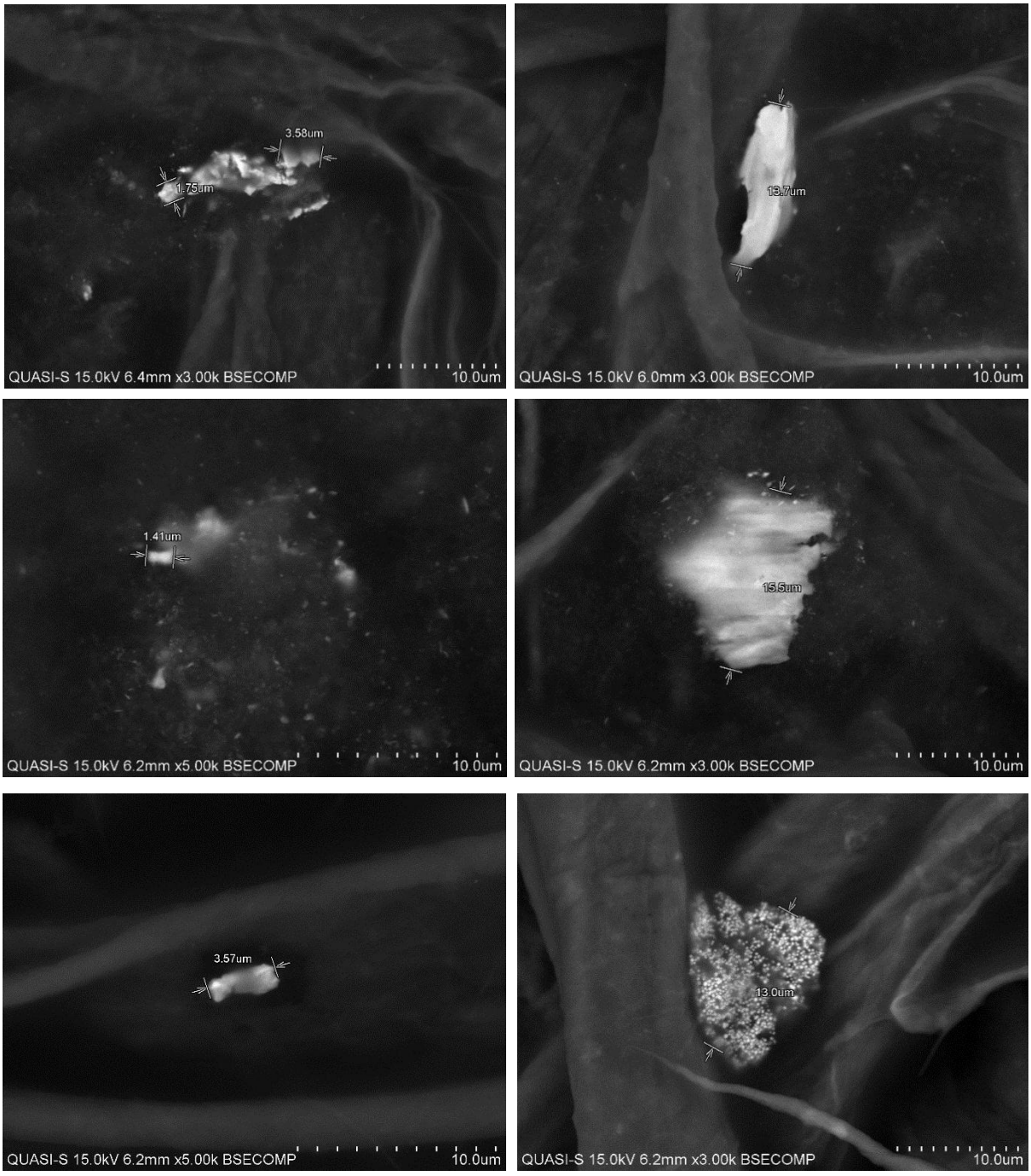

Figure 7.10: Minimum and maximum particle sizes of filtered wear debris by SEM/EDX microscopy

7.6.2. Wear surface analysis by SEM/EDX

The wear surface morphology of the stationary balls was evaluated using scanning electron microscopy (SEM) and the images of scar-worn surfaces are presented in Figure 7.11. The results reveal that significant surface deformation and cracks were identified for ULSD and the ManCr_Pa blend. Lots of micro cracks and corrosive delamination were also identified on the metal surfaces for ULSD and ManCr_Pa. The surface morphology reveals that the metal layers

were removed from the worn surface by the rotating balls in their sliding direction as shown in Figure 7.11. Adhesive wear was identified on the sliding surfaces due to the greater wear debris particle size as discussed above. The surface damage was identified to be more than 20 μm which implied this effect (Mosarof et al., 2016b).

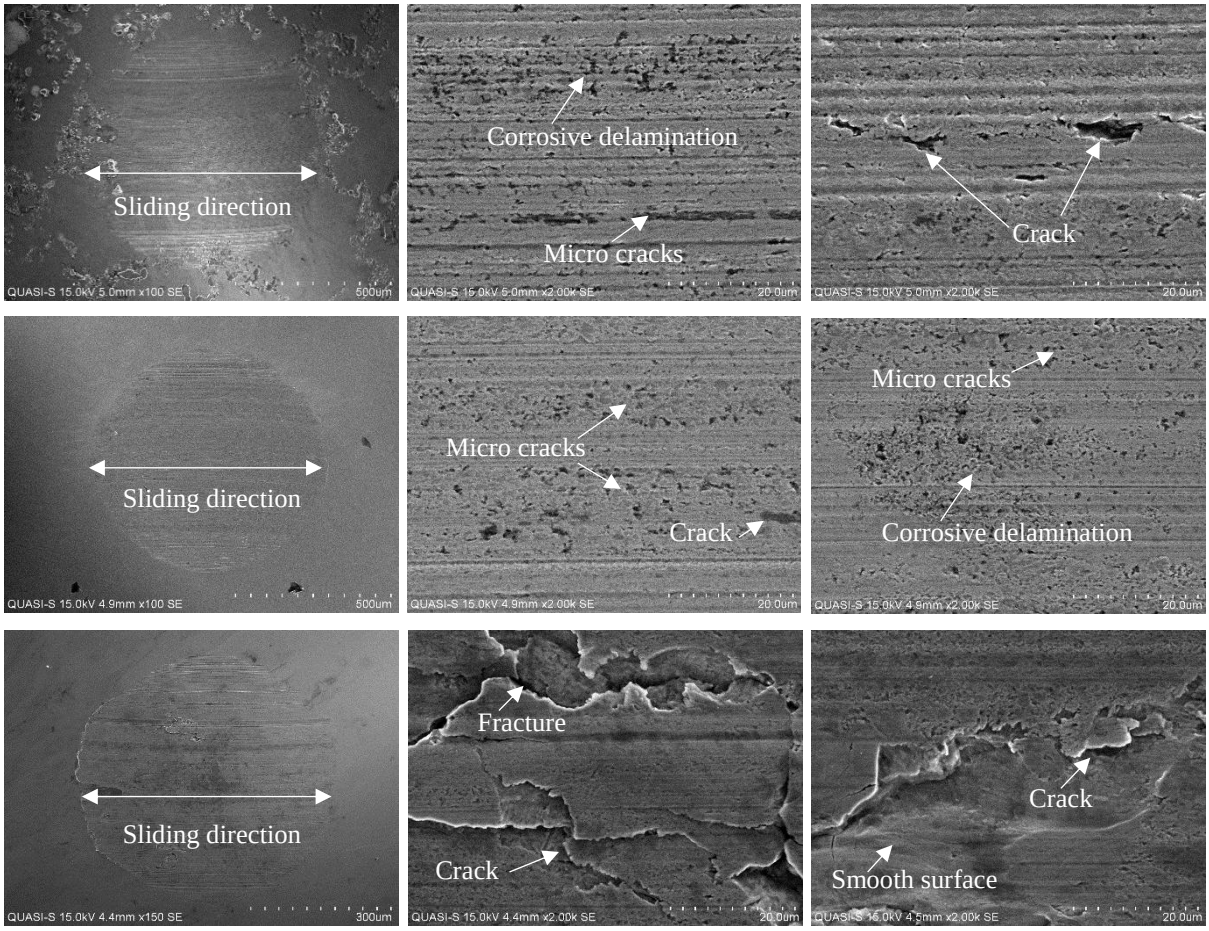

Figure 7.11: SEM worn surface images for ULSD, ManCr_Pa and AvBn_Pa fuels

The AvBn_Pa blend exhibits smaller worn surfaces (300 μm) whereas ULSD and ManCr_Pa had 500 μm worn surfaces as shown in Figure 7.11. In addition, bigger fractures and fewer cracks were identified for AvBn_Pa but lubricating film protected smooth surface was observed in major portions of the metal surface. This result is expected due to the longer CCL and DU and activated ester creates a monolayer film on the metal surface. On the contrary, higher oxygen content produced more metal oxides which enhance the lubrication film on the sliding surface. Hence, reduce friction and wear between the contact surfaces for AvBn_Pa blend.

The EDX analysis of the metal surfaces was conducted for all tested balls and identified Fe, C, O, Si, and Cr by both weight and atomic percentage. The results reveal a lower C content on the ball surfaces of about 4.44 wt.% for ULSD with 4.69 wt.% C for ManCr_Pa, and a high C of about 7.56 wt.% for AvBn_Pa. This higher percentage of C reinforces the conclusion of greater lubricating film stability on the metal surfaces which help to reduce friction and wear on the metal contact surfaces for the AvBn_Pa blend. In all aspects, the AvBn_Pa mixture blend demonstrated better tribological behaviour compared to the other fuels.

7.7. Chapter Conclusion

The tribological study was conducted on the three better-performing fuels derived from the engine tests on a four-ball tribotester using the ASTM D4172 test standard. It can be concluded from this study that the AvBn_Pa mixture blend shows less friction in both the run-in period and steady state conditions. This blend demonstrated more protected contact surface area and less mean WSD compared to other fuels. The higher FTP value of these blends exhibits a more reliable lubricating film that could sustain higher load and speeds without reaching the scuffing stage. The AvBn_Pa blend exhibits overall better lubrication performance on the four-ball tester which was further validated by the surface morphology analysis via SEM/EDX high-resolution microscopy. Thus, the AvBn_Pa blend is the best blend in all aspects of tribological characteristics for energy saving, engine reliability, and sustainable engine health.

Chapter 8

CONCLUSIONS AND RECOMMENDATIONS

This chapter sets out the conclusions based on the main findings from this study. The chapter also has some important recommendations for the further advancement of this research.

8.1. Conclusions

The world's future energy security and environmental sustainability are major concerns nowadays due to the very high consumption of liquid fuels. The history revealed that about one-third of the global energy demand has been met by liquid fuel which is mainly consumed by the fast growing transport sector. The high consumption of liquid fuel causes serious environmental pollution as well as uncertainty regarding future energy security. Biofuels could be one of the promising solutions to overcome these problems. This study investigated the prospect of the application of biofuels (including aviation biofuel produced from Mandarin peel and biodiesel produced from another five feedstocks) in CI engines to reduce emissions by improving combustion efficiency without the need for any modification to modern engines. This study produced aviation biofuel and biodiesels from industrial green waste and some Australian native feedstocks which could be prospective feedstocks for biofuel production. This study also experimentally investigated the engine performance, emissions, and the combustion phenomena of the newly developed biofuels. The tribological behaviour of the better performing fuels was also evaluated to assess the engine health using these fuels.

From the above discussion, it can be concluded that the aims laid out in **Chapter 1** have been satisfactorily achieved. The main conclusions that can be drawn from this study are as follows:

1) The study was undertaken in six main steps. This study assessed over 150 biofuel feedstocks and identified six most prospective feedstocks for detailed analysis to produce aviation biofuel and biodiesels. This study also assessed the prospect of aviation biofuel and biodiesel in the present context (**Chapter 2**).

2) The study developed experimental procedure and methodology (in **Chapter 3**) for evaluating new feedstocks for biodiesel production. This study also developed an Artificial Neural Network (Figure 3.5) which could help to design an experimental plan for investigation of performance, emissions and combustion parameters. The measurement techniques and the measured data are reliable and reproducible under the same examination conditions.

3) The fuel preparation techniques (including oil extraction and biofuel conversion) from the selected feedstocks were decided in **Chapter 4**. The transesterification reaction was conducted to convert triglyceride into methyl ester as biofuel. Maximum conversion rates of 96.55%, 98.21%, 86.72%, 97.79%, 98.37% and 95.11% were found for Mandarin, Crambe, Tamanu, Borage, Avocado and Bush nut, respectively. The fatty acid composition of the biodiesels was evaluated using the AOCS Ce 1a-13 standard methods. The FAMEs results of all the biodiesels satisfied the European standard EN 14214 requirements except for Mandarin biofuel which contains about 2.50% ester. The overall compositions of Mandarin biofuel were identified by GC analysis using the ISO 11024 standard. The results revealed that it contains 92 to 97% gasoline range of hydrocarbon which indicates a high potential as an aviation biofuel. The characteristics of this new fuel are similar to that of commercial jet fuel-A in addition to having a 4.34% higher CV (44.66 MJ/kg), higher FP (52 °C), lower viscosity, and being a self-oxygenated and is sulphur free aviation biofuel. The other properties of this biofuel were satisfactory within the range of standard jet fuel. The aviation biofuel developed from this new feedstock could be a promising alternative jet fuel for the aviation sector.

   The biodiesels (other than aviation biofuel from Mandarin rind) have satisfactory fuel properties within the acceptable range of the ASTM D6751 and EN 14214 standards. This study revealed biodiesels with high CVs of 40.63 MJ/kg with 10.49% O_2 content for Crambe and 40.00 MJ/kg with 11.75% O_2 for Avocado (CV) and a lower CV for Tamanu of 38.54 MJ/kg. The higher O_2 content reinforces a better combustion quality of the fuel. The physical behaviour of the developed biofuels was analysed and found to have similar trends to ULSD at varying temperatures. They could be used in a wide variety of weather conditions. The tested fuel samples were prepared by blending 5% to 20% by volume with ULSD for each biodiesel. Four ternary mixture blends, namely ManCr_Pa, TaMan_Pa, BoMan_Pa and AvBn_Pa were prepared by considering key research strategies such as

more oxygenated, lower density, viscosity with close CV to ULSD) to compare performance, emissions, and combustion with B5 blends and ULSD. The study found that the developed mixture blends show better results compared to each B5 blend in terms of performance, emissions and combustion characteristics.

4) The prepared fuel samples were examined in a DI diesel engine to evaluate engine performance and emissions for varying blend proportions, engine speeds and loads at steady state engine operating conditions (**Chapter 5**). The Mandarin aviation biofuel was also tested in the same lean combustion engine to investigate the pollutant formation due to non-availability of aviation engine test facilities. The study reveals that Mandarin biofuel blends demonstrate excellent comparative results with other blends due to their higher CV (44.66 MJ/kg) and closer density (838.00 kg/m^3) to ULSD (832.00 kg/m^3). On the other hand, Crambe, Avocado, Borage and Bush nut biodiesel blends exhibit similar performance throughout the range of engine test conditions. These later biodiesels could be used by blending up to 20% in a modern diesel engine with insignificant BP drop but about 5% to 10% more fuel consumption and around 2% to 7% lower thermal efficiency compared to ULSD. The BTE slightly decreases with the increase in biodiesel blend, and maximum BTE was achieved at 1600 rpm and 75% load for each fuel. On the other hand, Tamanu biodiesel demonstrates poor performance compared to ULSD and the other biodiesel blends due to its lower CV, and higher density and viscosity. This fuel can be used as a bio-lubricant due to the higher dynamic viscosity which is about 6.87 mPa.s. Between the mixture blends, MaCr_Pa and AvBn_PA mixture blends show better performance compared to other mixtures (as detailed below).

   Overall, BP increases with the increase in engine speed and load but decreases with the increase of the percentage of blended biodiesel. Additionally, BSFC increases with the increase of biodiesel blend percentage and decreases with the increase of engine load due to the lower CV of the biodiesels. By comparing with ULSD and other biodiesels, Mandarin and Borage show closer BP and BSFC at variable engine speeds and load conditions but Borage demonstrates better BTE compared to other biodiesel blends. By way of contrast, its BTE increases with the increase in engine load. Comparing Mandarin, Borage and Avocado biodiesels with ULSD, Avocado shows better BTE and closer BP and BSFC due to lower density and viscosity, higher CV and higher O_2 content which enhances the combustion efficiency of the Avocado biodiesel.

The biodiesels exhibited excellent capability to reduce toxic gas emissions such as CO, HC, and PM which were mainly formed due to incomplete combustion of rich air-fuel mixtures. This study revealed that the biodiesel blends of up to 20% can reduce up to 50% of CO, 47% of HC and 60% of PM emissions compared to ULSD. However, the emissions reduction was also impacted by several factors such as speed, load, fuel quality, operating condition, and incomplete combustion due to lack of sufficient oxygen. The self-oxygenation of biodiesels has a significant impact on reducing emissions by improving combustion quality of rich air-fuel mixtures. However, the higher in-cylinder peak temperature due to CO oxidation and higher BSFC increases NO_x emissions during combustion of biodiesel blends. In addition, biodiesel combustion slightly increases CO_2 emissions (CO converted to CO_2). Among biodiesel blends, B5 demonstrates better performance and B20 exhibits higher emissions reductions for each biodiesel.

This study identified that the most efficient mixture is a ternary blend which demonstrated better performance and more reduction of emissions compared to the pure B5 blend. The results reveal that the mixture blends improved efficiency with about 0.7% more BP, and up to 2.2% less BSFC which improved BTE by about 3.5% compared to B5 blends due to the improvement of fuel properties. The mixture blends demonstrated excellent capability to reduce emissions by up to 19.0% CO, up to 59.0% HC, and around 28.0% PM compared to B5 blends by improving combustion efficiency. These mixture blends mitigate one of the drawbacks of biodiesel combustion by reducing NO_x emissions (by about 1.2% to 8.8%) compared to B5 blends through reducing the cylinder peak temperature, but still result in about 10.0% to 20.0% higher NO_x as compared to ULSD. Among the mixture blends ManCr_Pa and AvBn_Pa blend shows closer performance with ULSD with significant emission reduction. For example, ManCr_Pa can reduce up to 39% CO emission, about 62% HC and around 21% PM compared to ULSD. On the other hand, AvBn_Pa can reduce up to 35% CO, 30% HC and 40% PM compared to ULSD. The maximum PM reduction of about 44% was recorded for BoMan_Pa blend. By comparing the performance and emission parameters, the study concluded that ManCr_Pa and AvBn_Pa mixture blends are a more efficient, fuel economy and environmentally sustainable biodiesel blend for the transport sector.

5) The combustion analysis was conducted on the better performing fuel blends (ManCr_Pa and AvBn_Pa) to analyse CP, HRR, ID and CD at the power stroke (**Chapter 6**). The study presented a relationship of CP and HRR to describe the combustion phenomena of the tested fuels which show CP increases with the increase in engine speed and load. The ULSD exhibits higher peak HRR at the rapid premixed combustion phase at variable speed. In contrast, ManCr_Pa and AvBn_Pa mixture blends show higher HRR with longer duration of the diffusion combustion phase which is the most powerful phase in combustion. The mixture blends also demonstrate closer combustion behavior with ULSD at full load condition and higher HRR at partial load. A knocking characteristic is identified for the ManCr_Pa blend at full load condition. By comparing the two mixture blends, AvBn_Pa demonstrates better combustion behaviour compared to ManCr_Pa blend due to the higher oxygen content, shorter ID and longer CD.

6) The tribological characteristics of the better performing blends were evaluated and compared with ULSD for assessing engine health (**Chapter 7**). This study was conducted using a four-ball tribotester under the ASTM D4172 standard. The study revealed that the AvBn_Pa mixture blend shows less friction in both the run-in period and steady state conditions and less mean WSD compared to other fuels. The higher FTP value of these blends implies a more reliable lubricating film and less possibility of scuffing occurring at TDC which have a significant impact on engine performance. The AvBn_Pa blend exhibits overall better self-lubrication performance which was further validated by the analysis of the metal surface morphology and filter debris analysis via SEM/EDX high-resolution microscopy.

This study reached the conclusion that the AvBn_Pa mixture blend is the best blend in all aspects of engine performance, emissions, combustion and tribology for the transport sector.

8.2. Recommendations for Future Work

This study satisfactorily achieved the objectives and identified new sources of aviation biofuel and biodiesel for the transport sector. The following suggestions and recommendations can be made for future research:

- The aviation biofuel satisfied the main commercial jet fuel properties, however, the octane number of this new aviation fuel is unknown which should be identified before any

application is made in an aviation engine. Due to the experimental limitation of the lack of an aviation engine, the study examined the performance of the newly developed aviation biofuel blends in a CI engine (as it is a lean combustion engine) to predict their performances and emissions formation. This study recommends the testing of this new aviation fuel in an actual aviation engine.

- Further analysis on the poor performing Tamanu biodiesel as a prospective bio-lubricant source should be undertaken as it has higher dynamic viscosity.

- This study recommends further assessment of engine performance and emissions by varying injecting pressure and injection timing of the fuel. Engine vibration and noise levels should be measured for better-performing blends as well as other blends.

- The combustion phenomena of these biodiesel blends could be effectively assessed by capturing combustion images from an optical engine to identify more affecting parameters to enhance combustion efficiency.

- Advanced turbulence combustion modelling by computational fluid dynamics (CFD) analysis using ANSYS IC Engine software should be developed to assess combustion and pollutant formation phenomena in detail.

- This study only dealt with the prospective newly developed biofuel by considering technical issues. Detailed economic analysis is recommended on the Mandarin aviation biofuel, the Crambe, Borage, Avocado and Bush nut biodiesel blends up to B20 and the better-performing mixture blends.

References

ABBASZAADEH, A., GHOBADIAN, B., OMIDKHAH, M. R. & NAJAFI, G. 2012. Current biodiesel production technologies: a comparative review. *Energy Conversion and Management,* 63**,** 138-148.

ABEDIN, M. J., MASJUKI, H. H., KALAM, M. A., SANJID, A., RAHMAN, S. M. A. & FATTAH, I. M. R. 2014. Performance, emissions, and heat losses of palm and jatropha biodiesel blends in a diesel engine. *Industrial Crops and Products,* 59**,** 96-104.

ACHTEN, W., VERCHOT, L., FRANKEN, Y. J., MATHIJS, E., SINGH, V. P., AERTS, R. & MUYS, B. 2008a. *Jatropha* bio-diesel production and use. *Biomass and bioenergy,* 32**,** 1063-1084.

ACHTEN, W. M. J., VERCHOT, L., FRANKEN, Y. J., MATHIJS, E., SINGH, V. P., AERTS, R. & MUYS, B. 2008b. Jatropha bio-diesel production and use. *Biomass and Bioenergy,* 32**,** 1063-1084.

AES 2016. Department of Industry, Innovation and Science, Office of the Chief Economist, Australian Energy Statistics, [cited 4 November 2016]; Available from: <http://www.industry.gov.au/Office-of-the-Chief-Economist/Publications/Pages/Australian-energy-statistics.aspx>.

AFGAN, N. H. & CARVALHO, M. G. 2004. Sustainability assessment of hydrogen energy systems. *International Journal of Hydrogen Energy,* 29**,** 1327-1342.

AGARWAL, A. K. 2007. Biofuels (alcohols and biodiesel) applications as fuels for internal combustion engines. *Progress in Energy and Combustion Science,* 33**,** 233-271.

AGARWAL, A. K., GUPTA, T. & KOTHARI, A. 2011. Particulate emissions from biodiesel vs diesel fuelled compression ignition engine. *Renewable and Sustainable Energy Reviews,* 15**,** 3278-3300.

AGARWAL, D., SINHA, S. & AGARWAL, A. K. 2006. Experimental investigation of control of NOx emissions in biodiesel-fueled compression ignition engine. *Renewable Energy,* 31**,** 2356-2369.

AL-SOHAIBANI, S. & MURUGAN, K. 2012. Anti-biofilm activity of Salvadora persica on cariogenic isolates of Streptococcus mutans: in vitro and molecular docking studies. *Biofouling,* 28**,** 29-38.

ALCANTARA, R., AMORES, J., CANOIRA, L., FIDALGO, E., FRANCO, M. J. & NAVARRO, A. 2000. Catalytic production of biodiesel from soy-bean oil, used frying oil and tallow. *Biomass and Bioenergy,* 18**,** 515-527.

AMIN, S. 2009. Review on biofuel oil and gas production processes from microalgae. *Energy Conversion and Management,* 50**,** 1834-1840.

AMIRI, H., KARIMI, K. & ZILOUEI, H. 2014. Organosolv pretreatment of rice straw for efficient acetone, butanol, and ethanol production. *Bioresource Technology,* 152**,** 450-456.

AN, H., YANG, W. M., MAGHBOULI, A., LI, J., CHOU, S. K. & CHUA, K. J. 2013. Performance, combustion and emission characteristics of biodiesel derived from waste cooking oils. *Applied Energy,* 112**,** 493-499.

AN, H., YANG, W. M., MAGHBOULI, A., LI, J. & CHUA, K. J. 2014. A skeletal mechanism for biodiesel blend surrogates combustion. *Energy Conversion and Management,* 81**,** 51-59.

ARAPOGLOU, D., VARZAKAS, T., VLYSSIDES, A. & ISRAILIDES, C. 2010. Ethanol production from potato peel waste (PPW). *Waste management,* 30**,** 1898-1902.

ARCAKLIOĞLU, E. & ÇELıKTEN, İ. 2005. A diesel engine's performance and exhaust emissions. *Applied Energy,* 80**,** 11-22.

ARUL MOZHI SELVAN, V., ANAND, R. & UDAYAKUMAR, M. 2009. Combustion characteristics of diesohol using biodiesel as an additive in a direct injection compression ignition engine under various compression ratios. *Energy & Fuels,* 23**,** 5413-5422.

ASHWATH, N. 2010. *Evaluating biodiesel potential of Australian native and naturalised plant species,* Rural Industries Research and Development Corporation (RIRDC Publication No. 10/216), Australia.

ATABANI, A., SILITONGA, A., ONG, H., MAHLIA, T., MASJUKI, H., BADRUDDIN, I. A. & FAYAZ, H. 2013a. Non-edible vegetable oils: A critical evaluation of oil extraction, fatty acid compositions, biodiesel production, characteristics, engine performance and emissions production. *Renewable and Sustainable Energy Reviews,* 18**,** 211-245.

ATABANI, A. E. & CÉSAR, A. D. S. 2014. Calophyllum inophyllum L.-A prospective non-edible biodiesel feedstock. Study of biodiesel production, properties, fatty acid composition, blending and engine performance. *Renewable and Sustainable Energy Reviews,* 37**,** 644-655.

ATABANI, A. E., MOFIJUR, M., MASJUKI, H. H., BADRUDDIN, I. A., KALAM, M. A. & CHONG, W. T. 2014. Effect of Croton megalocarpus, Calophyllum inophyllum, Moringa oleifera, palm and coconut biodiesel–diesel blending on their physico-chemical properties. *Industrial Crops and Products,* 60**,** 130-137.

ATABANI, A. E., SILITONGA, A. S., BADRUDDIN, I. A., MAHLIA, T. M. I., MASJUKI, H. H. & MEKHILEF, S. 2012. A comprehensive review on biodiesel as an alternative energy resource and its characteristics. *Renewable and Sustainable Energy Reviews,* 16**,** 2070-2093.

ATABANI, A. E., SILITONGA, A. S., ONG, H. C., MAHLIA, T. M. I., MASJUKI, H. H., BADRUDDIN, I. A. & FAYAZ, H. 2013b. Non-edible vegetable oils: A critical evaluation of oil extraction, fatty acid compositions, biodiesel production, characteristics, engine performance and emissions production. *Renewable and Sustainable Energy Reviews,* 18**,** 211-245.

ATADASHI, I., AROUA, M. & AZIZ, A. A. 2010. High quality biodiesel and its diesel engine application: a review. *Renewable and Sustainable Energy Reviews,* 14**,** 1999-2008.

AWAD, O. I., MAMAT, R., ALI, O. M., YUSRI, I. M., ABDULLAH, A. A., YUSOP, A. F. & NOOR, M. M. 2016. The effect of adding fusel oil to diesel on the performance and the emissions characteristics in a single cylinder CI engine. *Journal of the Energy Institute***,** 1-15 (In press).

AYDıN, S. & SAYıN, C. 2014. Impact of thermal barrier coating application on the combustion, performance and emissions of a diesel engine fueled with waste cooking oil biodiesel–diesel blends. *Fuel,* 136**,** 334-340.

AZAD, A. K., AMEER UDDIN, S. M. & ALAM, M. M. 2012. A Comprehensive Study of DI Diesel Engine Performance with Vegetable Oil: An Alternative Bio-fuel Source of Energy. *International Journal of Automotive and Mechanical Engineering,* 5**,** 576-586.

AZAD, A. K. & PRINCE, M. R. I. 2012. Preparation of bio-diesel from jatropha curcus seeds oil: performance and emission study of a 4-stroke single cylinder biodiesel fueled engine. *International Journal of Energy and Technology,* 4**,** 1-6.

AZAD, A. K., RASUL, M. G. & GIANNANGELO, B. Diesel Engine Performance and Emission Study Using Soybean Biodiesel Blends with Fossil Diesel. The Seventh International Exergy, Energy and Environment Symposium 2015a Valenciennes, France. 1-10.

AZAD, A. K., RASUL, M. G., GIANNANGELO, B. & ISLAM, R. 2015b. Comparative study of diesel engine performance and emission with soybean and waste oil biodiesel fuels. *International Journal of Automotive & Mechanical Engineering,* 12**,** 2866-2881.

AZAD, A. K., RASUL, M. G., KHAN, M. M. K., AHASAN, T. & AHMED, S. F. 2014a. Energy Scenario: Production, Consumption and Prospect of Renewable Energy in Australia. *Journal of Power and Energy Engineering,* 2**,** 19-25.

AZAD, A. K., RASUL, M. G., KHAN, M. M. K. & SHARMA, S. C. Review of biodiesel production from microalgae: a novel source of green energy. International Green Energy Conference, 2014b Tainjin, China. 879-888.

AZAD, A. K., RASUL, M. G., KHAN, M. M. K. & SHARMA, S. C. Review of non-edible biofuel resources in Australia for second generation (2G) biofuel conversion International Green Energy Conference, 2014c Tainjin, China. 867-878.

AZAD, A. K., RASUL, M. G., KHAN, M. M. K. & SHARMA, S. C. Socio-economic prospect of second generation bio-fuel in Australia: A Review International Conference on Clean Energy 2014d Istanbul, Turkey. 210-221.

AZAD, A. K., RASUL, M. G., KHAN, M. M. K., SHARMA, S. C. & BHUIYA, M. M. K. 2016a. *Biodiesel from Queensland bush nut (Macadamia Integrifolia)*, ELSEVIER.

AZAD, A. K., RASUL, M. G., KHAN, M. M. K., SHARMA, S. C., BHUIYA, M. M. K. & MOFIJUR, M. 2016b. A Review on Socio-economic Aspects of Sustainable Biofuels. *International Journal of Global Warming,* 10**,** 32-54.

AZAD, A. K., RASUL, M. G., KHAN, M. M. K., SHARMA, S. C. & HAZRAT, M. A. 2015c. Prospect of biofuels as an alternative transport fuel in Australia. *Renewable and Sustainable Energy Reviews,* 43**,** 331-351.

AZAD, A. K., RASUL, M. G., KHAN, M. M. K., SHARMA, S. C., MOFIJUR, M. & BHUIYA, M. M. K. 2016c. Prospects, feedstocks and challenges of biodiesel production from beauty leaf oil and castor oil: A nonedible oil sources in Australia. *Renewable and Sustainable Energy Reviews,* 61**,** 302-318.

AZAD, A. K. & UDDIN, S. M. A. 2013. Performance study of a diesel engine by first generation bio-fuel blends with fossil fuel: An experimental study. *Journal of Renewable and Sustainable Energy,* 5**,** 013118(1-12).

BAA. *Biofuels Association of Australia. Biodiesel production facilities in Australia; 2013 [cited 21 January 2014]; Available from: <http://www.biofuelsassociation.com.au/biodiesel-production-facilities-in-australia>.*

BAGAL, N. L., RUTLAND, C. J., FOSTER, D. E. & NARAYANASWAMY, K. 2009. CO Emission Model for an Integrated Diesel Engine, Emissions, and Exhaust Aftertreatment System Level Model. *SAE Int. J. Engines,* 2**,** 1460-1472.

BALAT, M. 2011. Potential alternatives to edible oils for biodiesel production-A review of current work. *Energy Conversion and Management,* 52**,** 1479-1492.

BALL, A., AHMAD, S., MCCLUSKEY, C., PHAM, P., AHN, I., NGUYEN, T. & NOWAKOWSKI, D. 2016. Bureau of Resources and Energy Economics. Australian Energy Update 2016; [citeed on 4 November 2016]; Available from: <http://www.industry.gov.au/Office-of-the-Chief-Economist/Publications/Documents/aes/2016-australian-energy-statistics.pdf>.

BANAPURMATH, N., TEWARI, P. & GAITONDE, V. 2012. Experimental investigations on performance and emission characteristics of Honge oil biodiesel (HOME) operated compression ignition engine. *Renewable Energy,* 48**,** 193-201.

BANAPURMATH, N., TEWARI, P. & HOSMATH, R. 2008a. Performance and emission characteristics of a DI compression ignition engine operated on Honge, Jatropha and sesame oil methyl esters. *Renewable energy,* 33**,** 1982-1988.

BANAPURMATH, N. R., TEWARI, P. G. & HOSMATH, R. S. 2008b. Performance and emission characteristics of a DI compression ignition engine operated on Honge, Jatropha and sesame oil methyl esters. *Renewable Energy,* 33**,** 1982-1988.

BANDI, A. K. R., LEE, D. U., TIH, R. G., GUNASEKAR, D. & BODO, B. 2012. Phytochemical and Biological Studies of Ochna Species. *Chemistry & Biodiversity,* 9**,** 251-271.

BASHA, S. A., GOPAL, K. R. & JEBARAJ, S. 2009. A review on biodiesel production, combustion, emissions and performance. *Renewable and Sustainable Energy Reviews,* 13**,** 1628-1634.

BENAJES, J., MOLINA, S., GARCÍA, A. & MONSALVE-SERRANO, J. 2015. Effects of direct injection timing and blending ratio on RCCI combustion with different low reactivity fuels. *Energy Conversion and Management,* 99**,** 193-209.

BENAJES, J., MOLINA, S., GARCÍA, A., MONSALVE-SERRANO, J. & DURRETT, R. 2014. Performance and engine-out emissions evaluation of the double injection strategy applied to the gasoline partially premixed compression ignition spark assisted combustion concept. *Applied Energy,* 134**,** 90-101.

BENJUMEA, P., AGUDELO, J. R. & AGUDELO, A. S. F. 2010. Effect of the Degree of Unsaturation of Biodiesel Fuels on Engine Performance, Combustion Characteristics, and Emissions. *Energy & Fuels,* 25**,** 77-85.

BERMAN, P., NIZRI, S. & WIESMAN, Z. 2011. Castor oil biodiesel and its blends as alternative fuel. *Biomass and Bioenergy,* 35**,** 2861-2866.

BHUIYA, M., RASUL, M., KHAN, M., ASHWATH, N. & AZAD, A. 2015a. Prospects of 2nd generation biodiesel as a sustainable fuel—Part: 1 selection of feedstocks, oil extraction techniques and conversion technologies. *Renewable and Sustainable Energy Reviews*.

BHUIYA, M., RASUL, M., KHAN, M., ASHWATH, N. & AZAD, A. 2015b. Prospects of 2nd generation biodiesel as a sustainable fuel—Part: 1 selection of feedstocks, oil extraction techniques and conversion technologies. *Renewable and Sustainable Energy Reviews,* 55**,** 1109-1128.

BHUIYA, M., RASUL, M., KHAN, M., ASHWATH, N., AZAD, A. & MOFIJUR, M. 2015c. Optimisation of Oil Extraction Process from Australian Native Beauty Leaf Seed (Calophyllum Inophyllum). *Energy Procedia,* 75**,** 56-61.

BHUIYA, M., RASUL, M., KHAN, M. M. K., ASHWATH, N., AZAD, A. K. & MOFIJUR, M. 2015d. Optimisation of oil extraction process from Australian native beauty leaf seed (Calophyllum Inophyllum). *Energy Procedia,* 75**,** 56-61.

BLANCA, A.-L. & JUAN, L. T.-G. 2008. Second-generation biofuels and local bioenergy systems. *Biofuels, Bioproducts and Biorefining,* 2**,** 455-469.

BLOK, K. 2005. Enhanced policies for the improvement of electricity efficiencies. *Energy Policy,* 33**,** 1635-1641.

BOZBAS, K. 2008. Biodiesel as an alternative motor fuel: production and policies in the European Union. *Renewable and Sustainable Energy Reviews,* 12**,** 542-552.

BP 2016. Statistical Review of World Energy June 2016, [cited on 10 November' 2016]; Available from: <http://www.bp.com/content/dam/bp/pdf/energy-economics/statistical-review-2016/bp-statistical-review-of-world-energy-2016-full-report.pdf>.

BRENNAN, L. & OWENDE, P. 2010. Biofuels from microalgae—A review of technologies for production, processing, and extractions of biofuels and co-products. *Renewable and Sustainable Energy Reviews,* 14**,** 557-577.

BRUNET, R., CARRASCO, D., MUÑOZ, E., GUILLÉN-GOSÁLBEZ, G., KATAKIS, I. & JIMÉNEZ, L. 2012. Economic and environmental evaluation of microalgae biodiesel

production using process simulation tools. *In:* IAN DAVID LOCKHART, B. & MICHAEL, F. (eds.) *Computer Aided Chemical Engineering.* Elsevier.
BUYUKKAYA, E. 2010. Effects of biodiesel on a DI diesel engine performance, emission and combustion characteristics. *Fuel,* 89**,** 3099-3105.
BUYUKKAYA, E., BENLI, S., KARAASLAN, S. & GURU, M. 2013. Effects of trout-oil methyl ester on a diesel engine performance and emission characteristics. *Energy Conversion and Management,* 69**,** 41-48.
CAMPBELL, M. N. 2008. Biodiesel: algae as a renewable source for liquid fuel. *Guelph Engineering Journal,* 1**,** 2-7.
CANAKCI, M., ERDIL, A. & ARCAKLIOĞLU, E. 2006. Performance and exhaust emissions of a biodiesel engine. *Applied energy,* 83**,** 594-605.
CANAKCI, M. & SANLI, H. 2008. Biodiesel production from various feedstocks and their effects on the fuel properties. *Journal of industrial microbiology & biotechnology,* 35**,** 431-441.
CAO, C.-Y. & ZHAO, Y.-H. 2013. Transesterification of castor oil to biodiesel using KOH/NaY as solid base catalyst. *International Journal of Green Energy,* 10**,** 219-229.
CARLUCCI, A. P., LAFORGIA, D., MOTZ, S., SARACINO, R. & WENZEL, S. P. 2014. Advanced closed loop combustion control of a LTC diesel engine based on in-cylinder pressure signals. *Energy Conversion and Management,* 77**,** 193-207.
CEFC. 2014. *Clean Energy Finance Corporation, Renewable energy. [cited 7 Janusary 2014]; Available from: <http://www.cleanenergyfinancecorp.com.au/renewable-energy.aspx?gclid=CNmrhuex67sCFeRKpgodIy0AOQ>*.
CHAKRABARTI, M., ALI, M., BAROUTIAN, S. & SALEEM, M. 2011. Techno-economic comparison between B10 of Eruca sativa L. and other indigenous seed oils in Pakistan. *Process Safety and Environmental Protection,* 89**,** 165-171.
CHANDEL, A. K., DA SILVA, S. S., CARVALHO, W. & SINGH, O. V. 2012. Sugarcane bagasse and leaves: foreseeable biomass of biofuel and bio-products. *Journal of chemical technology and biotechnology,* 87**,** 11-20.
CHEN, C.-Y., YEH, K.-L., AISYAH, R., LEE, D.-J. & CHANG, J.-S. 2011. Cultivation, photobioreactor design and harvesting of microalgae for biodiesel production: a critical review. *Bioresource Technology,* 102**,** 71-81.
CHEN, G.-Q., JIANG, Y. & CHEN, F. 2008. Variation of lipid class composition in *Nitzschia laevis* as a response to growth temperature change. *Food Chemistry,* 109**,** 88-94.
CHEN, Y.-H., CHIANG, T.-H. & CHEN, J.-H. 2012a. An optimum biodiesel combination: Jatropha and soapnut oil biodiesel blends. *Fuel,* 92**,** 377-380.
CHEN, Y.-H., HUANG, B.-Y., CHIANG, T.-H. & TANG, T.-C. 2012b. Fuel properties of microalgae (Chlorella protothecoides) oil biodiesel and its blends with petroleum diesel. *Fuel,* 94**,** 270-273.
CHERUBINI, F., BIRD, N. D., COWIE, A., JUNGMEIER, G., SCHLAMADINGER, B. & WOESS-GALLASCH, S. 2009. Energy- and greenhouse gas-based LCA of biofuel and bioenergy systems: Key issues, ranges and recommendations. *Resources, Conservation and Recycling,* 53**,** 434-447.
CHHETRI, A. & WATTS, K. 2013. Surface tensions of petro-diesel, canola, jatropha and soapnut biodiesel fuels at elevated temperatures and pressures. *Fuel,* 104**,** 704-710.
CHIARAMONTI, D., PRUSSI, M., BUFFI, M. & TACCONI, D. 2014. Sustainable bio kerosene: Process routes and industrial demonstration activities in aviation biofuels. *Applied Energy,* 136**,** 767-774.
CHISTI, Y. 2007. Biodiesel from microalgae. *Biotechnology advances,* 25**,** 294-306.

CHOI, I. S., LEE, Y. G., KHANAL, S. K., PARK, B. J. & BAE, H.-J. 2015. A low-energy, cost-effective approach to fruit and citrus peel waste processing for bioethanol production. *Applied Energy,* 140**,** 65-74.

CIFRE, P. G. & BADR, O. 2007. Renewable hydrogen utilisation for the production of methanol. *Energy Conversion and Management,* 48**,** 519-527.

COX, K., RENOUF, M., DARGAN, A., TURNER, C. & KLEIN-MARCUSCHAMER, D. 2014. Environmental life cycle assessment (LCA) of aviation biofuel from microalgae, Pongamia pinnata, and sugarcane molasses. *Biofuels, Bioproducts and Biorefining,* 8**,** 579-593.

CROWE, B., ATTALAH, S., AGRAWAL, S., WALLER, P., RYAN, R., VAN WAGENEN, J., CHAVIS, A., KYNDT, J., KACIRA, M. & OGDEN, K. L. 2012. A comparison of Nannochloropsis salina growth performance in two outdoor pond designs: conventional raceways versus the ARID pond with superior temperature management. *International Journal of Chemical Engineering,* 2012**,** 1-9.

DA SILVA CÉSAR, A. & OTÁVIO BATALHA, M. 2010. Biodiesel production from castor oil in Brazil: A difficult reality. *Energy Policy,* 38**,** 4031-4039.

DANTAS, M., ALBUQUERQUE, A., SOLEDADE, L. E., QUEIROZ, N., MAIA, A., SANTOS, I. M., SOUZA, A., CAVALCANTI, E. H., BARRO, A. & SOUZA, A. 2011. Biodiesel from soybean oil, castor oil and their blends. *Journal of thermal analysis and calorimetry,* 106**,** 607-611.

DEMIRBAS, A. 2005. Biodiesel production from vegetable oils via catalytic and non-catalytic supercritical methanol transesterification methods. *Progress in Energy and Combustion Science,* 31**,** 466-487.

DEMIRBAS, A. 2007. Importance of biodiesel as transportation fuel. *Energy Policy,* 35**,** 4661-4670.

DEMIRBAS, A. 2009a. Biodiesel from waste cooking oil via base-catalytic and supercritical methanol transesterification. *Energy Conversion and Management,* 50**,** 923-927.

DEMIRBAS, A. 2010. Use of algae as biofuel sources. *Energy conversion and management,* 51**,** 2738-2749.

DEMIRBAS, A. 2011a. Biodiesel from oilgae, biofixation of carbon dioxide by microalgae: A solution to pollution problems. *Applied Energy,* 88**,** 3541-3547.

DEMIRBAS, A. 2011b. Competitive liquid biofuels from biomass. *Applied Energy,* 88**,** 17-28.

DEMIRBAS, A. & FATIH DEMIRBAS, M. 2011. Importance of algae oil as a source of biodiesel. *Energy Conversion and Management,* 52**,** 163-170.

DEMIRBAS, M. F. 2009b. Biorefineries for biofuel upgrading: A critical review. *Applied Energy,* 86**,** S151-S161.

DEMIRBAS, M. F. 2011c. Biofuels from algae for sustainable development. *Applied Energy,* 88**,** 3473-3480.

DOE 2015. Department of Environment, Australia's Emission Projections 2014-2015, [cited on 10 November 2016]; Available from: <https://www.environment.gov.au/system/files/resources/f4bdfc0e-9a05-4c0b-bb04-e628ba4b12fd/files/australias-emissions-projections-2014-15.pdf>.

EPA 2016. US Environmental Protection Agency, Global Greenhouse Gas Emission Data, [cited on 10 November' 2016], Available from: <https://www.epa.gov/ghgemissions/global-greenhouse-gas-emissions-data>.

EXXONMOBIL 2016. World jet fuel specifications, 2005 Edition [cited on 15th November 2016]; Available from: <http://www.exxonmobile.com/AviationGlobal/Files/WorldJetFuelSpecifications2005.pdf>.

FAKAS, S., PAPANIKOLAOU, S., GALIOTOU-PANAYOTOU, M., KOMAITIS, M. & AGGELIS, G. 2008. Organic nitrogen of tomato waste hydrolysate enhances glucose uptake and lipid accumulation in Cunninghamella echinulata. *Journal of applied microbiology,* 105**,** 1062-1070.

FALASCA, S., MIRANDA DEL FRESNO, C. & ULBERICH, A. 2012. Possibilities for growing queen palm (*Syagrus romanzoffiana*) in Argentina as a biodiesel producer under semi-arid climate conditions. *International Journal of Hydrogen Energy,* 37**,** 14843-14848.

FARRELL, R. 2016. Australia Biofuels Annual 2016, Global Agricultural Information Network. GAIN Report number: AS1611, 1-19.

FATTAH, I. M. R., MASJUKI, H. H., KALAM, M. A., MOFIJUR, M. & ABEDIN, M. J. 2014. Effect of antioxidant on the performance and emission characteristics of a diesel engine fueled with palm biodiesel blends. *Energy Conversion and Management,* 79**,** 265-272.

FATTAH, I. M. R., MASJUKI, H. H., LIAQUAT, A. M., RAMLI, R., KALAM, M. A. & RIAZUDDIN, V. N. 2013. Impact of various biodiesel fuels obtained from edible and non-edible oils on engine exhaust gas and noise emissions. *Renewable and Sustainable Energy Reviews,* 18**,** 552-567.

FAZAL, M. A., HASEEB, A. S. M. A. & MASJUKI, H. H. 2010. Comparative corrosive characteristics of petroleum diesel and palm biodiesel for automotive materials. *Fuel Processing Technology,* 91**,** 1308-1315.

FAZAL, M. A., HASEEB, A. S. M. A. & MASJUKI, H. H. 2011. Biodiesel feasibility study: An evaluation of material compatibility; performance; emission and engine durability. *Renewable and Sustainable Energy Reviews,* 15**,** 1314-1324.

FAZAL, M. A., HASEEB, A. S. M. A. & MASJUKI, H. H. 2013. Investigation of friction and wear characteristics of palm biodiesel. *Energy Conversion and Management,* 67**,** 251-256.

FERNÁNDEZ, C. M., RAMOS, M. J., PÉREZ, Á. & RODRÍGUEZ, J. F. 2010. Production of biodiesel from winery waste: Extraction, refining and transesterification of grape seed oil. *Bioresource Technology,* 101**,** 7019-7024.

GARCÍA-MORENO, P. J., KHANUM, M., GUADIX, A. & GUADIX, E. M. 2014. Optimization of biodiesel production from waste fish oil. *Renewable Energy,* 68**,** 618-624.

GELLER, D. P. & GOODRUM, J. W. 2004. Effects of specific fatty acid methyl esters on diesel fuel lubricity. *Fuel,* 83**,** 2351-2356.

GHADGE, S. V. & RAHEMAN, H. 2005. Biodiesel production from mahua (Madhuca indica) oil having high free fatty acids. *Biomass and Bioenergy,* 28**,** 601-605.

GHALY, A. E., DAVE, D., BROOKS, M. & BUDGE, S. 2010. Production of biodiesel by enzymatic transesterification: review. *American Journal of Biochemistry and Biotechnology,* 6**,** 54.

GIAKOUMIS, E. G., RAKOPOULOS, C. D., DIMARATOS, A. M. & RAKOPOULOS, D. C. 2012. Exhaust emissions of diesel engines operating under transient conditions with biodiesel fuel blends. *Progress in Energy and Combustion Science,* 38**,** 691-715.

GOGOI, T. K. & BARUAH, D. C. 2011. The use of Koroch seed oil methyl ester blends as fuel in a diesel engine. *Applied Energy,* 88**,** 2713-2725.

GOIRIS, K., MUYLAERT, K., FRAEYE, I., FOUBERT, I., DE BRABANTER, J. & DE COOMAN, L. 2012. Antioxidant potential of microalgae in relation to their phenolic and carotenoid content. *Journal of Applied Phycology,* 24**,** 1477-1486.

GOUR, V. S. & KANT, T. 2012. Balanites aegyptiaca (l.) Del.: a multipurpose and potential biodiesel tree species of the arid regions. *International Journal of Science & Nature,* 3**,** 472-488.

GRACE, M. H., JIN, Y., WILSON, G. R. & COATES, R. M. 2006. Structures, biogenetic relationships, and cytotoxicity of pimarane-derived diterpenes from *Petalostigma pubescens*. *Phytochemistry,* 67**,** 1708-1715.

GUI, M. M., LEE, K. T. & BHATIA, S. 2008. Feasibility of edible oil vs. non-edible oil vs. waste edible oil as biodiesel feedstock. *Energy,* 33**,** 1646-1653.

GUIMARÃES, P. M., TEIXEIRA, J. A. & DOMINGUES, L. 2010. Fermentation of lactose to bio-ethanol by yeasts as part of integrated solutions for the valorisation of cheese whey. *Biotechnology Advances,* 28**,** 375-384.

GUTTI, B., BAMIDELE, S. S. & BUGAJE, I. M. 2012. Biodiesel kinematics viscosity analysis of *Balanite aegyptiaca* seed oil. *Journal of Engineering & Applied Sciences,* 7**,** 432-438.

GUZATTO, R., DE MARTINI, T. L. & SAMIOS, D. 2011. The use of a modified TDSP for biodiesel production from soybean, linseed and waste cooking oil. *Fuel Processing Technology,* 92**,** 2083-2088.

HABIBULLAH, M., MASJUKI, H. H., KALAM, M. A., GULZAR, M., ARSLAN, A. & ZAHID, R. 2015a. Tribological Characteristics of Calophyllum inophyllum–Based TMP (Trimethylolpropane) Ester as Energy-Saving and Biodegradable Lubricant. *Tribology Transactions,* 58**,** 1002-1011.

HABIBULLAH, M., MASJUKI, H. H., KALAM, M. A., ZULKIFLI, N. W. M., MASUM, B. M., ARSLAN, A. & GULZAR, M. 2015b. Friction and wear characteristics of Calophyllum inophyllum biodiesel. *Industrial Crops and Products,* 76**,** 188-197.

HAHN-HÄGERDAL, B., GALBE, M., GORWA-GRAUSLUND, M., LIDEN, G. & ZACCHI, G. 2006. Bio-ethanol–the fuel of tomorrow from the residues of today. *Trends in biotechnology,* 24**,** 549-556.

HALIM, R., GLADMAN, B., DANQUAH, M. K. & WEBLEY, P. A. 2011. Oil extraction from microalgae for biodiesel production. *Bioresource Technology,* 102**,** 178-185.

HAN, S., KIM, J. & BAE, C. 2014. Effect of air–fuel mixing quality on characteristics of conventional and low temperature diesel combustion. *Applied Energy,* 119**,** 454-466.

HARCH, C. A., RASUL, M. G., HASSAN, N. M. S. & BHUIYA, M. M. K. 2014. Modelling of Engine Performance Fuelled with Second Generation Biodiesel. *Procedia Engineering,* 90**,** 459-465.

HASEEB, A. S. M. A., SIA, S. Y., FAZAL, M. A. & MASJUKI, H. H. 2010. Effect of temperature on tribological properties of palm biodiesel. *Energy,* 35**,** 1460-1464.

HASSAN, N. M. S., RASUL, M. G. & HARCH, C. A. 2015. Modelling and experimental investigation of engine performance and emissions fuelled with biodiesel produced from Australian Beauty Leaf Tree. *Fuel,* 150**,** 625-635.

HAVET, L., BLOUET, J., VALLOIRE, F. R., BRASSEUR, E. & SLOMKA, D. 2001. Tribological characteristics of some environmentally friendly lubricants. *Wear,* 248**,** 140-146.

HEARD, T. A., CHAN, R. R., WILMOT SENARATNE, K., PALMER, W. A., LOCKETT, C. & LUKITSCH, B. 2009. *Agonosoma trilineatum* (Heteroptera: Scutelleridae) a biological control agent of the weed bellyache bush, *Jatropha, gossypiifolia* (Euphorbiaceae). *Biological control,* 48**,** 196-203.

HERBINET, O., PITZ, W. J. & WESTBROOK, C. K. 2010. Detailed chemical kinetic mechanism for the oxidation of biodiesel fuels blend surrogate. *Combustion and Flame,* 157**,** 893-908.

HILL, S. C. & DOUGLAS SMOOT, L. 2000. Modeling of nitrogen oxides formation and destruction in combustion systems. *Progress in Energy and Combustion Science,* 26**,** 417-458.

HOEKMAN, S. K., BROCH, A., ROBBINS, C., CENICEROS, E. & NATARAJAN, M. 2012. Review of biodiesel composition, properties, and specifications. *Renewable and Sustainable Energy Reviews,* 16**,** 143-169.

HOEKMAN, S. K. & ROBBINS, C. 2012. Review of the effects of biodiesel on NOx emissions. *Fuel Processing Technology,* 96**,** 237-249.

HOLMBERG, K., ANDERSSON, P. & ERDEMIR, A. 2012. Global energy consumption due to friction in passenger cars. *Tribology International,* 47**,** 221-234.

HOSAMANI, K., HIREMATH, V. & KERI, R. 2009. Renewable energy sources from *Michelia champaca* and *Garcinia indica* seed oils: A rich source of oil. *Biomass and Bioenergy,* 33**,** 267-270.

HOSSAIN, A. B. M. S., SALLEH, A., BOYCE, A. N., CHOWDHURY, P. & NAQIUDDIN, M. 2008. Biodiesel fuel production from algae as renewable energy. *American Journal of Biochemistry & Biotechnology,* 4**,** 250-254.

HOSSAIN, A. K. & DAVIES, P. A. 2012. Performance, emission and combustion characteristics of an indirect injection (IDI) multi-cylinder compression ignition (CI) engine operating on neat jatropha and karanj oils preheated by jacket water. *Biomass and Bioenergy,* 46**,** 332-342.

HOSSAIN, E., CHANDRA, G., NANDY, A. P., MANDAL, S. C. & GUPTA, J. K. 2012. Anthelmintic effect of a methanol extract of Bombax malabaricum leaves on Paramphistomum explanatum. *Parasitology research,* 110**,** 1097-1102.

HU, J., DU, Z., LI, C. & MIN, E. 2005. Study on the lubrication properties of biodiesel as fuel lubricity enhancers. *Fuel,* 84**,** 1601-1606.

HULWAN, D. B. & JOSHI, S. V. 2011. Performance, emission and combustion characteristic of a multicylinder DI diesel engine running on diesel–ethanol–biodiesel blends of high ethanol content. *Applied Energy,* 88**,** 5042-5055.

IEO 2016a. International Energy Outlook 2016, Chapter 1: World energy demand and economic outlook, [cited on 10 November 2016]; Available from: <https://www.eia.gov/forecasts/ieo/world.cfm>

IEO. 2016b. *International Energy Outlook 2016, US Energy Information Administration, [cited on 4 November' 2016], Available from: <http://www.eia.gov/forecasts/ieo/>*.

IMTENAN, S., MASJUKI, H. H., VARMAN, M., KALAM, M. A., ARBAB, M. I., SAJJAD, H. & ASHRAFUR RAHMAN, S. M. 2014a. Impact of oxygenated additives to palm and jatropha biodiesel blends in the context of performance and emissions characteristics of a light-duty diesel engine. *Energy Conversion and Management,* 83**,** 149-158.

IMTENAN, S., VARMAN, M., MASJUKI, H. H., KALAM, M. A., SAJJAD, H., ARBAB, M. I. & RIZWANUL FATTAH, I. M. 2014b. Impact of low temperature combustion attaining strategies on diesel engine emissions for diesel and biodiesels: A review. *Energy Conversion and Management,* 80**,** 329-356.

ISLAM, M. A., RAHMAN, M. M., HEIMANN, K., NABI, M. N., RISTOVSKI, Z. D., DOWELL, A., THOMAS, G., FENG, B., VON ALVENSLEBEN, N. & BROWN, R. J. 2015. Combustion analysis of microalgae methyl ester in a common rail direct injection diesel engine. *Fuel,* 143**,** 351-360.

IZAH, S. C. & OHIMAIN, E. I. 2013. The Challenge of Biodiesel Production from Oil Palm Feedstock in Nigeria. *Greener Journal of Biological Sciences,* 3**,** 1-12.

JACOBSON, M. Z. & DELUCCHI, M. A. 2011. Providing all global energy with wind, water, and solar power, Part I: Technologies, energy resources, quantities and areas of infrastructure, and materials. *Energy Policy,* 39**,** 1154-1169.

JAHIRUL, M. I., BROWN, J. R., SENADEERA, W., ASHWATH, N., LAING, C., LESKI-TAYLOR, J. & RASUL, M. G. 2013. Optimisation of Bio-Oil Extraction Process from Beauty Leaf (*Calophyllum Inophyllum*) Oil Seed as a Second Generation Biodiesel Source. *Procedia Engineering,* 56**,** 619-624.

JAIN, S. & SHARMA, M. 2010. Stability of biodiesel and its blends: a review. *Renewable and Sustainable Energy Reviews,* 14**,** 667-678.

JANAUN, J. & ELLIS, N. 2010. Perspectives on biodiesel as a sustainable fuel. *Renewable and Sustainable Energy Reviews,* 14**,** 1312-1320.

JEENNOR, S., LAOTENG, K., TANTICHAROEN, M. & CHEEVADHANARAK, S. 2008. Evaluation of inoculum performance for enhancing gamma-linolenic acid production from Mucor rouxii. *Letters in applied microbiology,* 46**,** 421-427.

JOTHIRAMALINGAM, R. & WANG, M. K. 2009. Review of recent developments in solid acid, base, and enzyme catalysts (heterogeneous) for biodiesel production via transesterification. *Industrial & Engineering Chemistry Research,* 48**,** 6162-6172.

KANSEDO, J., LEE, K. T. & BHATIA, S. 2009. Cerbera odollam (sea mango) oil as a promising non-edible feedstock for biodiesel production. *Fuel,* 88**,** 1148-1150.

KARMAKAR, A., KARMAKAR, S. & MUKHERJEE, S. 2010. Properties of various plants and animals feedstocks for biodiesel production. *Bioresource Technology,* 101**,** 7201-7210.

KARMAKAR, A., KARMAKAR, S. & MUKHERJEE, S. 2012. Biodiesel production from neem towards feedstock diversification: Indian perspective. *Renewable and Sustainable Energy Reviews,* 16**,** 1050-1060.

KARTHIKEYAN, A., VENKATESH, D. & RAMKUMAR, T. 2015. Experimental investigation on spark ignition engine using blends of bio-ethanol produced from citrus peel wastes. *International Journal of Ambient Energy***,** 1-4.

KAUR SANDHU, S., SINGH OBEROI, H., SINGH DHALIWAL, S., BABBAR, N., KAUR, U., NANDA, D. & KUMAR, D. 2012. Ethanol production from Kinnow mandarin (Citrus reticulata) peels via simultaneous saccharification and fermentation using crude enzyme produced by Aspergillus oryzae and the thermotolerant Pichia kudriavzevii strain. *Annals of Microbiology,* 62**,** 655-666.

KEERA, S., EL SABAGH, S. & TAMAN, A. 2011. Transesterification of vegetable oil to biodiesel fuel using alkaline catalyst. *Fuel,* 90**,** 42-47.

KELLY, G. 2007. Renewable energy strategies in England, Australia and New Zealand. *Geoforum,* 38**,** 326-338.

KIBAZOHI, O. & SANGWAN, R. 2011. Vegetable oil production potential from *Jatropha curcas*, *Croton megalocarpus*, *Aleurites moluccana*, *Moringa oleifera* and *Pachira glabra*: Assessment of renewable energy resources for bio-energy production in Africa. *Biomass and Bioenergy,* 35**,** 1352-1356.

KNOTHE, G. 2010. Biodiesel derived from a model oil enriched in palmitoleic acid, macadamia nut oil. *Energy & Fuels,* 24**,** 2098-2103.

KNOTHE, G. 2013a. Avocado and olive oil methyl esters. *Biomass and Bioenergy,* 58**,** 143-148.

KNOTHE, G. 2013b. Fuel properties of methyl esters of borage and black currant oils containing methyl γ-linolenate. *European Journal of Lipid Science and Technology,* 115**,** 901-908.

KNOTHE, G. 2014. A comprehensive evaluation of the cetane numbers of fatty acid methyl esters. *Fuel,* 119**,** 6-13.

KOH, L. P. & GHAZOUL, J. 2008. Biofuels, biodiversity, and people: understanding the conflicts and finding opportunities. *Biological conservation,* 141**,** 2450-2460.
KOMNINOS, N. P. & RAKOPOULOS, C. D. 2012. Modeling HCCI combustion of biofuels: A review. *Renewable and Sustainable Energy Reviews,* 16**,** 1588-1610.
KONG, K. W., MAT-JUNIT, S., AMINUDIN, N., ISMAIL, A. & ABDUL-AZIZ, A. 2012. Antioxidant activities and polyphenolics from the shoots of *Barringtonia racemosa* (L.) Spreng in a polar to apolar medium system. *Food Chemistry,* 134**,** 324-332.
KONGKASAWAN, J. & CAPAREDA, S. C. 2012. Jatropha Oil Refining Process and Biodiesel Conversion: Mass and Energy Balance. *International Energy Journal,* 13**,** 1-4.
KÖRBITZ, W. 1999. Biodiesel production in Europe and North America, an encouraging prospect. *Renewable Energy,* 16**,** 1078-1083.
KUMAR, A. & SHARMA, S. 2011. Potential non-edible oil resources as biodiesel feedstock: An Indian perspective. *Renewable and Sustainable Energy Reviews,* 15**,** 1791-1800.
KUMAR, N. & REDDY, M. P. 2012. Thidiazuron (TDZ) induced plant regeneration from cotyledonary petiole explants of elite genotypes of *Jatropha curcas*: A candidate biodiesel plant. *Industrial Crops and Products,* 39**,** 62-68.
KUMARI, V., SHAH, S. & GUPTA, M. N. 2007. Preparation of biodiesel by lipase-catalyzed transesterification of high free fatty acid containing oil from Madhuca indica. *Energy & fuels,* 21**,** 368-372.
KUSHWAH, Y. S., MAHANTA, P. & MISHRA, S. C. 2008. Some studies on fuel characteristics of Mesua Ferrea. *Heat Transfer Engineering,* 29**,** 405-409.
LAI, J. Y., LIN, K. C. & VIOLI, A. 2011a. Biodiesel combustion: Advances in chemical kinetic modeling. *Progress in Energy and Combustion Science,* 37**,** 1-14.
LAI, J. Y. W., LIN, K. C. & VIOLI, A. 2011b. Biodiesel combustion: Advances in chemical kinetic modeling. *Progress in Energy and Combustion Science,* 37**,** 1-14.
LAPUERTA, M., ARMAS, O. & HERREROS, J. M. 2008a. Emissions from a diesel–bioethanol blend in an automotive diesel engine. *Fuel,* 87**,** 25-31.
LAPUERTA, M., ARMAS, O. & RODRÍGUEZ-FERNÁNDEZ, J. 2008b. Effect of biodiesel fuels on diesel engine emissions. *Progress in Energy and Combustion Science,* 34**,** 198-223.
LARDON, L., HÉLIAS, A., SIALVE, B., STEYER, J.-P. & BERNARD, O. 2009. Life-cycle assessment of biodiesel production from microalgae. *Environmental science & technology,* 43**,** 6475-6481.
LEE, R. A. & LAVOIE, J.-M. 2013. From first-to third-generation biofuels: Challenges of producing a commodity from a biomass of increasing complexity. *Animal Frontiers,* 3**,** 6-11.
LEE, T., PARK, J., KWON, S., LEE, J. & KIM, J. 2013. Variability in operation-based NOx emission factors with different test routes, and its effects on the real-driving emissions of light diesel vehicles. *Science of The Total Environment,* 461–462**,** 377-385.
LI, J., YANG, W. M., AN, H., MAGHBOULI, A. & CHOU, S. K. 2014. Effects of piston bowl geometry on combustion and emission characteristics of biodiesel fueled diesel engines. *Fuel,* 120**,** 66-73.
LIM, S. & TEONG, L. K. 2010. Recent trends, opportunities and challenges of biodiesel in Malaysia: An overview. *Renewable and Sustainable Energy Reviews,* 14**,** 938-954.
LIN, C.-Y., CHEN, P.-N., HSIEH, Y.-S. & CHU, S.-C. 2014. *Koelreuteria formosana, extract impedes* in *vitro* human LDL and prevents oxidised LDL-induced apoptosis in human umbilical vein endothelial cells. *Food chemistry,* 146**,** 299-307.
LIN, L., CUNSHAN, Z., VITTAYAPADUNG, S., XIANGQIAN, S. & MINGDONG, D. 2011. Opportunities and challenges for biodiesel fuel. *Applied Energy,* 88**,** 1020-1031.

LIOR, N. 2002. Thoughts about future power generation systems and the role of exergy analysis in their development. *Energy Conversion and Management,* 43**,** 1187-1198.

LOTERO, E., LIU, Y., LOPEZ, D. E., SUWANNAKARN, K., BRUCE, D. A. & GOODWIN, J. G. 2005. Synthesis of biodiesel via acid catalysis. *Industrial & engineering chemistry research,* 44**,** 5353-5363.

LÜ, J., SHEAHAN, C. & FU, P. 2011. Metabolic engineering of algae for fourth generation biofuels production. *Energy & Environmental Science,* 4**,** 2451-2466.

LU, X., COTTER, J. & EADIE, D. 2005. Laboratory study of the tribological properties of friction modifier thin films for friction control at the wheel/rail interface. *Wear,* 259**,** 1262-1269.

LUNIN, V., SERGEEVA, Y. E., GALANINA, L., MYSYAKINA, I., IVASHECHKIN, A., BOGDAN, V. & FEOFILOVA, E. 2013. Biodiesel fuel production from lipids of filamentous fungi. *Applied Biochemistry and Microbiology,* 49**,** 46-52.

M. MOFIJUR, H. H. M., M.A. KALAM 2013. Experimental study of additive added palm biodiesel in a compression ignition engine. *Energy Education Science and Technology Part A,* 30**,** 737-748.

MACHADO CORRÊA, S. & ARBILLA, G. 2008. Carbonyl emissions in diesel and biodiesel exhaust. *Atmospheric Environment,* 42**,** 769-775.

MAGNO, A., MANCARUSO, E. & VAGLIECO, B. M. 2016. Analysis of combustion phenomena and pollutant formation in a small compression ignition engine fuelled with blended and pure rapeseed methyl ester. *Energy,* 106**,** 618-630.

MAHANTA, P. & SHRIVASTAVA, A. 2004. Technology development of bio-diesel as an energy alternative. *Department of Mechanical Engineering Indian Institute of Technology***,** 1-19.

MALEQUE, M., MASJUKI, H. & HASEEB, A. 2000. Effect of mechanical factors on tribological properties of palm oil methyl ester blended lubricant. *Wear,* 239**,** 117-125.

MARTÍN, C., MOURE, A., MARTÍN, G., CARRILLO, E., DOMÍNGUEZ, H. & PARAJÓ, J. C. 2010. Fractional characterisation of jatropha, neem, moringa, trisperma, castor and candlenut seeds as potential feedstocks for biodiesel production in Cuba. *Biomass and Bioenergy,* 34**,** 533-538.

MATA, T. M., MARTINS, A. A. & CAETANO, N. S. 2010. Microalgae for biodiesel production and other applications: A review. *Renewable and Sustainable Energy Reviews,* 14**,** 217-232.

MCHENRY, M. P. & ANWAR, M. J. 2013. Indigenous-owned pastoral land forestry carbon biosequestration and bioenergy options in arid, salt-affected Western Australian regions. In: Ren H (ed) Plantations: biodiversity, carbon sequestration, and restoration. Nova Science Publishers, Hauppauge, NY. . 53-76.

MEHER, L. C., VIDYA SAGAR, D. & NAIK, S. N. 2006. Technical aspects of biodiesel production by transesterification—a review. *Renewable and Sustainable Energy Reviews,* 10**,** 248-268.

MENEGHETTI, S. M. P., MENEGHETTI, M. R., WOLF, C. R., SILVA, E. C., LIMA, G. E., DE LIRA SILVA, L., SERRA, T. M., CAUDURO, F. & DE OLIVEIRA, L. G. 2006. Biodiesel from castor oil: a comparison of ethanolysis versus methanolysis. *Energy & Fuels,* 20**,** 2262-2265.

MENG, X., YANG, J., XU, X., ZHANG, L., NIE, Q. & XIAN, M. 2009. Biodiesel production from oleaginous microorganisms. *Renewable Energy,* 34**,** 1-5.

MISRA, B. B. & DEY, S. 2013. Shikimic Acid (Tamiflu Precursor) Production in Suspension Cultures of East Indian Sandalwood (Santalum album) in Air-lift Bioreactor. *Journal of Postdoctoral Research,* 1**,** 1-9.

MOFIJUR, M., RASUL, M., HYDE, J., AZAD, A., MAMAT, R. & BHUIYA, M. 2016a. Role of biofuel and their binary (diesel–biodiesel) and ternary (ethanol–biodiesel–diesel) blends on internal combustion engines emission reduction. *Renewable and Sustainable Energy Reviews,* 53**,** 265-278.

MOFIJUR, M., RASUL, M. G., HYDE, J., AZAD, A. K., MAMAT, R. & BHUIYA, M. M. K. 2016b. Role of biofuel and their binary (diesel–biodiesel) and ternary (ethanol–biodiesel–diesel) blends on internal combustion engines emission reduction. *Renewable and Sustainable Energy Reviews,* 53**,** 265-278.

MOHAMED ISMAIL, H., NG, H. K., GAN, S., LUCCHINI, T. & ONORATI, A. 2013. Development of a reduced biodiesel combustion kinetics mechanism for CFD modelling of a light-duty diesel engine. *Fuel,* 106**,** 388-400.

MOHIBBE AZAM, M., WARIS, A. & NAHAR, N. M. 2005. Prospects and potential of fatty acid methyl esters of some non-traditional seed oils for use as biodiesel in India. *Biomass and Bioenergy,* 29**,** 293-302.

MONIRUL, I. M., MASJUKI, H. H., KALAM, M. A., MOSAROF, M. H., ZULKIFLI, N. W. M., TEOH, Y. H. & HOW, H. G. 2016. Assessment of performance, emission and combustion characteristics of palm, jatropha and Calophyllum inophyllum biodiesel blends. *Fuel,* 181**,** 985-995.

MOSAROF, M., KALAM, M., MASJUKI, H., ARSLAN, A., MONIRUL, I., RUHUL, A., SHAHIR, S. & KHUONG, L. 2016a. Analysis of thermal stability and lubrication characteristics of Millettia pinnata oil. *RSC Advances,* 6**,** 81414-81425.

MOSAROF, M. H., KALAM, M. A., MASJUKI, H. H., ALABDULKAREM, A., ASHRAFUL, A. M., ARSLAN, A., RASHEDUL, H. K. & MONIRUL, I. M. 2016b. Optimization of performance, emission, friction and wear characteristics of palm and Calophyllum inophyllum biodiesel blends. *Energy Conversion and Management,* 118**,** 119-134.

MOSAROF, M. H., KALAM, M. A., MASJUKI, H. H., ALABDULKAREM, A., HABIBULLAH, M., ARSLAN, A. & MONIRUL, I. M. 2016c. Assessment of friction and wear characteristics of Calophyllum inophyllum and palm biodiesel. *Industrial Crops and Products,* 83**,** 470-483.

MOSER, B. R. 2011. Biodiesel production, properties, and feedstocks. *Biofuels.* Springer.

MOSER, B. R., ELLER, F. J., TISSERAT, B. H. & GRAVETT, A. 2011. Preparation of fatty acid methyl esters from osage orange (Maclura pomifera) oil and evaluation as biodiesel. *Energy & Fuels,* 25**,** 1869-1877.

MOSER, B. R. & VAUGHN, S. F. 2010. Coriander seed oil methyl esters as biodiesel fuel: Unique fatty acid composition and excellent oxidative stability. *Biomass and Bioenergy,* 34**,** 550-558.

MURALIDHARAN, K. & VASUDEVAN, D. 2011. Performance, emission and combustion characteristics of a variable compression ratio engine using methyl esters of waste cooking oil and diesel blends. *Applied Energy,* 88**,** 3959-3968.

MURALIDHARAN, K., VASUDEVAN, D. & SHEEBA, K. N. 2011. Performance, emission and combustion characteristics of biodiesel fuelled variable compression ratio engine. *Energy,* 36**,** 5385-5393.

MURILLO, S., MIGUEZ, J., PORTEIRO, J., GRANADA, E. & MORAN, J. 2007. Performance and exhaust emissions in the use of biodiesel in outboard diesel engines. *Fuel,* 86**,** 1765-1771.

MURUGESAN, A., UMARANI, C., SUBRAMANIAN, R. & NEDUNCHEZHIAN, N. 2009. Bio-diesel as an alternative fuel for diesel engines—a review. *Renewable and Sustainable Energy Reviews,* 13**,** 653-662.

MUSCULUS, M. P. B., MILES, P. C. & PICKETT, L. M. 2013. Conceptual models for partially premixed low-temperature diesel combustion. *Progress in Energy and Combustion Science,* 39**,** 246-283.

MUSSATTO, S. I., DRAGONE, G., GUIMARÃES, P. M., SILVA, J. P. A., CARNEIRO, L. M., ROBERTO, I. C., VICENTE, A., DOMINGUES, L. & TEIXEIRA, J. A. 2010. Technological trends, global market, and challenges of bio-ethanol production. *Biotechnology advances,* 28**,** 817-830.

NAGAR, P. & MIERS, S. 2011. Friction between Piston and Cylinder of an IC Engine: a Review. SAE Technical Paper.

NAIK, S. N., GOUD, V. V., ROUT, P. K. & DALAI, A. K. 2010. Production of first and second generation biofuels: A comprehensive review. *Renewable and Sustainable Energy Reviews,* 14**,** 578-597.

NIGAM, P. S. & SINGH, A. 2011. Production of liquid biofuels from renewable resources. *Progress in Energy and Combustion Science,* 37**,** 52-68.

NO, S.-Y. 2011. Inedible vegetable oils and their derivatives for alternative diesel fuels in CI engines: A review. *Renewable and Sustainable Energy Reviews,* 15**,** 131-149.

OJEDA, K., ÁVILA, O., SUÁREZ, J. & KAFAROV, V. 2011. Evaluation of technological alternatives for process integration of sugarcane bagasse for sustainable biofuels production—Part 1. *Chemical Engineering Research and Design,* 89**,** 270-279.

ONG, H., MAHLIA, T., MASJUKI, H. & NORHASYIMA, R. 2011. Comparison of palm oil, Jatropha curcas and Calophyllum inophyllum for biodiesel: a review. *Renewable and Sustainable Energy Reviews,* 15**,** 3501-3515.

ONG, H. C., MASJUKI, H. H., MAHLIA, T. M. I., SILITONGA, A. S., CHONG, W. T. & YUSAF, T. 2014. Engine performance and emissions using Jatropha curcas, Ceiba pentandra and Calophyllum inophyllum biodiesel in a CI diesel engine. *Energy,* 69**,** 427-445.

ONG, L. K., EFFENDI, C., KURNIAWAN, A., LIN, C. X., ZHAO, X. S. & ISMADJI, S. 2013. Optimization of catalyst-free production of biodiesel from *Ceiba pentandra* (kapok) oil with high free fatty acid contents. *Energy,* 57**,** 615-623.

ORTIZ, M. A., DORANTES, A. L., GALLNDEZ, M. J. & CARDENAS, S. E. 2004. Effect of a Novel Oil Extraction Method on Avocado (Persea americana Mill) Pulp Microstructure. *Plant Foods for Human Nutrition,* 59**,** 11-14.

OZSEZEN, A. N. & CANAKCI, M. 2011. Determination of performance and combustion characteristics of a diesel engine fueled with canola and waste palm oil methyl esters. *Energy Conversion and Management,* 52**,** 108-116.

PALASH, S. M., MASJUKI, H. H., KALAM, M. A., ATABANI, A. E., RIZWANUL FATTAH, I. M. & SANJID, A. 2015. Biodiesel production, characterization, diesel engine performance, and emission characteristics of methyl esters from Aphanamixis polystachya oil of Bangladesh. *Energy Conversion and Management,* 91**,** 149-157.

PANDEY, R. K., REHMAN, A. & SARVIYA, R. 2012. Impact of alternative fuel properties on fuel spray behavior and atomization. *Renewable and Sustainable Energy Reviews,* 16**,** 1762-1778.

PANWAR, N. L., SHRIRAME, H. Y., RATHORE, N. S., JINDAL, S. & KURCHANIA, A. K. 2010. Performance evaluation of a diesel engine fueled with methyl ester of castor seed oil. *Applied Thermal Engineering,* 30**,** 245-249.

PHAM, P., ALLISON BALL, SHAMIM AHMAD, GAYATHIRI BRAGATHESWARAN & CAITLIN MCCLUSKEY, E. A. 2016. Department of Industry, Innovation and Science, Office of Chief Economist, Energy in Australia 2015, [cited 10 November' 2016]; Available from: <http://www.industry.gov.au/Office-of-the-Chief-Economist/Publications/Documents/energy-in-aust/Energy-in-Australia-2015.pdf>.

PHAM, P., BODISCO, T., STEVANOVIC, S., RAHMAN, M., WANG, H., RISTOVSKI, Z., BROWN, R. & MASRI, A. 2013. Engine performance characteristics for biodiesels of different degrees of saturation and carbon chain lengths. *SAE International Journal of Fuels and Lubricants,* 6**,** 188-198.

PINZI, S., GARCIA, I., LOPEZ-GIMENEZ, F., LUQUE DE CASTRO, M., DORADO, G. & DORADO, M. 2009. The ideal vegetable oil-based biodiesel composition: a review of social, economical and technical implications. *Energy & Fuels,* 23**,** 2325-2341.

PURI, M., ABRAHAM, R. E. & BARROW, C. J. 2012. Biofuel production: Prospects, challenges and feedstock in Australia. *Renewable and Sustainable Energy Reviews,* 16**,** 6022-6031.

QI, D., CHEN, H., GENG, L., BIAN, Y. Z. & REN, X. C. 2010. Performance and combustion characteristics of biodiesel–diesel–methanol blend fuelled engine. *Applied Energy,* 87**,** 1679-1686.

QIN, S., SUN, Y., MENG, X. & ZHANG, S. 2010. Production and analysis of biodiesel from non-edible seed oil of Pistacia Chinensis. *Energy, Exploration & Exploitation,* 28**,** 37-46.

QURESHI, N., SAHA, B. C., DIEN, B., HECTOR, R. E. & COTTA, M. A. 2010. Production of butanol (a biofuel) from agricultural residues: Part I-Use of barley straw hydrolysate. *Biomass and Bioenergy,* 34**,** 559-565.

QURESHI, N., SAHA, B. C., HECTOR, R. E., HUGHES, S. R. & COTTA, M. A. 2008. Butanol production from wheat straw by simultaneous saccharification and fermentation using Clostridium beijerinckii: Part I—Batch fermentation. *Biomass and Bioenergy,* 32**,** 168-175.

RA, Y. & REITZ, R. D. 2011. A combustion model for IC engine combustion simulations with multi-component fuels. *Combustion and Flame,* 158**,** 69-90.

RACHIMOELLAH, H., RESTI, D. A., ZIBBENI, A. & SUSILA, I. W. 2010. Production of biodiesel through transesterification of avocado (Persea gratissima) seed oil using base catalyst. *Jurnal Teknik Mesin,* 11**,** pp. 85-90.

RAGIT, S. S., MOHAPATRA, S. K., KUNDU, K. & GILL, P. 2011. Optimization of neem methyl ester from transesterification process and fuel characterization as a diesel substitute. *Biomass and Bioenergy,* 35**,** 1138-1144.

RAHMAN, M., RASUL, M., HASSAN, N. & HYDE, J. 2016a. Prospects of Biodiesel Production from Macadamia Oil as an Alternative Fuel for Diesel Engines. *Energies,* 9**,** 403.

RAHMAN, M., RASUL, M., HASSAN, N. & HYDE, J. 2016b. Prospects of Biodiesel Production from Macadamia Oil as an Alternative Fuel for Diesel Engines. *Energies,* 9**,** 403 (1-15).

RAJENDRA PRASATH, B., TAMILPORAI, P. & SHABIR, M. F. 2010. Analysis of combustion, performance and emission characteristics of low heat rejection engine using biodiesel. *International Journal of Thermal Sciences,* 49**,** 2483-2490.

RAMOS, M. J., FERNÁNDEZ, C. M., CASAS, A., RODRÍGUEZ, L. & PÉREZ, Á. 2009. Influence of fatty acid composition of raw materials on biodiesel properties. *Bioresource Technology,* 100**,** 261-268.

RANZI, E., FRASSOLDATI, A., GRANA, R., CUOCI, A., FARAVELLI, T., KELLEY, A. & LAW, C. 2012. Hierarchical and comparative kinetic modeling of laminar flame speeds of hydrocarbon and oxygenated fuels. *Progress in Energy and Combustion Science,* 38**,** 468-501.

RASHID, U. & ANWAR, F. 2008. Production of biodiesel through optimized alkaline-catalyzed transesterification of rapeseed oil. *Fuel,* 87**,** 265-273.

RASHID, U., ANWAR, F., ASHRAF, M., SALEEM, M. & YUSUP, S. 2011. Application of response surface methodology for optimizing transesterification of Moringa oleifera oil: Biodiesel production. *Energy Conversion and Management,* 52**,** 3034-3042.

RASHID, U., IBRAHIM, M., YASIN, S., YUNUS, R., TAUFIQ-YAP, Y. H. & KNOTHE, G. 2013. Biodiesel from Citrus reticulata (mandarin orange) seed oil, a potential non-food feedstock. *Industrial Crops and Products,* 45**,** 355-359.

RAZON, L. F. 2009. Alternative crops for biodiesel feedstock. *CAB Reviews: Perspectives in agriculture, veterinary science, nutrition and natural resources,* 4**,** 1-15.

RAZON, L. F. & TAN, R. R. 2011. Net energy analysis of the production of biodiesel and biogas from the microalgae: *Haematococcus pluvialis* and *Nannochloropsis*. *Applied Energy,* 88**,** 3507-3514.

REN21 2016. Renewables 2016 Global Status Report, [cited on 10 November 2016], Available from: <http://www.ren21.net/status-of-renewables/global-status-report/>.

REŞITOĞLU, İ. A., ALTINIŞIK, K. & KESKIN, A. 2015. The pollutant emissions from diesel-engine vehicles and exhaust aftertreatment systems. *Clean Technologies and Environmental Policy,* 17**,** 15-27.

RET. 2013. *Australian Government, Department of Environment. Renewable Energy Target; 2013 [cited 7 January 2014]; Available from: <http://climatechange.gov.au/reducing-carbon/renewable-energy/renewable-energy-target>*.

REYES-TREJO, B., GUERRA-RAMÍREZ, D., ZULETA-PRADA, H., CUEVAS-SÁNCHEZ, J. A., REYES, L., REYES-CHUMACERO, A. & RODRÍGUEZ-SALAZAR, J. A. 2014. *Annona diversifolia* seed oil as a promising non-edible feedstock for biodiesel production. *Industrial Crops and Products,* 52**,** 400-404.

RODRIGUEZ, L. C., MAY, B., HERR, A., FARINE, D. & O'CONNELL, D. 2011. Biofuel excision and the viability of ethanol production in the Green Triangle, Australia. *Energy Policy,* 39**,** 1951-1957.

ROMEIRO, G. A., SALGADO, E. C., SILVA, R. V. S., FIGUEIREDO, M. K. K., PINTO, P. A. & DAMASCENO, R. N. 2012. A study of pyrolysis oil from soluble coffee ground using low temperature conversion (LTC) process. *Journal of Analytical and Applied Pyrolysis,* 93**,** 47-51.

ROSA, H. A., WAZILEWSKI, W. T., SECCO, D., CHAVES, L. I., VELOSO, G., DE SOUZA, S. N. M., DA SILVA, M. J. & SANTOS, R. F. 2014. Biodiesel produced from crambe oil in Brazil—A study of performance and emissions in a diesel cycle engine generator. *Renewable and Sustainable Energy Reviews,* 38**,** 651-655.

ROSEGRANT, M. W., ZHU, T., MSANGI, S. & SULSER, T. 2008. Global scenarios for biofuels: impacts and implications. *Applied Economic Perspectives and Policy,* 30**,** 495-505.

ROSENTHAL, A., PYLE, D. L., NIRANJAN, K., GILMOUR, S. & TRINCA, L. 2001. Combined effect of operational variables and enzyme activity on aqueous enzymatic extraction of oil and protein from soybean. *Enzyme and Microbial Technology,* 28**,** 499-509.

ROY, M. M., CALDER, J., WANG, W., MANGAD, A. & DINIZ, F. C. M. 2016. Emission analysis of a modern Tier 4 DI diesel engine fueled by biodiesel-diesel blends with a cold flow improver (Wintron Synergy) at multiple idling conditions. *Applied Energy,* 179**,** 45-54.

RUAN, Z., ZANOTTI, M., WANG, X., DUCEY, C. & LIU, Y. 2012. Evaluation of lipid accumulation from lignocellulosic sugars by *Mortierella isabellina* for biodiesel production. *Bioresource Technology,* 110**,** 198-205.

SAEED, A. & BASHIER, R. 2010. Physico-chemical analysis of Ximenia americana. L seed oil and structure elucidation of some chemical constituents of its seed oil and fruit pulp. *Journal of Pharmacognosy and Phytotherapy,* 2**,** 49-55.

SAHOO, P. K. & DAS, L. M. 2009. Combustion analysis of Jatropha, Karanja and Polanga based biodiesel as fuel in a diesel engine. *Fuel,* 88**,** 994-999.

SAHOO, P. K., DAS, L. M., BABU, M. K. G. & NAIK, S. N. 2007. Biodiesel development from high acid value polanga seed oil and performance evaluation in a CI engine. *Fuel,* 86**,** 448-454.

SAJJAD, H., MASJUKI, H. H., VARMAN, M., KALAM, M. A., ARBAB, M. I., IMTENAN, S. & ASHRAFUL, A. M. 2015. Influence of gas-to-liquid (GTL) fuel in the blends of Calophyllum inophyllum biodiesel and diesel: An analysis of combustion–performance–emission characteristics. *Energy Conversion and Management,* 97**,** 42-52.

SAKA, S. & KUSDIANA, D. 2001. Biodiesel fuel from rapeseed oil as prepared in supercritical methanol. *Fuel,* 80**,** 225-231.

SAKTHIVEL, G. 2016. Prediction of CI engine performance, emission and combustion characteristics using fish oil as a biodiesel at different injection timing using fuzzy logic. *Fuel,* 183**,** 214-229.

SALVI, B. & PANWAR, N. 2012a. Biodiesel resources and production technologies–A review. *Renewable and Sustainable Energy Reviews,* 16**,** 3680-3689.

SALVI, B. L. & PANWAR, N. L. 2012b. Biodiesel resources and production technologies-A review. *Renewable and Sustainable Energy Reviews,* 16**,** 3680-3689.

SÁNCHEZ-BORROTO, Y., PILOTO-RODRIGUEZ, R., ERRASTI, M., SIERENS, R. & VERHELST, S. Prediction of cetane number and ignition delay of biodiesel using Artificial Neural Networks. Energy Procedia, 2014. 877-885.

SANFORD, S. D., WHITE, J. M., SHAH, P. S., WEE, C., VALVERDE, M. A. & MEIER, G. R. 2009. Feedstock and biodiesel characteristics report. *Renewable Energy Group,* 416**,** 1-136.

SANJID, A., MASJUKI, H., KALAM, M., RAHMAN, S., ABEDIN, M. & PALASH, S. 2013. Impact of palm, mustard, waste cooking oil and *Calophyllum inophyllum* biofuels on performance and emission of CI engine. *Renewable and Sustainable Energy Reviews,* 27**,** 664-682.

SANJID, A., MASJUKI, H. H., KALAM, M. A., RAHMAN, S. M. A., ABEDIN, M. J. & PALASH, S. M. 2014. Production of palm and jatropha based biodiesel and investigation of palm-jatropha combined blend properties, performance, exhaust emission and noise in an unmodified diesel engine. *Journal of Cleaner Production,* 65**,** 295-303.

SARAVANAN, S., NAGARAJAN, G., ANAND, S. & SAMPATH, S. 2012. Correlation for thermal NOx formation in compression ignition (CI) engine fuelled with diesel and biodiesel. *Energy,* 42**,** 401-410.

SARAVANAN, S., NAGARAJAN, G., LAKSHMI NARAYANA RAO, G. & SAMPATH, S. 2010. Combustion characteristics of a stationary diesel engine fuelled with a blend of crude rice bran oil methyl ester and diesel. *Energy,* 35**,** 94-100.

SARI, Y. W., BRUINS, M. E. & SANDERS, J. P. M. 2013. Enzyme assisted protein extraction from rapeseed, soybean, and microalgae meals. *Industrial Crops and Products,* 43**,** 78-83.

SARıBıYıK, O. Y., ÖZCANLı, M., SERIN, H., SERIN, S. & AYDıN, K. 2010. Biodiesel production from ricinus communis oil and its blends with soybean biodiesel. *Strojniški vestnik-Journal of Mechanical Engineering,* 56**,** 811-816.

SARIN, A. 2012. *Biodiesel: production and properties*, Royal Society of Chemistry.

SARIN, A., ARORA, R., SINGH, N., SARIN, R., MALHOTRA, R. & SARIN, S. 2010a. Blends of biodiesels synthesized from non-edible and edible oils: effects on the cold filter plugging point. *Energy & Fuels,* 24**,** 1996-2001.

SARIN, A., ARORA, R., SINGH, N. P., SARIN, R., MALHOTRA, R. K., SHARMA, M. & KHAN, A. A. 2010b. Synergistic effect of metal deactivator and antioxidant on oxidation stability of metal contaminated Jatropha biodiesel. *Energy,* 35**,** 2333-2337.

SARIN, R., KUMAR, R., SRIVASTAV, B., PURI, S. K., TULI, D. K., MALHOTRA, R. K. & KUMAR, A. 2009a. Biodiesel surrogates: Achieving performance demands. *Bioresource Technology,* 100**,** 3022-3028.

SARIN, R., SHARMA, M. & KHAN, A. A. 2009b. Studies on *Guizotia abyssinica* L. oil: Biodiesel synthesis and process optimization. *Bioresource technology,* 100**,** 4187-4192.

SCHINAS, P., KARAVALAKIS, G., DAVARIS, C., ANASTOPOULOS, G., KARONIS, D., ZANNIKOS, F., STOURNAS, S. & LOIS, E. 2009. Pumpkin (Cucurbita pepo L.) seed oil as an alternative feedstock for the production of biodiesel in Greece. *Biomass and Bioenergy,* 33**,** 44-49.

SCOTT, S. A., DAVEY, M. P., DENNIS, J. S., HORST, I., HOWE, C. J., LEA-SMITH, D. J. & SMITH, A. G. 2010. Biodiesel from algae: challenges and prospects. *Current Opinion in Biotechnology,* 21**,** 277-286.

SEO, Y. H., SUNG, M., OH, Y.-K. & HAN, J.-I. 2015. Lipid extraction and esterification for microalgae-based biodiesel production using pyrite (FeS2). *Bioresource Technology,* 191**,** 420-425.

SHAH, S., SHARMA, A. & GUPTA, M. N. 2005. Extraction of oil from Jatropha curcas L. seed kernels by combination of ultrasonication and aqueous enzymatic oil extraction. *Bioresource Technology,* 96**,** 121-123.

SHAHID, E. M. & JAMAL, Y. 2011. Production of biodiesel: a technical review. *Renewable and Sustainable Energy Reviews,* 15**,** 4732-4745.

SHARMA, A. & MURUGAN, S. 2015. Combustion, performance and emission characteristics of a DI diesel engine fuelled with non-petroleum fuel: A study on the role of fuel injection timing. *Journal of the Energy Institute,* 88**,** 364-375.

SHARMA, M., KHAN, A. A., DOHHEN, K. C., CHRISTOPHER, J., PURI, S. K., TULI, D. K. & SARIN, R. 2012. A Heterogeneous Catalyst for Transesterification of Argemone mexicana Oil. *Journal of the American Oil Chemists' Society,* 89**,** 1545-1555.

SHARMA, Y., SINGH, B. & UPADHYAY, S. 2008. Advancements in development and characterization of biodiesel: a review. *Fuel,* 87**,** 2355-2373.

SHARMA, Y. C. & SINGH, B. 2010. An ideal feedstock, kusum (*Schleichera triguga*) for preparation of biodiesel: Optimization of parameters. *Fuel,* 89**,** 1470-1474.

SHUSTER, M., COMBS, D., KARRIP, K. & BURKE, D. 2000. Piston ring cylinder liner scuffing phenomenon studies using acoustic emission technique. SAE Technical Paper.

SIAUT, M., CUINÉ, S., CAGNON, C., FESSLER, B., NGUYEN, M., CARRIER, P., BEYLY, A., BEISSON, F., TRIANTAPHYLIDÈS, C. & LI-BEISSON, Y. 2011. Oil accumulation in the model green alga Chlamydomonas reinhardtii: characterization, variability between common laboratory strains and relationship with starch reserves. *BMC biotechnology,* 11**,** 1-15.

SILITONGA, A., MASJUKI, H., MAHLIA, T., ONG, H., CHONG, W. & BOOSROH, M. 2013a. Overview properties of biodiesel diesel blends from edible and non-edible feedstock. *Renewable and Sustainable Energy Reviews,* 22**,** 346-360.

SILITONGA, A., ONG, H., MAHLIA, T., MASJUKI, H. & CHONG, W. 2013b. Characterization and production of *Ceiba pentandra* biodiesel and its blends. *Fuel,* 108**,** 855-858.

SINGH, K. K., WIESENBORN, D. P., TOSTENSON, K. & KANGAS, N. 2002. Influence of moisture content and cooking on screw pressing of crambe seed. *Journal of the American Oil Chemists' Society,* 79**,** 165-170.

SINGH, S. & SINGH, D. 2010a. Biodiesel production through the use of different sources and characterization of oils and their esters as the substitute of diesel: a review. *Renewable and Sustainable Energy Reviews,* 14**,** 200-216.

SINGH, S. P. & SINGH, D. 2010b. Biodiesel production through the use of different sources and characterization of oils and their esters as the substitute of diesel: A review. *Renewable and Sustainable Energy Reviews,* 14**,** 200-216.

SOLOIU, V., DUGGAN, M., HARP, S., VLCEK, B. & WILLIAMS, D. 2013. PFI (port fuel injection) of n-butanol and direct injection of biodiesel to attain LTC (low-temperature combustion) for low-emissions idling in a compression engine. *Energy,* 52**,** 143-154.

SOLOVCHENKO, A., KHOZIN-GOLDBERG, I., DIDI-COHEN, S., COHEN, Z. & MERZLYAK, M. 2008. Effects of light and nitrogen starvation on the content and composition of carotenoids of the green microalga Parietochloris incisa. *Russian Journal of Plant Physiology,* 55**,** 455-462.

SOMASHEKAR, D., VENKATESHWARAN, G., SAMBAIAH, K. & LOKESH, B. 2003. Effect of culture conditions on lipid and gamma-linolenic acid production by mucoraceous fungi. *Process Biochemistry,* 38**,** 1719-1724.

SOTO, C., CHAMY, R. & ZÚÑIGA, M. E. 2007. Enzymatic hydrolysis and pressing conditions effect on borage oil extraction by cold pressing. *Food Chemistry,* 102**,** 834-840.

STAVARACHE, C. E., MORRIS, J., MAEDA, Y., OYANE, I. & VINATORU, M. 2008. Syringa (Melia azedarach L.) berries oil: a potential source for biodiesel fuel. *Revista de Chimie,* 59**,** 672-677.

STEINBERG, A. M., DRISCOLL, J. F. & SWAMINATHAN, N. 2012. Statistics and dynamics of turbulence–flame alignment in premixed combustion. *Combustion and Flame,* 159**,** 2576-2588.

STEVENS, C. & VERHÉ, R. 2004. *Renewable bioresources: scope and modification for non-food applications*, Wiley-Interscience.

SUN, J., CATON, J. A. & JACOBS, T. J. 2010. Oxides of nitrogen emissions from biodiesel-fuelled diesel engines. *Progress in Energy and Combustion Science,* 36**,** 677-695.

SYAHRULLAIL, S., WIRA, J. Y., WAN NIK, W. & FAWWAZ, W. Friction characteristics of RBD palm olein using four-ball tribotester. Applied Mechanics and Materials, 2013. Trans Tech Publ, 936-940.

TAHA, E. M., OMAR, O., YUSOFF, W. M. W. & HAMID, A. A. 2010. Lipid biosynthesis in Cunnin ghamella bainieri 2A1 in N-li mited and N-excess media. *Ann Microbiol,* 60**,** 615-622.

TALEBI, A. F., MOHTASHAMI, S. K., TABATABAEI, M., TOHIDFAR, M., BAGHERI, A., ZEINALABEDINI, M., HADAVAND MIRZAEI, H., MIRZAJANZADEH, M., MALEKZADEH SHAFAROUDI, S. & BAKHTIARI, S. 2013. Fatty acids profiling: A selective criterion for screening microalgae strains for biodiesel production. *Algal Research,* 2**,** 258-267.

TAN, P.-Q., HU, Z.-Y., LOU, D.-M. & LI, Z.-J. 2012. Exhaust emissions from a light-duty diesel engine with Jatropha biodiesel fuel. *Energy,* 39**,** 356-362.

TANG, H., SALLEY, S. O. & NG, K. S. 2008. Fuel properties and precipitate formation at low temperature in soy-, cottonseed-, and poultry fat-based biodiesel blends. *Fuel,* 87**,** 3006-3017.

TARABET, L., LOUBAR, K., LOUNICI, M. S., HANCHI, S. & TAZEROUT, M. 2012. Eucalyptus biodiesel as an alternative to diesel fuel: preparation and tests on DI diesel engine. *BioMed Research International,* 2012**,** 235485 (1-8).

TASHTOUSH, G. M., AL-WIDYAN, M. I. & AL-JARRAH, M. M. 2004. Experimental study on evaluation and optimization of conversion of waste animal fat into biodiesel. *Energy conversion and Management,* 45**,** 2697-2711.

TESFA, B., MISHRA, R., ZHANG, C., GU, F. & BALL, A. D. 2013. Combustion and performance characteristics of CI (compression ignition) engine running with biodiesel. *Energy,* 51**,** 101-115.

TONG, D., HU, C., JIANG, K. & LI, Y. 2011. Cetane number prediction of biodiesel from the composition of the fatty acid methyl esters. *Journal of the American Oil Chemists' Society,* 88**,** 415-423.

TRAN, D.-T. & CHANG, J.-S. 2014. Kinetics of enzymatic transesterification and thermal deactivation using immobilized Burkholderia lipase as catalyst. *Bioprocess and biosystems engineering,* 37**,** 481-491.

TRAN, M. K., DUNN-RANKIN, D. & PHAM, T. K. 2012. Characterizing sooting propensity in biofuel–diesel flames. *Combustion and Flame,* 159**,** 2181-2191.

TÜCCAR, G. & AYDıN, K. 2013. Evaluation of methyl ester of microalgae oil as fuel in a diesel engine. *Fuel,* 112**,** 203-207.

TÜCCAR, G., ÖZGÜR, T. & AYDıN, K. 2014a. Effect of diesel–microalgae biodiesel–butanol blends on performance and emissions of diesel engine. *Fuel,* 132**,** 47-52.

TÜCCAR, G., TOSUN, E., ÖZGÜR, T. & AYDıN, K. 2014b. Diesel engine emissions and performance from blends of citrus sinensis biodiesel and diesel fuel. *Fuel,* 132**,** 7-11.

TUNG, S. C. & MCMILLAN, M. L. 2004. Automotive tribology overview of current advances and challenges for the future. *Tribology International,* 37**,** 517-536.

UDDIN, M. S. 2009. Prospect of Jatropha Curcas and Pithraj Cultivation in Bangladesh. *Journal of Engineering and Technology Vol,* 7**,** 42.

ULLAH, Z., BUSTAM, M. A. & MAN, Z. 2015. Biodiesel production from waste cooking oil by acidic ionic liquid as a catalyst. *Renewable Energy,* 77**,** 521-526.

UMERIE, S., OKONKWO, I., NWADIALOR, N. & OKONKWO, J. 2010. Studies on the oil and nutritive value of seeds of Crotalaria retusa L.(Fabaceae). *Pakistan Journal of Nutrition,* 9**,** 912-914.

USTA, N., AYDOĞAN, B., ÇON, A. H., UĞUZDOĞAN, E. & ÖZKAL, S. G. 2011. Properties and quality verification of biodiesel produced from tobacco seed oil. *Energy Conversion and Management,* 52**,** 2031-2039.

VALLINAYAGAM, R., VEDHARAJ, S., YANG, W. M., LEE, P. S., CHUA, K. J. E. & CHOU, S. K. 2014. Pine oil–biodiesel blends: A double biofuel strategy to completely eliminate the use of diesel in a diesel engine. *Applied Energy,* 130**,** 466-473.

VARATHARAJAN, K. & CHERALATHAN, M. 2012. Influence of fuel properties and composition on NO_x emissions from biodiesel powered diesel engines: A review. *Renewable and Sustainable Energy Reviews,* 16**,** 3702-3710.

VASHIST, D. & AHMAD, M. 2011. A comparative study of castor and jatropha oil source and its methyl ester test on the diesel engine. *Int J Eng Sci Technol,* 3**,** 4765-4773.

VASUDEVAN, P. T. & BRIGGS, M. 2008. Biodiesel production—current state of the art and challenges. *Journal of Industrial Microbiology & Biotechnology,* 35**,** 421-430.

VEYNANTE, D. & VERVISCH, L. 2002. Turbulent combustion modeling. *Progress in energy and combustion science,* 28**,** 193-266.

WAN, M., LIU, P., XIA, J., ROSENBERG, J. N., OYLER, G. A., BETENBAUGH, M. J., NIE, Z. & QIU, G. 2011. The effect of mixotrophy on microalgal growth, lipid content,

and expression levels of three pathway genes in Chlorella sorokiniana. *Applied microbiology and biotechnology,* 91**,** 835-844.

WANG, L. & YU, H. 2012. Biodiesel from Siberian apricot (Prunus sibirica L.) seed kernel oil. *Bioresource Technology,* 112**,** 355-358.

WANG, R., HANNA, M. A., ZHOU, W.-W., BHADURY, P. S., CHEN, Q., SONG, B.-A. & YANG, S. 2011. Production and selected fuel properties of biodiesel from promising non-edible oils: *Euphorbia lathyris* L., *Sapium sebiferum* L. and *Jatropha curcas* L. *Bioresource Technology,* 102**,** 1194-1199.

WANG, R., ZHOU, W.-W., HANNA, M. A., ZHANG, Y.-P., BHADURY, P. S., WANG, Y., SONG, B.-A. & YANG, S. 2012. Biodiesel preparation, optimization, and fuel properties from non-edible feedstock,*Datura stramonium* L. *Fuel,* 91**,** 182-186.

WANG, Y., LIU, H. & LEE, C.-F. F. 2016. Particulate matter emission characteristics of diesel engines with biodiesel or biodiesel blending: A review. *Renewable and Sustainable Energy Reviews,* 64**,** 569-581.

WAZILEWSKI, W. T., BARICCATTI, R. A., MARTINS, G. I., SECCO, D., SOUZA, S. N. M. D., ROSA, H. A. & CHAVES, L. I. 2013. Study of the methyl crambe (Crambe abyssinica Hochst) and soybean biodiesel oxidative stability. *Industrial Crops and Products,* 43**,** 207-212.

WORLD BANK 2016. The World Bank, Total population data, [cited on 20th November, 2016]; Available from: <http://data.worldbank.org/indicator/SP.POP.TOTL?end=2015&start=1960&view=chart>.

WU, C.-W., CHEN, R.-H., PU, J.-Y. & LIN, T.-H. 2004. The influence of air–fuel ratio on engine performance and pollutant emission of an SI engine using ethanol–gasoline-blended fuels. *Atmospheric Environment,* 38**,** 7093-7100.

WU, L., LIU, H., ZHANG, R., LI, L., LI, J., HU, H. & HUANG, H. 2013. Chondroprotective Activity of Murraya exotica through Inhibiting β-Catenin Signaling Pathway. *Evidence-Based Complementary and Alternative Medicine,* 2013**,** 1-8.

WU, S., ZHAO, X., SHEN, H., WANG, Q. & ZHAO, Z. K. 2011. Microbial lipid production by *Rhodosporidium toruloides* under sulfate-limited conditions. *Bioresource technology,* 102**,** 1803-1807.

WYNN, J. P., HAMID, A. A., LI, Y. & RATLEDGE, C. 2001. Biochemical events leading to the diversion of carbon into storage lipids in the oleaginous fungi Mucor circinelloides and Mortierella alpina. *Microbiology,* 147**,** 2857-2864.

XUE, F., MIAO, J., ZHANG, X. & TAN, T. 2010. A new strategy for lipid production by mix cultivation of Spirulina platensis and Rhodotorula glutinis. *Applied biochemistry and biotechnology,* 160**,** 498-503.

XUE, J., GRIFT, T. E. & HANSEN, A. C. 2011. Effect of biodiesel on engine performances and emissions. *Renewable and Sustainable Energy Reviews,* 15**,** 1098-1116.

YAMADA, H., MISAWA, K., SUZUKI, D., TANAKA, K., MATSUMOTO, J., FUJII, M. & TANAKA, K. 2011. Detailed analysis of diesel vehicle exhaust emissions: Nitrogen oxides, hydrocarbons and particulate size distributions. *Proceedings of the Combustion Institute,* 33**,** 2895-2902.

YAN, Y., LI, X., WANG, G., GUI, X., LI, G., SU, F., WANG, X. & LIU, T. 2014. Biotechnological preparation of biodiesel and its high-valued derivatives: A review. *Applied Energy,* 113**,** 1614-1631.

YANG, F.-X., SU, Y.-Q., LI, X.-H., ZHANG, Q. & SUN, R.-C. 2009. Preparation of biodiesel from Idesia polycarpa var. vestita fruit oil. *Industrial Crops and Products,* 29**,** 622-628.

YUSUF, N. N. A. N., KAMARUDIN, S. K. & YAAKUB, Z. 2011. Overview on the current trends in biodiesel production. *Energy Conversion and Management,* 52**,** 2741-2751.

ZAHEDI, G. & AZARPOUR, A. 2011. Optimization of supercritical carbon dioxide extraction of *Passiflora* seed oil. *The Journal of Supercritical Fluids,* 58**,** 40-48.

ZHANG, J., LU, J., ZHANG, Q., DAI, L., LIU, Y., TU, P. & QIAO, Y. 2013. Simultaneous Screening and Identifying Four Categories of Particular Flavonoids in the Leaves of Murraya exotica L. by HPLC–DAD–ESI-MS-MS. *Journal of chromatographic science,* 52**,** 103-114.

ZHANG, Y., ADAMS, I. P. & RATLEDGE, C. 2007. Malic enzyme: the controlling activity for lipid production? Overexpression of malic enzyme in Mucor circinelloides leads to a 2.5-fold increase in lipid accumulation. *Microbiology,* 153**,** 2013-2025.

ZHAO, B. & SU, Y. 2014. Process effect of microalgal-carbon dioxide fixation and biomass production: A review. *Renewable and Sustainable Energy Reviews,* 31**,** 121-132.

ZHAO, X., HU, C., WU, S., SHEN, H. & ZHAO, Z. K. 2011. Lipid production by Rhodosporidium toruloides Y4 using different substrate feeding strategies. *Journal of industrial microbiology & biotechnology,* 38**,** 627-632.

ZHOU, J. H., LU, Y. J., HUANG, B. H., HUO, Y. P. & ZHANG, K. 2011. Preparation of Biodiesel from Tung Oil Catalyzed by Sulfonic-Functional Brŏnsted Acidic Ionic Liquids. *Advanced Materials Research,* 314**,** 1459-1462.

ZHU, J., RONG, J. & ZONG, B. 2013. Factors in mass cultivation of microalgae for biodiesel. *Chinese Journal of Catalysis,* 34**,** 80-100.

ZHU, L., CHEUNG, C. S. & HUANG, Z. 2016. A comparison of particulate emission for rapeseed oil methyl ester, palm oil methyl ester and soybean oil methyl ester in perspective of their fatty ester composition. *Applied Thermal Engineering,* 94**,** 249-255.

ZHU, L., CHEUNG, C. S., ZHANG, W. G. & HUANG, Z. 2011. Combustion, performance and emission characteristics of a DI diesel engine fueled with ethanol–biodiesel blends. *Fuel,* 90**,** 1743-1750.

ZULKIFLI, N. W. M., KALAM, M. A., MASJUKI, H. H., SHAHABUDDIN, M. & YUNUS, R. 2013. Wear prevention characteristics of a palm oil-based TMP (trimethylolpropane) ester as an engine lubricant. *Energy,* 54**,** 167-173.

Appendix-I

This Appendix contains some important information of the above study. Some results illustrated in these Figures have been discussed in previous chapters.

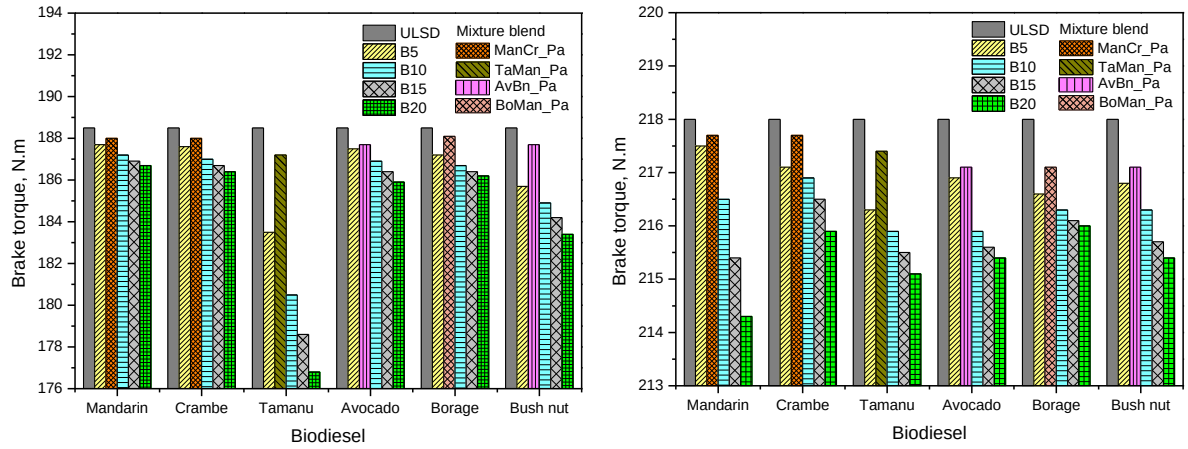

(a) (b)

Appendix Figure 1: Effect of biodiesel blends on brake torque at (a) rated power at 2400 rpm and (b) rated torque at 1400 rpm

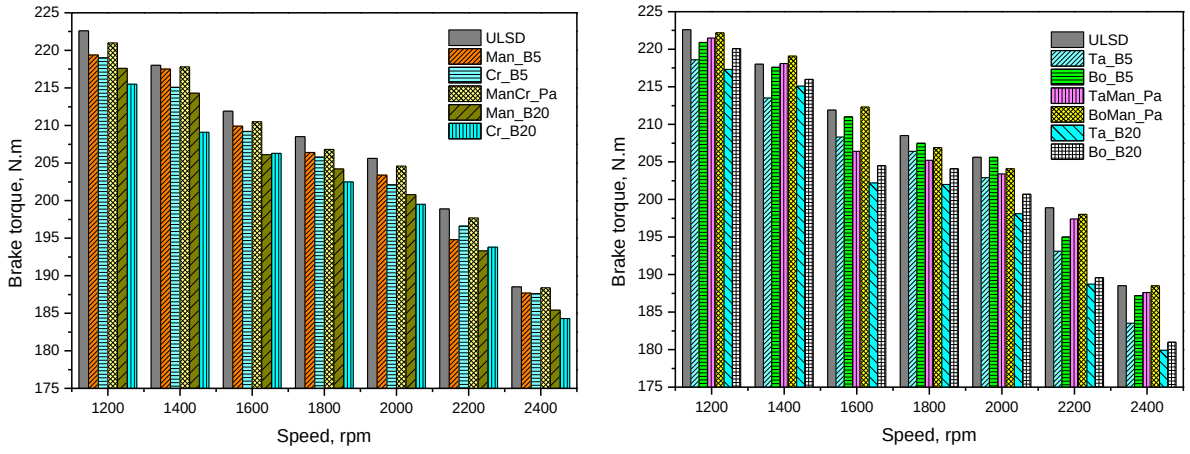

(a) (b)

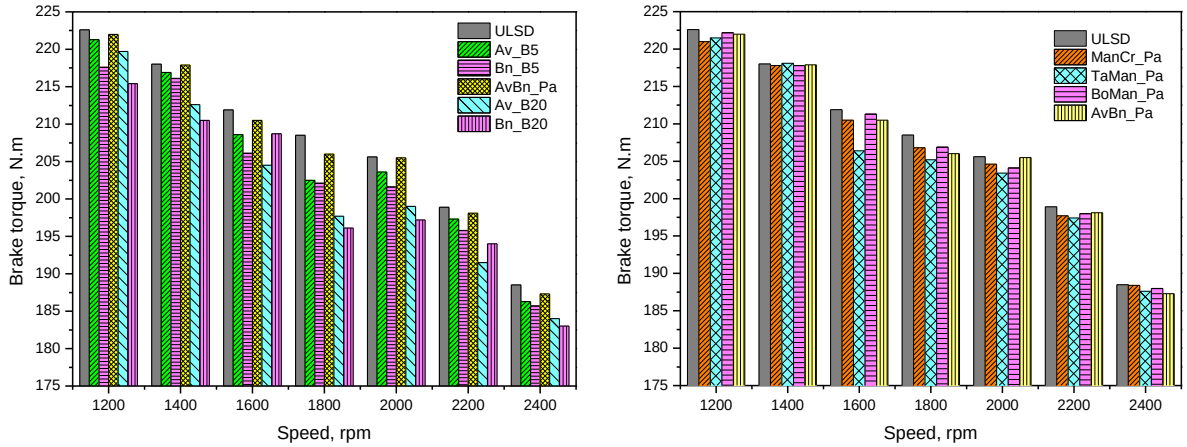

(c) (d)

Appendix Figure 2: Variation of BT by varying engine speed for (a) Mandarin-Crambe, (b) Tamanu-Borage, (c) Avocado-Bush nut and (d) Biodiesels and paraffin mixture blends

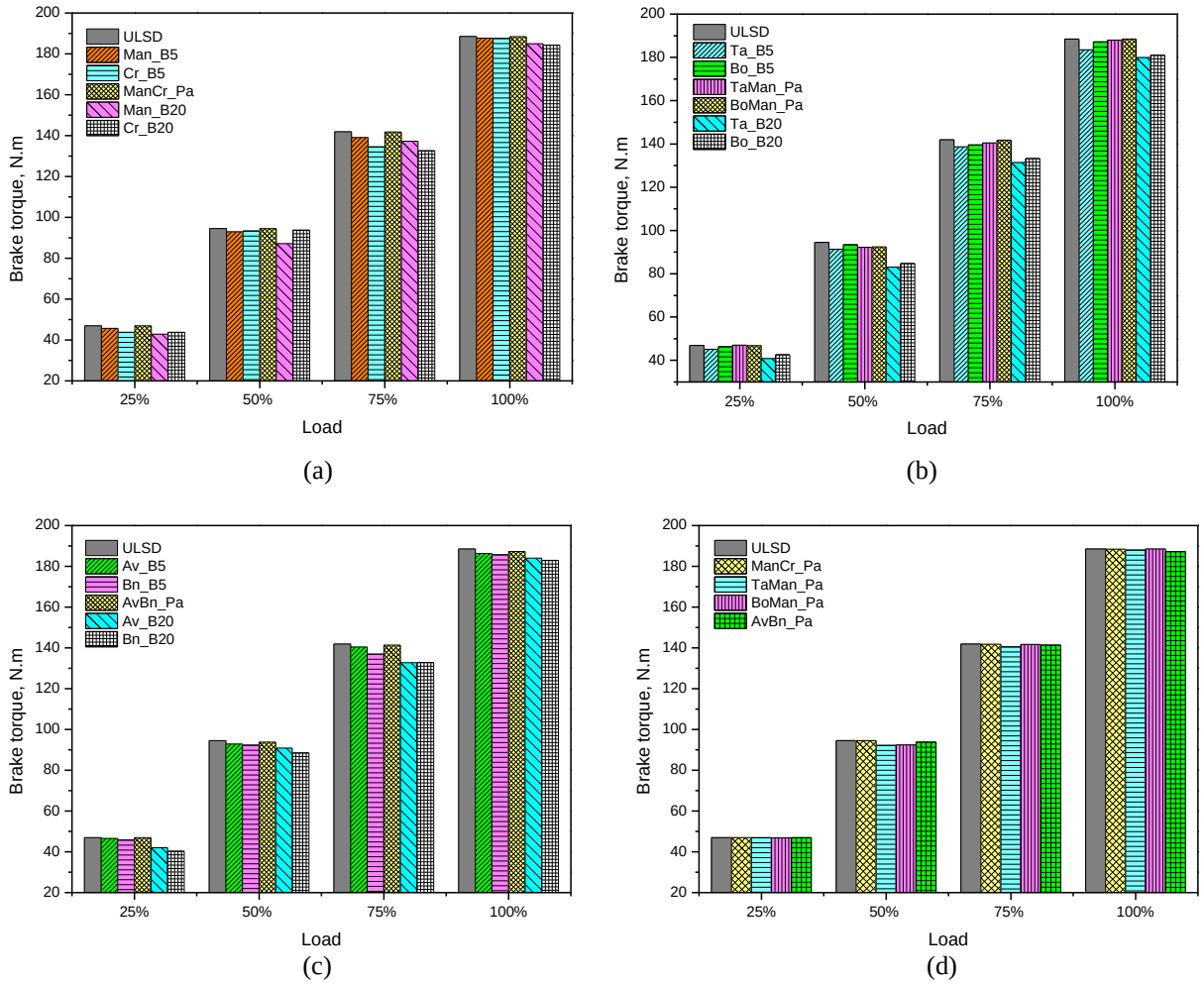

(a) (b)

(c) (d)

Appendix Figure 3: Variation of BT by varying engine load at 2400 rpm for (a) Mandarin-Crambe, (b) Tamanu-Borage, (c) Avocado-Bush nut and (d) Biodiesels and paraffin mixture blends

BMEP Variation

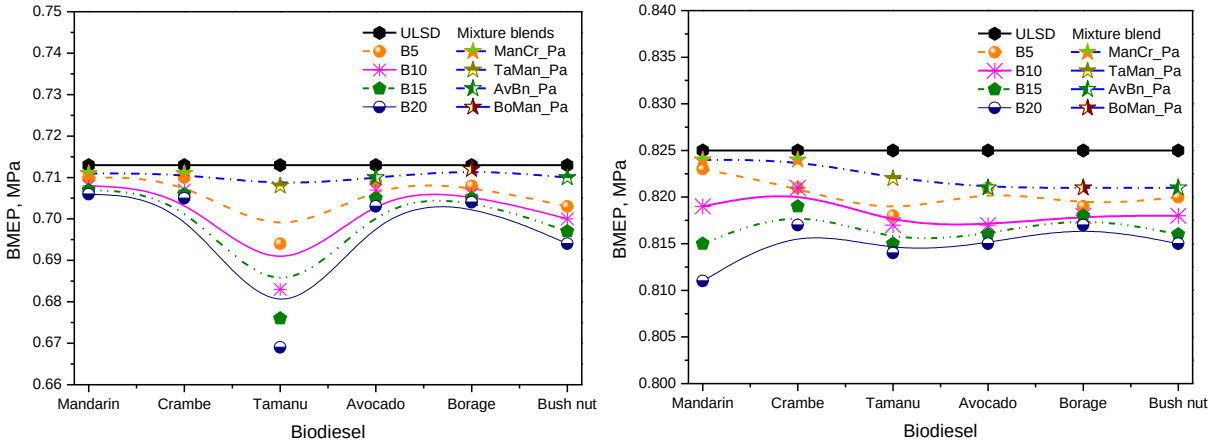

(a) (b)

Appendix Figure 5: Effect of biodiesel blends on BMEP at (a) rated power at 2400 rpm and (b) rated torque at 1400 rpm

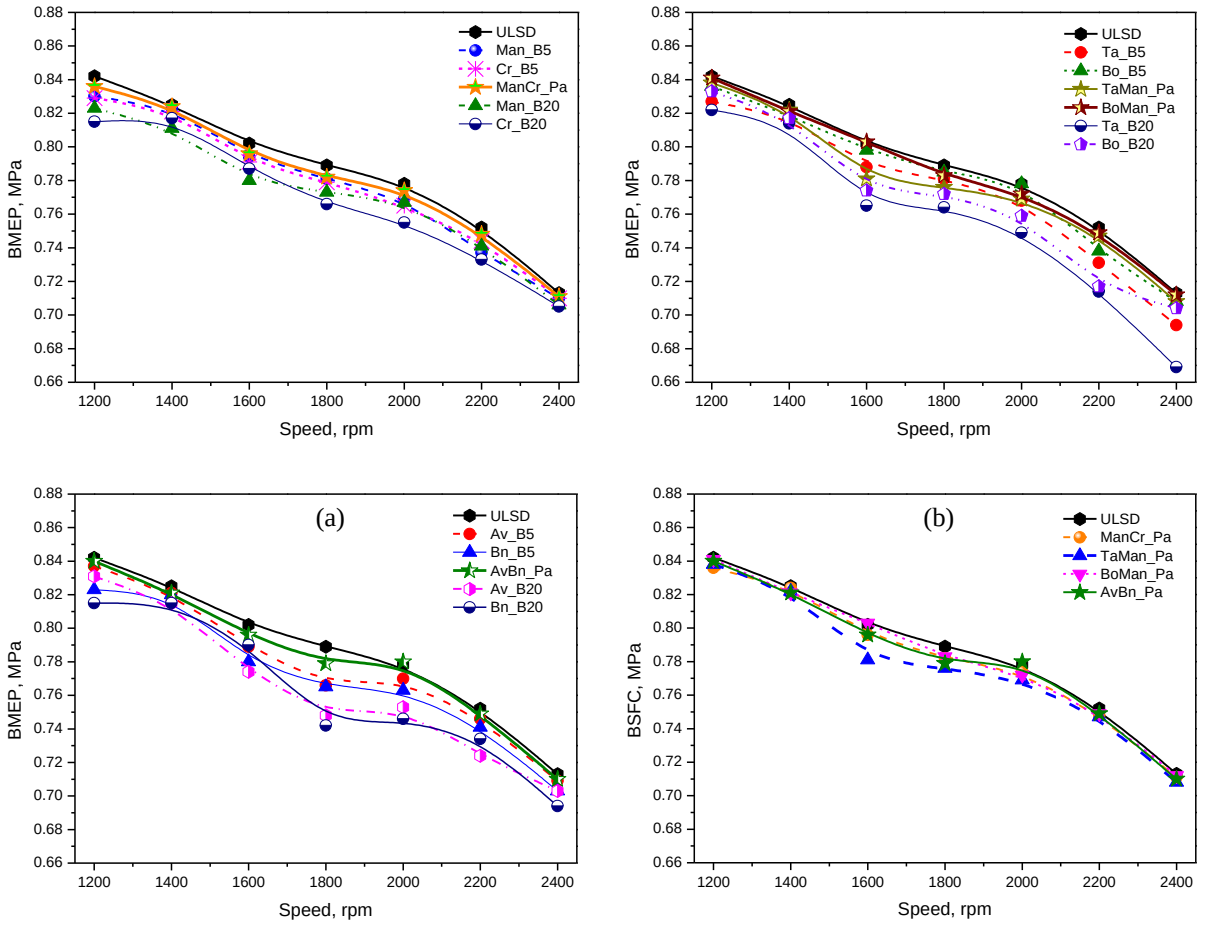

(c) (d)

Appendix Figure 6: Variation of BMEP by varying engine speed for (a) Mandarin-Crambe, (b) Tamanu-Borage, (c) Avocado-Bush nut and (d) Biodiesels and paraffin mixture blends

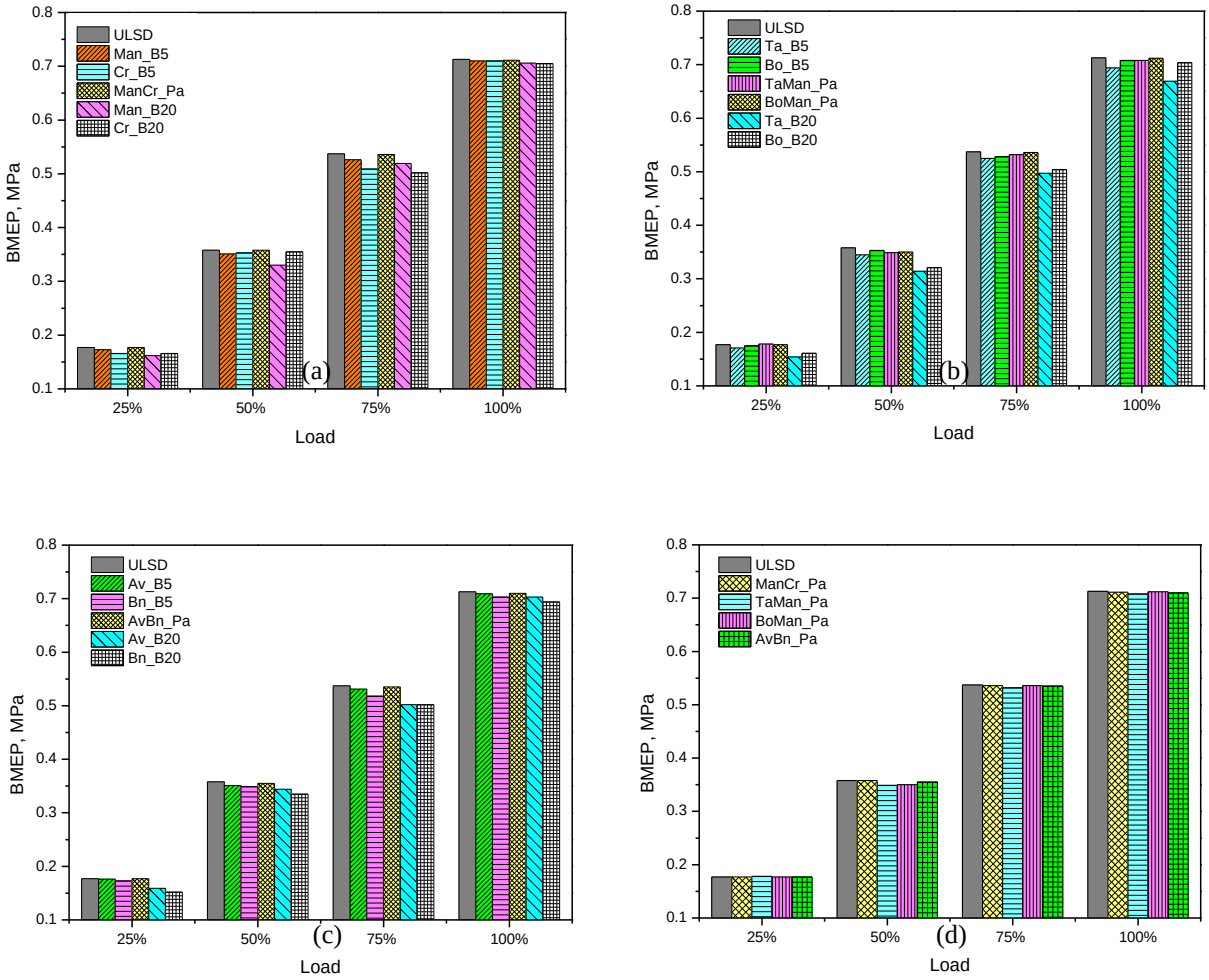

Appendix Figure 7: Variation of BMEP by varying engine load at 2400 rpm for (a) Mandarin-Crambe, (b) Tamanu-Borage, (c) Avocado-Bush nut and (d) Biodiesels and paraffin mixture blends